

# Meereswissenschaftliche Berichte

## Marine Science Reports



No 99 2016

Deglaciation history, coastal development, and environmental change in West Greenland during the Holocene:

Results of the R/V “Maria S. Merian” expedition MSM05/03, 15<sup>th</sup> June to 4<sup>th</sup> July 2007

Jan Harff, Kerstin Perner, Matthias Moros (eds.)

"Meereswissenschaftliche Berichte" veröffentlichen Monographien und Ergebnisberichte von Mitarbeitern des Leibniz-Instituts für Ostseeforschung Warnemünde und ihren Kooperationspartnern. Die Hefte erscheinen in unregelmäßiger Folge und in fortlaufender Nummerierung. Für den Inhalt sind allein die Autoren verantwortlich.

"Marine Science Reports" publishes monographs and data reports written by scientists of the Leibniz-Institute for Baltic Sea Research Warnemünde and their co-workers. Volumes are published at irregular intervals and numbered consecutively. The content is entirely in the responsibility of the authors.

Schriftleitung: Dr. Norbert Wasmund  
([norbert.wasmund@io-warnemuende.de](mailto:norbert.wasmund@io-warnemuende.de))

Die elektronische Version ist verfügbar unter / The electronic version is available on:  
<http://www.io-warnemuende.de/meereswissenschaftliche-berichte.html>



© Dieses Werk ist lizenziert unter einer Creative Commons Lizenz CC BY-NC-ND 4.0 International. Mit dieser Lizenz sind die Verbreitung und das Teilen erlaubt unter den Bedingungen: Namensnennung - Nicht-kommerziell - Keine Bearbeitung.

© This work is distributed under the Creative Commons License which permits to copy and redistribute the material in any medium or format, requiring attribution to the original author, but no derivatives and no commercial use is allowed, see:  
<http://creativecommons.org/licenses/by-nc-nd/4.0/>

ISSN 2195-657X

---

Jan Harff<sup>1,2</sup>, Kerstin Perner<sup>1</sup>, Matthias Moros<sup>1</sup> (eds.): Deglaciation history, coastal development, and environmental change in West Greenland during the Holocene: Results of the R/V "Maria S. Merian" expedition MSM05/03, 15th June to 4th July 2007. Meereswiss. Ber., Warnemünde, 99 (2016), doi:10.12754/msr-2016-0099

Adressen der Editoren:

<sup>1</sup> Leibniz Institute for Baltic Sea Research (IOW), Seestraße 15, D-18119 Rostock

<sup>2</sup> University of Szczecin, Institute of Marine and Coastal Sciences, ul. Mickiewicza 18. Szczecin 70-383. Polen

E-mail des verantwortlichen Editor: [jan.harff@io-warnemuende.de](mailto:jan.harff@io-warnemuende.de)

## List of authors and cruise participants

Harff, J.	<i>Chief Scientist</i>	IOW
Endler, R.	Sedimentacoustic profiling (watch)	IOW
Nickel, G.	Sedimentacoustic profiling (watch)	IOW
Waniek, J.	CTD/ADCP measurements (watch)	IOW
Hentzsch, B.	CTD/ADCP measurements (watch)	IOW
Weinrebe, W.	Bathymetric measurements	IFM-GEOMAR
Moros, M.	Sedimentology	IOW
Mikkelsen, N.	Sedimentology	GEUS
Jensen, J. B.	Sedimentacoustic profiling (watch)	GEUS
Kotov, S.	Data exploration	MARUM
Kujpers, A.	Sedimentacoustic profiling (watch)	GEUS
Lloyd, J.	Paleoceanography	DU
Shevchenko, V.	SPM / aeolian dust investigation	IORAS
Leipe, T	Geochemical sampling	IOW
Trost, E.	Hydrochemical/geochemical sampling	IOW
Rysgaard, S.	Biogeochemical sampling	GINR
Risgaard-Pettersen, N.	Biogeochemical sampling	AU
Richter, T.	XRF-Scanner	NIOZ
Witkowski, A.	Mikropalaeontology	US
Krauss, N.	Sedimentological Recording (watch)	EMAU
Perner, K.	Geochemistry	EMAU
Sandgren, P.	Paleomagnetic/sedimentological sampling	GBSC
Snowball, I.	Paleomagnetic/sedimentological sampling	GBSC
Frahm, A.	Technical operation of geological sampling	IOW
Pötzsch, M.	Technical operation of geological sampling	IOW
Dietrich, R.	Geodetical measurements	TUD
Richter, A.	Geodetical measurements	TUD
Kotov, S.**		MARUM

\*\*) did not attend the cruise

## Contributing Institutes

1. Leibniz Institute for Baltic Sea Research Warnemünde, Germany (IOW)
2. Leibniz Institute of Marine Sciences Kiel, Germany (IfM-GEOMAR)
3. Technische Universität Dresden, Germany (TUD)
4. Geological Survey of Denmark and Greenland, Copenhagen, Denmark (GEUS)
5. Durham University, UK (DU)
6. Greenland Institute of Natural Resources, Nuuk, Greenland (GINR)
7. Royal Netherlands Institute of Sea Research, Texel, The Netherlands (NIOZ)
8. Szczecin University, Poland (US)
9. Lund University, Sweden (GBSC)
10. Shirshov Institute of Oceanology, Russian Academy of Science Moscow, Russia (IORAS)
11. Ernst-Moritz-Arndt-University Greifswald, Germany (EMAU)
12. Aarhus University, Denmark (AU)
13. Center for Marine Environmental Sciences, University of Bremen (MARUM)

## Table of contents

Abstract

Kurzfassung

1.	Introduction (J. Harff)	6
2.	Methods and devices	8
2.1	Subbottom profiling (R. Endler, G. Nickel)	8
2.2	Multibeam echo-sounding (W. Weinrebe)	10
2.2.1	Kongsberg (Simrad) EM-120 deep-water multibeam echosounder	10
2.2.2	Kongsberg (Simrad) EM-120 shallow-water echosounder	11
2.2.3	EM-120 multibeam data processing	11
2.3	Hydrography (J. Waniek, E. Trost)	12
2.3.1	Continous underway measurements	15
2.3.2	Hydrochemistry	15
2.4	Sediment Sampling (M. Moros)	17
2.5	Lithological core description (K. Perner)	18
2.6	Diatomological investigation (A. Witkowski)	19
2.7	Biogeochemistry (S. Rysgaard, N. Risgaard-Petersen)	23
2.8	Magnetic susceptibility measurements (P. Sandgren, I. Snowball)	26
2.9	XRF-Scanning (T. Richter)	26
2.10	Geodetic measurements (R. Dietrich, A. Richter)	28
2.11	SPM and aerial dust sampling (V. Shevshenko)	31
3.	First results	31
3.1	Mapping (W. Weinrebe)	31
3.1.1	Mapping Ilulissat Icefjord	31
3.1.2	Morphology of the Ilulissat Ice fjord area	33
3.1.3	Mapping ice berg drift in the Davis strait	36
3.2	Biogeochemistry - early diagenesis in fjord and bay sediments (S. Rysgaard, N. Risgaard-Petersen)	38
3.3	Disko Bay, fjord, and shelf sediments – paleoceanographic / paleoclimatological Interpretation	40
3.3.1	Analyses during the expedition (J. Lloyd, M. Moros, K. Perner, P. Sandgren, I. Snowball, J. Harff, T. Richter)	39
3.3.2	Data Analyses (J. Harff, S. Kotov, K. Perner)	39
3.4	Anthropogenic impact on Qaumarujuk Fjord environment (K. Perner, T. Leipe, T. Richter, P. Sandgren)	45
3.5	Geodetic measurements (R. Dietrich, A. Richter)	49
3.6	SPM an aerial dust (V. Shevshenko)	49
4.	Summary (J. Harff)	50
	References	52
	Enclosures	55

## Abstract

An international and interdisciplinary team of geoscientists collected a series of water and sediment samples and performed geophysical mapping of the sea floor as well as glacio-isostatic measurements during the expedition MSM 05/03 of the R/V “Maria S. Merian” in West Greenland waters between June 15 and July 4, 2007. This expedition improved our understanding of the interaction between hydrosphere, geosphere, and climatic changes in West Greenland coastal waters and its impact on environmental change during the Late Quaternary. Using a set of hydrographic, geophysical, sedimentological, paleontological, and geodetical methods the following results have been achieved during the expedition and during post-cruise studies: i) Finalizing a geodetical network that records glacio-isostatic adjustment in the central West Greenland area led to the identification of vertical dislocations of the earth’s crust in West Greenland, which has been used for model parameterization. ii) Using multibeam echosounder survey, mapping of the sea floor in the Disko Bay area and along the expeditions cruise track along the shelf has been performed. Identification of ploughmarks illustrate different drift directions of icebergs, indicating variations in the flow path of ocean currents. iii) On board measurements of geochemical and sediment-physical parameters revealed the good quality of the collected marine sediment cores for high-resolution, millennial to decadal scale, paleoceanographic reconstructions and periodicity analyses. iv) The impact of anthropogenic activity on sediment properties and on the aquatic ecosystem that resulted from lead/zink mining close to Maarmorilik („Black Angel Mine“) has been studied within the Qaumarujuk Fjord.

## Kurzfassung

Die Expedition MSM 05/03 führte das F/S “Maria S. Merian” vom 15.6. bis 4.7.2007 in Fjorde und Schelfgebiete Westgrönlands. Ein internationales und interdisziplinäres Team von Geowissenschaftlern untersuchte die Wechselbeziehung zwischen Hydrosphäre, Geosphäre, Anthroposphäre und Klimaänderungen in Westgrönländischen küstennahen Gewässern sowie dessen Einfluss auf die Umweltbedingungen im Spätquartär. Durch Anwendung von hydrographischen, geophysikalischen, sedimentologischen, paläontologischen und geodätischen Methoden konnten während und nach der Expedition bisher folgende Ergebnisse erzielt werden: i) Ein geodätisches Meßnetz zur Identifikation von glazio-isostischen Bewegungen in Westgrönland wurde komplettiert und Daten für die Parametrisierung von Modellen gewonnen. ii) Seismoakustische Aufnahmen vom Meeresboden im Bereich der Disko Bucht und entlang der Expeditionsroute auf dem Schelf ermöglichte eine morphologische Kartierung von Eisberg-„Ploughmark“ Richtungen, welche auf strömungsbedingte Änderungen der Driftrouten hindeuten. iii) Die bereits auf dem Schiff erfolgten Messung von geochemischen und physikalischen Parametern verdeutlichten, das die gewonnenen marinen Sedimentkernen das Potenzial haben paläozeanographische Änderungen auf tausendjährigen bis multidekadischen Skalen aufzulösen und sich zur Durchführung von Zeitreihenanalysen eignen. iv) Spuren anthropogener Aktivitäten zeigen sich in Sedimenten des Qaumarujuk Fjords anhand erhöhter Schwermetallkonzentrationen. Diese Anomalien sind auf den Blei/Zink Bergbau in Bereich Maarmorilik („Black Angel Mine“) zurückzuführen.

## 1. Introduction

The expedition MSM 05/03 on the German RV “Maria S. Merian” took place between June 15 and July 4 in 2007 on the shelf and fjords of West Greenland, on board scientists from Denmark/Greenland, Germany, Russia, Sweden, and The Netherlands. Their general aim was to study the interaction between hydrosphere, geosphere, and climatic change in the coastal waters of West Greenland and to improve our knowledge on its impact on environmental change during the Late Quaternary. The team of geologists, geophysicists, marine geochemists, palaeontologists, geodesists, and paleo-oceanographers performed an interdisciplinary measuring and sampling campaign along transects from the head of three Fjords, i.e. the Nuuk Fjord, Nordre Strømfjord, and Ummannaq Fjord, towards the shelf edge, as well as in the Disko Bay, and therefore contributed to following research topics:

- (1.) Reconstruction of climate and ice dynamics in West Greenland during the late Pleistocene and Holocene.
- (2.) Influence of climate change and anthropogenic forcing on biogeochemical cycles during the Holocene.
- (3.) Glacio-isostatic deformation of the Earth crust and its influence on coastal processes.

The sampling program and on-board measurements and post-cruise work aimed to identify drivers of environmental and oceanographic changes within the fjords (East-West transects) as well as along the shelf between 64° N and 72° N (South-North transect). Figure 1 shows the work areas:

- Nordre Strømfjord
- Disko Bay
- Vaigat and Ummannaq Fjord
- Nuuk Fjord

The spatiotemporal pattern of climatic, oceanographic and isostatic changes has been investigated at selected sediment core sites within the Nuuk Fjord, the Nordre Strømfjord, the outer Ummannaq Fjord and Disko Bugt area, using micropaleontological and geochemical proxies. Within the Disko Bay area, extensive seismoacoustic profiling led to the identification of sedimentary basins that contained undisturbed and massive sediment packages of Holocene origin, which were particularly needed for oceanic and climatic reconstructions within the area and the potential influence of meltwater pulses from the Greenland Ice Sheet on regional environmental conditions. Extensive sea floor mapping provided valuable information about iceberg drift in the Disko Bay area.

The Nordre Strømfjord is a suitable area to study changes in the behavior of the vertical crust movements from the edge of the Greenland Ice Sheet toward the shelf area in West Greenland. In order to identify and improve our knowledge on recent vertical crustal deformations and the range of sea-level variations, geodetic observations have been carried out in the fjord using autonomously operated GPS receivers and pressure tides gauges. The impact of anthropogenic activity via lead/zinc mining of the “Black Angel Mine” at Marmorilik on local environmental conditions has been studied within the Qumarjuruk Fjord using geochemical analyses on set of short sediment cores.

This report presents all data collected during the expedition MSMo5/03, i.e. onboard measurements on water and sediment samples and provides an overview about post-cruise studies, including publications.

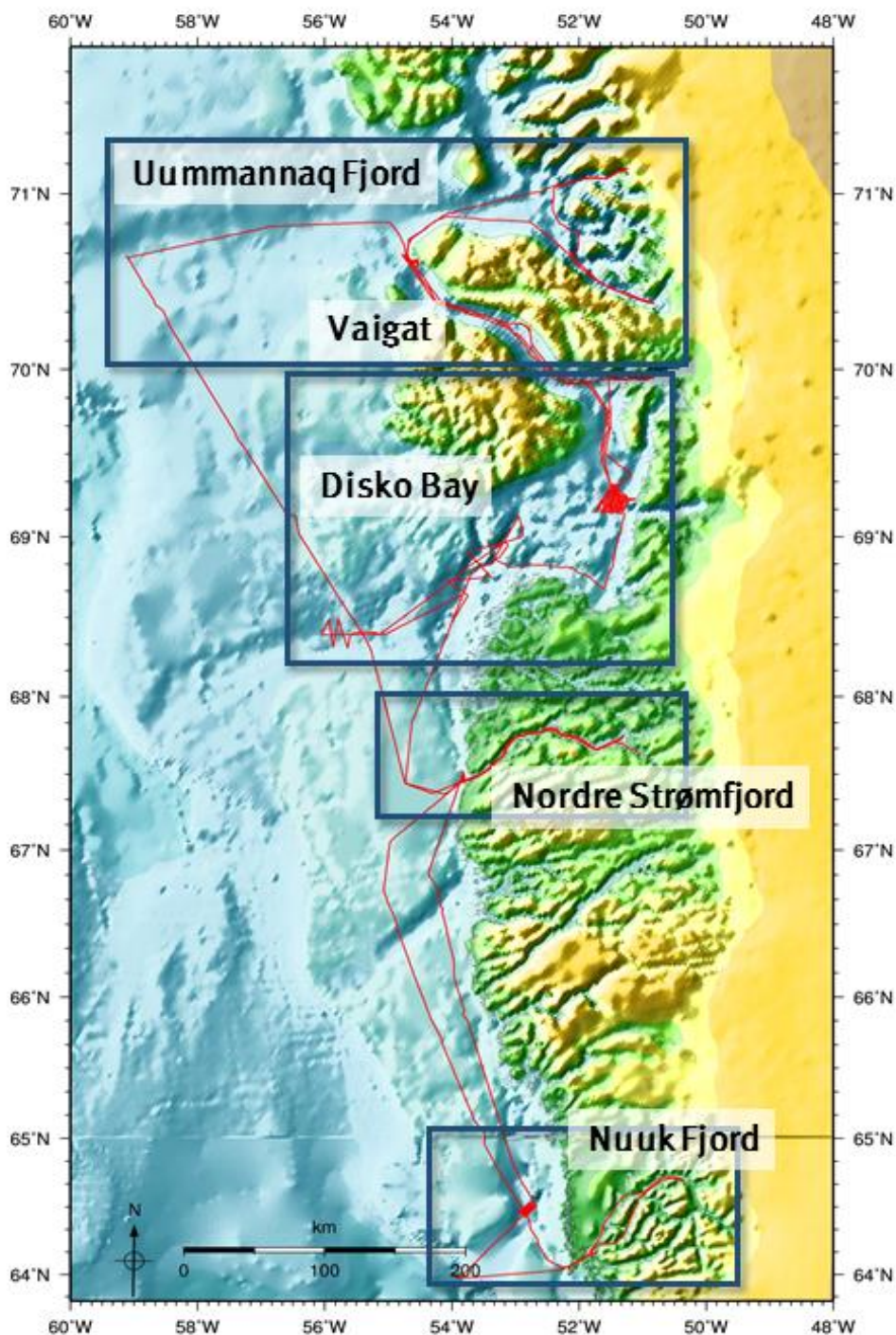


Fig. 1.1: Bathymetric map of central West Greenland including cruise track (red line) and the study areas (blue boxes) of the MSMo5/03 cruise in June/July 2007.

## 2. Methods and devices

### 2.1 Subbottom profiling (R. Endler, G. Nickel)

Morphology, distribution, and layering of sediments was investigated using the “ATLAS PARASOUND P70” subbottom profiling system. The main task was to find optimal sampling locations in the predefined working areas. Parametric echosounders work both as low-frequency sediment echosounders and as high-frequency narrow beam echsounders (to measure water depth). They make use of the so called “parametric” effect which produces additional (secondary) frequency components through non-linear interaction of two signals with high, slightly different (primary) frequencies at high sound pressures. The new, low (secondary) frequency components propagate within the narrow cone of the high (primary) frequencies. Therefore, the footprint size is comparably small and both lateral and vertical resolution are significantly improved. The directivity pattern of the low frequency components shows no significant side lobes and remains nearly constant for different secondary frequencies. The insonified volume is the same and comparable results are obtained for different secondary frequencies. Parametric systems have a high system bandwidth and can therefore transmit short pulses without ringing (e.g. 1 period of 12 kHz). This makes parametric systems particularly useful for high resolution surveys in shallow water areas. Furthermore, short pulses, narrow beams and the absence of side lobes result in less volume and bottom surface reverberation compared to linear systems. This improves the signal to noise ratio and therefore the usable depth range (penetration depth). Suitable for operations from 10 m to 10 000 m the ATLAS PARASOUND P70 operates at primary frequencies of 18-39 kHz to provide secondary frequencies as low as 500 Hz. With a secondary parametric source level of approximately 206 dB this provides bottom penetration >200 m with resolution <15 cm depending on bottom characteristics. A detailed description of the system can be found at [www.atlashydro.com](http://www.atlashydro.com).

The Parasound echosounder was permanently operated during the cruise. The profile trackplots are depicted in Fig. 2.1.1. The system worked very unstable. Nearly one total system reset per day was required to keep the echosounder properly in operation. This caused data gaps, sometimes more than one hour per day. Parasound seismograms of the “secondary low frequency” were digitized, preprocessed, printed and stored on harddisk in a SEGY-type “.ps3” format using the “Parastore” - program. Unfortunately, the program stores only the envelope, not the full wave form. This makes the file handling easier, but a lot of information is lost and the postprocessing possibilities of these data are limited. Therefore, rawdata were stored as “xxx.asd” files. To get the full wave form data in a segy format out of the “xxx.asd” files new software tools has to be written. But up to now the data format of the “xxx.asd” is not available. The online prints were used for the selection of the coring stations. Acoustic profile images (from ps3 – files) of sampling stations were created using IOW – software (see enclosure). An overview about the morphology and the sediment cover of the Nordre Stroemfjord is depicted in Fig. 2.1.2, as a composite of Parasound records.

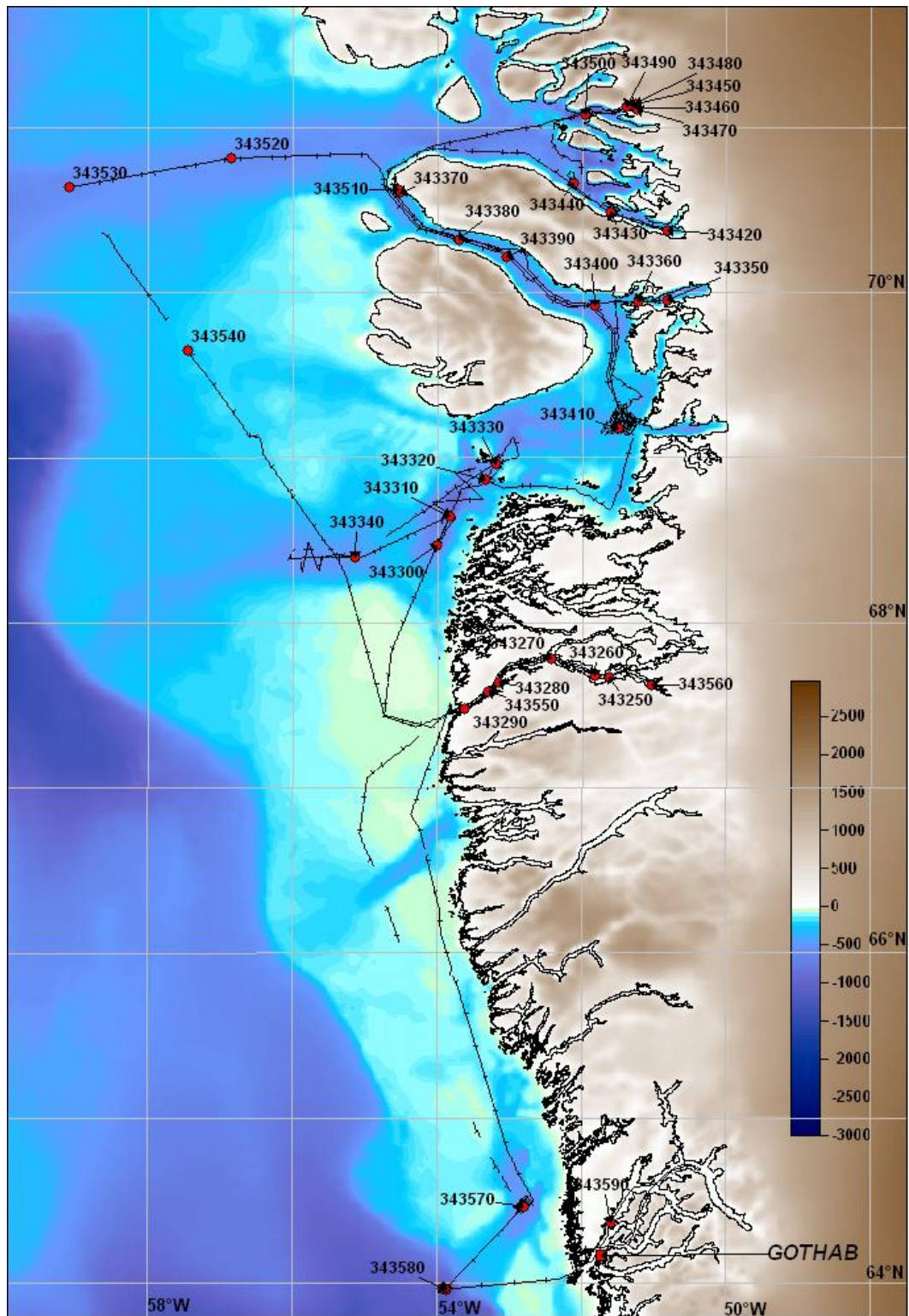


Fig 2.1.1: Trackplot of “Parasound” profiles (black lines) and sampling stations (red dots) obtained during MSM05/03.

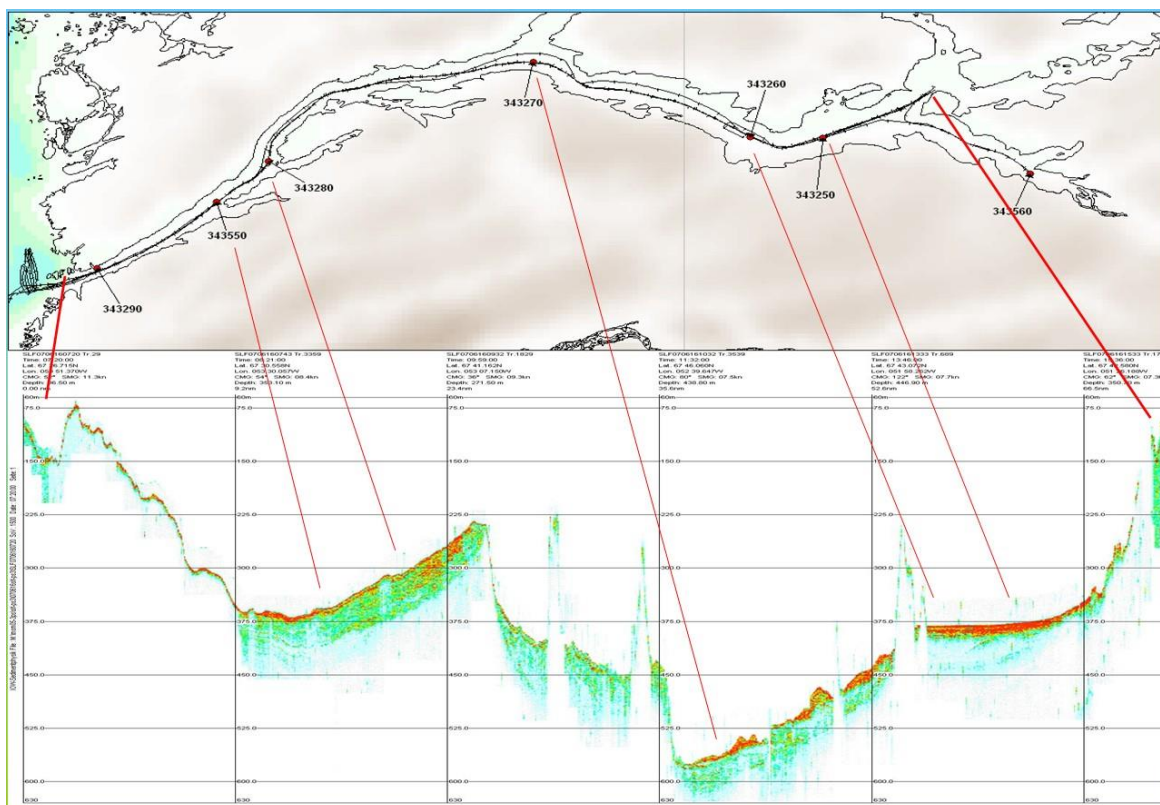


Fig.2.1.2.: Stacked “Parasound” profile (lower part) of the “Nordre Stroemfjord” with trackplot (upper part) and locations of the sampling stations.

## 2.2 Multibeam echo-sounding (W. Weinrebe)

### 2.2.1 Kongsberg (Simrad) EM-120 deep-water multibeam echosounder

The EM 120 system is a deep-water multibeam echosounder providing accurate bathymetric mapping up to full ocean depth. A system overview is presented in Fig. 2.2.1. Basic components of the system are two linear transducer arrays in a Mills cross configuration with separate units for transmit and receive. The nominal sonar frequency is 12 kHz with an angular coverage sector of up to  $150^\circ$  and 191 beams per ping. The emission beam is  $150^\circ$  wide across track, and  $2^\circ$  along track direction. The reception is obtained from 191 beams, with widths of  $2^\circ$  across track and  $20^\circ$  along track. Thus the actual footprint of a single beam has a dimension of  $2^\circ$  by  $2^\circ$ . Achievable swath width on a flat bottom will normally be up to six times the water depth dependent on the character of the seafloor. The angular coverage sector and beam pointing angles may be set to vary automatically with depth according to achievable coverage. This maximizes the number of usable beams. The beam spacing is normally equidistant with equiangle available.

For depth measurements, 191 isolated depth values are obtained perpendicular to the track for each ping. Using the 2-way-travel-time and the beam angle known for each beam, and taking into account the ray bending due to refraction in the water column by sound speed variations, depth is calculated for each beam. A combination of amplitude (for the central beams) and phase (slant beams) is used to provide a measurement accuracy practically independent of the beam pointing angle.

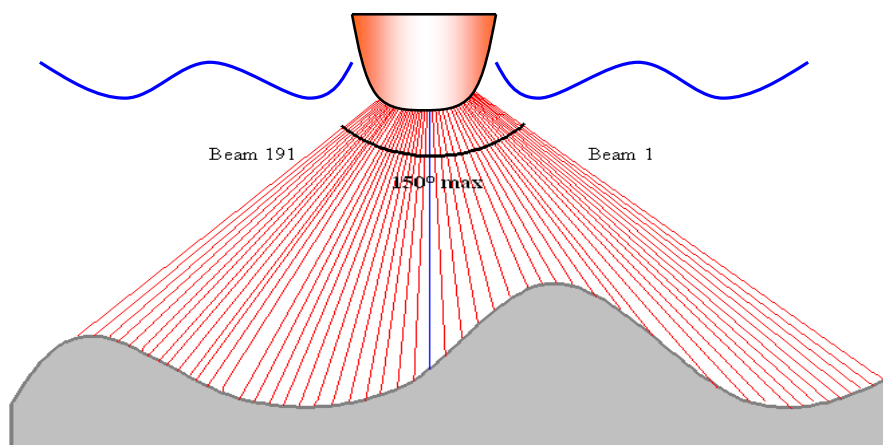


Fig. 2.2.1: Overview of the Kongsberg EM120 beam pattern.

### 2.2.2 Kongsberg (Simrad) EM-1002 shallow-water multibeam echosounder

The EM1002 multibeam echosounder is a shallow-water system for surveying the seafloor down to a depth of 1,000 m. The nominal sonar frequency is 95 kHz with an angular coverage sector of up to  $150^\circ$  and 111 beams per ping. The actual footprint of a single beam has a dimension of  $2.3^\circ$  by  $2^\circ$ . Achievable swath width on a flat bottom will normally be up to 1,500 m or more than seven times the water depth dependent on depth and the character of the seafloor. The angular coverage sector and beam pointing angles may be adjusted in order to get better quality data or wider coverage. The beam spacing is normally equidistant with equiangle available.

The transducer of the EM1002 is cylindrically shaped. It is not permanently installed under the hull of RV Maria S. Merian. Instead, when the EM1002 is used the transducer has to be mounted in the moonpool of the vessel. As the transducer sticks out about 1 m below the keel, the system can not be operated when sea ice or floating ice is present. The survey speed is limited to a maximum of 7 knots.

Onboard R/V Maria S. Merian only one operator station is used to control both multibeam echosounder. Thus only one of the systems can be used at any time, which is not optimal particularly while surveying in areas with water depths varying from very shallow to deep.

### 2.2.3 EM-120 Multibeam data processing

The raw data from the multibeam echosounder were continuously processed onboard R7V Maria S. Merian during the cruise. Generally, processing of multibeam data requires two sequences of processing steps: a profile-oriented sequence followed by an area-based processing. The profile-oriented processing of multibeam data comprises the check of navigation data, interpolating missing navigation values, the calculation of the water depth and position a of the footprints of the beams by raytracing through the water-column taking into

account the sound velocity profile, and removing artefacts and erroneous data points. Area-based processing comprises the calculation of a digital terrain model (DTM) and the visualisation of the data in various different presentations. For these purposes a software package from Kongsberg is available onboard RV Maria S. Merian. During cruise MSM05/3, the “open software” packages MB-System (CARESS and CHAYES, 1996) and GMT (WESSEL and SMITH, 1995) were used beside the Kongsberg applications for the processing of the multibeam data. Processed data sets from the surveys during the cruise are presented in chapter 3.1 and within the enclosure (p. 83).

### 2.3 Hydrography (J. Waniek, E. Trost)

CTD measurements were carried out using a Seabird sbeg11 system combined with a 24 10L HYDROBIOS-FREEFLOW bottle rosette at 32 stations (Fig. 2.3.1). Continuous profiles of temperature, conductivity for determination of salinity, pressure and dissolved oxygen. The system was operated with an altimeter for the determination of the distance between the CTD and sea floor. At all stations discrete samples for the determination of chlorophyll a concentration, suspended particulate matter (SPM) content and the nutrient concentration were taken at selected depth (Fig. 2.3.2 and 2.3.3). Samples for nutrients, chlorophyll a were stored on board in a -20°C room and transported frozen to the home laboratory after the cruise for chemical analysis.

Nutrient concentrations (nitrate, nitrite, silicate and phosphate) were measured using an auto-analyser device in the laboratory at the IOW in August 2007 according to the methods described by HANSEN and KOROLEFF 1999. The detection limit was 0.05  $\mu\text{mol l}^{-1}$  for nitrate, 0.02  $\mu\text{mol l}^{-1}$  for nitrite, 0.02  $\mu\text{mol l}^{-1}$  for phosphate and 0.1  $\mu\text{mol l}^{-1}$  for silicate respectively. The GFF filters for the determination of chlorophyll a were measured fluorometrically according to the JGOFS protocols following the method described by Herbland et al. 1985. For the determination of the SPM content 2L of seawater were filtered through 45 mm filter, which were dried and weighted in the home laboratory prior to the cruise. Each filter was stored in a Petri-dish and a plastic back in order to keep them dry.

After filtration the filter were frozen at -20°C until analysis at IOW. Here the filters were dried in the drying chamber at 60°C over a period of 12h and weighted. The SPM concentration was calculated using the difference of the weight of the filter (prior and after filtration) and the filtrated volume of water, and was expressed in  $\text{mg l}^{-1}$  (Fig. 2.3.3). For continuative results see KRAWCZYK et al. (2012, 2014).

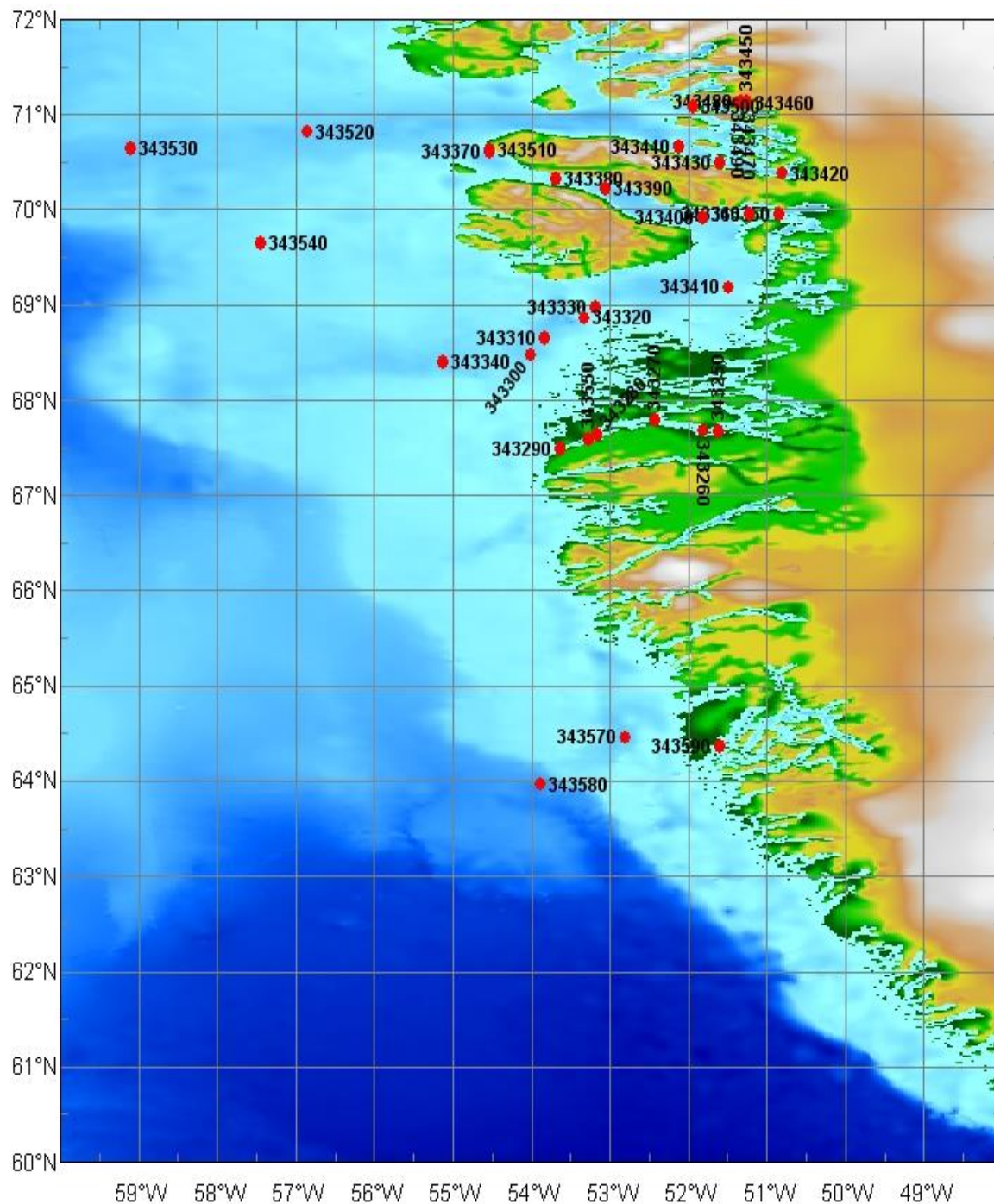


Fig. 2.3.1: Locations of CTD profiling performed at sediment coring sites (red dots). Samples for chlorophyll a, SPM and nutrient measurements were taken at discrete depth from all stations.

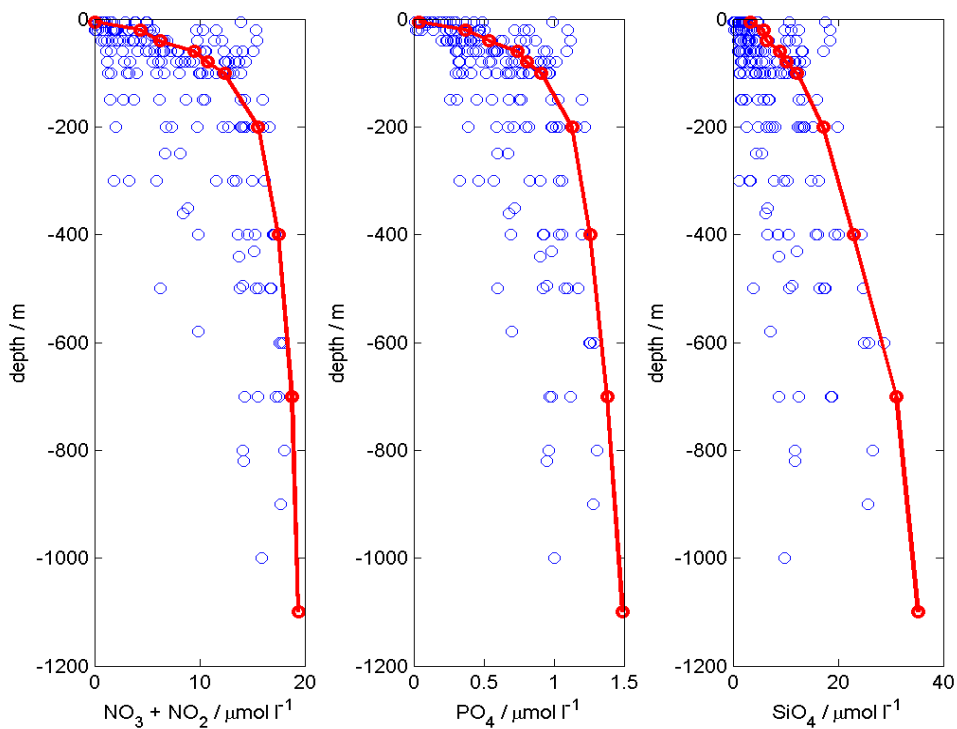


Fig. 2.3.2: Discrete samples from CTD profiling, measured during MSM05/3 for nutrients (nitrate+nitrite, phosphate and silicate).

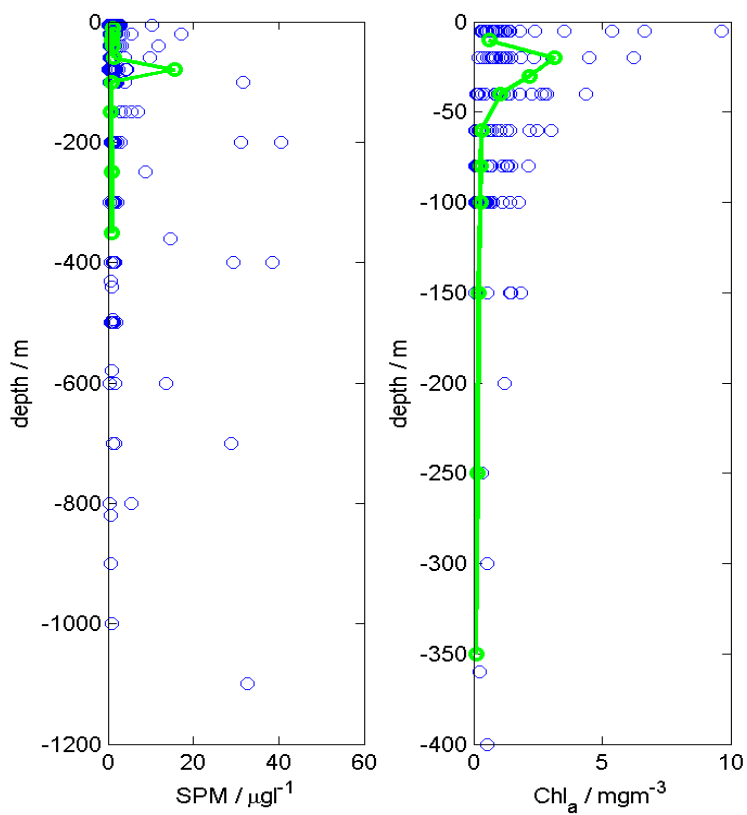


Fig. 2.3.3: Discrete samples measured during MSM05/3 for chlorophyll a and suspended particulate matter (SPM).

### 2.3.1 Continuous underway measurements

Over the duration of the cruise, continuous measurements of surface temperature and conductivity (for determination of salinity) by means of a thermosalinograph were carried out. The system from Sea & Sun technology GmbH in Trappenkamp (Germany) is installed permanently on board. The company gives its accuracy with  $\leq 5 \mu\text{S cm}^{-1}$  for conductivity and  $\pm 0.002^\circ\text{C}$  for temperature (Fig. 2.3.1.1).

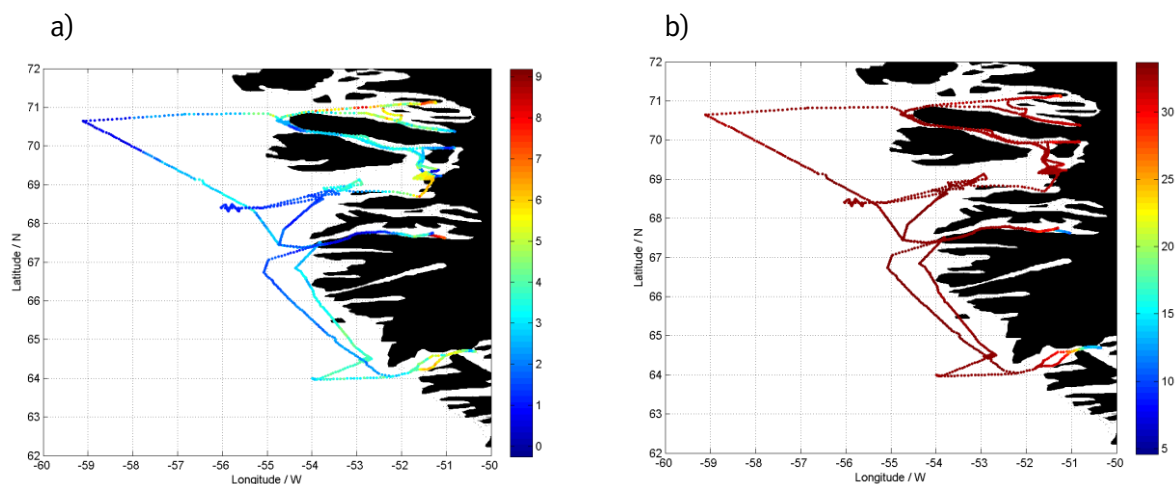


Fig.2.3.1.1: Surface temperature (a) and salinity (b) along the cruise track of MSM05/03 as measured using the ship own thermosalinograph.

For chlorophyll a determination in the surface near water a flow-through fluorometer was continuously operated over the entire cruise. The microFlu-Chl from TriOS Optical Sensors GmbH in Oldenburg (Germany) has an accuracy of  $0.1 \mu\text{g l}^{-1}$  and can be operated optionally in the range  $0-10 \mu\text{g l}^{-1}$  or  $1-100 \mu\text{g l}^{-1}$ .

The RV Maria S. Merian operates an automatic weather station on behalf on the DWD (Deutsches Wetterdienst). The meteorological station contains sensors for monitoring of the wind speed, wind direction, air temperature, humidity, water temperature (2 m below surface) and air pressure. Details of the installed sensors are listed in the ship handbook. An Acoustic Doppler Current Meter (ADCP) Ocean Surveyor Narrowband operated at 75 kHz in low resolution mode (long range profile) was used to monitor the currents in the water column over the entire cruise. The ADCP was set up to record the currents in 45 layers each 16 m wide with a blanking distance set to 8 m.

### 2.3.2 Hydrochemistry

An in-situ pump was deployed at selected positions to collect large volume samples for the determination of PCBs, PAHs and DDTs. Additionally large volume samples were obtained along selected transects (Fig. 2.3.2.1, Tab. 2.3.2.1) hereby a phase separation between the dissolved and particulate phase was carried out. The determination of the organic compounds will be performed with a gas chromatograph and mass spectrometer (GS-MS) according to ICES standard procedures (ICES 1996, 1997 & 1998, Annex B-11) in the laboratory at IOW.

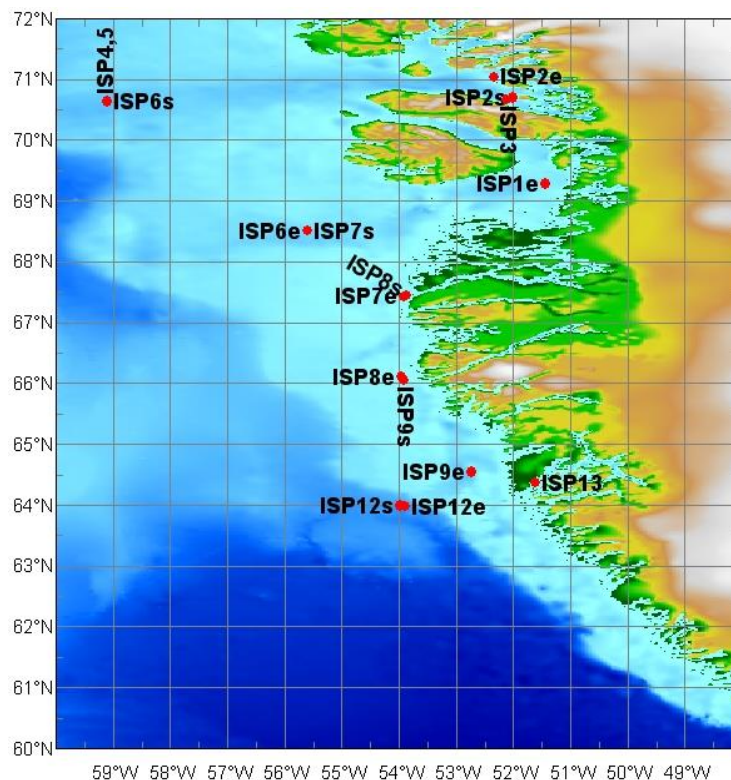


Fig. 2.3.2.1: In-situ pump stations and ISP surface transects carried out during the cruise MSM05/03. Letters (s & e) indicate the start and the end of transects, where ISP was deployed pumping water from the surface (5 m) to collect large volume samples.

Table 3.3.2.1: List of in-situ pump stations carried out during the MSM05/03 cruise.

Sample	Description	Date	Time (UTC)	Latitude (N)	Longitude (W)	Duration
ISP1	transect I	21.06.2007	14:00	68°18.87	51°22.48	3h
			17:00	69°16.61	51°26.40	
ISP2	transect 2	27.06.2007	00:45	70°41.87	52°01.05	4h
			04:15	71°02.42	52°19.92	
ISP3	surface (20m)	26.06.2007	17:45	70°39.75	52°06.86	4h
			21:34			
ISP4,5	at 5 m & 400 m	29.06.2007	00:15	70°38.79	59°6.83	6h
			06:15			
ISP6	transect IIIa,b	29.06.2007	08:35	70°38.4	59°06.00	12h
			20:35	68°30.52	55°35.55	
ISP7	transect IIIc	29.06.2007	22:00	68°30.52	55°35.55	
		30.06.2007	05:10	67°25.57	53°54.42	7h
ISP8	transect IVa	01.07.2007	13:35	67°26.72	53°51.96	7h
			20:50	66°06.60	53°56.83	
ISP9	transect IVb	01.07.2007	21:05	66°03.37	53°54.52	8h
		02.07.2007	05:00	64°32.71	52°43.37	
ISP10,11	20 m & 500 m	02.07.2007	19:20	53°57.94	53°55.4	4h
			23:20			
ISP12	transect V	03.07.2007	01:55	63°59.45	53°58.21	
			06:00	63°58.72	53°52.83	
ISP13	surface (20 m)	03.07.2007	08:20	64°21.96	51°36.34	4h
			12:20			

## 2.4 Sediment Sampling (M. Moros)

For sedimentological sampling a Multi-Corer, a Giant Box-Corer (50x50x60 cm) and a Gravity-Corer (6, 12, 18 m) were used during the cruise. The Multi-Corer of the Leibniz-Institute for Baltic Sea Research and the Giant Box-Corer shown in Fig. 2.4.1 A and B were used to obtain up to 54 cm long cores of undisturbed surface sediments in order to obtain a well-preserved fluffy surface layer and including the bottom water. To gain long sediment cores a Gravity-Corer up to 18 m in length was used in the soft sediments.

The Gravity-corer (Fig 2.4.2) consists of a steel tube with 6 m, 12 m or 18 m length and top section with discs of lead-weights, each 60 kg. The RV “Maria S. Merian” offers a rack for the handling of Gravity-Corers with steel tubes of up to 24 m length. The 6 m steel tube (in a few cases 12 m) was used with foil to gain cores, which were opened on board for description. Gravity-Corer steel tubes loaded with plastic liners (diameter 125 mm) were used to obtain cores which were cut into sections of 1 m and split on board. Splitted sections were run in the Avaatech XRF scanner and surface magnetic susceptibility was measured using TAMISCAN provided by the GBSC Lund. A few closed cores will be studied in the labs of the participating institutes.

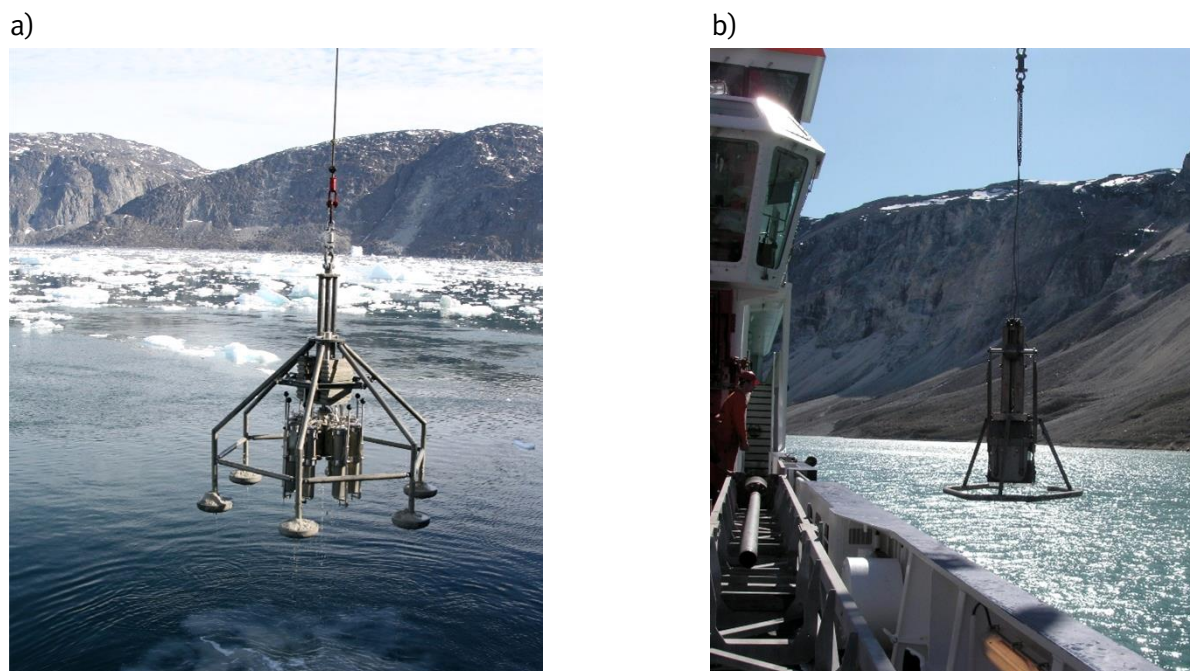


Fig 2.4.1: Multi-Corer (a) equipped with six tubes and the Giant Box-Corer (b) from Leibniz-Institute for Baltic Sea Research during station works of the MSM05/03 cruise.



Fig 2.4.2: During station works within Disko Bay the Gravity-Corer was equipped with a 18 m long steel tube.

## 2.5 Lithological core description (K. Perner)

Back on board the gravity corer have been brought to a horizontal position and afterwards the liner, filled with sediments, was pulled out of the device and cut into 1m sections. The sections have been split into two halves by a core-cut-device. The working part was prepared for following lithological description and further measurements on board, by cleaning with a knife or an old credit card to receive a clean and undisturbed sediment surface (Fig. 2.5.1 A and B)



Fig. 2.5.1: (A) Plastic liner from the Gravity-Core splitted using a core cut device. (B) Splitted gravity core with cleaned sediment surface.

Furthermore, photographic documentation of each core section was conducted for all cores. The lithological description based on grain size composition, structure, consolidation and also fossil content of the sediment. If possible, molluscs were determined to species level and collected. The sediment colour was determined by using the Munsill Soil Color Chart. In this connection is to note that variations in determining colour probably created by the artificial light at the hangar.

## 2.6 Diatomological investigation (A. Witkowski)

Samples collected during Maria S. Merian Cruise

### 1. Inland samples collected from 4 GPS stations

Moss – 19 samples

Sands/sediments – 19 samples

Moss squeeze – 11 samples

Scarpe/pool rocks – 12 samples

Macroalgae – 4 samples

### 2. Samples collected onboard for the diatom species composition of phytoplankton and of the uppermost sediment layer

Gravity Corer – 1 sample

MUC – 19 samples of the uppermost sediments layer

Boxcorer – 2 samples (0-1 cm interval)

### 3. On October 23-24th in Warnemünde selected MUC and gravity cores for diatom species composition and palaeotemperature evaluation were sampled. The samples were taken at high resolution intervals e.g. 0-10 cm at 0.5 cm and 10-downward at 1 cm interval. The most important of which is MUC and gravity corer site 343320. From this site MUC corer samples (35) have already been processed for LM study and await analysis.

So far 77 samples were prepared for microscopic analysis. Some samples were already studied by means of Scanning Electron Microscope (SEM) and Light Microscope (LM). In addition 24 phytoplankton samples collected within the Nuuk Fjord were qualitatively and quantitatively analyzed.

In samples collected during the cruise special focus was paid to:

1. The patchiness of diatom distribution in the surface sediments of the Western Greenland Waters and of Disko Bay in particular
2. The species composition. This issue is of special importance as the dominant diatom species are indicative of particular water masses (temperate versus cold waters) and therefore important in evaluation of palaeotemperatures.

In addition freshwater acidic habitats were sampled for terrestrial diatoms and representatives of genus *Eunotia* in particular. The diatom species belonging in this genus inhabit pristine waters though very little studied in Greenland so far. The material collected during the cruise gives an

excellent opportunity to broaden our knowledge on diatom flora of habitats which are very sensitive to human impact and endangered in many places world wide.

To achieve the expected results of the above scheduled issues during the cruise superficial sediment samples from multicorer (MUC) were collected. From a single MUC up to 6 samples were collected. Selected were samples collected from sites: 343300 (3 samples), 343310 (4), 343420 (5), 343330 (6), and 343340 (2). From each of the corers permanent slides for LM were prepared and two of them were subject to SEM analysis. The samples were processed as follow. ca. 1 g of the dry sediment was treated by means of 10 % HCl to remove carbonates. Then samples were washed several times with distilled water. Next samples were boiled in hydrogen peroxide (37%) to remove organic matter and again washed with distilled water. Naphrax® was used as the mounting medium. Diatoms were examined by means of light and electron microscopy. Light microscope observations were made with a Leica DMLB with a Plan-apochromatic 100x (1.4 n.a.) oil immersion objective. For SEM, cleaned material was air-dried onto cover slips. The cleaned suspension was mounted onto stubs and after drying sputter-coated with gold. Observations were made on a Hitachi S-4500 at the Faculty Biology, Institute of Ecology, Phylogeny, Diversity, J.-W. Goethe-University, Frankfurt am Main with an assistance of Manfred Ruppel. All the LM slides are deposited in Diatom Collection of Andrzej Witkowski (AW) at the Institute of Marine Sciences, University of Szczecin and their numbers are 12111-12135; 12194-12212; 12213-12248.

1. Analysis of the slides prepared from different MUC sites from superficial sediments indicated that diatom abundance differed between particular cores. Distinct differences in diatom abundance were observed. At one MUC site in some cores diatoms were abundant in others rare. However, the dominant forms were always the same.
2. Usually the most abundant were undetermined resting spores of *Chaetoceros* spp. resting spores of *Ch. furcellatus* and numerous *Thalassiosira* species two of which i.e. *T. kushirensis* and *T. antarctica* var. *borealis* are the most abundant. Less abundant were representatives of cold water *Fragilariopsis* taxa and other cosmopolitan species e.g. *Thalassionema nitzschioides*. The resting stages of *Ch. furcellatus* are indicative of cold Arctic water inflow. The major problem of palaeotemperature significance is distribution of two above mentioned *Thalassiosira* species. *T. antarctica* var. *borealis* is thought to represent plankton diatom association of Arctic cold waters. In earlier diatomological investigations carried out in the Disko Bay area (even involving SEM application) only this taxon was recognized in the Holocene sediments (e.g. MOROS et al. 2006). Therefore the palaeotemperature interpretation based on such identification was strongly biased towards cold impact. Routine application of SEM analysis in this study and the careful interpretation of its results has revealed that in fact in the surface sediments (but also down core) two taxa of *Thalassiosira* are present. One of them, which in superficial sediments is less abundant is *T. antarctica* var. *borealis*. The most abundant, however, as clearly shown in our SEM study is *T. kushirensis*. This species has an optimum of occurrence in temperate zone ocean waters (e.g. HASLE & SYVERSTSEN 1996). Therefore its abundant occurrence in Disko Bay area must be indicative for an inflow of West Greenland Current waters. An implication of this discovery must be reevaluation of

palaeotemperatures distribution and of palaeoclimatic conditions during the Holocene in the Western Greenland and in the North Atlantic area.

The diatom assemblage studies have been continuously pursued in co-operation between the University of Szczecin, the Leibniz Institute for Baltic Sea Research Warnemünde and the Greenland Institute of Natural Resources, Nuuk. Main results are published by KRAWCZYK et al. (2012), KRAWCZYK et al. (2013), KRAWCZYK et al. (2014).

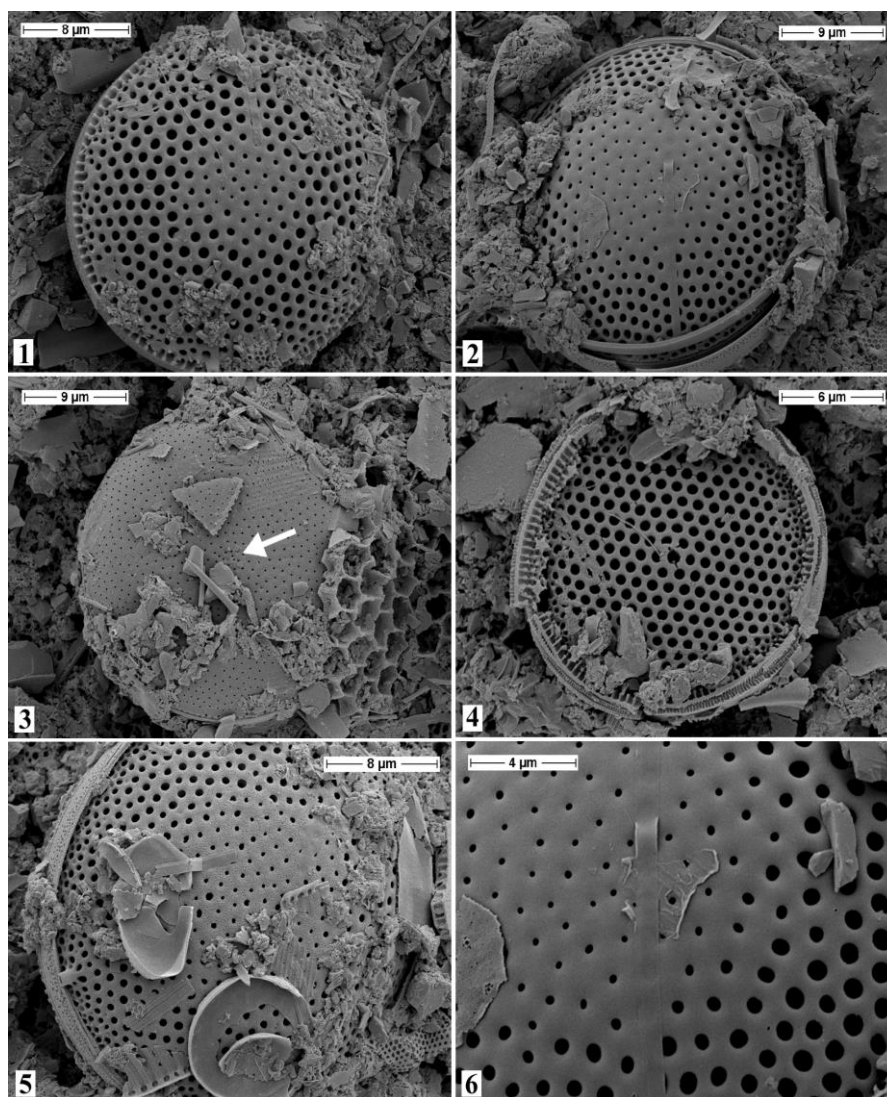


Plate I

(1, 2, 5, 6) *Thalassiosira kushirensis* (resting spores); (3) *Thalassiosira antarctica* var. *borealis* (resting spore), note the presence of central strutted process (arrow) which are missing in *T. kushirensis*; (4) *Thalassiosira tenera*.

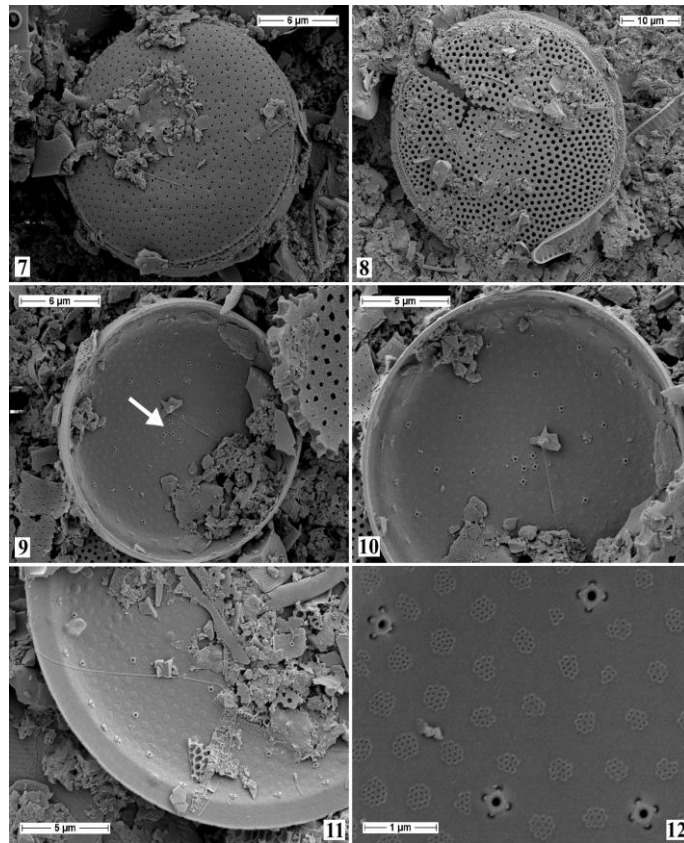


Plate II – (7-12) *Thalassiosira antarctica* var. *borealis*.

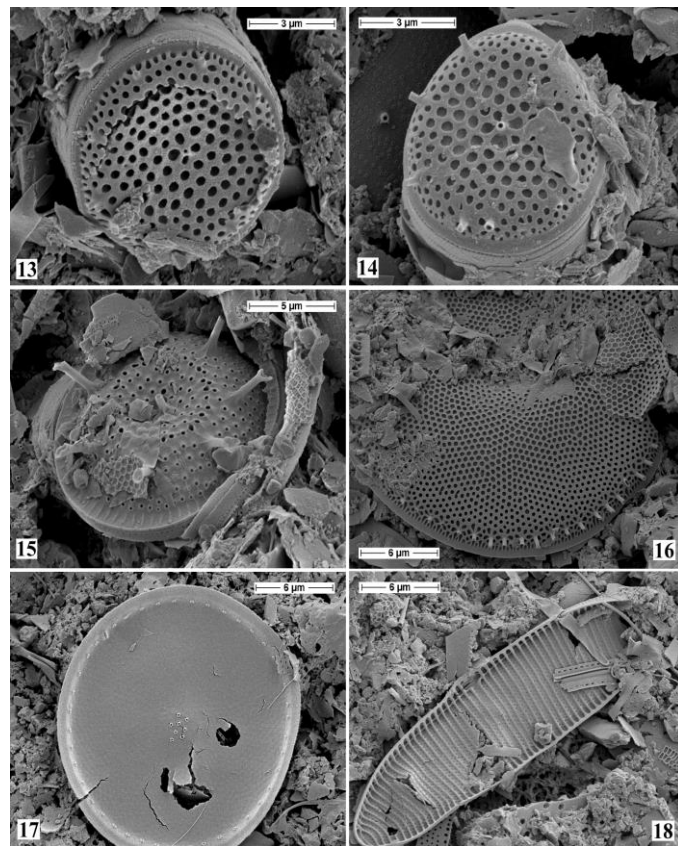


Plate III

(13) *Thalassiosira oestrupii*; (14) *Thalassiosira* spec; (15) *Thalassiosira nordenskiöldii*; (16) *Thalassiosira rotula*; (17) *Thalassiosira rotula*; (18) *Fragilariopsis atlantica*.

## 2.7 Biogeochemistry (S. Rysgaard, N. Risgaard-Petersen)

The upper sediment layers were used to describe present-day carbon and nutrient cycling in Arctic sediments. Rate measurements covered oxygen respiration, denitrification, anammox and carbon mineralization as well as fluxes of dissolved inorganic carbon and nutrients across the sediment-water interface. Furthermore, sampling in the upper sediment layers for identification and activity measurements of benthic foraminifera was made on various stations. In addition, the depth distribution of  $O_2$ ,  $NH_4^+$ ,  $NO_3^-$ , dissolved inorganic carbon,  $CH_4$ , organic carbon and nitrogen as well as  $^{13}C$  and  $^{15}N$  in the sediment will form basis for interpretation and modeling biogeochemical transformations in the sediment (RYSGAARD et al. 1998, BERG et al. 1998, BERG et al. 2003). Our investigations will be combined with a detailed ongoing sampling program in Godthåbsfjord in the Nuuk area including annual measurements of the vertical flux of particulate matter (total flux, carbonate, chlorophyll, particulate organic carbon and nitrogen) to the sediment and will serve as input to model present carbon and nutrient cycling. Combining our data with sedimentation records and proxy data of palaeo-climate conditions from the other research teams during MSM 05/03 we will attempt to model historical carbon and nutrient cycling.

Material for completion of four tasks was collected during the cruise:

- a) Investigation of the decomposition of organic carbon as function of age and composition.
- b) Investigation of nitrate accumulation and nitrate respiration in Arctic for-aminifers.
- c) Investigation of temperature adaptation of aerobe Arctic bacteria.
- d) Investigation of the biogeography of thermophilic sulphate reducing bacteria.
- e) Investigation of factors controlling  $pCO_2$  in surface waters of the Arctic.

a) A 6 m long gravity core were collected from station # 343340, and sliced into 7 sections, each representing c. 500 years. In addition one multicore was sliced into 3 sections. All sections were transferred to gastight plasticbags and incubated at 4 °C. Sampling from the bags were initiated on board and will continue at the GRNI in order to follow changes in central parameters (mainly dissolved inorganic carbon ( $TCO_2$ ),  $NH_4^+$  and  $CH_4$ ) and rates of decomposition. Sediment samples for DNA extractions were transferred to PCR vials and frozen. On return to laboratory the microbial diversity in the different sections will be analysed using PCR, DGGE cloning and sequencing on the extracted DNA. Sediment samples for enumeration of bacteria were transferred to vials with buffered formaldehyde. Counting will be performed after DAPI- staining in the lab. Samples for analysis of amino-acid composition in the different layers were transferred to plastic vials and frozen. Amino acids (D and L-forms) will be determined after hydrololization using HPLC. Samples for  $TCO_2$  and  $NH_4^+$  determinations were extracted from the sediment porewater and transferred to vials. Dissolved inorganic carbon samples were conserved with  $HgCl_2$ .  $NH_4^+$  samples were frozen.  $TCO_2$  and  $NH_4^+$  will be analysed in the laboratory using flow-injection. Sediment samples for  $CH_4$  determinations were transferred to gastight vials together with distilled water and  $ZnCl_2$ . Methane will be determined on a gas chromatograph. Samples for determination of organic carbon/nitrogen content and isotopic composition were frozen for later analysis in the laboratory using an elemental analyzer coupled to an IR-MS. In addition samples for the porewater concentration of  $NH_4^+$ ,  $NO_3^-$ , intracellular  $NO_3^-$  and  $TCO_2$  were collected from the

top 10 cm of the sediment with a resolution of 1 cm. The microdistribution of  $O_2$  were measured with an  $O_2$  microsensor with a depth resolution of 0.5 mm. Exchange of  $O_2$ ,  $TCO_2$ ,  $NO_3^-$  and  $NH_4^+$  between the sediment and the water were measured on board on cores collected with the multicorer. Bacterial N-transformations (denitrification and anammox) were measured on the same cores using  $^{15}N$ -techniques.

b) We have recently discovered that some foraminifers, with preference for anoxic environments accumulate nitrate intracellular, which is subsequently respired to dinitrogen gas (RISGAARD-PETERSEN et al. 2006). During the cruise we have collected foraminifers from the Norde Stroem Fjord and the Disko Bay and transferred individuals to PCR-tubes. The foraminifers will be analysed for presence of intracellular  $NO_3^-$  as described in RISGAARD-PETERSEN et al. (2006) on return to the GINR. On board the ability to respire with  $NO_3^-$  was tested using acetylene inhibition and  $N_2O$  microsensors (RISGAARD-PETERSEN et al. 2006).

c) Bacterial oxygen consumption in intact sediments has been measured using  $O_2$  microsensors on several stations. In addition material for determination of organic carbon in these sediments has been collected. The relationship between organic carbon and bacterial respiration will be compared with relationship derived from data from temperate marine environments. Depending on the outcome further studies focusing specifically on temperature regulation of bacterial activity will be performed in the laboratory.

d). It has been shown that arctic sediments from Svalbard contains bacteria that only are active at temperatures above  $4^{\circ}C$ . (KNOBLAUCH and JØRGENSEN 1999). In order to obtain more information about the distribution of these bacteria and their origin, samples from several stations, has been collected and transferred to gastight plastic bag. Presence of the bacteria will be determined on Max Planck Bremen using molecular techniques.

*e) It has recently been suggested (RISGAARD et al. 2007) that sea ice may act as carbon pump in polar seas. During sea ice formation in polar seas, brine rejection increases the density in the underlying water column and thereby contributes to the formation of deep and intermediate water masses in the world ocean. Evidence has been presented that  $TCO_2$  is rejected together with brine from growing sea ice and that low temperatures may result in a significant change in the ratio of  $TCO_2$  and alkalinity in Arctic sea ice compared with surface waters. At MSM05/03 we collected surface water samples in the ice melt zone to be able to verify previous model calculation showing that this sea ice-driven carbon pump affects surface water partial pressure of  $CO_2$  significantly in polar seas and potentially sequesters large amounts of  $CO_2$  to the deep ocean. In short, surface samples from the water column were collected at each CTD station for the determination of dissolved inorganic carbon ( $TCO_2$ ), total alkalinity (TA),  $^{18}O$ , nutrients and chlorophyll contents. Care was taken when filling the gas tight glass bottles (250 ml) for  $TCO_2$ , TA and  $^{18}O$  determination to avoid bubble trapping and to ensure sufficient overflow. Samples were preserved with 50  $\mu$ l  $HgCl_2$  (saturated solution) and kept cold ( $2^{\circ}C$ ) until analysis. Water samples for nutrients and Chlorophyll determination were frozen ( $-18^{\circ}C$ ) until analysis. Standard methods of analysis will be performed on these samples on the return to the laboratory in Nuuk.*

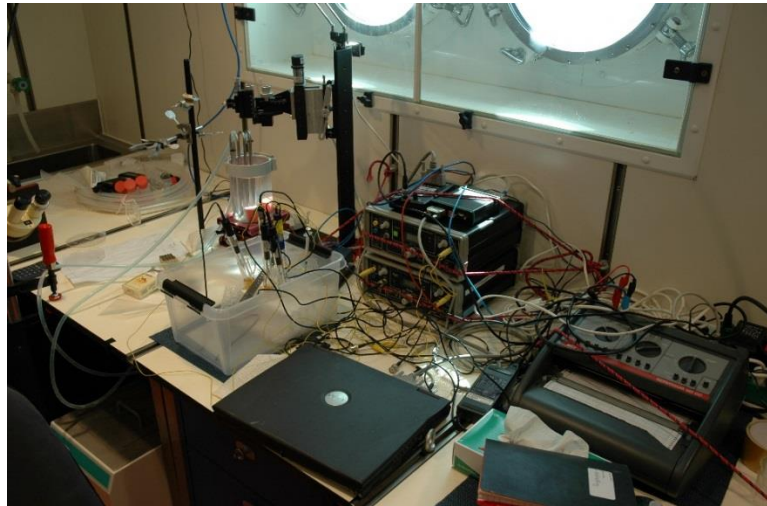
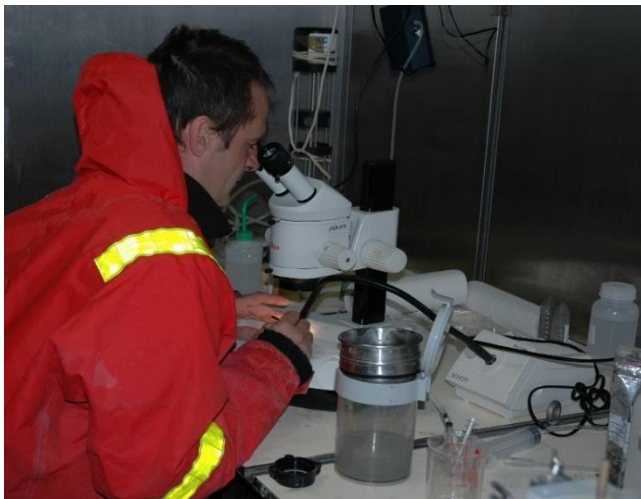


Fig. 2.7.1 Sensors: Set up used for measuring oxygen concentration in surface sediments

a)



b)



Fig. 2.7.2: a) Microscopy: Looking for live foraminifers in mud at in situ temperature. b) Flux: Set up used for measuring bacterial N-transformations and exchange of nutrient between the surface sediment and the overlying water.



Fig. 2.7.3: Porewater presser: Equipment used for extracting porewater from sediments.

## 2.8 Surface scanning magnetic susceptibility (P. Sandgren, I. Snowball)

Magnetic susceptibility is a measure of the ease by which material can be magnetized (THOMPSON and OLDFIELD 1986). It can provide an independent stratigraphic record of sediment sequences and quantitative information about the concentration of magnetic minerals. Sliced sediment samples of 0.5-1 cm intervals from individual Multi-Cores, which contained the surface sediments, were placed in Petri dishes and covered with thin plastic film. The magnetic susceptibility was measured with a Bartington Instruments MS2E1 high-resolution surface scanning sensor connected to a MS2 meter. Split gravity core sections were covered with plastic film and measured with the MS2E1 sensor coupled to a TAMISCAN-TS1 automatic logging conveyor (SANDGREN and SNOWBALL 2002). Units are expressed in the SI system.

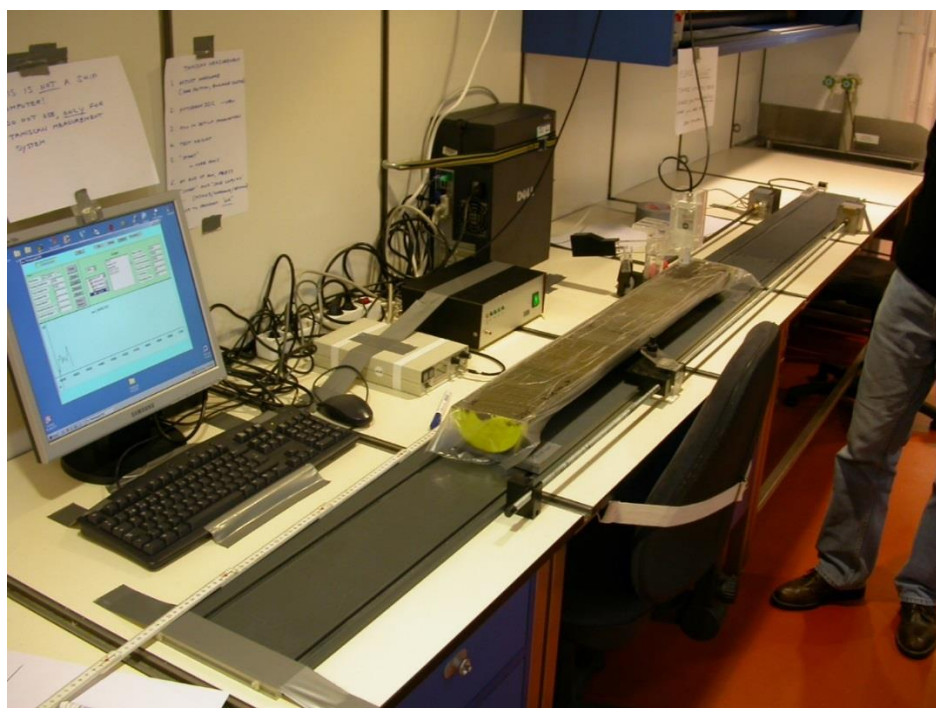


Fig. 2.8.1: The TAMISCAN-TS1 magnetic susceptibility automatic logging system onboard RV Maria S. Merian.

## 2.9 X-ray fluorescence (XRF) logging (T. Richter)

X-ray fluorescence (XRF) logging is a non-destructive method tracking downcore changes in chemical composition. Compared to XRF analyses with conventional laboratory instruments, results are somewhat less accurate and may display a lower signal-to-noise ratio: Conventional X-ray fluorescence is carried out on homogenous and dry samples with a flat and smooth surface. Split sediment cores do not meet these requirements; accordingly, results are also affected by changes in other sediment properties (grain size, water content, porosity) and by irregularities of the core surface. On the other hand, XRF logging provides non-destructive and rapid results

(~1 minute per multi-element analysis) with minimal sample preparation. Effects of sample inhomogeneity and surface roughness are particularly pronounced for sediments containing abundant medium-coarse sand-sized particles, but less significant in most fine-grained sediments. Applications of XRF logging include, among others, preliminary stratigraphic interpretation, provenance studies of terrigenous material, lithological characterization and assessment of (anthropogenic) heavy metal input. Results can provide constraints on sampling strategies for various subsequent (shore-based) analyses on discrete samples, commonly at lower resolution and/or over selected core intervals.

For the duration of the cruise, the containerized Avaatech XRF Core Scanner (RICHTER et al., 2006) of the Royal Netherlands Institute for Sea Research (NIOZ) was temporarily installed onboard RV Maria S. Merian. XRF analyses were performed on the surface of split sediment cores, generally within hours to days after core retrieval. Sample preparation includes careful flattening of the sediment surface to remove irregularities from core slicing. Subsequently, the sediment surface is covered with thin ( $4\mu\text{m}$ ) Ultralene film, further diminishing surface roughness and preventing contamination of the measurement unit during core logging. During XRF scanning, a prism unit is lowered onto the core surface at each measurement position. Incoming radiation generated in the X-ray tube enters at an angle of  $45^\circ$ ; the detector for outgoing radiation is likewise installed at an angle of  $45^\circ$  (see Figure 2.9.1). The entire measurement system is flushed with helium to prevent partial or complete absorption of emitted radiation by air.

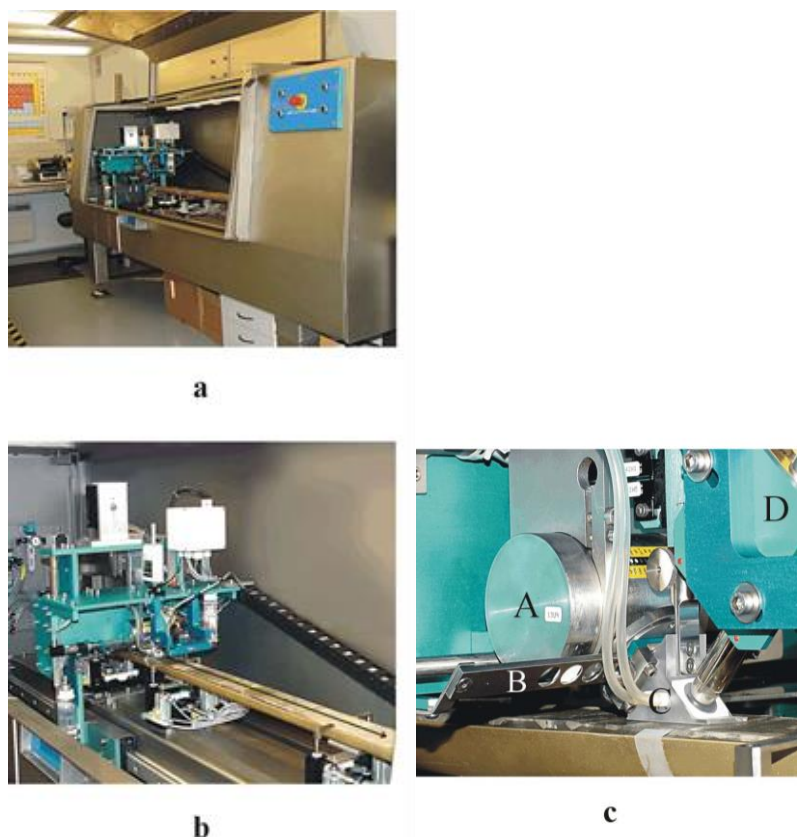


Figure 2.9.1: Views of the Avaatech XRF Core Scanner. a) General overview of the instrument. b) Measurements on a split sediment core. Arrow on core surface depicts (stepwise) movement of measurement system along the core surface. c) Detailed view of X-ray tube (A), filters that can be placed in the incoming X-ray beam (B), prism lowered onto the sediment surface covered with Ultralene film (C), and XRF detector (D).

A step size of 1cm was applied; analyzed elements comprise Al, Si, S, Cl, K, Ca, Ti, Mn and Fe. The response depth of elements to incoming radiation depends on their atomic weight; varying from 0.05mm (Al) to 1mm (Fe). For selected core sections from Qaumarujuk Fjord, additional measurements (separate analytical runs) were performed for the (anthropogenic) heavy metals Pb and Zn. The processing software provides total XRF counts (peak areas for each element, corrected for spectral background), data are exported into Excel files. Long-term stability of the instrument was verified through daily analyses of reference standards.

## 2.10 Geodetic measurements (R. Dietrich, A. Richter)

The geodetic fieldwork during the MSM05/3 cruise was focussed on the installation and first observation of new GPS markers on bedrock for the determination of recent deformations of the earth crust – with an emphasis on east-west gradients of the vertical deformations – after a repetition of the GPS observations. An additional aim was the determinations of the tidal signal in the Nordre Strømfjord.

The first GPS station was put into operation on June 16, 2007 on the already existing GPS marker NOSF located at the easternmost end of Nordre Strømfjord. New GPS markers were erected on the northern shore of the central part (NOSC) as well as at the mouth (NOSW) of this fjord. Further GPS markers were established near the western tip of Nugssuaq Peninsula (NUGS) and at the north-eastern end of the Qaumarujuk fjord (WGNR). The latter thus represents now the northernmost marker of our West Greenland GPS network (Fig. 2.10.1). The coordinates and occupation times for the GPS markers are summarised in Table 2.10.1.

The markers consist of specially designed threaded bolts screwed into bedrock that have proven effective in West Greenland for many years (Fig. 2.10.2). In this way they are well suited for repeated observations after several years guaranteeing an exact relocation of the antenna onto the screw. The exact locations of the new markers were chosen considering:

- a) a spatial distribution suitable for the determination of recent crustal deformations,
- b) a minimum horizon shadowing for the reception of a maximum of satellite signals,
- c) a solid, reliable rock basement guaranteeing long-term stability,
- d) an effective and flexible access for repeated occupations.

Immediately after their installation, the markers were occupied with GPS receivers for a first observation. At this geodetic dual-frequency receivers Trimble 4000SSi were used. At the already existing sites, exactly the same antennas were used as for the previous occupations in order to minimise systematic effects. At the beginning and the end of the observations, the azimuth orientation of the antennas was documented. The GPS data were logged in most cases with a rate of 15 sec, or 30 sec otherwise (Table 2.10.1). In order to provide the autonomous receivers with power for two weeks, accumulators and solar panels were used (Fig. 2.10.3).

Near the GPS sites NOSF and NOSW, two pressure tide gauges Aanderaa WLR7 were deployed on the bottom of the Nordre Strømfjord at water depths of about 5 m in order to record continuously the water level changes in the fjord. The instruments were mounted in rugged steel

frames ensuring a stable position throughout the observation period. The tide gauges were recovered successfully after 13 days of observations each.

After the deployment of the tide gauges, as well as at 20 additional locations during the entire cruise, kinematic GPS measurements were carried out using a GPS buoy in order to determine exact instantaneous sea-level heights. While the measurements near the tide gauge sites are used to refer the obtained sea-level records to a global height reference system, the other measurements can be used to validate both ocean tide and geoid models.

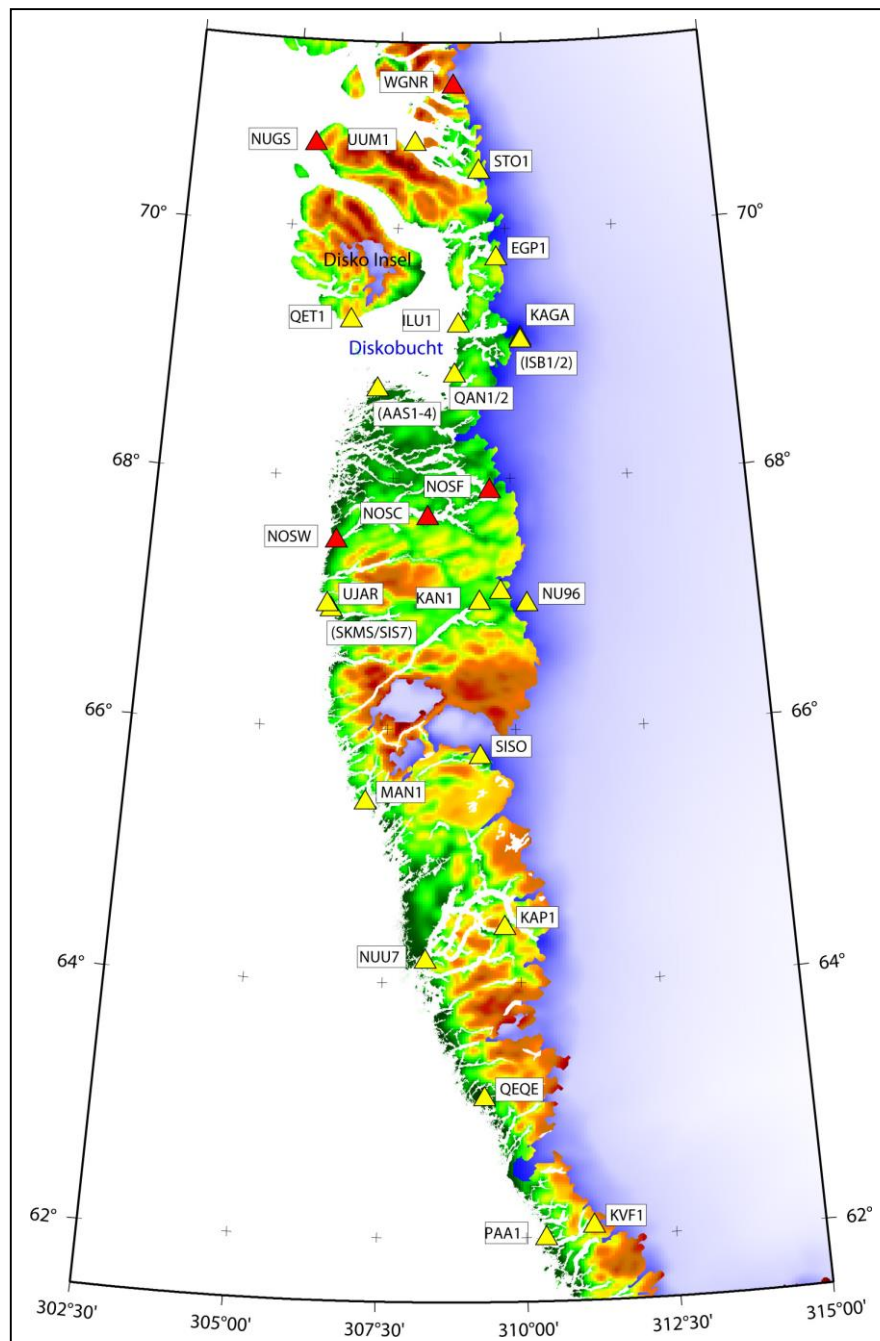


Fig. 2.10.1: Map of the West Greenland GPS network. New markers established during the MSM05/3 cruise are displayed in red color.

Table 2.10.1: Coordinates (in the IGB00 reference system) and occupation times of the geodetic GPS markers observed during the MSM05/03 cruise.

Marker	Latitude [N]	Longitude [W]	Height [m]	Start obs.	End obs.
NOSF	67°53,982	50°26,748	224,94	16.06.07	30.06.07
NOSC	67°41,128	51°44,917	73,72	16.06.07	30.06.07
NOSW	67°29,175	53°38,887	52,23	18.06.07	31.06.07
NUGS	70°39,484	54°32,343	51,10	23.06.07	28.06.07
WGNR	71°08,684	51°12,441	46,30	27.06.07	27.06.07



Fig. 2.10.2: Installation of the new GPS marker WGNR, Qaumarujuk Fjord.



Fig. 2.10.3: Example for the setup of a GPS station at the site NSFC. On top of the rock outcrop, the antenna is mounted. The GPS receiver and the accumulators are stored in an aluminium box, solar panels are used for the power supply.

## 2.11 SPM and aeolian dust (V. Shevshenko)

Water samples were obtained from the water column by Niskin bottles and from the surface by plastic bucket. The filtration of water samples was carried out through pre-weighted Nuclepore filters 47 mm in diameter (pore size 0.45  $\mu\text{m}$ ) and Whatman GF/F filters. After filtration filters were washed with distilled water and dried at 50–55°C, packed in plastic Petry dishes and then sealed in plastic envelopes for later analyses in the land laboratory. In more detail working procedures are described elsewhere (LISITZIN et al., 2003).

Air was filtered through AFA-KhP-20 acetate-cellulose filters with working surface of 20 cm<sup>2</sup>, which trap all particles  $>0.5 \mu\text{m}$ , including particles of sea salt. Blank filters were treated similarly with sample filters, except the air was passed through for only 1 min. The content of chemical elements in filters will be determined by instrumental neutron activation analysis (INAA, SCHEVCHENKO et al., 2005). In more details the aerosol studies are described elsewhere (SHEVCHENKO, 2003).

In 3 places (near NOSF and NOSW GPS stations and on the shore of Nuuk Fjord) mosses and lichens were collected to study aeolian input of heavy metals. Samples were collected in clean plastic bags using plastic gloves. In the land laboratories the elemental composition of mosses and lichens will be determined by INAA and ICP-MS).

One snow sample was collected on the July 1 on the land (on the shore near NOSW GPS station). Snow was collected in precleaned plastic bucket. Sample was melted at +20°C and filtered the same way as water samples.

## 3. First Results

### 3.1 Mapping (W. Weinrebe)

#### 3.1.1 Mapping Illulissat Icefjord

The most remarkable feature in the Disko-Bay area is the Illulissat Icefjord, a UNESCO world heritage site since 2004. The 25 km long and about 1 km wide fjord connects the inland ice with the sea. The fjord is filled completely with large icebergs. The front of icebergs spanning the entire width of the fjord is moving with a speed of about 1 meter per hour towards Disko Bay where the icebergs start floating towards the open sea. This area is denoted as the most productive iceberg generating area of the northern hemisphere.

The area adjacent to the mouth of Illulissat Icefjord has never been mapped before with multibeam echosounder systems, as navigation is difficult for survey vessels due to the abundant number of floating icebergs. As icegoing vessels such as R/V Maria S. Merian are well suited to map such areas, a survey of the area was planned and successfully completed during the cruise MSM05/03.

Water depths in Disko Bay range between about 200 m and 500 m according to the GEBCO global bathymetry data set. This depth range is very well suited for the shallow water multibeam echosounder Kongsberg EM1002 of R/V Maria S. Merian. However, this system cannot be used

in areas with sea ice or iceberg covering, as its transducer has to be mounted in the moonpool and sticks out about 1 meter below the keel of the vessel. Therefore the deep water multibeam echosounder Kongsberg EM120 was used on profiles close to the icefront. The transducers of this system are permanently installed in the hull and protected by an “ice window”. Whenever ice conditions allowed, the transducer of the shallow water system was mounted in the moonpool and the EM1002 was used, which performed considerably better in this depth range. The survey was started on June 21 in the morning close to the icefront. Profiles were planned in south – north direction, however the vessel could not always maintain to follow the straight profile lines as it had to detour around floating icebergs frequently. In total an area of about 250 km<sup>2</sup> was mapped in 32 hours along 397.66 km profile lines applying 72,509 pings (Fig. 3.1.1.1)

Table 3.1.1.1: Details of multibeam surveys off Ilulissat Icefjord.

Date	System	No. of pings	Duration (h)	Length (km)
21.06.2007	EM120	21,345	9,55	108,16
21/22.06.2007	EM1002	22,311	10,08	125,98
24.06.2007	EM120	28,853	12,36	163,52

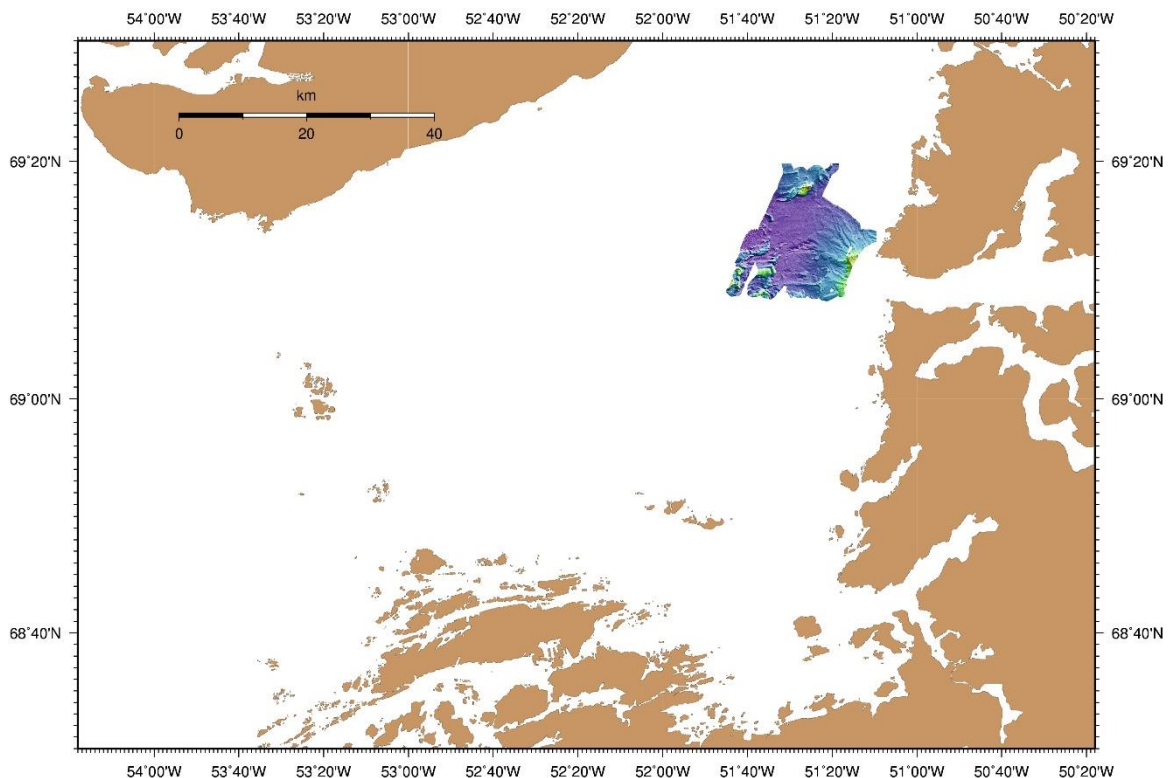


Fig. 3.1.1.1: Southern Disko Bay with surveyed area off the mouth of Ilulissat Icefjord.

### 3.1.2 Morphology of the Ilulissat Icefjord Area

The area off the mouth of Ilulissat Icefjord is dominated by a large basin with a diameter of at least 15 km. The rims of the basin to the South, West, and North have only partly been mapped. Generally the basin shows a smooth surface gently dipping westward from a water depth of about 250 m in the vicinity of the ice front to about 450 m at the western rim of the surveyed area. The western rim of the basin is marked by a series of elongated ridges or highs, partly crescent-shaped. These ridges have lengths of 2 km to 5 km, widths of about 1 km and heights of 50 m and more. The sides facing the ice front are generally very steep whereas the far sides are dipping gently. The ridges probably act as a kind of a backstop for larger, deep-reaching icebergs. This is documented by abundant iceberg plow marks on top of some of the ridges, particularly on the hill at  $69^{\circ}10.8'N$ ,  $51^{\circ}35.8'W$  in a water depth of 260 m which is intensively scoured by drifting icebergs. The plow marks do not show a distinct pattern indicating probable changes of the prevailing drift directions in history. More plow marks are found close to the ice front. Generally the surveyed area is divided into two parts. The southern part is characterized by fluvio-glacial denudation and deposition processes displayed in some elongated depressions and steep holes about 20 m deep and 120 m in diameter (kettle holes?). The northern part shows slightly less water depths and is shaped by the drift of icebergs which have been detached from the ice front of Ilulissat Icefjord. Elongated ridges and grooves stretching in northwest direction clearly document the prevailing drift direction. This is also demonstrated in the satellite image shown in Fig. 3.1.2.6. Large ice blocks and icebergs, which can be identified at the surface of the ice stream close to its mouth, seem to follow this direction.

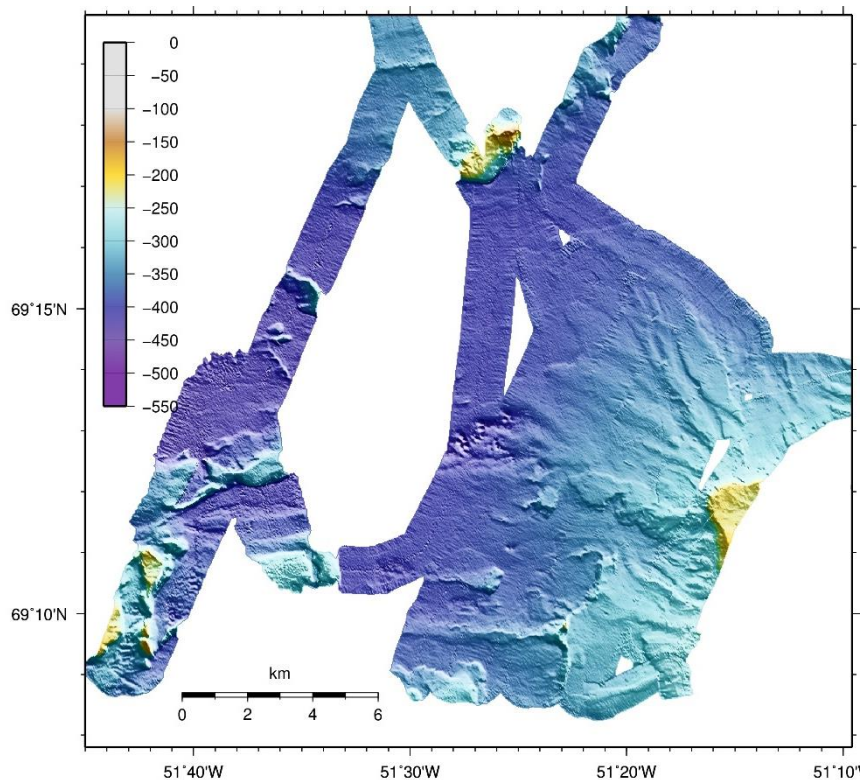


Fig. 3.1.2.1: Area off the mouth of Ilulissat Icefjord surveyed with deep-water multibeam echosounder Kongsberg EM120.

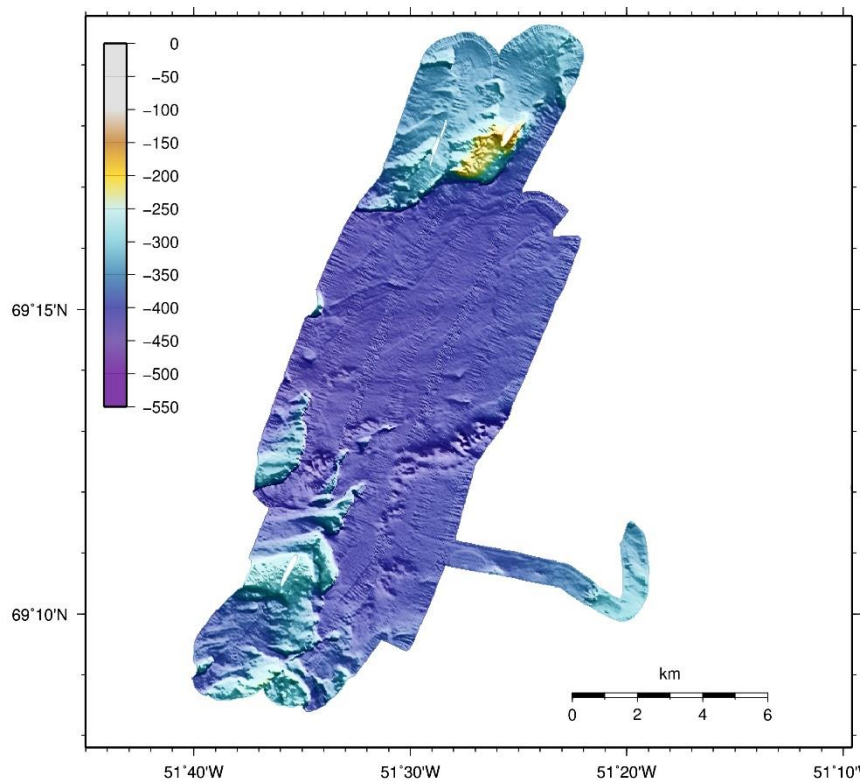


Fig. 3.1.2.2: Area off the mouth of Ilulissat Icefjord surveyed with shallow-water multibeam echosounder Kongsberg EM1002.

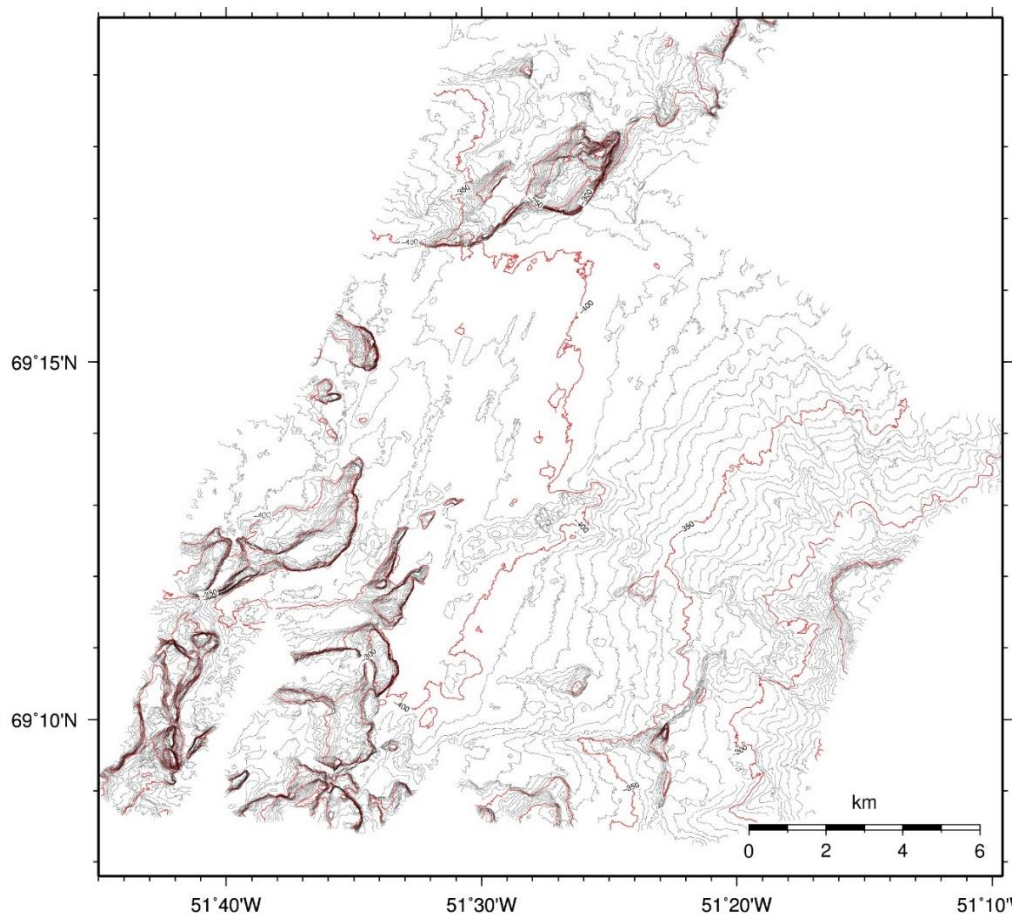


Fig. 3.1.2.3: Isocontour map of the surveyed area off the mouth of Ilulissat Icefjord.

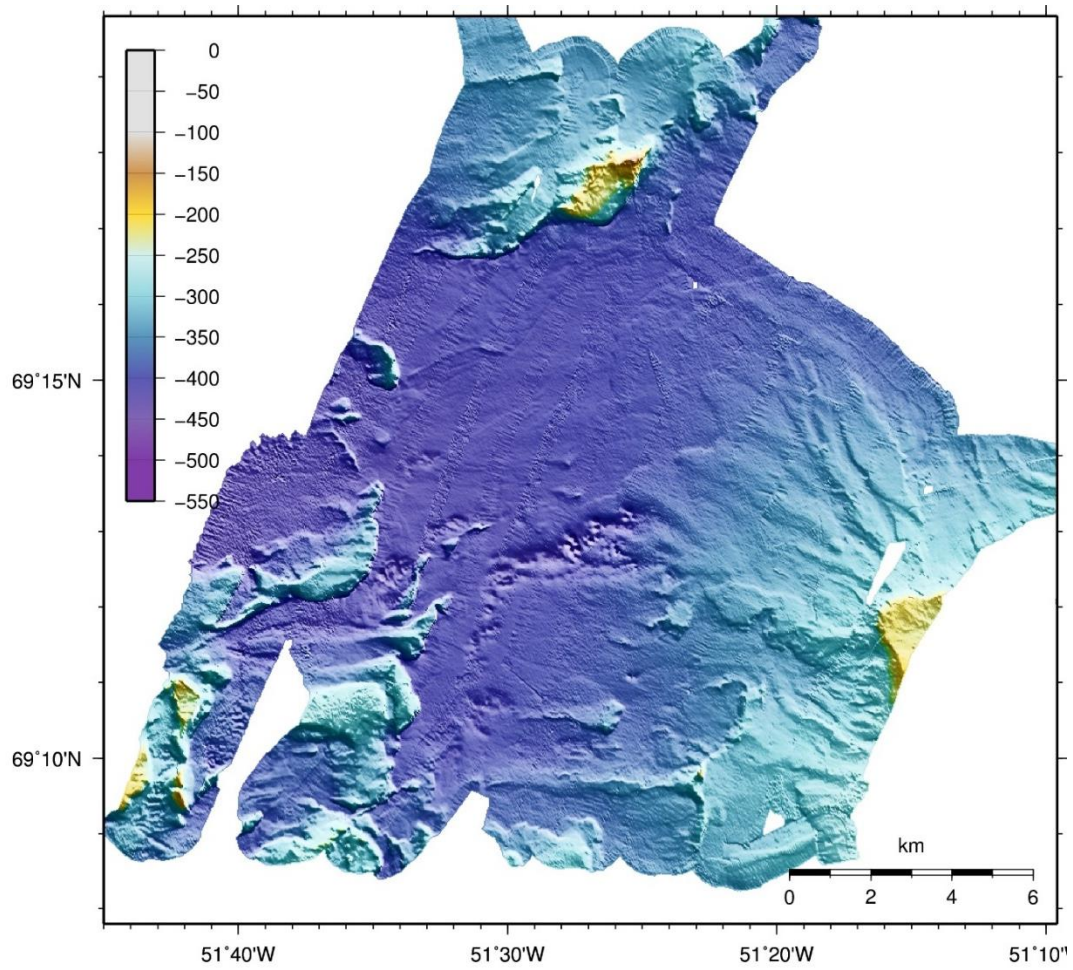


Fig. 3.1.2.4: Relief map of the surveyed area off the mouth of Ilulissat Icefjord.

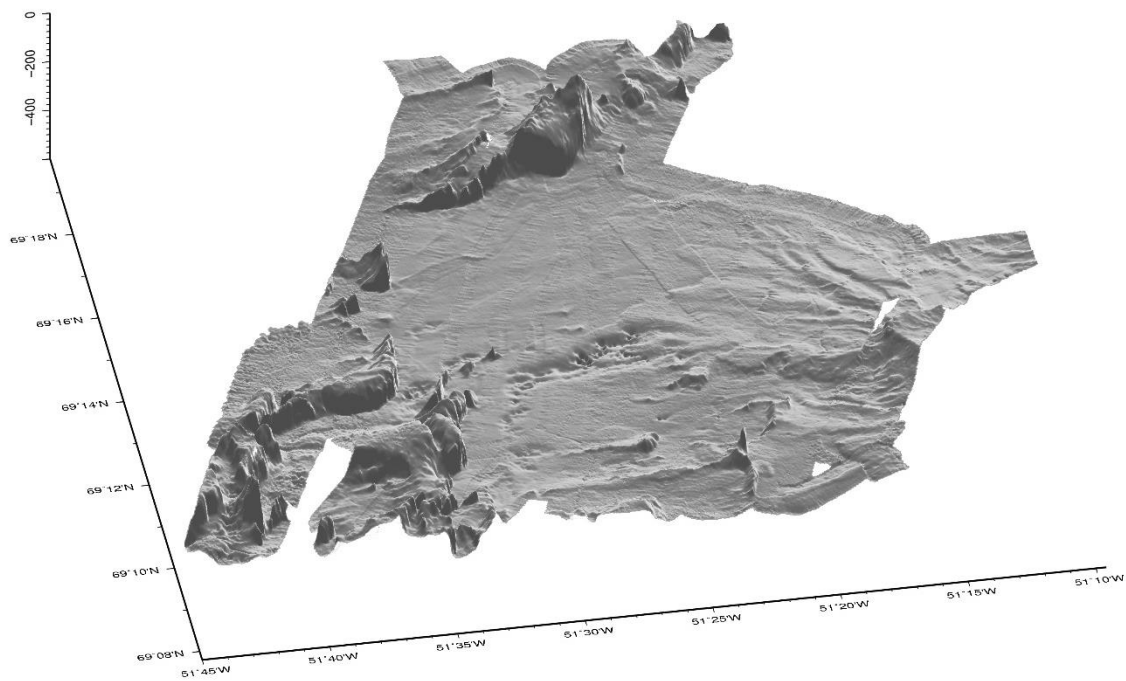


Fig. 3.1.2.5: Perspective image of the surveyed area off the mouth of Ilulissat Icefjord, view from the south (190°) elevation angle 33°, illumination from north (24°).

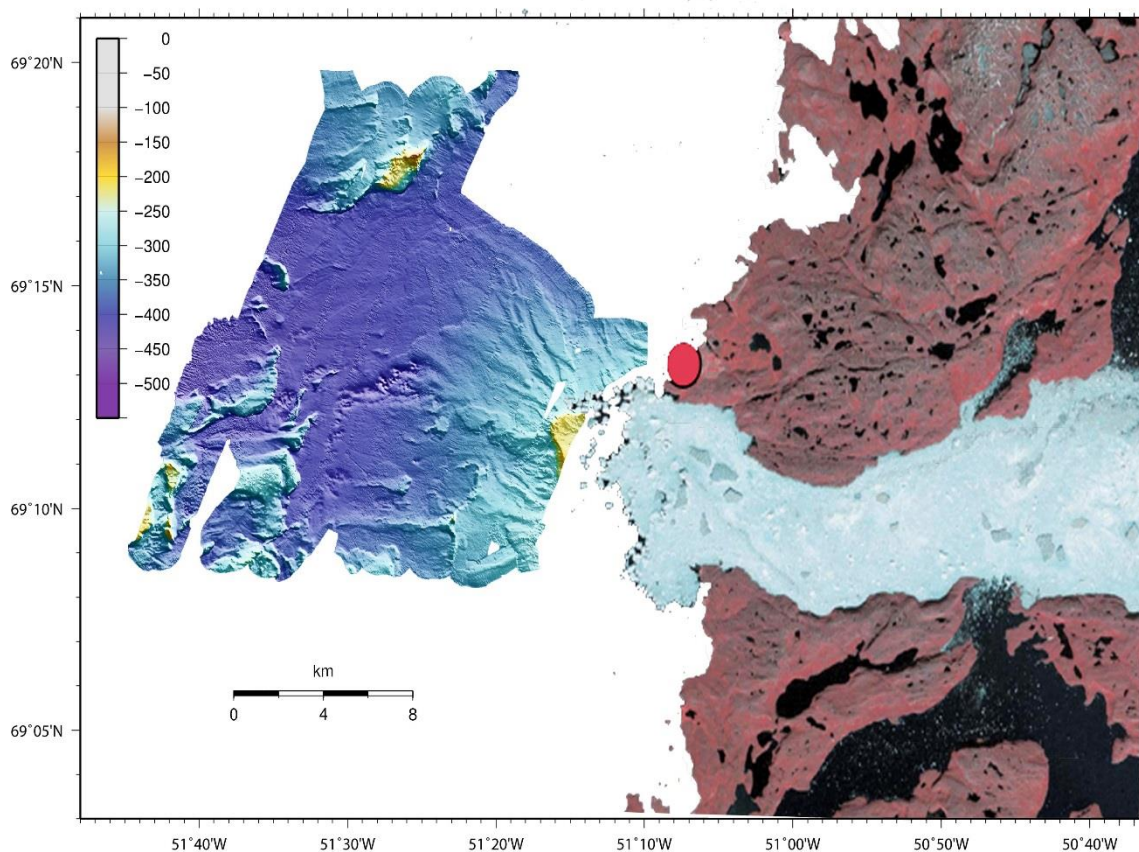


Fig. 3.1.2.6: Shaded relief image of the bathymetry of the surveyed area off Ilulissat Icefjord combined with a satellite image of onshore areas and the Icefjord.

### 3.1.3 Mapping iceberg drift in the Davis Strait

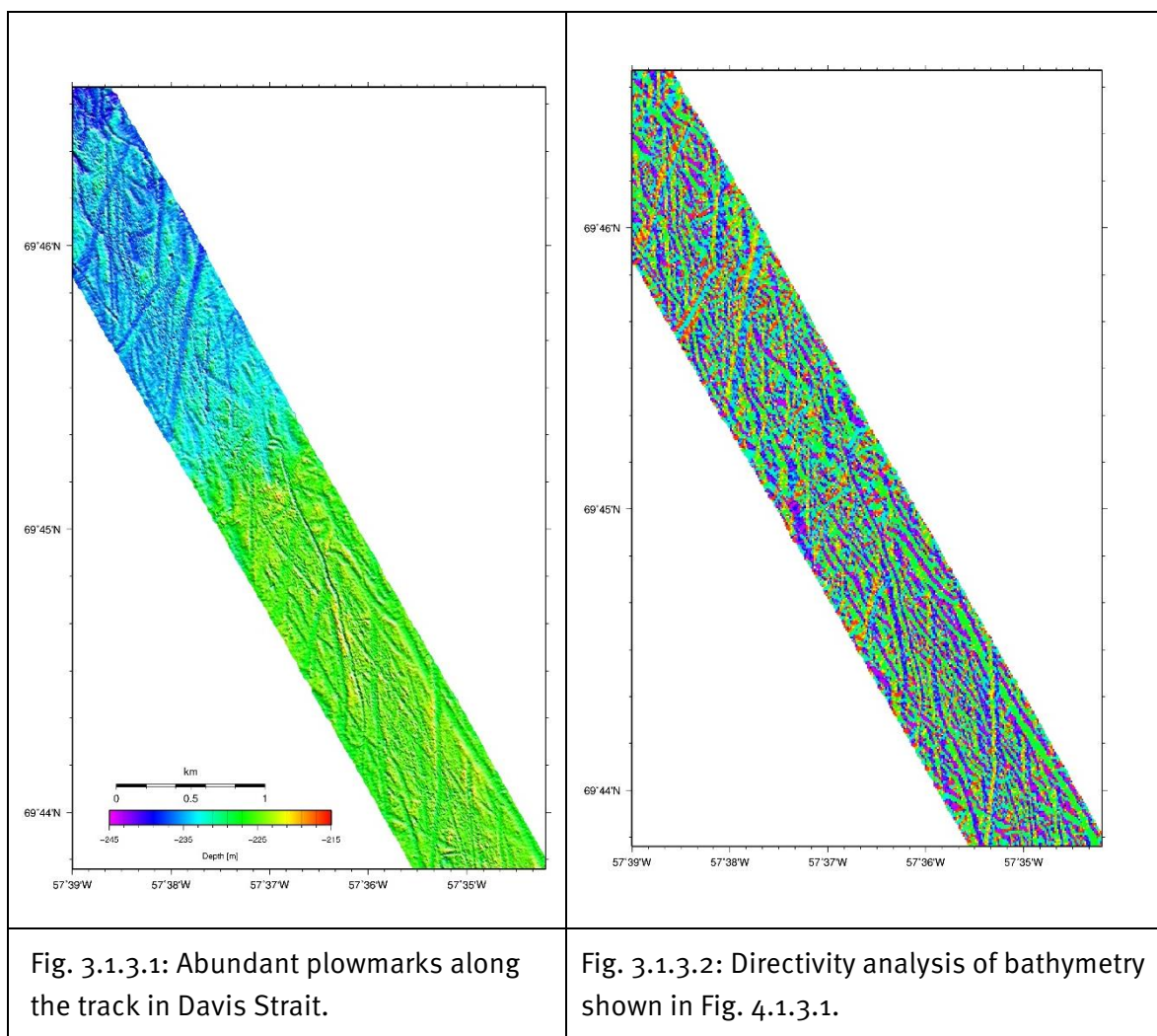
The multibeam system was operated continuously also during transits between different working areas. During such a transit an area tremendously sculptured by iceberg plowmarks was mapped by chance at 69°45'N, 57°36.5'W (Fig. 3.1.3.1). Several distinct patterns of directions of iceberg drifts can be identified, which represent different phases of drift. This is displayed even more clearly in Fig. 3.1.3.2, in which the directivity of the digital terrain model is shown. Different directions of the gradient (direction of steepest slope) of the digital terrain model are coded with different colors, enhancing the directivity of the seafloor morphology. Broader, wider and probably older grooves in the surveyed area are oriented more towards the north, whereas steeper, narrower furrows are oriented towards the northwest. The water depth in this area varies between 200 m and 240 m documenting rather deep going icebergs.

The planned geodetic fieldwork has been conducted successfully. Our GPS network of West Greenland has been densified and extended to the north by the establishment and first observation of four new GPS markers. Based on the obtained observation data, exact marker coordinates have been determined in a global reference frame. The inference of recent crustal deformation rates, however, requires the repetition of the GPS observations on these markers. The pressure tide gauge records obtained at two locations in the Nordre Strømfjord allow the determination and analysis of the water-level changes in the fjord. The water-level variations are

clearly dominated by the tidal signal with a range of 4 m. At this, the tidal amplitudes seem to increase towards the east. The tidal constituents resulting from a harmonic tidal analysis of the sea-level signal can be compared to the predictions of ocean tide models for

- a) a regional validation of the tide models, and
- b) investigating the modification of the tidal signal within a long, narrow fjord.

In addition, high-frequency sea-level changes such as surface seiches can be studied, and the simultaneously registered water temperature and conductivity records can be analysed regarding oceanographical questions.



The observed tidal signals were compared to the predictions of the global ocean tide model FES2004. At the outer coast, a good agreement was found. Inside the fjord, however, the model performs worse and tide gauge observations may still be indispensable when accurate tidal signals are required. The tide gauge records reveal also significant shallow-water tidal effects, in particular compound and overtide amplitudes reaching several cm.

### 3.2 Biogeochemistry - early diagenesis in fjord and bay sediments (S. Rysgaard, N. Risgaard-Petersen)

We are continuing the experiments in the labs of GRNI and still need to perform both chemical and genetic analysis of much of the material sampled during the cruise. First experimental and analytical work was expected to be finished by the end of 2007 – beginning 2008. Below we describe briefly the preliminary results obtained so far. The presentation is focused on data obtained through the study of microbial activity in the 6 m long core collected at station # 343340. The presentation is only based on a subset of expected data and should therefore be regarded only as very preliminary.

DIC increases with depth from app 2 mM in the surface to more than 10mM at 5 m depth (Fig. 3.2.1a) The profile indicates DIC production in the upper m and DIC consumption at 4-6 meters depth, the latter being due to methanogenesis. Direct measurements of DIC production and consumption confirm this pattern. Yet the activity estimates are still based on few data and more a will be provided during the next months together with data for distribution and turnover of methane. The depth integrated DIC production (estimated as DIC efflux from incubated cores of surface sediment), is 100% balanced by the oxygen consumption of the sediment indicating complete reoxidation of reduction equivalents produced during organic matter decomposition (e.g.  $\text{H}_2\text{S}$ ,  $\text{Fe}^{++}$ ,  $\text{NH}_4^+$ ). Oxygen consumption is confined to the upper two cm of the sediment (Fig. 3.2.1b), while we can measure DIC net production down to at least 60 cm. Nitrate respiration, measured as denitrification (i.e. the respiratory pathway that succeeds oxygen respiration) is probably confined to the upper 2-4 cm of the core (which will be confirmed by data from  $\text{NO}_3^-$  profile measurements) and accounts for less than 1% of DIC production.

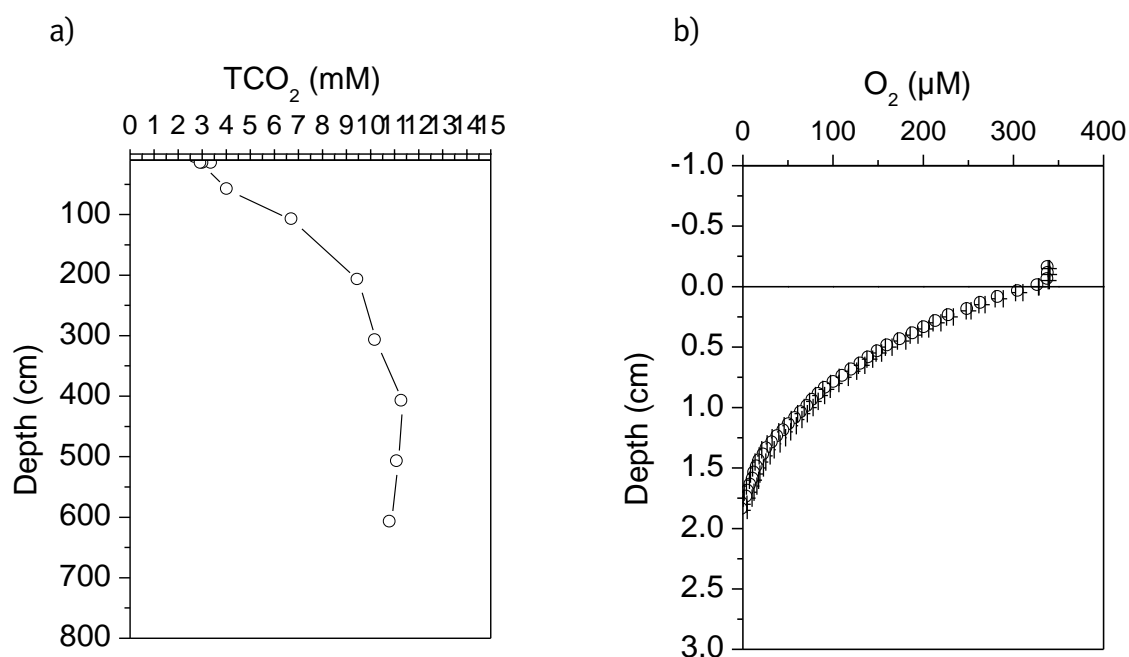


Fig 3.2.1: a) Concentration of DIC in core 343340 and b) Concentration of O<sub>2</sub> in core 343340 from the south-western Disko Bay shelf.

### 3.3 Disko Bay, fjord, and shelf sediments – paleoceanographic / paleoclimatological interpretation

#### 3.3.1 Analyses during the expedition (J. Lloyd, M. Moros, K. Perner, P. Sandgren, I. Snowball, J. Harff, T. Richter)

During the cruise a series of long (up to 12 m) gravity cores and short multicores were collected from a series of locations within Nordre Strömfjord, shelf west of Disko Bay, the Vaigat and the Ummannaq fjord complex and shelf. The exact timing and nature of deglaciation from the LGM maximum position near the shelf edge is rather poorly constrained for this section of the Greenland Ice Sheet. Long gravity cores were collected to investigate this deglaciation history from a number of locations, particularly in the Disko Bay and Ummannaq areas. Long cores were also collected from locations of known or assumed high accumulation rate for high resolution studies of oceanographic variability linked to climate change and also possible ice sheet instability during the Holocene. Multicores were collected from each location to provide an undisturbed record of sedimentation over the recent past (often lost during the gravity coring process). These samples can also be used to investigate the present day distribution of foraminifera and diatoms to help in the palaeoenvironmental studies from the long cores.

To investigate the deglaciation history from the shelf into the coastal areas a series of core transects were collected. The first transect runs from mid way to the shelf break west of Disko Bay into the deep trough (Egedesminde Dyb) that runs into Disko Bay. These cores will provide an extension of previous coring expeditions within Disko Bay itself. A second transect was collected along the Vaigat, the deep water trough exiting north from Disko Bay into the Ummannaq fjord system, into Torsukattak Fjord northeast Disko Bay. This transect will provide evidence of deglaciation of the trough itself, but also a history of northwards ice flux from Disko Bay. The final transect of cores was collected from the shelf into Ummannaq Fjord.

Preliminary investigation of the foraminifera from the surface samples of the multicores shows a clear trend of faunal change in relation to the temperature and salinity of bottom waters at each site. This clearly relates to the relative weakening/dilution of the relatively warm and saline West Greenland Current from south to north and also the absence of the WGC from Nordre Strömfjord (dominated by relatively cold and lower salinity bottom waters).

Preliminary investigation of the cores from west of Disko Bay also provides some insight into the deglacial history of the area. The magnetic susceptibility and the abundance of certain elements identified from the XRF scanning (e.g. Ti and S) completed onboard provides particularly valuable information. In this report we will discuss preliminary results from 343340, 343300 and 343310 from the Disko shelf area, from 343260 from the Nordre Strömfjord, and from 343520 from the Ummannaq shelf area

The magnetic susceptibility (MS) record from 343340 and 343300 (Fig. 3.3.1.1.) show initially high values in the basal sections of the cores (550 – 1150 cm and 300 – 1050 cm respectively), then low values for the upper sections of the cores. Based on previous analyses from long cores in eastern Disko Bay the high magnetic susceptibility is interpreted as a signal produced by high concentration of terrestrially sourced glacial detritus (rock flour and coarser material). The concentration of Ti from the XRF scanning shows similar trends in both cores, high in the lower sections and low in the upper sections. This also relates to increased levels of Ti from glacially

eroded material from the Greenland landmass. The high MS and Ti levels from the lower sections of both cores therefore suggest when this sediment was deposited the ice margin must have been very close to the respective core sites. As MS and Ti values decrease the ice margin must have been retreating eastwards, as the ice margin becomes more distal from the core sites the high MS and Ti signature from the glacial detritus is reduced and sedimentation is dominated by in situ marine productivity (supported by the increase in S values from the XRF scanning data). These cores therefore provide an accurate history of the timing and nature of deglaciation of the Greenland Ice Sheet east across the shelf and into Disco Bay during the earliest Holocene.

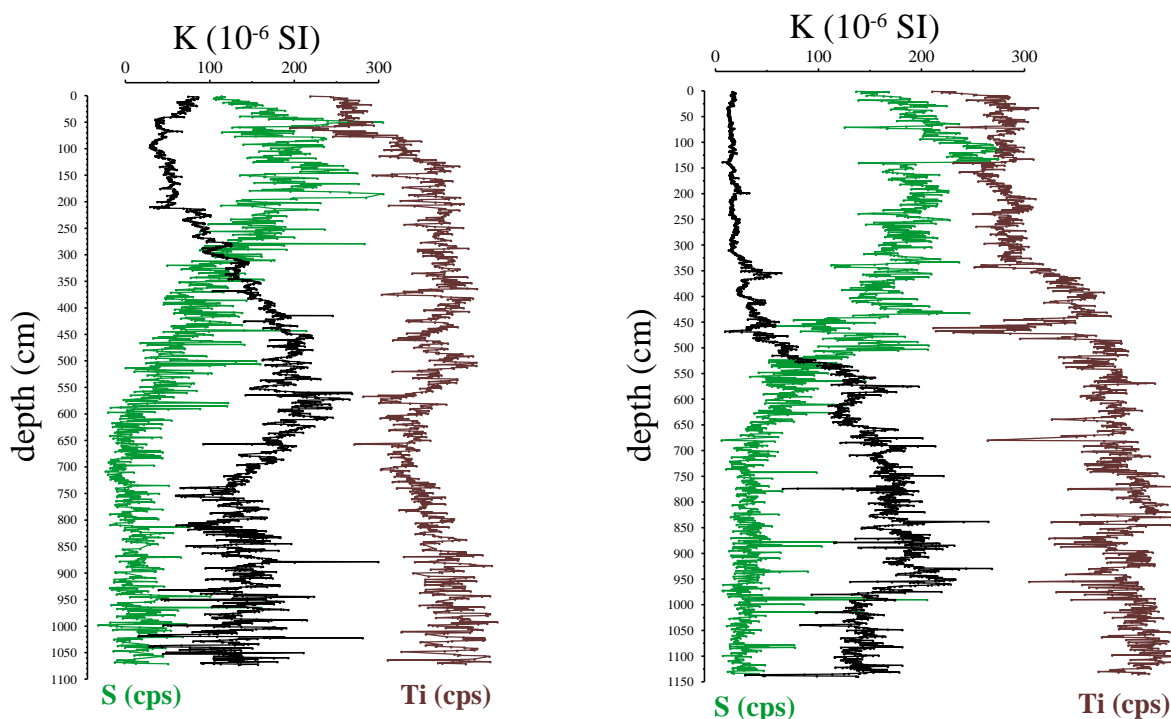


Fig. 3.3.1.1: On-board magnetic susceptibility (K) and XRF scanner (sulphur and titanium, counts per second) data of 343340 (left) and 343300 (right).

Typical signals for the fjord environments can be read from the MS of core 343260 from the Nordre Strömfjord (Fig. 3.3.1.2a). As one can see from the Parasound record (Enclosures, Fig. E6.2) the core were taken within an isolated basin sheltered against marine influences by a dominant sill. The rhythmic structure of the MS signal of a change between high and low values is due to the lithological sequence of pelitic/silty to sandy sediments. By an first interpretation the corser layers reflect events due to warmer periods causing increased melt water inflow into the fjord together with increased transport energy and, probably, slumping of sandy sediments. A dating of the sedimentary sequence will allow the analysis of the periodicity of these events.

Preliminary results from 343310 (Fig. 3.3.1.2b) highlights the suitability of this core for high resolution investigation of mid to late Holocene oceanographic evolution along the west Greenland margin. The MS record for the whole of this core (10 m gravity core) is relatively low (similar values to the top sections of 343340 and 343300). This suggests the full record from this

core dates from a period after the ice had retreated eastwards into Disko Bay. This core will, therefore, provide an excellent record of variability in the relative strength of the WGC through the Holocene (based on benthic foraminifera fauna) and also the history of sea ice concentration (based on diatom flora).

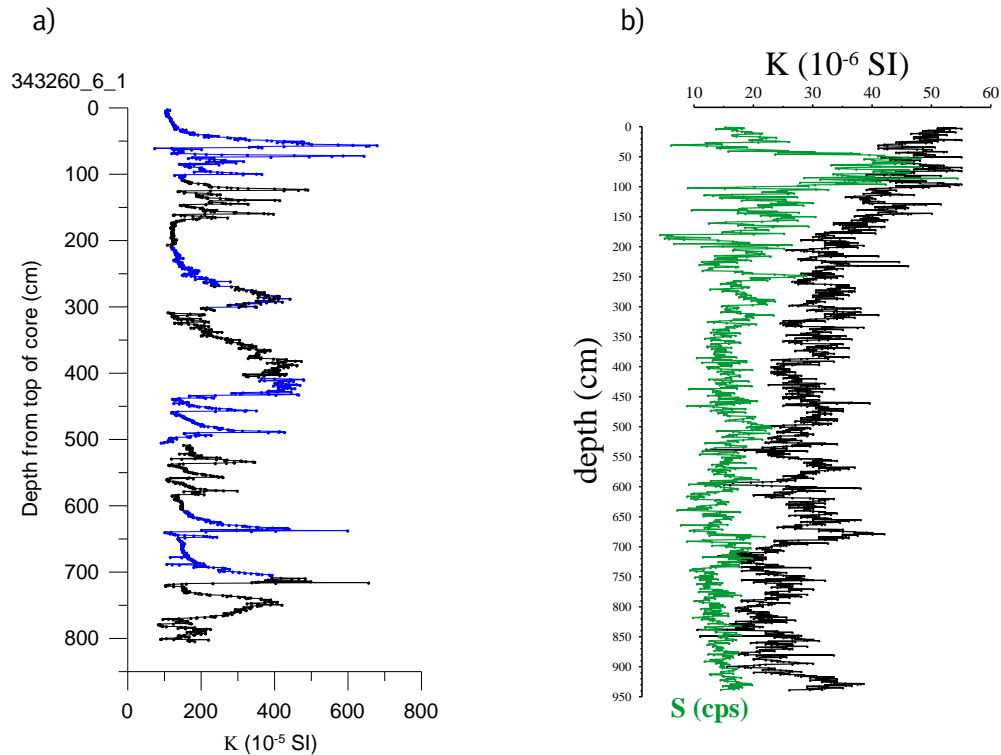


Fig. 3.3.1.2: a) Magnetic susceptibility data from a long sediment core in Nørdre Strømfjord and b) on-board magnetic susceptibility (K) and sulphur content (counts per second, cps) obtained via XRF scanning from site 343310 from Egedesminde Dyb in souther-western Disko Bay.

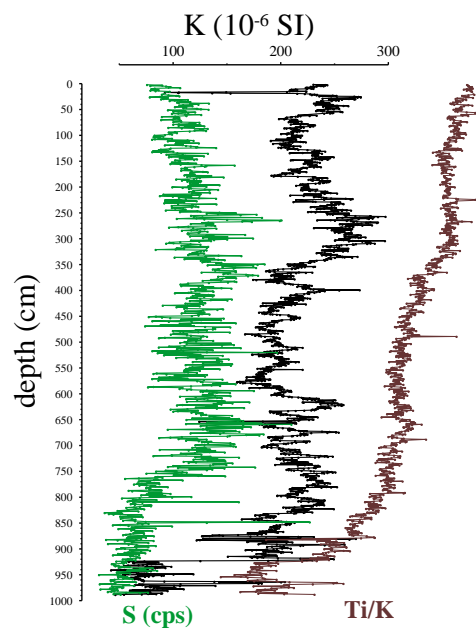


Fig. 3.3.1.3: On-board magnetic susceptibility (K) and results for sulphur and the Ti/K ratio (cps) obtained via XRF scanning from core site 343520 on the outer Uummanaq shelf.

A rather different record has been identified from 343520 (Fig. 3.3.1.3) retrieved from the Ummannak shelf. The MS results from this core are relatively high throughout the core – lowest values from the base of the core, Ti values mirror this trend. The trend in S is relatively low initially, then increases from 750 cm. Our initial interpretation is that the MS and Ti values are generally higher throughout this record because this core lies to the north and west of the Vaigat and west of the major Ummannak fjord complex supplying large volumes of IRD throughout the Holocene.

Once the ice sheet had retreated into Disko Bay we hypothesise that the majority of iceberg flux from the major ice streams draining into Disko Bay was then routed through the Vaigat rather than out westwards beyond Disko Bay. This is supported by present day iceberg drift patterns that carry most icebergs northwards through the Vaigat (carried by the predominant northerly currents in the area). This leads to significant IRD flux north and west of the Vaigat across the location of 343520. This site would also receive the significant flux of meltwater and icebergs from the major ice streams draining through the Ummannak fjord complex. So in this location the record from S provides a more reliable signal for deglaciation. The increase in S from 750 cm suggests deglaciation of this location sometime after this point (increasing S from marine productivity results from reduced dilution from glacially derived sedimentation). This core will also provide a high resolution record of oceanographic variability since deglaciation (over 700 cm of sedimentation since deglaciation).

These preliminary results provide evidence of the deglaciation of the shelf west of Disko Bay for the first time. Also long cores have been collected from the Ummannak fjord complex and shelf east of the fjord for the first time. These cores also provide evidence for deglaciation of the shelf west of the Ummannaq fjord. The MS and XRF scanning data also provides evidence for cores with very high resolution records of oceanographic and climate evolution from the west Greenland margin that will be investigated in more detail during further post cruise research. After the expedition several publications (MOROS et al. 2016, PERNER et al. 2011, 2013a,b, LLOYD et al. 2011, RIBEIRO et al. 2012) have contributed to a deeper understanding of the paleoceanographic and paleoclimate development of western Greenland.

#### **4.3.2 Data Analyses (J. Harff, S. Kotov, K. Perner)**

Time series analyses have been performed using proxy data from cores 343300 and 343310 in order to investigate the possible link between Northern Atlantic paleoceanographic changes and regional oceanic, climatic, and ice-dynamical variability in the West Greenland study area. Selected geochemical proxy data (MS-, TOC- and XRF-scanning data) have been converted to time series applying the age model published by PERNER et al. (2011; 2013a). Periodicity analyses have been performed using classical approaches of Fourier methods (FFT, MTM etc.). Similarities in the periodicity of the proxy data with those reconstructed for the Northern Atlantic have been used to test hypotheses about the link between the large scale North Atlantic current systems as driving forces for paleoceanographic changes in West Greenland. For signal-to-noise enhancement, we have used a singular spectral analysis method (SSA) specially designed for noised climatic series (GHIL et al. 2002). SSA was used not only for noise reduction but also for signal decomposition into statistically uncorrelated components (sub signals). The last ones can be regarded as a reflection of independent geo-climatic processes.

In Fig. 3.3.2.1, TOC-, Fe-, Ti-concentration, and magnetic susceptibility (MS) are given for cores 343300 and 3433100. For each of the curves the nonlinear trend has been determined as the 1-st component of Singular Spectrum Decomposition. The Fe-, Ti-, and MS-data stand mainly for the influence of meltwater delivering detrital material to the receiving basin - due to changes in atmospheric and oceanic changes. However, these data also reflect changes in the sources region due to changes in the iceberg drift. TOC (total organic carbon) serves as a proxy for paleoproductivity. The Fe- and Ti-trends show a clear shift at 6.2 ka BP. This shift is interpreted by the change in current system in the Disko Bugt after it became ice-free due to the warming phase and influence of the WGC from 8 to 6 ka BP (PERNER et al., 2013b, MOROS et al., 2016). But, all curves show a periodicity with an inflection point, which can be well correlated between the curves. For comparison with Holocene climatic changes and variations in current system of the Northern Atlantic, the curves in Fig. 4.3.2.1 are superimposed with Bond-events 0 to 5 (Bond et al. 2001) but also with cooling phases (“Wanner events”) after WANNER et al. (2011). Bond events have been derived from fluctuations in ice-rafted debris data and stand for cooling events and low SST of the North Atlantic, while the “Wanner events” incorporate a more complex interpretation of climate proxies reflecting atmospheric temperature, precipitation and humidity. The 8.2 ka BP Bond (5) event is clearly marked by the corresponding minimum of 343300 Ti-curve. Warming and cooling phase thereafter are reflected by increasing and decreasing meltwater discharge in the Fe- and Ti-curves of cores 343300 and 343310 as well as the TOC curve of core 343300. The remarkable inflection points, alongside minimum values of Ti and Fe at 6.2 ka BP, at 5.9 ka Bond (4) event and coincides with the 6.5-5.9 cold event. After the Disko Bugt became ice-free inflection points in the Ti, Fe-, MS- and TOC-curves in Fig. 4.3.6 correlate in general with Bond 3-1 events. Further, it has to be mentioned that the clear correspondence with the “Wanner cold events” 4.8-4.5, 3.3-2.5, , 1.75-135 ka BP lead to the conclusion that a complex process including paleoceanographic and climatic triggered changes determine the sediment accumulation in Disko Bugt. Paleoclimatic (cooling) events can be correlated in general with the non-linear trend functions shown in Fig. 3.3.2.1. In this study it is hypothesized that the energy supply to the Disko Bugt – and in this sense the glacier dynamics is related to the paleoceanographic variability of the WGC which is for its part depending on the large-scale North Atlantic circulation system - the Irminger Current (IC), and the East Greenland Current (EGC). Similarities in sediment proxy variability with North Atlantic paleoclimatic changes provide additional arguments to accept the hypothesis mentioned above. For further comparison of periodicities in climatic and oceanographic changes we have investigated the spectral densities of selected sediment proxies of core 343300 (Fig. 3.3.2.2). As the downcore sampling rate is 1 cm, t.e. about 50 years time lag, we can consider (according to Nyquist–Shannon–Kotelnikov theorem) only periods more than 100 years – for analytical signals. Taking in account natural and analytical noise plus errors of space-time models we assume that frequencies higher than 200 years should not be taken into consideration here. Correspondingly, for the analysed variables periods of  $\approx 450$ ,  $\approx 550$ ,  $\approx 750$ ,  $\approx 900$ , and 1500 to 1600 should be considered.

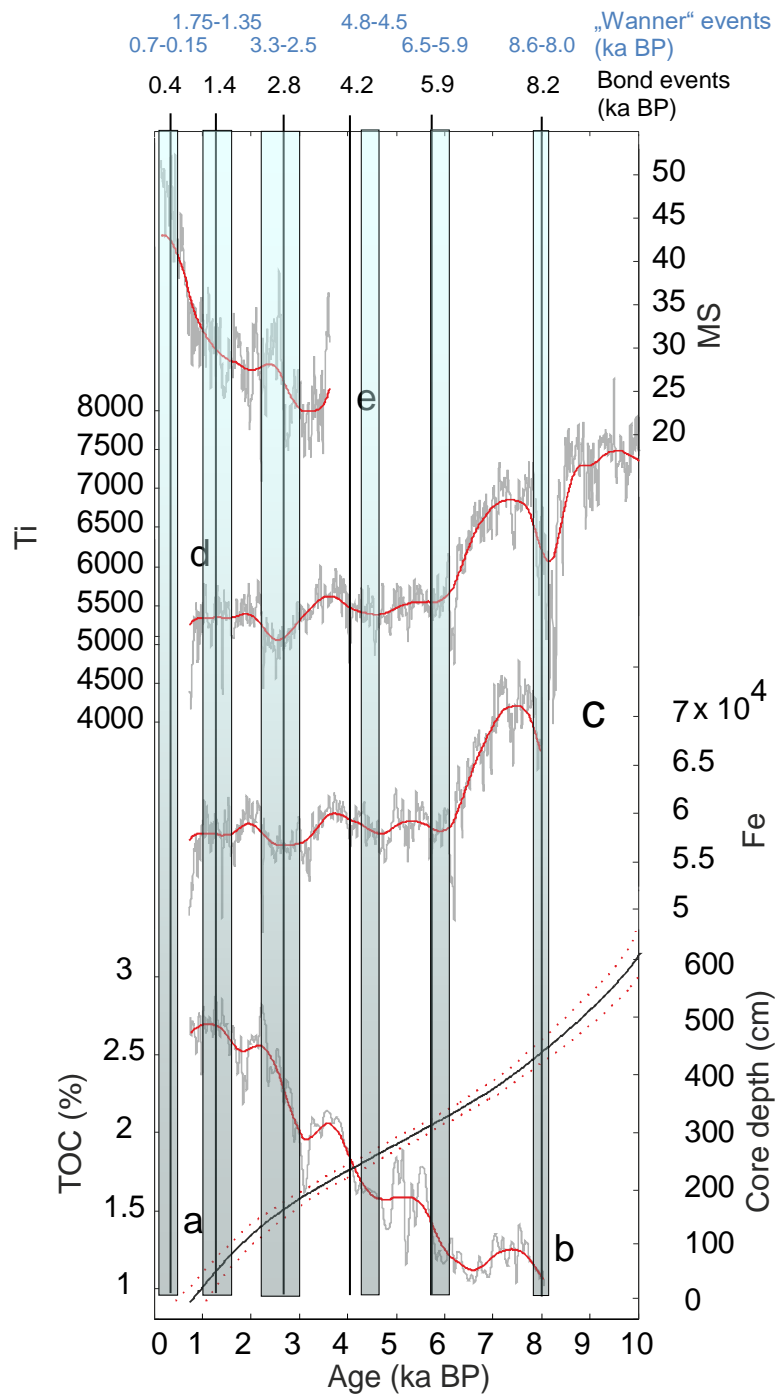


Fig. 3.3.2.1: TOC, Fe-, Ti-concentration, and the magnetic susceptibility (MS) for cores 343300 and 3433100 (grey curves). The red curves show the nonlinear trend for each variable determined as the 1-st component of Singular Spectrum Decomposition. a) age model for core 343300 after Perner et al. (2013a) improved by additional data (Perner pers. commun.), b) TOC (%) for core 343300, c) Fe concentration as XRF-scanning counts/sec. (core 343300), d) Ti concentration as XRF-scanning counts/sec. (core 343300), e) Magnetic susceptibility for core 3433100 (SI).

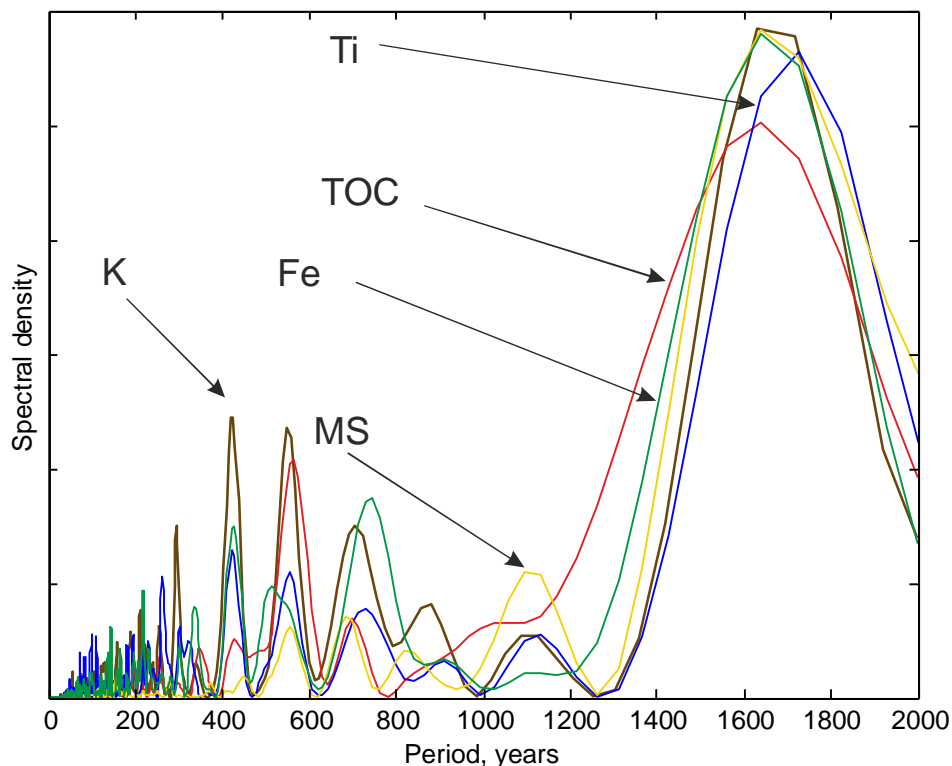


Fig. 3.3.2.2: Spectral density for time series, TOC (total organic carbon), Ti, Fe, K, MS (magnetic susceptibility) for sediment core 343300.

The latter one is dominant within the graph (Fig. 3.3.2.2) and is interpreted here as a signal of North Atlantic oceanographic (ant climatic) variability. This period can be regarded a reflection of the Bond-cyclicity of  $1470 \pm 500$  years (BOND et al. 1997). Also the 750 years period is to be interpreted in this light. Bond cycles have been identified in many marine records not only from the Atlantic ocean (WANNER et al. 2008), but also in terrestrial records or marginal seas as the Baltic (HARFF et al. 2011). From western Greenland it is the first time that it has been measured in such a pronounced manner. For the periods of of  $\approx 450$ ,  $\approx 550$ , and  $\approx 900$ years it has to be mentioned that KOTOV and HARFF (2006) have reported similar periods for Greenland ice proxy data and sediments from the Baltic Sea. According to LAMY et al. (2006), preliminarily, these periods are interpreted here, as results of AO/NAO variation due to changes in solar activity.

### 3.4 Anthropogenic impact on Qaumarujuk Fjord environment (K. Perner, T. Leipe, T. Richter, P. Sandgren)

The northern most coring stations were chosen in the northern part of the Uummanaq-Fjord near an former lead-zinc mine “The Black Angel Mine” at Maarmorilik ( $71^{\circ} 07'N / 51^{\circ} 16'W$ ), about 500 km north of the arctic cycle. Mining activities involves significant influences on the environment. The deposition of mine wastes and tailings into the Fjords caused an evident impact on the fjord environment by release of heavy metals into the water column.

The Black Angel mine is located at the entrance of the 4 km long Affarlikassaa Fjord, which is separated by a small sill with a maximum depth of 23 m, from the bigger 8 km long Qaumarujuk Fjord. From 1973 to 1990 the Canadian mining company Greenex A/S operated the lead-zinc mine. In total approximately 11 000 000 million tonnes of ore have been mined, processed into 135 000 tons of zinc concentrate and 35 000 tons of lead concentrate (ASMUND et al 1994).

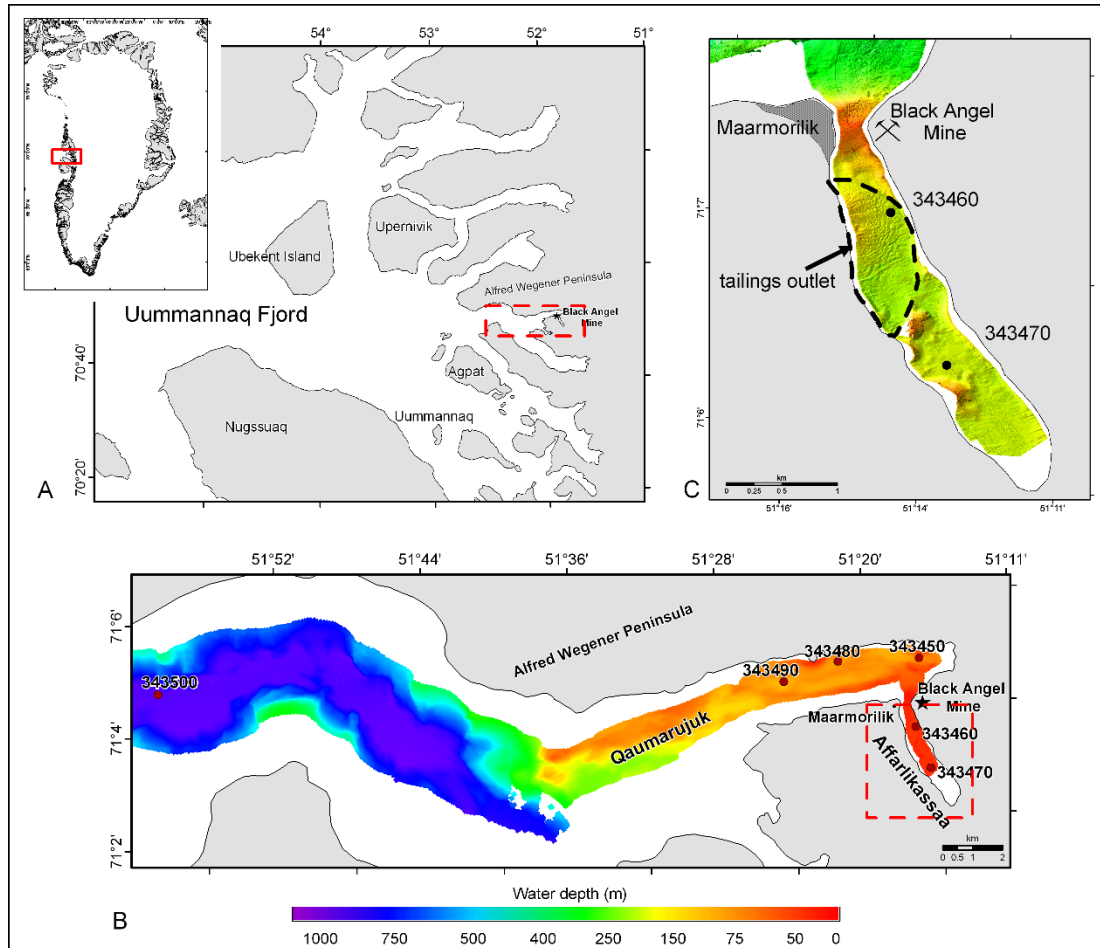


Fig. 3.4.1: Survey map of the investigation area and close up of the Uummannaq Fjord, with sample locations and bathymetric map (Perner et al., 2010).



Fig. 3.4.2: Black Angel Mountain. (Photo: K. Perner)

The aim of our study was to take short cores with the multi corer as well as long cores with the gravity corer from the polluted areas, for analysing the concentration and distribution of heavy metals in the sediment under vertical and horizontal aspects, from the main polluted area through less polluted area at the outermost part of the Q-fjord (Fig. 3.4.1).

The Black Angel Mine took its name from a pelite outcrop that forms a dark angel-like figure on a precipitous cliff face of marble above A-Fjord (see Fig. 3.4.2). At an average height of 700 m the mineralized zone crops out just above the angel like figure (THOMASSEN 2003). The ore bodies hosted in the Maarmorilik Formation, containing widespread stratabound lead-zinc sulphide mineralization in the metamorphosed limestone, come from the Palaeoproterozoic and formed by three main phases of folding and thrusting. From the Black Angel Mountain on the east side of the A-fjord the mined ore was transported by an areal tramway to the mining town on the west side for further processing

During the mine operation time from 1973 until 1990, 11.3 million tones of ore were processed with average ore grades of 4.1 % Pb, 12.5 % Zn and 30 g/t Ag. First, the mined ore was grinded by rod- and ball mills, than recovered by conventional selective flotation. Tailing were discharged into the A-fjord with an total amount of nearly 8 million tones. The chemical composition of the deposited tailings is approximatly 50% carbonate (marble and dolomite), 50% FeS<sub>2</sub> (pyrite), 1% Zn (mainly as ZnS, sphalerite), 0.5% Pb (mainly as PbS, galena) and 0.01 % Cd (ASMUND 1980).

Fig. 3.4.1C shows the Maarmorilik area with a detailed bathymetric map, created during the cruise with the Kronsberg shallow-water multi beam system. The sediment sampling was conducted at 6 locations near Maarmorilik. At each location short cores were collected using a multicorer or a boxcorer. It was possible to go with R/V Maria S. Merian into the small A-Fjord, taking two short cores and two long cores in the high-polluted area.

The short cores reached an average penetration of 35 cm and were sliced into 5 mm peaces untill a depth of 10 cm and than sliced in 1 cm intervals downcore. The samples were stored into small Petridishes and brought into the cold-storage chamber at 4°C onboard R/V Maria S. Merian after measuring the magnetic suszeptibility.

The long cores taken by a gravity corer with a 6 m stainless steel tube, were cut into one meter sections and afterwards splitted in two halves, lithological described and measured with TAMI-Scan for magnetic suszeptibility and also with the Aavatech XRF-Scanner for maja element detection. The lithological description of the gravity core 343460 showed that the whole core consisted of olive to dark grey silty clay with fine sand, arraged in fine alternating layers. Downcore pyrite was visible and especially in the coraser fine sand layers it seemed to be concentrated. That indicates that this core was taken directly from the tailings outfall originate from the processed mining material.

Results of magnetic suszeptibility measurements for core 343460 show relative low values downcore with some higher values between 90 and 100 cm depth and at the bottom at depths between 520 cm and 540 cm, resulting eventually from some stronger discharging processes by the mining activity.

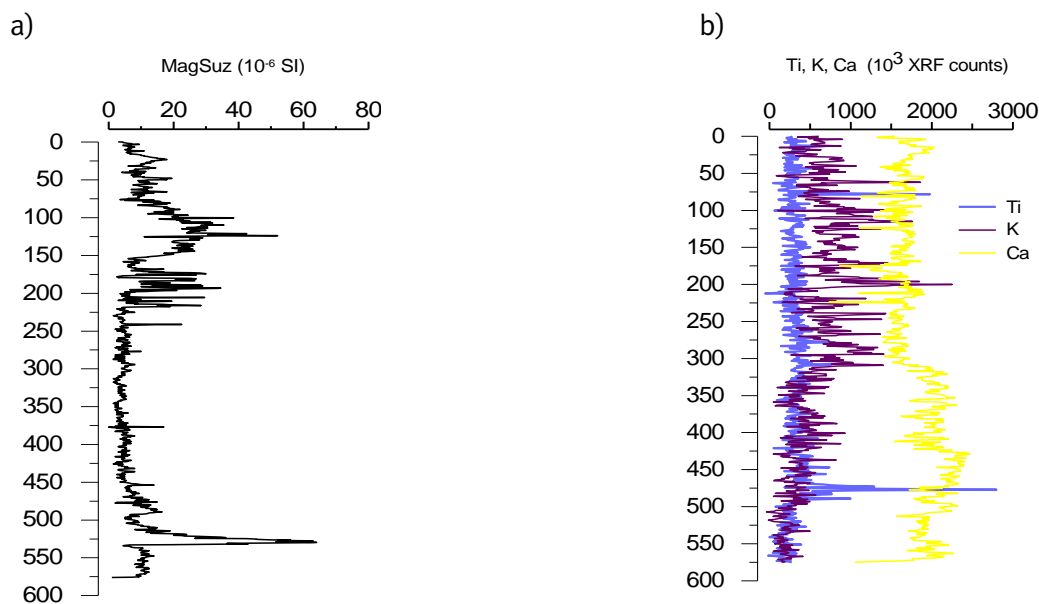


Fig. 3.4.3: a) Magnetic Suszeptibility and b) Titanium, Potassium and Calcium profiles from XRF scanning from gravity core 343 460 from the central Affarlikassaa fjord.

The preliminary results from XRF-scan, plotted for Ti, K and Ca in Fig.4.4.3b, show relatively low values. The values of Ti ranging between 300 to 400 ( $10^3$ XRF counts) downcore, with two peaks at depth of 75 cm and 475 cm. Values measured for K indicate at the base of the core similar values to Ti, at a depth of 350 cm the values increases with some strengthened variations. A different trend than K exhibit the curve shape of Ca. Untill a depth of 300 cm the values ranging between 1500 and 2000 ( $10^3$ XRF counts), than the values are increasing with toward the bottom of the core.

In order to identify signals of lead and zinc, the detector have been modified with a copper-filter and the whole core was measured downcore at a level of 30 kV. Figure 3.4.4 shows the XRF-counts/sec. for lead and zinc as well as sulphur and iron of core 343 460.

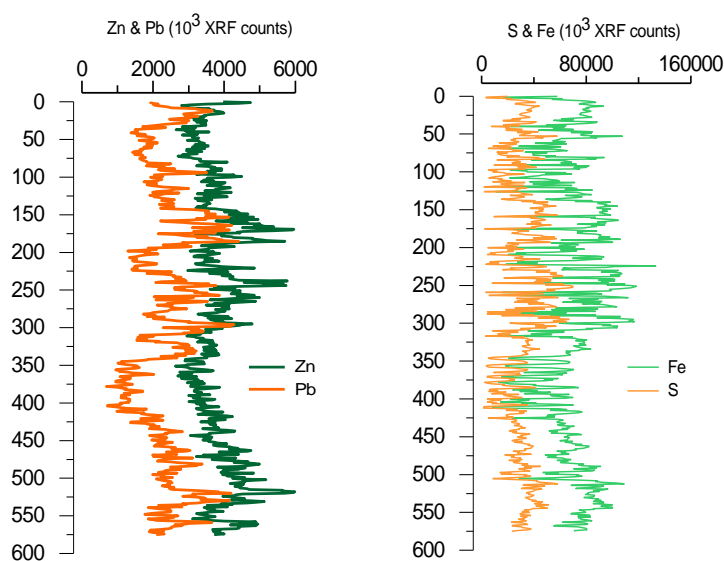


Fig.3.4.4: XRF scans of Pb and Zn as well as S and Fe from station 343460-2-1 (tailings outfall).

Within the sediment, relatively high values for Zn as well as for Pb have been detected, indicating with some variations through the depth. Therefore it can be assumed, that the whole core consists of processed material, containing ore minerals. In addition, the detected values of sulphur and iron are relative high through the whole core, besides both elements show a similar behavior downcore to lead and zinc. Certainly, the detected values of iron, sulphur, lead and zinc will not reach any natural background level. Nevertheless, this can probably be shown within the sediments of station 343470, this gravity core will be also measured with a special filter to detect the signals for lead and zinc. Further analyses of the short cores and long cores had been focussed on: trace elements with ICP-OES, detection of the total mercury content with DMA (Direct Mercury Analyser), grain size analyses, determination of organic and inorganic carbon and total sulphur as well as  $^{210}\text{Pb}$  and  $^{137}\text{Cs}$  dating. Results have been published by PERNER et al. (2010).

### 3.5 Geodetic measurements (R. Dietrich, A. Richter)

The planned geodetic fieldwork has been conducted successfully. Our GPS network of West Greenland has been densified and extended to the north by the establishment and first observation of four new GPS markers. Based on the obtained observation data, exact marker coordinates have been determined in a global reference frame. The inference of recent crustal deformation rates, however, requires the repetition of the GPS observations on these markers. The pressure tide gauge records obtained at two locations in the Nordre Strømfjord allow the determination and analysis of the water-level changes in the fjord. The water-level variations are clearly dominated by the tidal signal with a range of 4 m. At this, the tidal amplitudes seem to increase towards the east. The tidal constituents resulting from a harmonic tidal analysis of the sea-level signal can be compared to the predictions of ocean tide models for

- a) a regional validation of the tide models, and
- b) investigating the modification of the tidal signal within a long, narrow fjord.

In addition, high-frequency sea-level changes such as surface seiches can be studied, and the simultaneously registered water temperature and conductivity records can be analysed regarding oceanographical questions.

The observed tidal signals were compared to the predictions of the global ocean tide model FES2004. At the outer coast, a good agreement was found. Inside the fjord, however, the model performs worse and tide gauge observations may still be indispensable when accurate tidal signals are required. The tide gauge records reveal also significant shallow-water tidal effects, in particular compound and overtide amplitudes reaching several cm.

### 3.6 SPM and aerial dust – Preliminary Results

SPM concentrations in Uummannaq Fjord at the surface varied from 1.12 mg/l at St. 343440 to 1.26 mg/l at St. 343430. With depth it decreased to 0.22–0.50 mg/l below the pycnocline. In eastern end of Qaumaruujuk fjord at St. 343450–343490 the SPM concentrations at the surface

were higher (1.65–3.27 mg/l). Much higher concentrations of SPM were registered in melt-water stream (salinity was close to 0 psu) flowing from Qaumarujuk glacier (136 mg/l) and in fjord near-shore zone near Qaumarujuk glacier with salinity 20.7 psu (59.2 mg/l).

In the mouths of Qaumarujuk and Uummannaq fjords and in open sea SPM concentration was low. Most part of stream SPM sediments at the salinity barrier. The lowest value (0.19 mg/l) was registered at St. 343530, the mostly remote from the land). In eastern part of Nordre-Strømfjord SPM concentration at the surface was high – 23.1 mg/l.

## 5. Summary (J. Harff)

The expeditions has been executed according to the research plan.

The following **methods** have been applied:

*Hydrography:* The currents in the water column have been observed continuously using the ship mounted Acoustic Doppler Current Profiler (ADCP). Within the fjords and outside the fjords on the shelf average CTD stations (20 nm distance) have been executed. CTD-measurements have been also carried out for each of the coring stations selected on the base of seismo-acoustic data.

*Geophysical methods:* For the identification of sedimentary basins we have used multibeam echo sounder and the new parametric echo sounder PARASOUND DS3 mounted at the R/V Maria S. Merian. In addition, multi-beam bathymetric data acquisition has been used for the interpretation of the origin of various seabed features (e.g. iceberg drift).

*Sedimentological sampling:* In order to investigate environmental and climatic changes during the Late Quaternary we samples marine sediment sequences using a gravity corer. Sampling of the recent sediments (last 100 years) has been conducted using the MUC (multi-corer). These cores have been used for detailed studies of biochemical cycles and anthropogenic impacts on the marine environment during the past decades. For surface sediment sampling a box-corer have been used in selected areas.

*Geodesy:* To measure the recent vertical deformations of the Earths crust in the vicinity of the Greenland Ice Sheet, a GPS network has been established within the frame of previous research projects and extendet/completed during the MSM05/03 cruise. This included installation and a of new GPS stations located along the Nordre Strømfjord, the Vaigat and the Qaumarujuk Fjord, as well as a re-observation of one site of an already existing network. From the repeated observation of this GPS network, the detailed spatial pattern of the present-day uplift rates in the area of investigation can be deduced.

The following **results** have been achieved during the MSM05/03 cruise:

1. The geodetical network that measures the glacio-isostatic adjustment of the earths cruiss in West Greenland has been completed. Now, it is possible to identify and quantify vertical crust dislocations for model parameterization.

2. Sediment cores have been collected from the West Greenland shelf. Geochemical and sedimentological parameters have been measured on board. These data presented first insights into the history of Holocene climatic changes and variability of the West Greenland Current at a high resolution.
3. The technical equipment of the MSM did allow sampling of sediments within Fjords with active calving glaciers. These cores describe the climatically controlled ice-dynamics of tide water glaciers that drain the Greenland Ice Sheet.
4. Using the multibeam echosounder allowed detailed mapping of the sea floor close along the cruise track and within the fjords. The identification of Ploughmarks show different drift directions of icebergs pointing to variations in the flow path of marine currents.
5. Traces of anthropogenic impact have been identified through geochemical proxies within sediments of the Qaumarujuk Fjord. Here, the lead/zink mining close to Maarmorilik, conducted during the 1970s, caused pollution pressure on the aquatic ecosystem and is still recorded within the fjords sediments.

During the expedition MSM05/03, a social meeting of the scientists with local school teachers, students and citizens of the Uummannaq commune provided interesting information about the effect of climate warming on hunting habits of the Inuit in West Greenland.

Following the MSM05/03 expeditions a number of multi-proxy analyses have been performed on selected sediment cores from the cruise. These investigations have resulted in numerous publications that contribute to an improved understanding of climatic and oceanic changes in West Greenland and to ice-ocean dynamics within the area on a decadal to millennial time scale for the last 100 years and for the Holocene time period.

## **Acknowledgements**

The expedition MSM05/03 was financed by the Deutsche Forschungsgemeinschaft (DFG). Results assigned to the topic “Disko Bay, fjord, and shelf sediments – paleoceanographic/paleoclimatological interpretation Interaction between ocean forcing, climate change and the West Greenland ice sheet during the mid- to late Holocene” have been elaborated within the frame of an DFG-funded research project (MO 1422/2-1). The editors and the authors of this report express their sincere thank to Capitain Friedhelm von Staa, the officers and the crew of R/V “Maria S. Merian” for professional service and excellent work conditions on board during the expedition MSM05/03.

## References

- ASMUND, G., 1980: Water movements traced by metals dissolved from mining tailings deposited in a fjord in north west Greenland. In: FREELAND, H.J., FARMER, D.M., LEVINGS, C.D. (eds): Fjord oceanography. Volume 4 of the series NATO Conference Series. Plenum- New York and London, pp.219-225.
- ASMUND, G., BROMAN, P.G., LINDGREN, G., 1994: Managing the environment at the Black Angel Mine, Greenland. - *International Journal of Surface Mining, Reclamation and Environment* **8**, 37-40.
- BERG, P., RISGAARD-PETERSEN, N., RYSGAARD, S., 1998: Interpretation of measured concentration profiles in sediment porewater. - *Limnology and Oceanography* **43**, 1500-1510.
- BERG, P., RYSGAARD, S., THAMDRUP, B., 2003: Dynamic modelling of early diagenesis and nutrient cycling: A case study in an Arctic marine sediment. - *American Journal of Science* **303**, 905-955.
- BOND, G., SHOWERS, W., CHESEBY, M., LOTTI, R., ALMASI, P., DE MENOCAL, P., PRIORE, P., CULLEN, H., HAJDAS, I., BONANI, G., 1997: A pervasive millennial-scale cycle in the North Atlantic Holocene and glacial climates. - *Science* **294**, 2130-2136.
- BOND, G., KROMER, B., BEER, J., MUSCHELER, R., EVANS, M.N., SHOWERS, W., HOFFMANN, S., LOTTI-BOND, R., HAJDAS, I., BONANI, G., 2001: Persistent solar influence on North Atlantic climate during the Holocene. - *Science* **278**, 1257-1266.
- GHIL, M., ALLEN, M.R., DETTINGER, M.D., IDE, K., KONDRASHOV, D., MANN, M.E., ROBERTSON, A.W., SAUNDERS, A., TIAN, Y., VARADI, F., YIOU, P., 2002: Advanced spectral methods for climatic time series. - *Rev. Geophys.* **40**(1), 3.1-3.41.
- GRAY, S.T., GRAUMLICH, L.J., BETANCOURT, J.L., PEDERSON, G.T., 2004: A tree-ring based reconstruction of the Atlantic Multidecadal Oscillation since 1567 A.D. - *Geophysical Research Letters* **31**, L12205, doi:10.1029/2004GL019932.
- HANSEN, H.P., KOROLEFF, F., 1999: Determination of nutrients. In: GRASSHOFF, K., KREMLING, K., EHRHARDT, M. (eds): *Methods of Seawater Analysis*. - Wiley-VCH, New York, pp.159-229.
- HARFF, J., ENDLER, R., EMELYANOV, E., KOTOV, S., LEIPE, T., MOROS, M., OLEA, R.A., TOMCZAK, M., WITKOWSKI, A., 2011: Late Quaternary Climate Variations reflected in Baltic Sea Sediments. In: HARFF, J., BJÖRCK, S., HOTH, P. (eds): *The Baltic Sea Basin*. Springer: Berlin et al., pp.99-132.
- HASLE, G.R., SYVERTSEN, E.E., 1996: Marine diatoms. In: THOMAS, C.R. (ed.): *Identifying Marine Phytoplankton*. - Academic Press, San Diego, pp.5-386.
- HERBLAND, A., LE BOUTELLER, A., RAIMBAULT, P., 1985: Size structure of phytoplankton biomass in the equatorial Atlantic Ocean. - *Deep-Sea Research* **32**, 819-836.
- HILLAIRE-MARCEL, C., DE VERNAL, A., BILODEAU, G., WEAVER, A., 2001: Absence of Deepwater formation in the Labrador Sea during the last interglacial period. - *Nature* **410**, 1073-1077.
- JENNINGS, A.E., KNUDSEN, K.L., HALD, M., HANSEN, C.V., LAMY, F., ARZ, H.W., BOND, G.C., BAHR, A., PÄTZOLD, J., 2006: Multicentennial-scale hydrological changes in the Black Sea and northern Red Sea during the Holocene and the Arctic/North Atlantic oscillation. - *Paleoceanography* **21**, PA1008.
- KNOBLAUCH, C., JØRGENSEN, B., 1999: Effect of temperature on sulfate reduction, growth rate and growth yield in five psychrophilic sulphate-reducing bacteria from arctic sediments. - *Environ. Microbiol* **1**, 457-467.

- KOTOV, P., HARFF, J., 2006: A Comparison of Greenland Ice and Baltic Sea Sediment Record - A Contribution to Climate Change Analysis. - *Mathematical Geology* **38**(6): 721-733.
- KRAWCZYK, D., WITKOWSKI, A., MOROS, M., LLOYD, J.M., KUIJPERS, A., KIERZEK, A., 2010: Late-Holocene diatom-inferred reconstruction of temperature variations of the west Greenland current from Disko Bugt, central west Greenland. - *Holocene* **20**, 659-666.
- KRAWCZYK, D.W., WITKOWSKI, A., WRONIECKI, M., WANIEK, J.J., KURZYDŁOWSKI, K.J., PLOCINSKI, T., 2012: Hydrological consequences of the reinterpretation of two diatom species from the West Greenland margin - *Thalassiosira kushirensis* and *Thalassiosira antarctica* var. *borealis*. - *Marine Micropaleontology* **88-89**, 1-14.
- KRAWCZYK, D.W., WITKOWSKI, A., LLOYD, J.M., MOROS, M., HARFF, J., KUIJPERS, A., 2013: Late-Holocene diatom derived seasonal variability in hydrological conditions off Disko Bugt, west Greenland. - *Quat. Sci. Rev.* **67**, 93-104.
- KRAWCZYK, D.W., WITKOWSKI, A., WANIEK, J.J., WRONIECKI, M., HARFF, J., 2014: Description of diatoms from the Southwest to West Greenland coastal and open marine waters. - *Polar Biology* **37**, 1589-1606.
- LISITZIN, A.P., SHEVCHENKO, V.P., BURENKOV, V.I., KOPELEVICH, O.V., VASILIEV, L.YU., 2003: Suspended matter and hydrooptics of the White Sea – new regularities of quantitative distribution and granulometry. In: LAVEROV, N.P., VINOGRADOV, M.E., LISITZIN, A.P., LAPPO, S.S., LOBKOVSKY, L.I. (eds): *Actual Problems of Oceanology*, Nauka, pp.554-605 (in Russian).
- LLOYD, J.M., MOROS, M., PERNER, K., TELFORD, R.J., KUIJPERS, A., JANSEN, E., MCCARTHY, D., 2011: A 100 year record of ocean temperature control on the stability of Jakobshavn Isbrae, West Greenland. - *Geology* **39**, 867-870.
- MOROS, M., JENSEN, K.G., KUIJPERS, A., 2006: Mid- to late-Holocene hydrological and climatic variability in Disko Bugt, central West Greenland. - *The Holocene* **16**(3), 357-367.
- MOROS, M., LLOYD, J.M., PERNER, K., KRAWCZYK, D., BLANZ, T., DE VERNA, A., OUELLET-BERNIER, M.M., KUIJPERS, A., JENNINGS, A.E., WITKOWSKI, A., SCHNEIDER, R., JANSEN, E., 2016: Surface and sub-surface multi-proxy reconstruction of mid to late Holocene palaeoceanographic changes in Disko Bugt, West Greenland. - *Quaternary Science Reviews* **132**, 146-160.
- OUELLET-BERNIER, M.-M., DE VERNAL, A., HILLAIRE-MARCEL, C., MOROS, M., 2014: Paleoceanographic changes in the Disko Bugt area, west Greenland, during the Holocene. - *Holocene* **24**, 1573-1583.
- PERNER, K., LEIPE, T., DELLWIG, O., KUIJPERS, A., MIKKELSEN, N., ANDERSEN, T.J., HARFF, J., 2010: Contamination of arctic Fjord sediments by Pb-Zn mining at Maarmorilik in central West Greenland. - *Marine pollution bulletin* **60**, 1065-1073.
- PERNER, K., MOROS, M., LLOYD, J.M., KUIJPERS, A., TELFORD, R.J., HARFF, J., 2011: Centennial scale benthic foraminiferal record of late Holocene oceanographic variability in Disko Bugt, West Greenland. - *Quaternary Science Reviews* **30**, 2815-2826.
- PERNER, K., MOROS, M., JENNINGS, A., LLOYD, J.M., KNUDSEN, K.L., 2013a: Holocene palaeoceanographic evolution off West Greenland. - *Holocene* **23**, 374-387.
- PERNER, K., MOROS, M., SNOWBALL, I., LLOYD, J.M., KUIJPERS, A., RICHTER, T., 2013b: Establishment of modern circulation pattern at c. 6000 cal a BP in Disko Bugt, central West Greenland: opening of the Vaigat Strait. - *Journal of Quaternary Science* **28**, 480-489.

- RIBEIRO, S., MOROS, M., ELLEGAARD, M., KUIJPERS, A., 2012: Climate variability in west Greenland during the past 1500 years: evidence from a high-resolution marine palynological record from Disko Bay. - *Boreas* **41**, 68-83.
- RICHTER, T.O., VAN DER GAAST, S., KOSTER, B., VAARS, A., GIELES, R., DE STIGTER, H.C., DE HAAS, H., VAN WEERING, T.C.E., 2006: The Avaatech XRF Core scanner: technical description and applications to NE Atlantic sediments. In: ROTHWELL, R.G. (ed.): *New Techniques in Sediment Core Analysis*, Geol. Soc. London Spec. Publ. **267**, 39-50.
- RICHTER, A., RYSGAARD, S., DIETRICH, R., MORTENSEN, J., PETERSEN, D., 2010: Coastal tides in West Greenland derived from tide gauge records. - *Ocean Dynamics* **61**(1), 39-49.
- RISGAARD-PETERSEN, N., LANGEZAAL, A.M., INGVARSDEN, S., SCHMID, M.C., JETTEN, M.S.M., OP DEN CAMP, H.J.M., DERKENSEN, J.W.M., PINA-OVHOA, E., ERIKSSON, S.P., NIELSEN, L.P., REVSBECH, N.P., CEDHAGEN, T., VAN DER ZWAAN G.J., 2006: Evidence for complete denitrification in a benthic foraminifer. - *Nature* **443**, 93-96.
- RYSGAARD, S., THAMDRUP, B., RISGAARD-PETERSEN, N., FOSSING, H., BERG, P., CHRISTENSEN, P.B., DALSGAARD, T., 1998: Seasonal carbon and nitrogen mineralization in a high-Arctic coastal marine sediment, Young Sound Northeast Greenland. - *Marine Ecology Progress Series* **175**, 261-276.
- SHEVCHENKO, V., 2003: The influence of aerosols on the oceanic sedimentation and environmental conditions in the Arctic. - *Berichte zur Polar- und Meeresforschung* **464**, 149 pp.
- SHEVCHENKO, V.P., DOLOTOV, Y.S., FILATOV, N.N., ALEXEEVA, T.N., FILIPPOV, A.S., NÖTHIG, E.-M., NOVIGATSKY, A.N., PAUTOVA, L.A., PLATONOV, A.V., POLITOVA, N.V., RAT'KOVA, T.N., STEIN, R., 2005: Biogeochemistry of the Kem' River estuary, White Sea (Russia). - *Hydrology and Earth System Sciences* **9**, 57-66.
- THOMASSEN, B., 2003: The Black Angel lead zinc mine at Maarmorilik in West Greenland. - *Geology and ore* **2**, 12 pp.
- WANNER, H., BEER, J., BÜTIKOFER, J., CROWLEY, T.J., CUBASCH, U., FLÜCKIGER, J., GOOSSE, H., GROSJEAN, M., JOOS, F., KAPLAN, J.O., KÜTTEL, M., MÜLLER, S., PRENTICE, I.C., SOLOMINA, O., STOCKER, T.F., TARASOV, P., WAGNER, M., WIDMANN, M., 2008: Mid- to late Holocene climate change: an overview. - *Quaternary Sci. Rev.* **27**, 1791-1828.
- WANNER, H., SOLOMINA, O., GROSJEAN, M., RITZ, S. P., JETEL, M., 2011: Structure and origin of Holocene cold events. - *Quaternary Science Reviews* **30**, 3109-3123.
- ICES ACME Report, 1996: Guidelines for the determination of chlorbiphenyls in sediments: Analytical Methods.
- ICES ACME Report, 1997: Determination of Polycyclic Aromatic Hydrocarbons (PAHs) in Sediments: Analytical Methods.
- ICES ACME Report 1998 and Annex B-11, Determination of Polycyclic Aromatic Hydrocarbons (PAHs) in Biota: Analytical Methods.

## Enclosures

1. Cruise protocol
2. Cruise track plot
3. Station / Profile List
4. Nutrient, chlorophyll a and SPM data
5. Multibeam echosounder maps
6. Parasound Profiles / Core stations
7. Core Lists
8. Sample Lists
9. Lithological core descriptions
10. XRF-Scans / Metadata plus selected plots
11. Magnetic susceptibility (MS) scanning of sediment cores collected during MSM05/03
12. Abstracts of seminars

## 1. Cruise protocol

MSM 05/03  
Protocol

Date y:2007	UTC	Action	Device/ Scientist	Profile / Station
June 14	12:00	boarding		
		Scientific presentation		
	19:00	J. Harff: Expedition MSM 05/03 – targets and program.-		
June 15	12:30-	Departure Nuuk harbour		
	12:30- 24:00	Profiling	Parasound, multibeam echosounder (deep), ADCP / Dr. Endler, Dr. Jensen, G. Nickel, W. Weinrebe	Transit 1
		Scientific presentation		
	21:00	R. Dietrich, A. Richter: Vertical crustal movement in Western Greenland.-		
June 16	00:00- 09:45	Profiling	Parasound, multibeam echosounder (deep) / Dr. Endler, Dr. Jensen, G. Nickel, W. Weinrebe ADCP / Dr. J. Waniek	Transit 1
	09:45- 17:00	Profiling	Parasound, multibeam echosounder (deep) / Dr. Endler, Dr. Jensen, G. Nickel, W. Weinrebe ADCP / Dr. J. Waniek	PN
	17:10- 02:00 (16.6.)	Boat expedition to install geodetic stations	GPS-receiver / Prof. R. Dietrich, Dr. A. Richter, Dr. T. Leipe	Land- station NSOF
	17:25- 20:45	Hydrographic measurement, Hydrochemical sampling, Sediment sampling	CTD, boxcorer, multicorer, gravity corer / Dr. J. Waniek, Dr. B. Hentzsch, Dr. M. Moros, Dr. T. Leipe	343250
June 17	02:45- 04:25	Profiling	Parasound, multibeam echosounder (shallow) / Dr. Endler, Dr. Jensen, G. Nickel, W. Weinrebe ADCP / Dr. J. Waniek	PN

	10:45-13:05	Boat expedition to install geodetic stations, sampling diatoms	GPS-receiver, pressure gauge / Prof. R. Dietrich, Dr. A. Richter, Prof. A. Witkowski	Land-station NS-Center
	11:15-17:20	Hydrographic measurement, Hydrochemical sampling, Sediment sampling	GPS-boye / Prof. R. Dietrich; CTD, multicorer, gravity corer / Dr. J. Waniek, Dr. B. Hentzsch, Dr. M. Moros, Dr. T. Leipe	343260
	17:25-19:30	Profiling	Parasound, multibeam echosounder (shallow) / Dr. Endler, Dr. Jensen, G. Nickel, W. Weinrebe ADCP / Dr. J. Waniek	PN
	19:40-21:00	Hydrographic measurement, Hydrochemical sampling, Sediment sampling	GPS-boye / Prof. R. Dietrich; CTD / Dr. J. Waniek, Dr. B. Hentzsch; multicorer, Dr. M. Moros, Dr. T. Leipe	343270
	21:10-00:10 (18.6.)	Profiling	Parasound, multibeam echosounder (shallow) / Dr. Endler, Dr. Jensen, G. Nickel, W. Weinrebe ADCP / Dr. J. Waniek	PN
June 18	00:20-04:00	Hydrographic measurement, Hydrochemical sampling, Sediment sampling	CTD, multicorer, gravity corer / Dr. J. Waniek, Dr. B. Hentzsch, Dr. M. Moros, Dr. T. Leipe	243280
	04:00-06:30	Profiling (continuation)	Parasound, multibeam echosounder (shallow) / Dr. Endler, Dr. Jensen, G. Nickel, W. Weinrebe ADCP / Dr. J. Waniek	PN
	10:45-13:35	Boat expedition to install geodetic stations, sampling diatoms	GPS-receiver, pressure gauge / Prof. R. Dietrich, Dr. A. Richter, Prof. A. Witkowski, A. Frahm	Land-station NS-Mouth
	11:30-11:55	Hydrographic measurement, Hydrochemical sampling: Failed due to strong currents Sediment sampling: Failed	GPS-boye / Prof. R. Dietrich; CTD / Dr. J. Waniek, Dr. B. Hentzsch; Boxcorer, Dr. M. Moros, Dr. T. Leipe	343290
	15:00-16:45	Maintainance of multi-channel echosounder DG1		

	17:00-24:00	Profiling	Parasound, multibeam echosounder (deep) / Dr. Endler, Dr. Jensen, G. Nickel, W. Weinrebe ADCP / Dr. J. Waniek	PDB1
	Scientific presentations			
	16:30	J. Lloyd: Ice streams, climate and ocean circulation in Disko Bugt.-		
	21:00	T. Richter: XRF core scanning: Principles and applications to North Atlantic paleoceanography.-		
June 19	00:00-09:30	Profiling	Parasound, multibeam echosounder (deep) / Dr. Endler, Dr. Jensen, G. Nickel, W. Weinrebe ADCP / Dr. J. Waniek	PDB1
	11:05-14:15	Hydrographic measurement, Hydrochemical sampling, Sediment sampling	GPS-boye / Prof. R. Dietrich; CTD / Dr. J. Waniek, Dr. B. Hentzsch; Multicorer, Garvity corer / Dr. M. Moros, Dr. T. Leipe	343300
	15:50-23:15	Hydrographic measurement, Hydrochemical sampling, Sediment sampling	CTD / Dr. J. Waniek, Dr. B. Hentzsch; Multicorer, Garvity corer / Dr. M. Moros, Dr. T. Leipe	343310
June 20	02:35-09:25	Profiling	Parasound, multibeam echosounder (deep) / Dr. Endler, Dr. Jensen, G. Nickel, W. Weinrebe ADCP / Dr. J. Waniek	PDB1
	10:15-15:45	Hydrographic measurement, Hydrochemical sampling, Sediment sampling	GPS-boye / Prof. R. Dietrich; CTD / Dr. J. Waniek, Dr. B. Hentzsch; Multicorer, Garvity corer / Dr. M. Moros, Dr. T. Leipe	343340
	20:30-23:30	Hydrographic measurement, Hydrochemical sampling, Sediment sampling	GPS-boye / Prof. R. Dietrich; CTD / Dr. J. Waniek, Dr. B. Hentzsch; Multicorer, Garvity corer / Dr. M. Moros, Dr. T. Leipe	343320
June 21	00:40-02:20	Hydrographic measurement, Hydrochemical sampling, Sediment sampling	CTD / Dr. J. Waniek, Dr. B. Hentzsch; Multicorer, Garvity corer / Dr. M. Moros, Dr. T. Leipe	343320

	02:30-15:40	Profiling	Parasound, multibeam echosounder (deep) / Dr. Endler, Dr. Jensen, G. Nickel, W. Weinrebe ADCP / Dr. J. Waniek	PDB2
	16:05-24:00	Profiling	Parasound, multibeam echosounder (shallow) / Dr. Endler, Dr. Jensen, G. Nickel, W. Weinrebe ADCP / Dr. J. Waniek	PDB2
	Scientific presentations			
	12:00	N. Mikkelsen: Ilulissat Icefjord – a UNESCO World Heritage area seen in climatic perspective.-		
	14:30	I. Snowball, P. Sandgren, R. Muscheler: Palaeomagnetic secular variations and palaeointensity at high northern latitudes.-		
	21:00	S. Rysgaard, N. Risgaard-Petersen et al.: Early diagenesis in Greenlandic marine sediments.-		
June 22	00:00-14:15	Profiling	Parasound, multibeam echosounder (shallow) / Dr. Endler, Dr. Jensen, G. Nickel, W. Weinrebe ADCP / Dr. J. Waniek	PDB3
	14:20-15:00	Hydrographic measurement, Hydrochemical sampling,	GPS-boye / Prof. R. Dietrich; CTD / Dr. J. Waniek, Dr. B. Hentzsch;	343350
	17:30 - 21:55	Hydrographic measurement, Hydrochemical sampling, Sedimentological sampling	GPS-boye / Prof. R. Dietrich; CTD / Dr. J. Waniek, Dr. B. Hentzsch; Multicorer, Gravity corer / Dr. M. Moros, Dr. T. Leipe	343360
	22:10-23:30	Profiling	Parasound, multibeam echosounder (shallow) / Dr. Endler, Dr. Jensen, G. Nickel, W. Weinrebe ADCP / Dr. J. Waniek	PV
June 23	00:00-08:45	Profiling	Parasound, multibeam echosounder (shallow) / Dr. Endler, Dr. Jensen, G. Nickel, W. Weinrebe ADCP / Dr. J. Waniek	PV
	11:00-13:30	Boat expedition to install geodetic stations, sampling diatoms	GPS-receiver, pressure gauge / Prof. R. Dietrich, Dr. A. Richter, Prof. A. Witkowski, Dr. Mikkelsen	NUGS

	11:50-12:20	Hydrographic measurement, Hydrochemical sampling, sediment sampling	CTD / Dr. J. Waniek, Dr. B. Hentzsch;	343370
	14:10-16:50	Profiling	Parasound, multibeam echosounder (shallow) / Dr. Endler, Dr. Jensen, G. Nickel, W. Weinrebe ADCP / Dr. J. Waniek	PV
	17:45-19:55	Hydrographic measurement, Hydrochemical sampling, sediment sampling	CTD / Dr. J. Waniek, Dr. B. Hentzsch; Multicorer, Garvity corer / Dr. M. Moros, Dr. T. Leipe	343380
	20:00-22:00	Profiling	Parasound, multibeam echosounder (shallow) / Dr. Endler, Dr. Jensen, G. Nickel, W. Weinrebe ADCP / Dr. J. Waniek	PV
	22:10-23:50	Hydrographic measurement, Hydrochemical sampling, sediment sampling	GPS-boye / Prof. R. Dietrich; CTD / Dr. J. Waniek, Dr. B. Hentzsch; Multicorer, Garvity corer / Dr. M. Moros, Dr. T. Leipe	343390
24.6.07	00:00-03:40	Profiling	Parasound, multibeam echosounder (shallow) / Dr. Endler, Dr. Jensen, G. Nickel, W. Weinrebe ADCP / Dr. J. Waniek	PDB2
	03:50-04:20	Hydrographic measurement,	CTD / Dr. J. Waniek, Dr. B. Hentzsch;	343400
	04:25-11:50	Profiling	Parasound, multibeam echosounder (shallow) / Dr. Endler, Dr. Jensen, G. Nickel, W. Weinrebe ADCP / Dr. J. Waniek	PDB2
	12:00-12:55	Hydrographic measurement, Hydrochemical sampling, sediment sampling	CTD / Dr. J. Waniek, Dr. B. Hentzsch; Multicorer / Dr. M. Moros, Dr. T. Leipe	343410
	13:00-19:50	Profiling	Parasound, multibeam echosounder (deep) / Dr. Endler, Dr. Jensen, G. Nickel, W. Weinrebe ADCP / Dr. J. Waniek	PDB2
	20:00-21:30	Exchange of visitors		

	21:30-24:00	Profiling	Parasound, multibeam echosounder (deep) / Dr. Endler, Dr. Jensen, G. Nickel, W. Weinrebe ADCP / Dr. J. Waniek	PV
25.6.07	00:00-19:00	Profiling	Parasound, multibeam echosounder (deep) / Dr. Endler, Dr. Jensen, G. Nickel, W. Weinrebe ADCP / Dr. J. Waniek	PU1
	Scientific presentation			
	12:00-13:00	A. Witkowski: Limnology of western Iran.-		
	19:00-21:00	Exchange of scientists		
	21:00-24:00	Profiling	Parasound, multibeam echosounder (deep) / Dr. Endler, Dr. Kuijpers, G. Nickel, W. Weinrebe ADCP / Dr. J. Waniek	PU1
26.6.07	00:00-04:30	Profiling	Parasound, multibeam echosounder (deep) / Dr. Endler, Dr. Kuijpers, G. Nickel, W. Weinrebe ADCP / Dr. J. Waniek	PU1
	04:30-05:15	Hydrographic measurement, Hydrochemical sampling	CTD / Dr. J. Waniek, Dr. B. Hentzsch;	343420
	05:00-10:10	Profiling	Parasound, multibeam echosounder (deep) / Dr. Endler, Dr. Kuijpers, G. Nickel, W. Weinrebe ADCP / Dr. J. Waniek	PU1
	10:10-15:10	Hydrographic measurement, Hydrochemical sampling, sediment sampling	CTD / Dr. J. Waniek, Dr. B. Hentzsch; Multicorer, gravity corer / Dr. M. Moros, Dr. T. Leipe	343430
	15:15-17:55	Profiling	Parasound, multibeam echosounder (deep) / Dr. Endler, Dr. Kuijpers, G. Nickel, W. Weinrebe ADCP / Dr. J. Waniek	PU1
	18:30-22:00	Hydrographic measurement, Hydrochemical sampling	CTD, water pump / Dr. J. Waniek, E. Trost	343440

	22:00-24:00	Profiling	Parasound, multibeam echosounder (deep) / Dr. Endler, Dr. Kuijpers, G. Nickel, W. Weinrebe ADCP / Dr. J. Waniek	PU2
27.6.07	00:00-09:00	Profiling	Parasound, multibeam echosounder (deep) / Dr. Endler, Dr. Kuijpers, G. Nickel, W. Weinrebe ADCP / Dr. J. Waniek	PU2
	11:20-13:30	Boat expedition to install geodetic stations, sampling diatoms, surface water	GPS-receiver / Prof. J.Harff. Dr. T. Leipe, Dr. A. Richter, M. Donnerhak	WGNR
	11:30-13:30	Hydrographic measurement, Hydrochemical sampling, sediment sampling	CTD / Dr. J. Waniek, Dr. B. Hentzsch; Multicorer, gravity corer, box-corer / Dr. M. Moros, Dr. T. Leipe	343450
	13:35-14:50	Profiling	Parasound, multibeam echosounder (deep) / Dr. Endler, Dr. Kuijpers, G. Nickel, W. Weinrebe ADCP / Dr. J. Waniek	PU2
	14:55-16:20	sediment sampling	GPS-boye / Prof. R. Dietrich; Boxcorer, gravity corer / Dr. M. Moros, Dr. T. Leipe	343460
	16:25-17:10	Profiling	Parasound, multibeam echosounder (shallow) / Dr. Endler, Dr. Kuijpers, G. Nickel, W. Weinrebe ADCP / Dr. J. Waniek	PU2
	17:15-19:15	sediment sampling	Boxcorer, gravity corer / Dr. M. Moros, Dr. T. Leipe	343470
	19:20-20:05	Profiling	Parasound, multibeam echosounder (shallow) / Dr. Endler, Dr. Kuijpers, G. Nickel, W. Weinrebe ADCP / Dr. J. Waniek	PU2
	20:10-21:30	Hydrographic measurement, Hydrochemical sampling, sediment sampling	GPS-boye / Prof. R. Dietrich; CTD / Dr. J. Waniek, Dr. B. Hentzsch; Multicorer / Dr. M. Moros, Dr. T. Leipe	343480

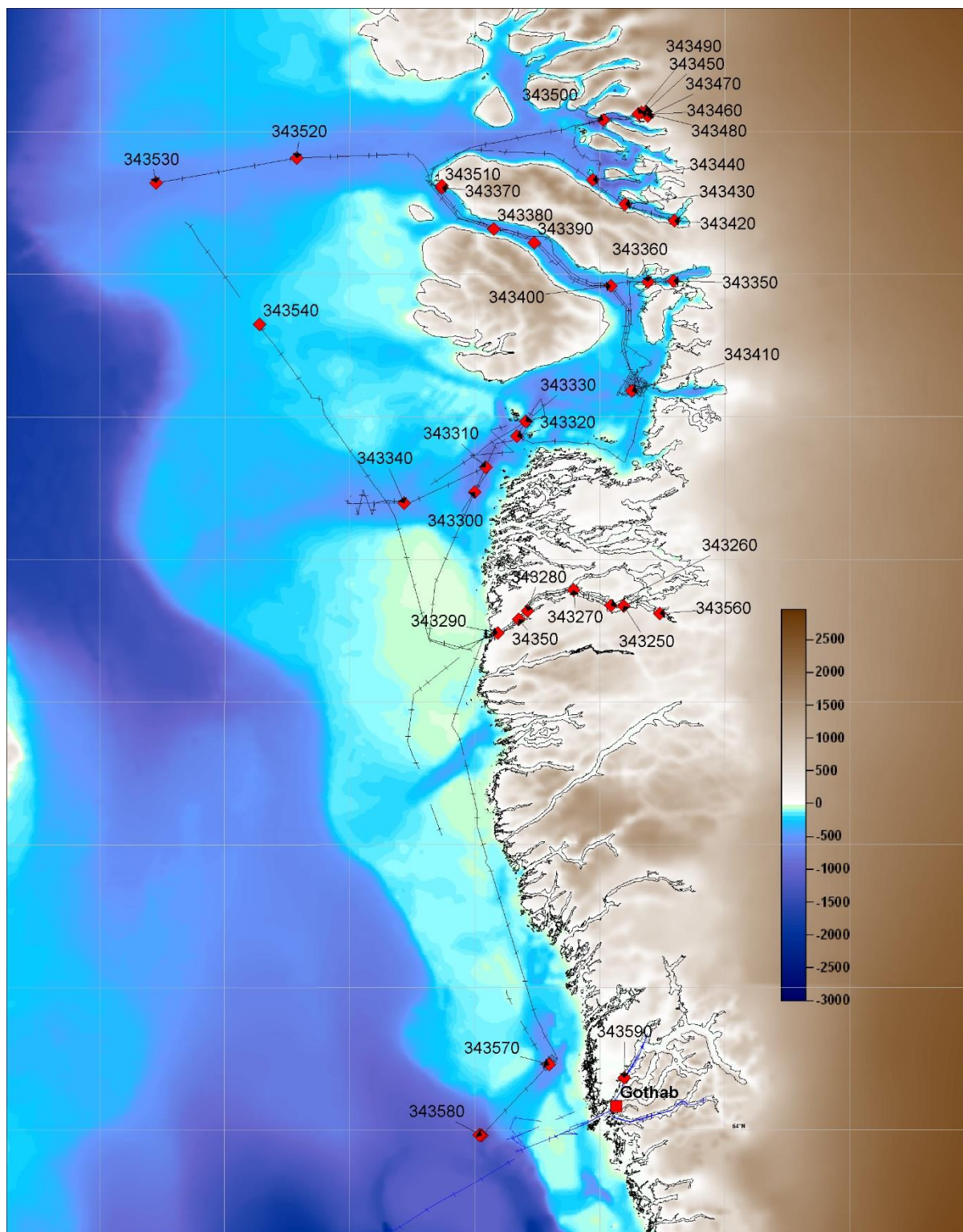
	21:35-21:55	Profiling	Parasound, multibeam echosounder (shallow) / Dr. Endler, Dr. Kuijpers, G. Nickel, W. Weinrebe ADCP / Dr. J. Waniek	PU2
	22:00-23:10	Hydrographic measurement, Hydrochemical sampling, sediment sampling	GPS-boye / Prof. R. Dietrich; CTD / Dr. J. Waniek, Dr. B. Hentzsch; Multicorer / Dr. M. Moros, Dr. T. Leipe	343490
	23:15-00:40 (28.6.07)	Profiling	Parasound, multibeam echosounder (shallow) / Dr. Endler, Dr. Kuijpers, G. Nickel, W. Weinrebe ADCP / Dr. J. Waniek	PU2
28.6.07	00:45-03:20	Hydrographic measurement, Hydrochemical sampling, sediment sampling	CTD / Dr. J. Waniek, Dr. B. Hentzsch; Multicorer, gravity corer / Dr. M. Moros, Dr. T. Leipe	343500
	03:25-10:55	Profiling	Parasound, multibeam echosounder (deep) / Dr. Endler, Dr. Kuijpers, G. Nickel, W. Weinrebe ADCP / Dr. J. Waniek	PU3
	11:00-12:50	Boat expedition to pick up geodetic stations, sampling surface water	GPS-receiver / Prof. R. Dietrich, Dr. A. Richter, M. Donnerhak	NUGS
	11:15-11:45	Hydrographic measurement, Hydrochemical sampling	CTD / Dr. J. Waniek, Dr. B. Hentzsch;	343510
	13:00-17:25	Profiling	Parasound, multibeam echosounder (deep) / Dr. Endler, Dr. Kuijpers, G. Nickel, W. Weinrebe ADCP / Dr. J. Waniek	PU3
	17:30-19:30	Hydrographic measurement, Hydrochemical sampling, sediment sampling	GPS-boye / Prof. R. Dietrich; CTD / Dr. J. Waniek, Dr. B. Hentzsch; Multicorer, gravity corer / Dr. M. Moros, Dr. T. Leipe	343520
	19:40-23:40	Profiling	Parasound, multibeam echosounder (deep) / Dr. Endler, Dr. Kuijpers, G. Nickel, W. Weinrebe ADCP / Dr. J. Waniek	PU3

	23:45-08:30 (29.6.)	Hydrographic measurement, Hydrochemical sampling, sediment sampling Water pumping	GPS-boye / Prof. R. Dietrich; CTD, water pump / Dr. J. Waniek, Dr. B. Hentzsch, E. Trost; Multicorer / Dr. M. Moros, Dr. T. Leipe	343530
June 29	08:35-14:20	Profiling	Parasound, multibeam echosounder (deep) / Dr. Endler, Dr. Kuijpers, G. Nickel, W. Weinrebe ADCP / Dr. J. Waniek	PUN
	14:25-15:15	Hydrographic measurement, Hydrochemical sampling, sediment sampling	GPS-boye / Prof. R. Dietrich; CTD, / Dr. J. Waniek, Dr. B. Hentzsch; Multicorer / Dr. M. Moros, Dr. T. Leipe	343540
	15:20-00:00	Profiling	Parasound, multibeam echosounder (deep) / Dr. Endler, Dr. Kuijpers, G. Nickel, W. Weinrebe ADCP / Dr. J. Waniek	PUN
	Scientific presentation			
	21:00-22:00	A. Kuijpers: Icebergs and palaeoceanographic changes around Greenland.-		
June 30	00:00-05:25	Profiling	Parasound, multibeam echosounder (deep) / Dr. Endler, Dr. Kuijpers, G. Nickel, W. Weinrebe ADCP / Dr. J. Waniek	PN
	06:00-12:00	Boat expedition to pick up geodetic stations, sampling surface water	GPS-receiver / Prof. R. Dietrich, Dr. A. Richter, M. Donnerhak	NSOF, NS Center
	12:00-14:00	Profiling	Parasound, multibeam echosounder (deep) / Dr. Endler, Dr. Kuijpers, G. Nickel, W. Weinrebe ADCP / Dr. J. Waniek	PN
	14:10-16:25	Hydrographic measurement, Hydrochemical sampling, sediment sampling	GPS-boye / Prof. R. Dietrich; UW Camera / A.Frahm; Multicorer, gravity corer / Dr. M. Moros, Dr. T. Leipe	343560

	16:30-00:40 (1.7.07)	Profiling	Parasound, multibeam echosounder (deep) / Dr. Endler, Dr. Kuijpers, G. Nickel, W. Weinrebe ADCP / Dr. J. Waniek	PNS
Scientific presentation				
	22:00-23:00	V. Shevshenko: Eolian and ice transport of sedimentary matter in the Arctic.-		
July 1	00:55-02:50	Hydrographic measurement, Hydrochemical sampling, sediment sampling	GPS-boye / Prof. R. Dietrich; CTD,/ Dr. J. Waniek, Dr. B. Hentzsch; Multicorer, gravity-corer / Dr. M. Moros, Dr. T. Leipe	343550
	03:10-00:00	Profiling	Parasound, multibeam echosounder (deep) / Dr. Endler, Dr. Kuijpers, G. Nickel, W. Weinrebe ADCP / Dr. J. Waniek	PNS
	09:00-11:30	Boat expedition to pick up geodetic stations, sampling surface water	GPS-receiver / Prof. R. Dietrich, Dr. A. Richter, M. Donnerhak	NSOF, NS Mouth
Scientific presentations				
	22:00-23:00	J. Harff, R. Endler, S. Kotov: Variation of Late Quaternary climate of the North Atlantic – Baltic realm as reflected in the sediments of the central Baltic Sea.- N. Mikkelsen, J. Harff, J. Thiede: Alfred Wegener in Greenland and his time.-		
July 2	00:00-10:20	Profiling	Parasound, multibeam echosounder (deep) / Dr. Endler, Dr. Kuijpers, G. Nickel, W. Weinrebe ADCP / Dr. J. Waniek	PNS
	11:00-12.45	Hydrographic measurement, Hydrochemical sampling, sediment sampling	GPS-boye / Prof. R. Dietrich; UW Camera / A.Frahm; CTD / Dr. J. Waniek, Dr. B. Hentzsch; Multicorer, gravity-corer / Dr. M. Moros, Dr. T. Leipe	343570
	13:00-16:20	Profiling	Parasound, multibeam echosounder (deep) / Dr. Endler, Dr. Kuijpers, G. Nickel, W. Weinrebe ADCP / Dr. J. Waniek	PNN

	16:30-01:40 (3.7.07)	sediment sampling	GPS-boye / Prof. R. Dietrich; CTD, water pump / Dr. J. Waniek, Dr. B. Hentzsch; Multicorer / Dr. M. Moros, Dr. T. Leipe	343580
July 3	01:45-05:50	Profiling	Parasound, multibeam echosounder (deep) / Dr. Endler, Dr. Kuijpers, G. Nickel, W. Weinrebe ADCP / Dr. J. Waniek	PG
	06:40-08:00	Profiling	Parasound, multibeam echosounder (deep) / Dr. Endler, Dr. Kuijpers, G. Nickel, W. Weinrebe ADCP / Dr. J. Waniek	PG
	08:10-16:00	Hydrographic measurement, Hydrochemical sampling, sediment sampling	GPS-boye / Prof. R. Dietrich; CTD / Dr. J. Waniek, Dr. B. Hentzsch; Multicorer, gravity-corer / Dr. M. Moros, Dr. T. Leipe	343590
	16:30-00:00	Profiling	Parasound, multibeam echosounder (deep) / Dr. Endler, Dr. Kuijpers, G. Nickel, W. Weinrebe ADCP / Dr. J. Waniek	PG
	Scientific presentation			
	22:00-23:00	J. Waniek: Azores Front, Saharan dust, and the biogeochemical properties of the Madeira Abyssal Plain (subtropical NE Atlantic).-		
July 4	00:00-10:00	Profiling	Parasound, multibeam echosounder (deep) / Dr. Endler, Dr. Kuijpers, G. Nickel, W. Weinrebe ADCP / Dr. J. Waniek	PG
	14:00	Nuuk: End of expedition		

## 2. Cruise track plot





## MSM 05/03 Station list

<b>Nordre Strømfjord</b>					
<b>IOW-Station</b>	<b>Station</b>	<b>Yd-°N</b>	<b>ymin</b>	<b>Xd-°w</b>	<b>xmin</b>
343250	CTD, multicorer, boxcorer, gravity corer	67	40.478	51	36.930
Land station NSOF	GPS site Pressure gauge deployment	67	54.00	50	27.00
Land station NS Center	GPS site Pressure gauge deployment	67	41.00	51	45.00
Land station NS Mouth	GPS site Pressure gauge deployment	67	29.00	53	38.00
343260	CTD, MUC, GC	67	40.60	51	49.06
343270	CTD	67	47.16	52	25.2
343280	CTD, MUC, GC	67	38.46	53	09.46
343290	GPS-Boye, CTD, BC	67	29.00	53	38.00
343550	GPS-Boye, CTD, MUC, GC	67	34.891	53	17.998
343560	Camera, MUC, GC	67	37.335	51	02.249
<b>Disko Bay/Vaigat</b>					
343300	GPS-Boye, CTD, MUC, GC	68	28.312	54	00.122
343310	GPS-Boye, CTD, MUC, GC	68	38.872	53	49.493
343320	GPS-Boye, CTD, MUC, GC	68	51.880	53	19.720
343330	GPS-Boye, CTD, MUC, GC	68	58.077	53	11.109
343340	GPS-Boye, CTD, MUC, GC	68	23.838	55	07.790
343350	GPS-Boye, CTD	69	57.20	50	49.34
343360	GPS-Boye, CTD, MUC, GC	69	56.836	51	13.637
343370	GPS-Boye, CTD	70	41.80	54	35.80
343380	CTD, MUC, GC	70	19.043	53	41.697
343390	CTD, MUC, GC	70	13.178	53	03.320
343400	CTD	69	55.09	51	49.310
343410	CTD	69	10.998	51	29.499
<b>Uummannaq Fjord</b>					
343420	CTD	70	22.62	50	48.72
343430	CTD, MUC, GC	70	29.570	51	37.117
343440	CTD, water pump	70	39.786	52	06.479
343450	CTD, MUC, GC	71	08.368	51	15.409
343460	BC, GC	71	07.152	51	15.321
343470	BC, GC	71	06.490	51	13.952
343480	GPS-Boye, CTD, MUC	71	08.030	51	20.230
343490	GPS-Boye, CTD, MUC	71	07.474	51	22.966
343500	GPS-Boye, CTD, MUC	71	04.889	51	56.855
<b>Westgreenland Shelf</b>					
343510	CTD	70	37.38	54	32.05
343520	CTD, MUC	70	48.95	56	50.90
343530	CTD, MUC, Pump station	70	38.40	59	06.00
343540	GPS-Boye, CTD, MUC	69	38.959	57	26.931
343570	GPS-Boye, CTD, MUC, GC	64	27.586	52	48.380
343580	GPS-Boye, CTD, MUC, Pump ST.	63	57.802	53	53.012
<b>Godthabsfjord</b>					
343590	GPS-Boye, CTD, MUC, Pump station	64	18.836	51	37.936

#### 4. Nutrient, chlorophyll a and SPM data

Nutrient, chlorophyll a and SPM samples measured during MSM05/03 (n.d.= no data; red numbers indicate measurements at detection limit) are listed within the table below.

Station No.	Date	UTC	Latitude		Longitude		Depth m	SPM mg/l	Chla $\mu\text{g/l}$	NO <sub>2</sub>	NO <sub>3</sub>	PO <sub>4</sub>	SiO <sub>4</sub>
			N	W	$\mu\text{mol/l}$								
34 32 50	16.06.07	17:50	67°40,479'	51°36,926	350	0,91	0,103	0,14	8,74	0,72	6,55		
					250	0,96	0,152	0,14	8,05	0,67	5,55		
					150	0,71	0,195	0,13	8,56	0,68	5,80		
					100	0,85	0,269	0,12	7,92	0,66	5,15		
					80	15,62	0,294	0,13	7,62	0,66	4,50		
					60	1,44	0,307	0,11	7,17	0,58	4,10		
					40	1,05	1,044	0,12	6,48	0,55	3,45		
					30	0,91	2,170	0,11	5,36	0,47	2,90		
					20	1,06	3,158	0,10	4,20	0,40	3,00		
					10	1,07	0,611	0,04	0,12	0,09	1,35		
34 32 60	17.06.07	11:11	67°40,599'	51°45,059	360	14,62	0,246	0,13	8,29	0,68	6,25		
					250	8,74	0,320	0,10	6,59	0,60	4,50		
					150	5,52	0,517	0,11	6,07	0,56	4,70		
					100	1,14	0,743	0,12	6,51	0,59	4,20		
					80	1,32	1,131	0,11	6,22	0,55	3,45		
					60	1,17	0,909	0,11	6,48	0,56	3,35		
					40	0,74	1,796	0,10	4,89	0,45	2,85		
					20	17,26	6,207	0,07	1,66	0,26	1,80		
5	10,28	1,380	0,05	0,11	0,09	1,40							
34 32 70	17.06.07	20:10	67°47,158'	52°25,198	500	1,06	0,525	0,10	6,16	0,60	3,90		
					400	n.d.	0,508	n.d.	n.d.	n.d.	n.d.		
					300	0,36	0,516	0,11	5,83	0,57	3,35		
					200	n.d.	1,211	n.d.	n.d.	n.d.	n.d.		
					150	1,26	1,433	0,06	3,68	0,45	2,50		
					100	1,75	1,735	0,11	3,21	0,41	1,40		
					80	4,17	2,134	0,08	3,29	0,40	1,80		
					60	1,35	2,152	0,10	3,96	0,42	1,40		
					40	3,28	2,842	0,10	3,65	0,40	1,00		
					20	1,40	4,477	0,08	2,07	0,27	0,90		
5	2,64	1,132	0,05	0,07	0,10	1,30							
34 32 80	18.06.07	00:42	67°38,459'	53°9,458	300	1,58	n.d.	0,08	1,74	0,33	1,20		
					200	n.d.	n.d.	n.d.	n.d.	n.d.	n.d.		
					150	0,52	1,448	0,07	1,45	0,31	1,70		
					100	2,18	1,394	0,07	1,52	0,30	1,20		
					80	n.d.	1,329	n.d.	n.d.	n.d.	n.d.		
					60	0,52	1,412	0,08	1,51	0,30	0,95		
					40	0,62	1,401	0,07	1,56	0,30	1,30		
					20	1,31	1,193	0,06	1,52	0,30	1,20		
5	1,58	0,968	0,07	1,43	0,29	1,05							
34 33 00	19.06.07	12:00	68°28,311'	54°0,118	495	1,13	n.d.	0,03	14,06	0,95	11,30		
					400	n.d.	n.d.	n.d.	n.d.	n.d.	n.d.		
					300	1,09	n.d.	0,03	13,48	0,90	9,60		
					200	1,45	n.d.	0,10	12,15	0,80	8,05		
					100	1,42	0,601	0,14	10,11	0,69	5,15		
					80	1,19	1,114	0,13	9,24	0,66	4,40		
					60	1,00	3,000	0,09	5,06	0,38	2,00		
					40	1,61	4,355	0,07	2,65	0,24	1,30		

					20	1,37	1,060	0,03	0,13	0,06	0,70
					5	0,47	0,488	0,03	0,08	0,05	0,40
34 33 10	19.06.07	16:30	68°38,872'	53°49,485	820	0,70	n.d.	0,02	14,19	0,95	11,80
					700	n.d.	n.d.	n.d.	n.d.	n.d.	n.d.
					500	1,42	n.d.	n.d.	n.d.	n.d.	10,75
					300	n.d.	n.d.	n.d.	n.d.	n.d.	n.d.
					200	0,92	n.d.	n.d.	n.d.	n.d.	4,70
					150	3,96	1,847	0,05	2,66	0,26	1,45
					100	1,36	1,135	0,08	3,00	0,35	2,00
					80	0,79	1,290	0,06	2,80	0,33	2,05
					60	1,06	1,401	0,07	2,57	0,31	1,80
					40	2,12	2,245	0,06	2,04	0,27	1,55
					20	2,92	3,065	0,08	1,83	0,26	1,50
				5	1,33	3,535	0,05	0,85	0,20	1,30	
34 33 40	20.06.07	11:08	68°23,837'	55°7.788	430	0,60	n.d.	0,01	15,15	0,98	12,10
					300	n.d.	n.d.	n.d.	n.d.	n.d.	n.d.
					200	1,05	n.d.	0,03	12,70	0,82	7,45
					150	n.d.	0,149	n.d.	n.d.	n.d.	n.d.
					100	1,92	0,455	0,12	11,49	0,76	5,70
					80	n.d.	1,344	n.d.	n.d.	n.d.	n.d.
					60	0,47	2,475	0,11	6,27	0,46	1,20
					40	n.d.	2,759	n.d.	n.d.	n.d.	n.d.
					20	0,50	0,516	0,01	0,01	0,02	0,30
					5	0,37	1,014	0,02	0,00	0,01	0,00
34 33 30	20.06.07	21:30	68°58,076'	53°11,102	700	1,68	n.d.	0,02	14,22	0,97	12,50
					500	n.d.	n.d.	n.d.	n.d.	n.d.	n.d.
					300	1,76	n.d.	0,16	13,04	0,90	10,35
					200	n.d.	n.d.	n.d.	n.d.	n.d.	n.d.
					150	2,93	0,244	0,12	10,24	0,75	6,85
					100	n.d.	0,384	n.d.	n.d.	n.d.	n.d.
					80	0,29	0,532	0,09	5,95	0,54	3,60
					60	n.d.	0,479	n.d.	n.d.	n.d.	n.d.
					40	0,77	0,439	0,06	3,23	0,34	1,45
					20	n.d.	0,747	n.d.	n.d.	n.d.	n.d.
				5	0,83	0,729	0,03	0,04	0,06	0,45	
34 33 20	20./21.06.07	01:00	68°51,879'	53°19,719	800	0,50	n.d.	0,04	14,05	0,96	11,80
					600	n.d.	n.d.	n.d.	n.d.	n.d.	n.d.
					400	1,18	n.d.	0,03	13,60	0,93	10,60
					200	n.d.	n.d.	n.d.	n.d.	n.d.	n.d.
					150	6,88	0,203	0,13	10,39	0,77	6,75
					100	n.d.	0,485	n.d.	n.d.	n.d.	n.d.
					80	0,60	0,666	0,10	5,40	0,54	3,60
					60	n.d.	0,717	n.d.	n.d.	n.d.	n.d.
					40	0,38	0,423	0,06	3,58	0,36	2,05
					20	n.d.	0,744	n.d.	n.d.	n.d.	n.d.
				5	0,54	0,846	0,03	0,10	0,05	0,35	
34 33 50	22.06.07	14:15	69°57,196'	50°49,338	700	1,12	n.d.	0,03	17,25	1,12	18,60
					600	n.d.	n.d.	n.d.	n.d.	n.d.	n.d.
					500	1,91	n.d.	0,02	16,70	1,08	17,30
					400	n.d.	n.d.	n.d.	n.d.	n.d.	n.d.
					200	2,81	n.d.	0,04	15,44	1,04	15,20
					150	1,26	n.d.	0,05	14,23	0,98	12,50
					100	1,17	n.d.	0,08	13,83	0,96	11,80
					80	1,12	n.d.	0,06	14,35	0,97	13,55
					60	1,76	n.d.	0,09	13,39	0,93	13,15
40	1,62	n.d.	0,08	12,04	0,87	11,95					

					20	2,03	n.d.	0,08	9,62	0,72	9,90
					5	2,84	n.d.	0,04	0,37	0,14	2,90
34 33 60	22.06.07	18:00	69°56,832'	51°13,661	700	1,02	n.d.	0,04	17,44	1,12	18,90
					500	n.d.	n.d.	n.d.	n.d.	n.d.	n.d.
					300	1,48	n.d.	0,02	16,19	1,06	16,30
					150	n.d.	n.d.	n.d.	n.d.	n.d.	n.d.
					100	0,94	0,209	0,10	13,09	0,90	10,35
					80	2,30	0,229	0,08	13,27	0,91	10,70
					60	1,30	0,300	0,10	14,01	0,95	13,25
					40	1,19	0,855	0,07	11,34	0,80	10,75
					20	1,95	2,342	0,07	11,48	0,82	11,00
					5	2,01	5,388	0,06	3,86	0,30	4,65
34 33 70	23.06.07	11:50	70°36,277'	54°31,640	20	0,87	1,265	0,07	5,17	0,46	4,10
					5	2,16	1,218	0,07	3,77	0,37	3,35
34 33 80	23.06.07	18:00	70°19,041'	53°41,693	500	1,46	n.d.	0,04	15,56	1,10	17,60
					400	1,45	n.d.	0,03	15,22	1,04	15,70
					200	0,83	n.d.	0,05	14,14	0,98	13,15
					100	0,41	0,215	0,06	9,86	0,78	7,15
					80	1,76	0,253	0,07	8,19	0,72	5,50
					60	0,45	0,357	0,06	6,57	0,59	4,35
					40	1,63	1,059	0,07	4,76	0,46	3,10
					20	5,36	1,315	0,06	3,13	0,40	2,15
					5	1,35	1,247	0,06	2,89	0,29	1,95
34 33 90	23.06.07	22:30	70°13,176'	53°3,194	500	0,79	n.d.	0,05	15,29	1,08	16,45
					400	1,49	n.d.	0,03	15,20	1,06	16,10
					200	1,26	n.d.	0,07	13,87	0,98	12,70
					100	0,33	0,128	0,08	10,71	0,83	7,70
					80	0,76	0,153	0,08	8,99	0,75	6,20
					60	0,37	0,172	0,07	7,88	0,70	5,35
					40	0,97	0,178	0,07	6,86	0,64	4,50
					20	0,90	0,741	0,09	5,57	0,50	3,95
					5	1,12	1,387	0,04	1,66	0,18	1,80
34 34 20	26.06.07	04:28	70°22,620	50°48,72	800	5,53	n.d.	0,03	18,01	1,31	26,50
					600	13,58	n.d.	0,04	17,94	1,29	25,85
					400	38,48	n.d.	0,03	17,09	1,20	20,10
					200	40,58	n.d.	0,04	16,59	1,22	19,90
					100	1,74	0,123	0,15	13,03	0,97	12,75
					80	4,39	0,183	0,17	12,60	0,93	12,75
					60	9,79	0,052	0,10	15,03	1,09	17,25
					40	11,77	0,085	0,09	15,35	1,12	18,45
					20	3,41	0,170	0,09	15,31	1,10	18,45
					5	2,29	1,193	0,09	13,87	0,99	17,60
34 34 30	26.06.07	10:00	70°29,409'	51°35,859	900	0,57	n.d.	0,02	17,72	1,28	25,60
					600	1,68	n.d.	0,03	17,72	1,25	24,90
					400	1,60	n.d.	0,02	16,92	1,20	19,45
					200	2,06	n.d.	0,04	15,93	1,16	17,30
					100	0,80	0,159	0,13	12,12	0,91	11,55
					80	0,14	0,098	0,13	12,36	0,93	11,80
					60	1,51	0,248	0,17	10,36	0,79	9,85
					40	1,30	0,424	0,17	9,59	0,76	10,15
					20	1,59	0,767	0,15	10,18	0,79	12,50
					5	2,16	9,650	0,11	4,92	0,43	10,80
34 34 40	26.06.07	18:30	70°39,614'	52°7,122	150	0,59	0,081	0,06	13,90	1,03	13,30
					100	1,50	0,098	0,09	12,55	0,94	11,75
					60	3,88	0,183	0,15	9,91	0,78	8,70
					20	1,84	0,512	0,13	4,88	0,50	4,80

					5	3,04	6,625	0,03	0,09	0,05	3,15
34 34 50	27.06.07	11:30	71°08,391'	51°15,841'	150	0,89	0,059	0,12	15,87	1,20	16,00
					80	1,37	0,082	0,12	13,58	1,02	11,55
					60	1,36	0,126	0,14	12,15	0,93	9,75
					40	1,20	0,317	0,06	1,12	0,20	1,00
					20	1,41	1,843	0,03	0,30	0,14	2,35
					5	2,22	0,810	0,03	0,17	0,04	2,50
34 34 60	27.06.07	15:00	71°07,153'	51°15,326'	5	168,2	0,621	0,03	0,10	0,05	2,25
34 34 70	27.06.07	16:57	71°06,469'	51°13,920'	5	1,24	0,525	0,03	0,03	0,04	2,00
34 35 00	27.06.07	00:30	71°04,888'	51°56,846'	1100	32,70	n.d.	0,02	19,36	1,49	35,30
					700	28,84	n.d.	0,02	18,78	1,38	31,10
					400	29,31	n.d.	0,02	17,49	1,26	22,95
					200	31,05	n.d.	0,03	15,55	1,13	17,20
					100	31,76	0,091	0,08	12,31	0,91	12,20
					80	0,08	0,139	0,13	10,60	0,81	10,10
					60	1,41	0,213	0,15	9,38	0,74	9,00
					40	2,76	0,431	0,14	6,08	0,54	6,45
					20	1,18	0,625	0,10	4,26	0,37	5,85
5	1,50	0,425	0,04	0,01	0,04	3,40					
34 35 20	28.06.07	17:00	70°48,949'	56°50,893'	500	0,63	n.d.	0,02	16,80	1,17	24,80
					300	0,94	n.d.	0,01	15,03	1,04	14,80
					200	0,63	n.d.	0,03	13,97	0,99	13,50
					60	0,73	1,052	0,19	6,32	0,60	5,95
					20	0,50	3,118	0,08	3,24	0,40	3,85
					5	1,86	2,371	0,03	0,04	0,12	2,00
34 35 30	28.06.07	23:49	70°38,399'	59°5,992'	600	0,42	n.d.	0,02	17,61	1,26	28,70
					400	1,28	n.d.	0,02	17,05	1,20	24,50
					200	0,67	n.d.	0,02	15,12	1,02	13,60
					100	0,89	0,075	0,04	10,05	0,82	9,15
					80	1,10	0,207	0,07	8,52	0,70	8,05
					60	1,24	0,485	0,15	7,71	0,71	7,90
					40	1,30	1,168	0,14	6,34	0,62	6,70
					20	0,85	1,103	0,08	3,60	0,47	4,10
					5	0,16	0,293	0,11	4,83	0,49	4,75
34 35 40	29.06.07	14:30	69°38,959'	57°26,934'	200	0,52	n.d.	0,04	14,34	0,99	12,40
					100	1,03	0,536	0,09	12,76	0,90	9,85
					80	0,25	1,451	0,17	12,22	0,88	8,55
					60	0,73	1,283	0,12	10,45	0,78	6,00
					40	0,98	2,632	0,05	0,62	0,23	2,15
					20	0,89	0,347	0,02	0,06	0,03	1,15
					5	0,72	0,377	0,03	0,13	0,04	1,10
34 35 50	01.07.07	00:50	67°34,891'	53°17,998'	300	1,05	n.d.	0,11	3,17	0,46	3,10
					200	1,54	n.d.	0,08	1,94	0,39	2,55
					100	1,14	0,654	0,07	1,28	0,32	2,05
					80	1,08	0,688	0,06	1,17	0,32	1,55
					60	1,03	0,690	0,07	1,10	0,32	1,75
					40	1,00	0,802	0,05	0,93	0,28	2,40
					20	0,98	0,853	0,07	0,73	0,26	2,00
5	1,02	0,886	0,05	0,71	0,26	2,30					
34 35 70	02.07.07	11:35	64°27,586'	52°48,380'	440	1,01	n.d.	0,06	13,64	0,90	8,80
					300	2,05	n.d.	0,30	11,26	0,83	7,75
					200	0,66	n.d.	0,14	6,68	0,67	4,85
					100	0,77	0,078	0,11	3,88	0,52	3,55
					80	1,78	0,082	0,11	3,23	0,48	3,15
					60	0,62	0,068	0,09	2,57	0,44	2,45
					40	1,37	0,155	0,10	2,30	0,41	2,95

					20	0,60	0,714	0,08	1,77	0,35	2,40
					5	0,83	1,433	0,05	1,04	0,26	2,05
34 35 80	02.07.07	16:15	63°57,834'	53°53,572	1000	0,83	n.d.	0,03	15,91	1,00	9,75
					700	1,24	n.d.	0,02	15,52	0,98	8,70
					400	0,68	n.d.	0,05	14,53	0,92	8,55
					200	1,16	n.d.	0,49	11,76	0,82	6,95
					100	3,91	0,403	0,18	7,85	0,68	6,00
					60	1,04	0,631	0,12	5,56	0,57	4,75
					40	1,26	0,968	0,10	4,31	0,43	4,20
					20	0,61	0,878	0,10	3,55	0,40	3,95
				5	1,08	0,325	0,04	0,92	0,23	2,55	
34 35 90	03.07.07	08:00	64°21,959'	51°36,340	580	0,96	n.d.	0,05	9,83	0,70	7,15
					400	1,75	n.d.	0,07	9,76	0,69	6,50
					200	0,95	n.d.	0,12	9,64	0,71	6,40
					100	0,90	0,352	0,15	5,71	0,52	4,40
					60	0,73	0,491	0,15	4,73	0,46	4,10
					40	1,33	1,311	0,11	2,62	0,29	3,55
					20	1,39	1,437	0,11	1,91	0,23	3,40
									5	0,90	1,796

## 5. Multibeam Echosounder surveys

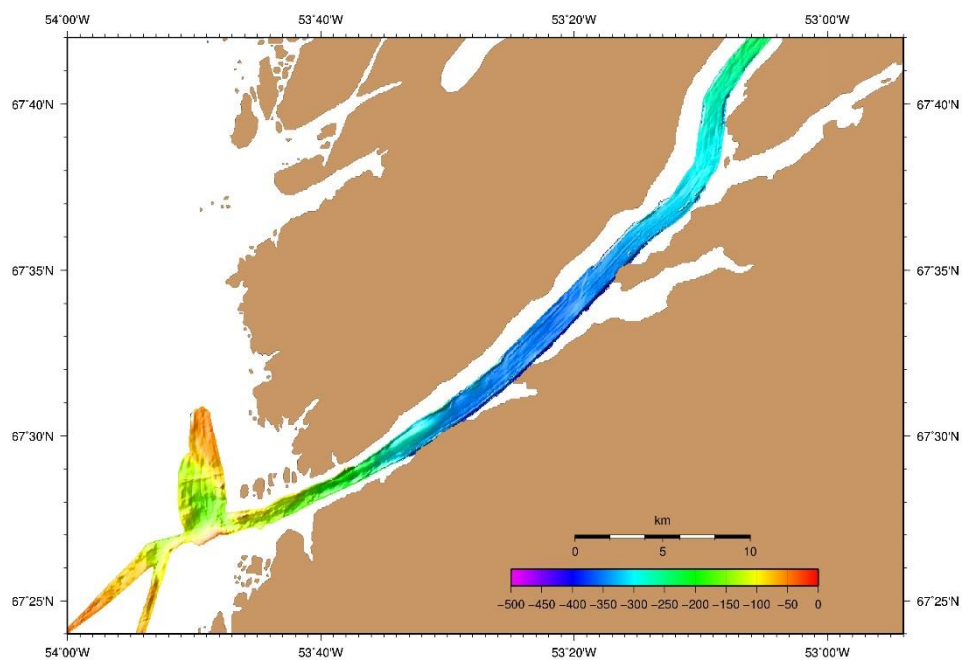


Fig. E5.1 Multibeam survey of Nordre Strömfjord; entrance and outer parts.

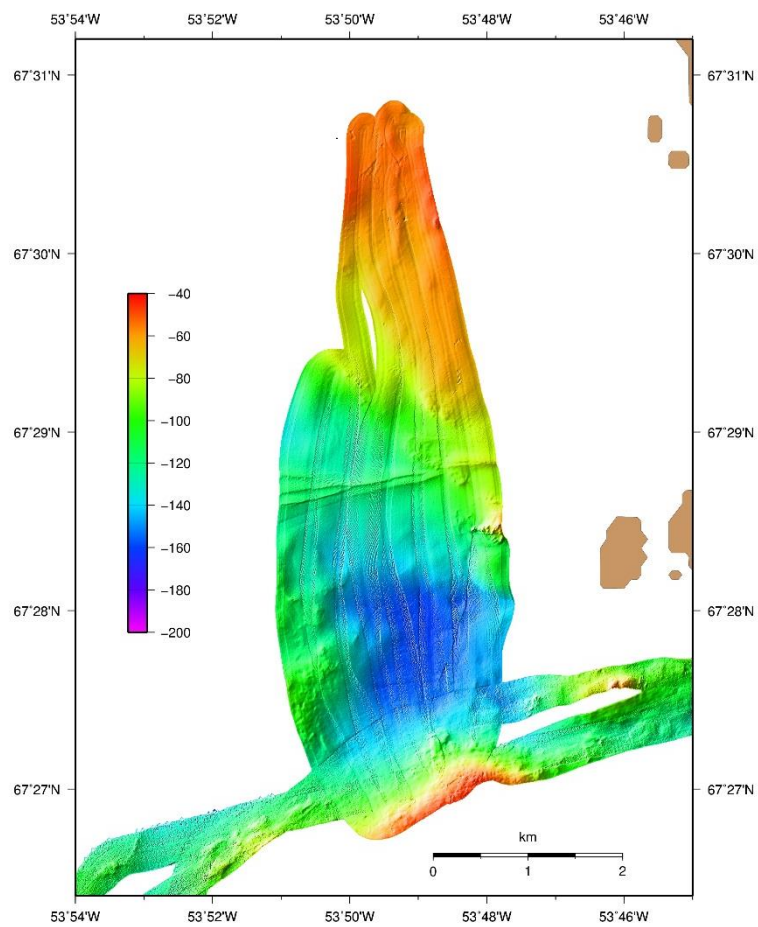


Fig. E5.2: Basin off the entrance to Nordre Strömfjord.

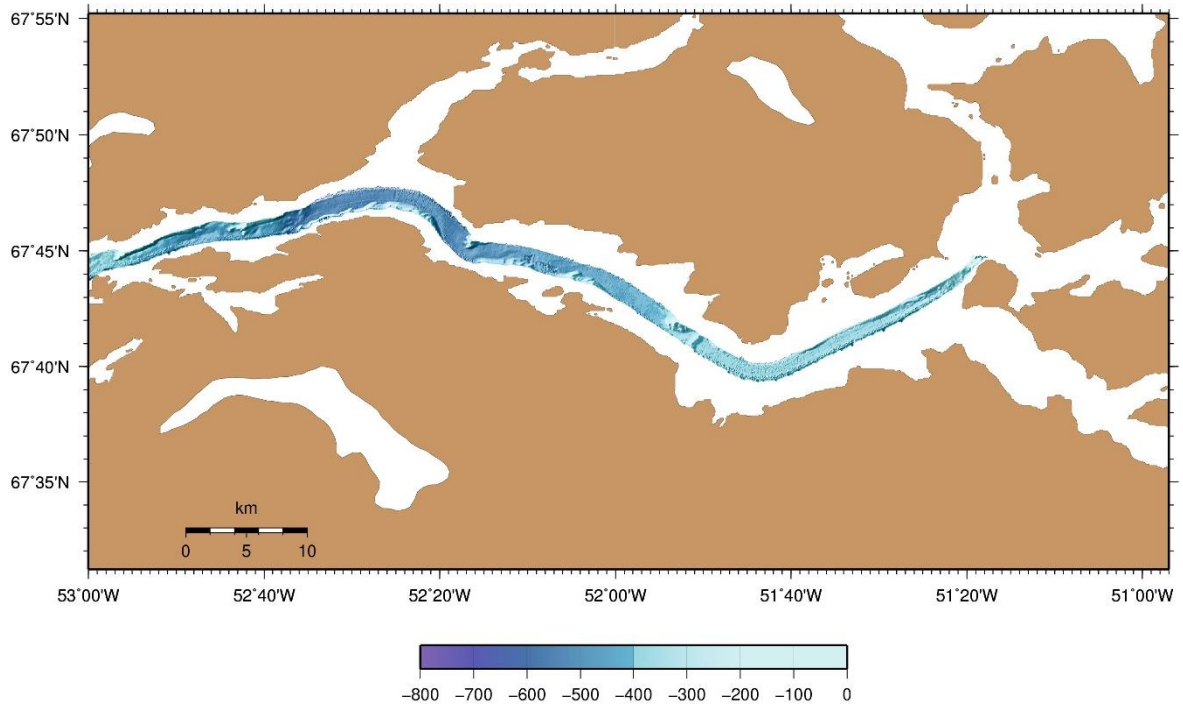


Fig. E5.3 Multibeam survey of Nordre Strömfjord; inner part.

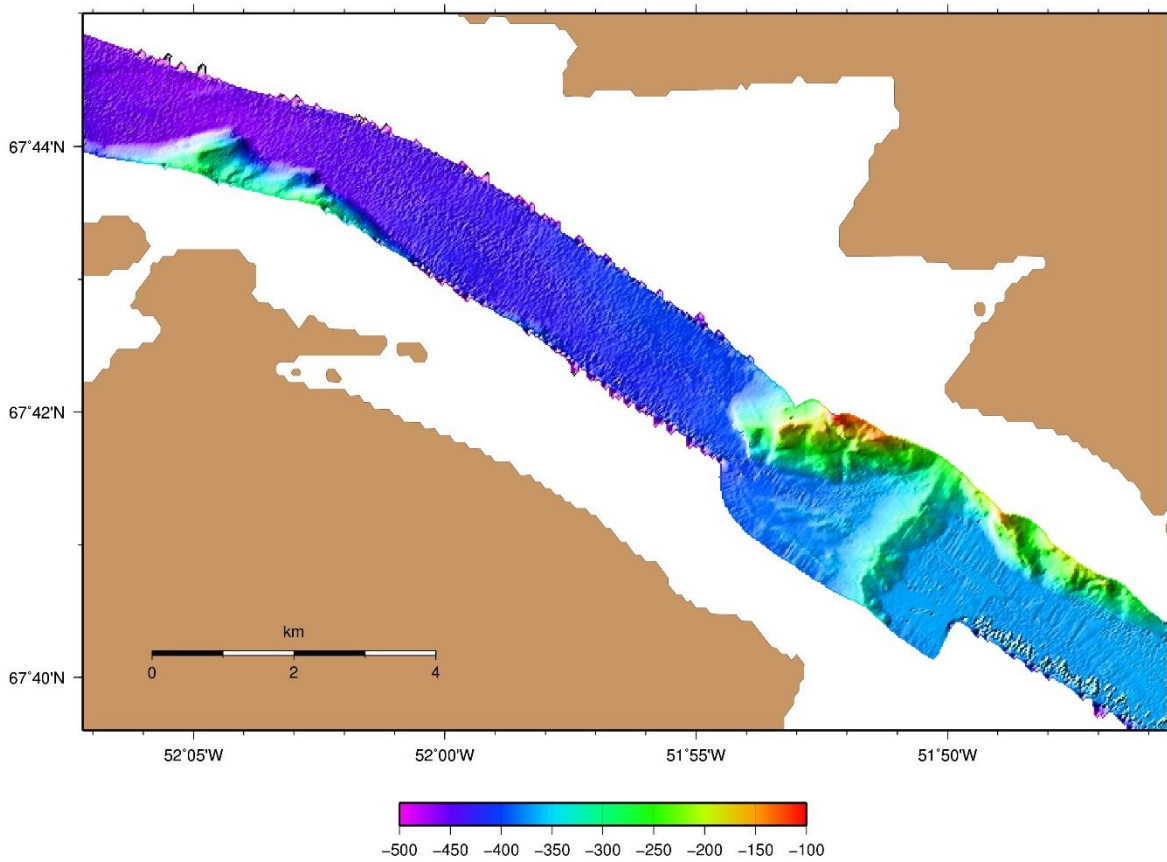


Fig. E5.4: Multibeam survey of Nordre Strömfjord; inner part.

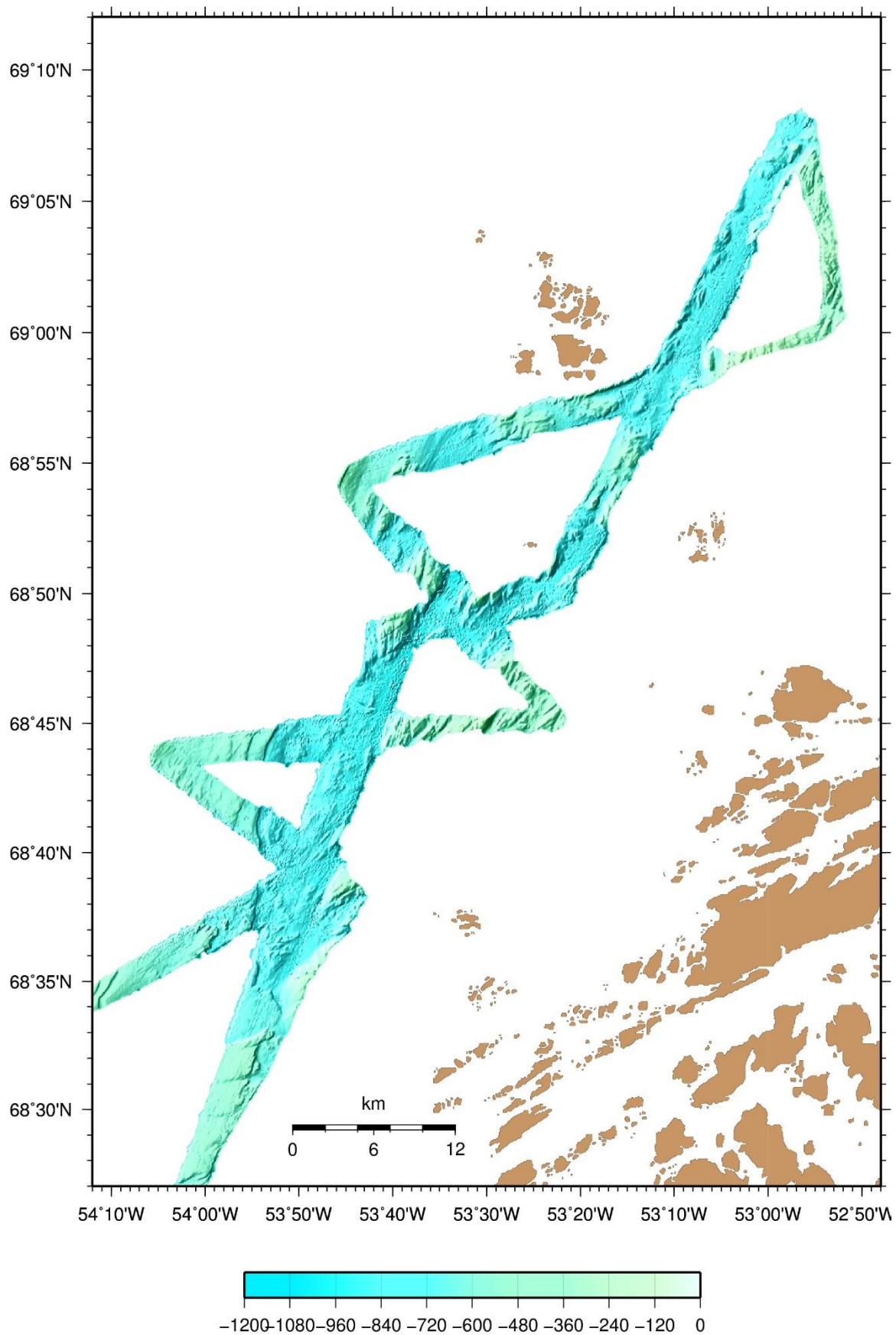


Fig. E5.5: Multibeam survey of area outside Disko Bay.

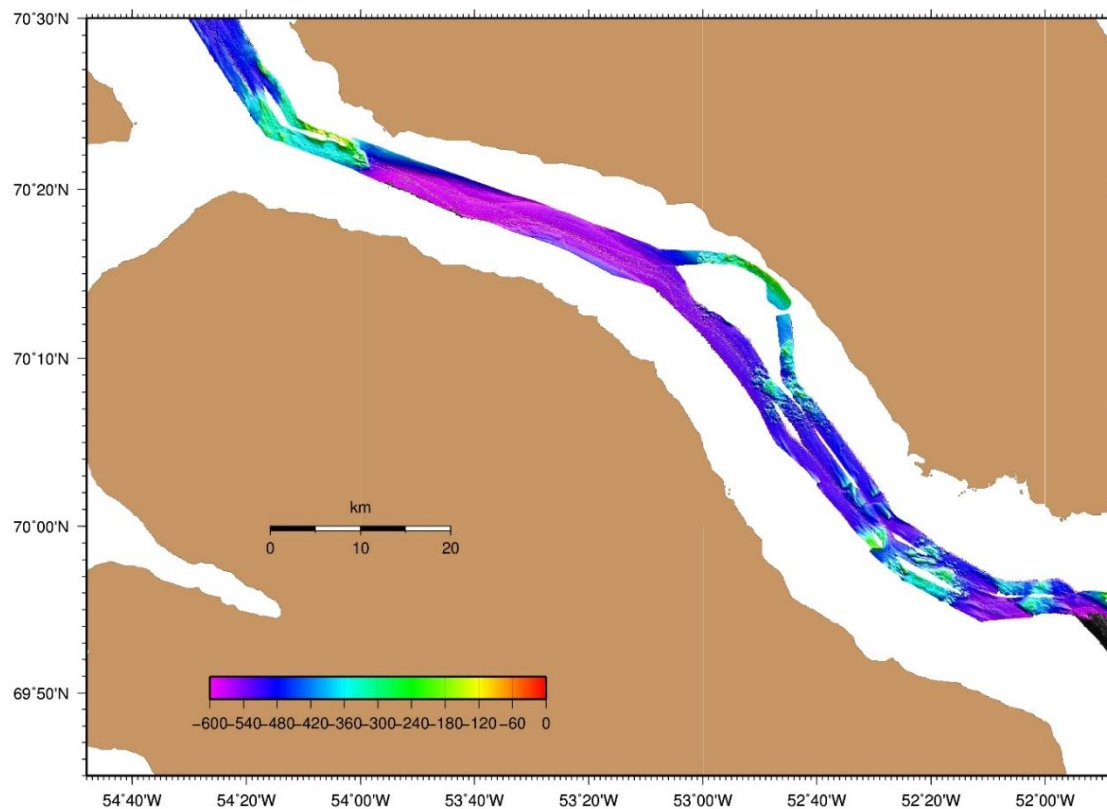


Fig. E5.6: Multibeam survey of Vaigat.

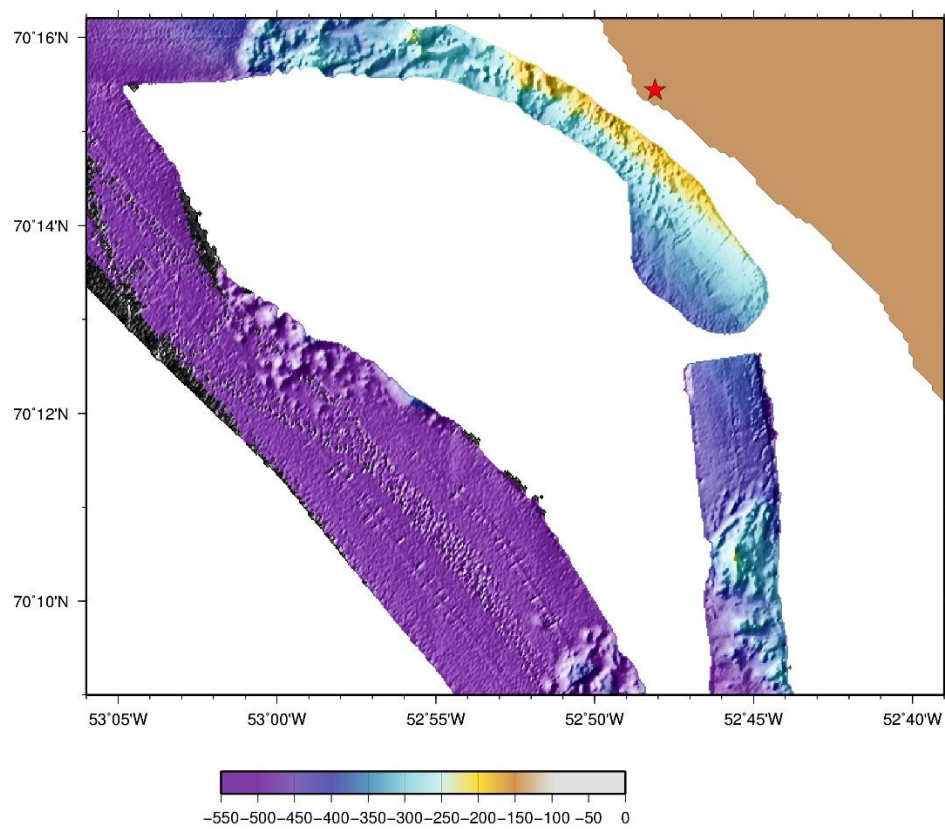


Fig. E5.7: Multibeam survey of tsunami area in Vaigat..

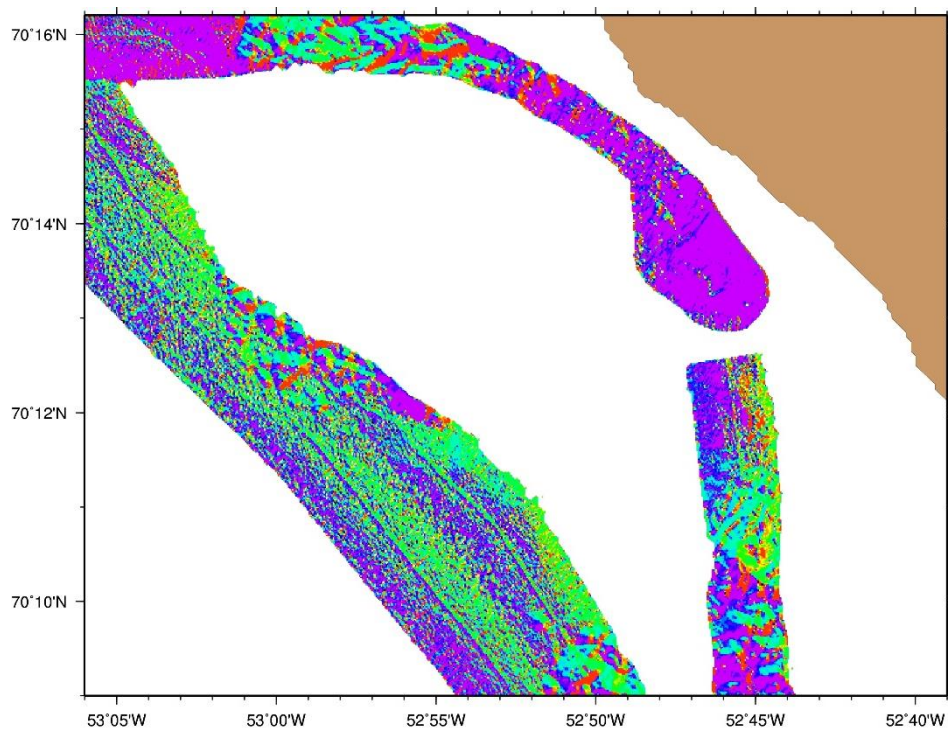


Fig. E5.8: Directivity analysis of tsunami area in Vaigat.

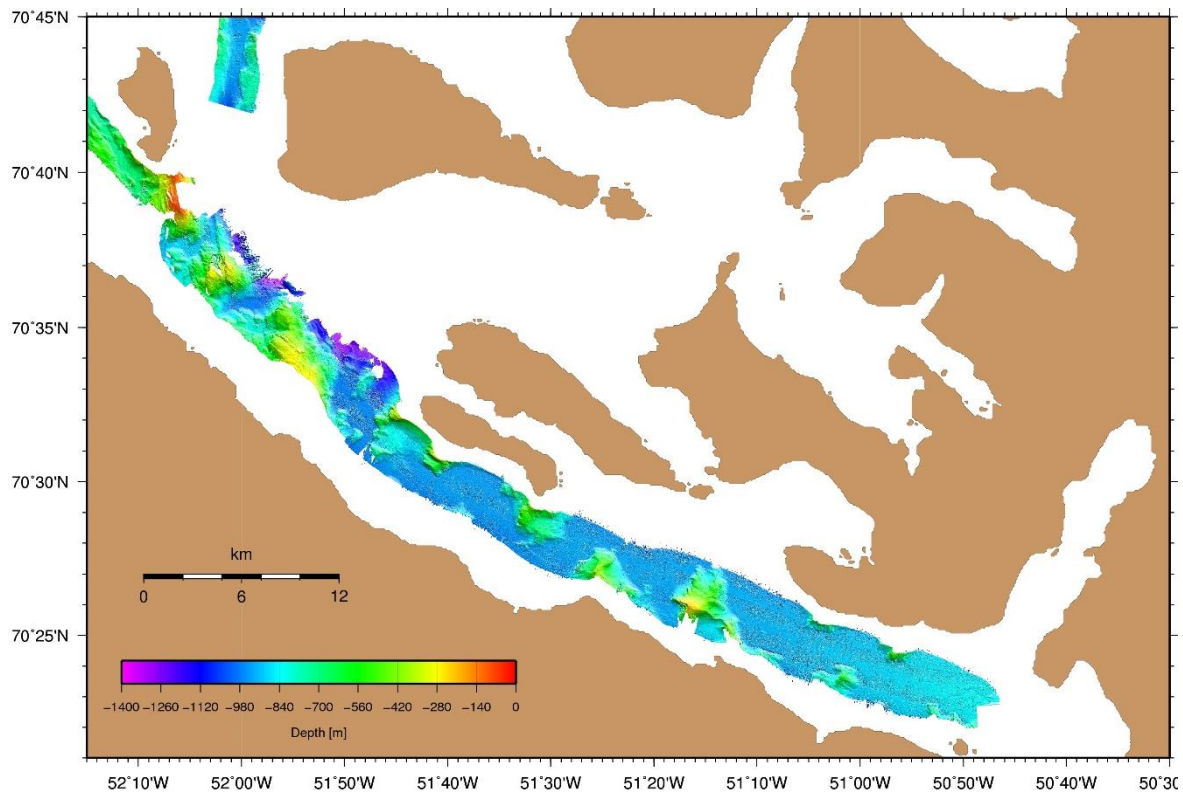


Fig. E5.9: Multibeam survey of Uumannaq Fjord.

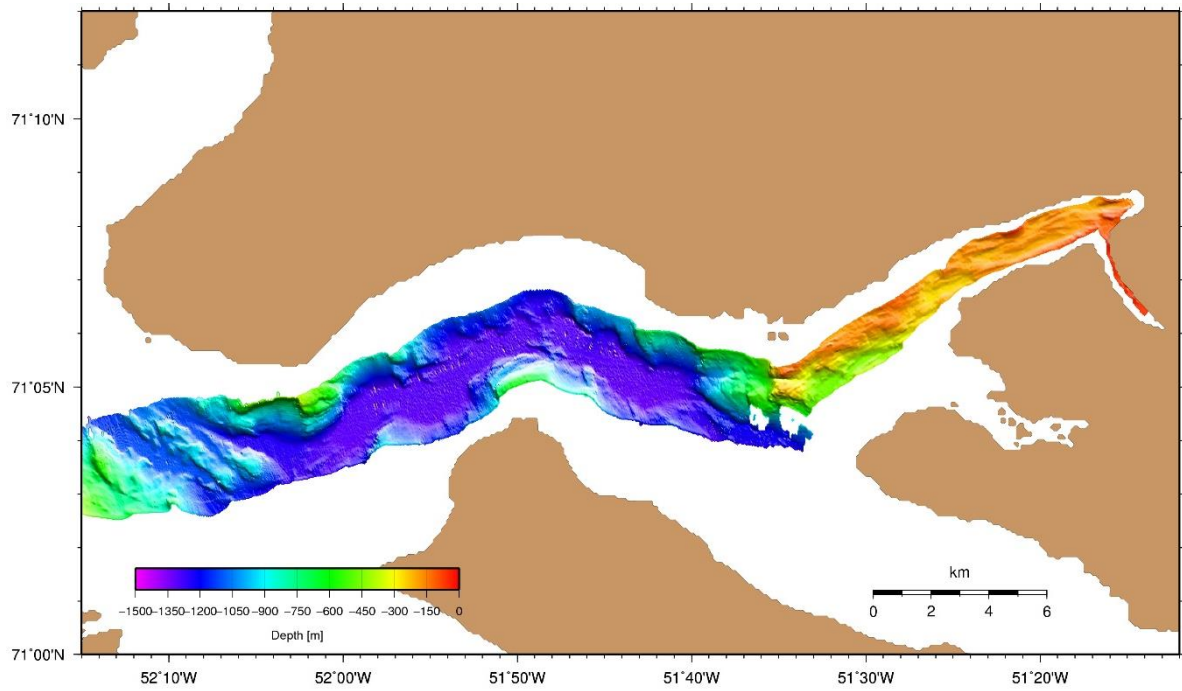


Fig. E5.10: Multibeam survey of Quamarujuk Fjord; inner part.

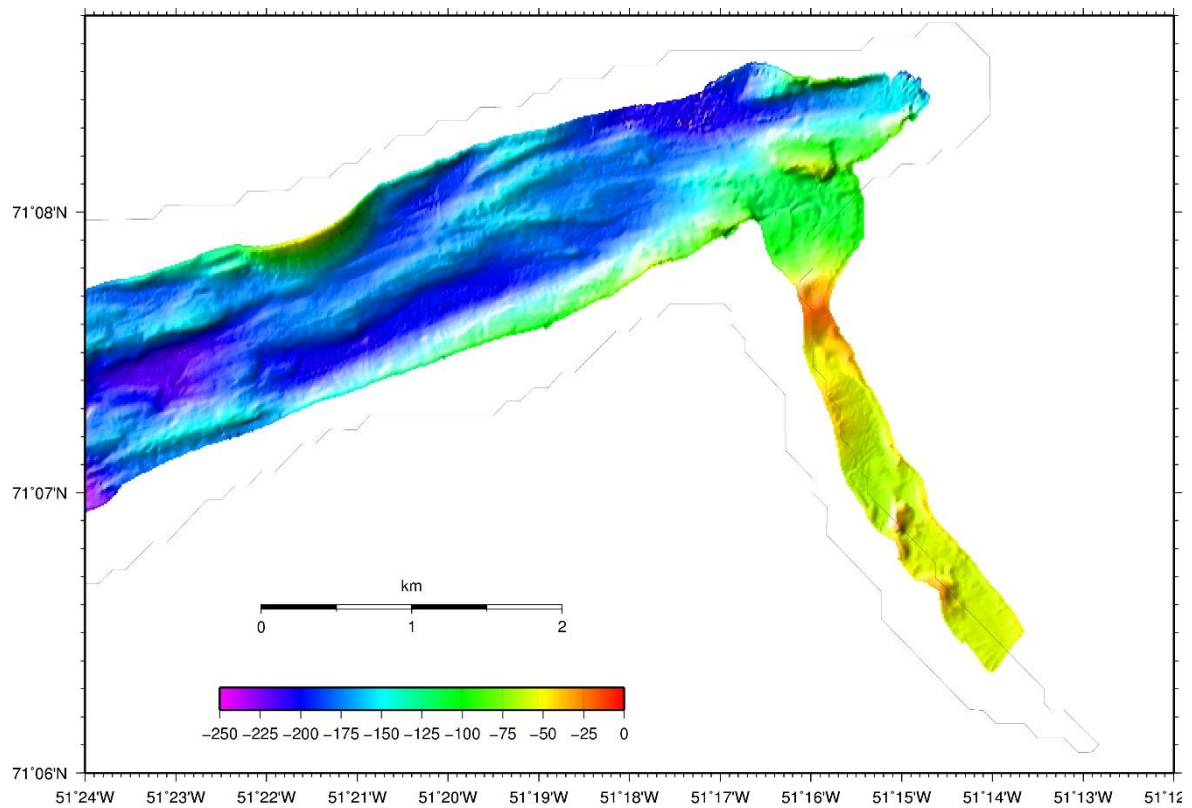


Fig. E5.11: Multibeam survey of the inner part of Quamarujuk Fjord and Marmorilik.

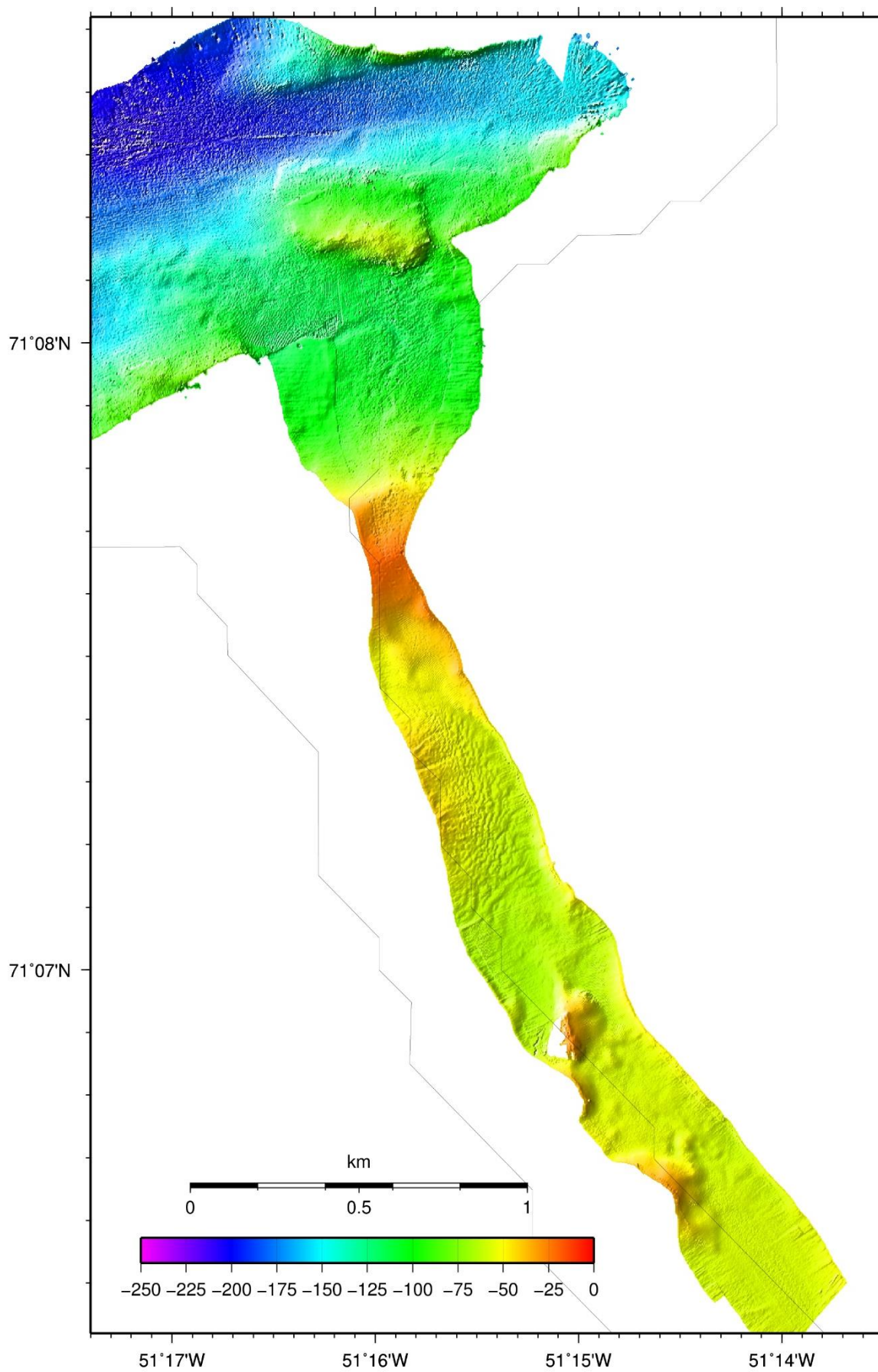


Fig. E5.12: Multibeam survey of Marmorilik area.

## 6. Parasound profiles / coring stations

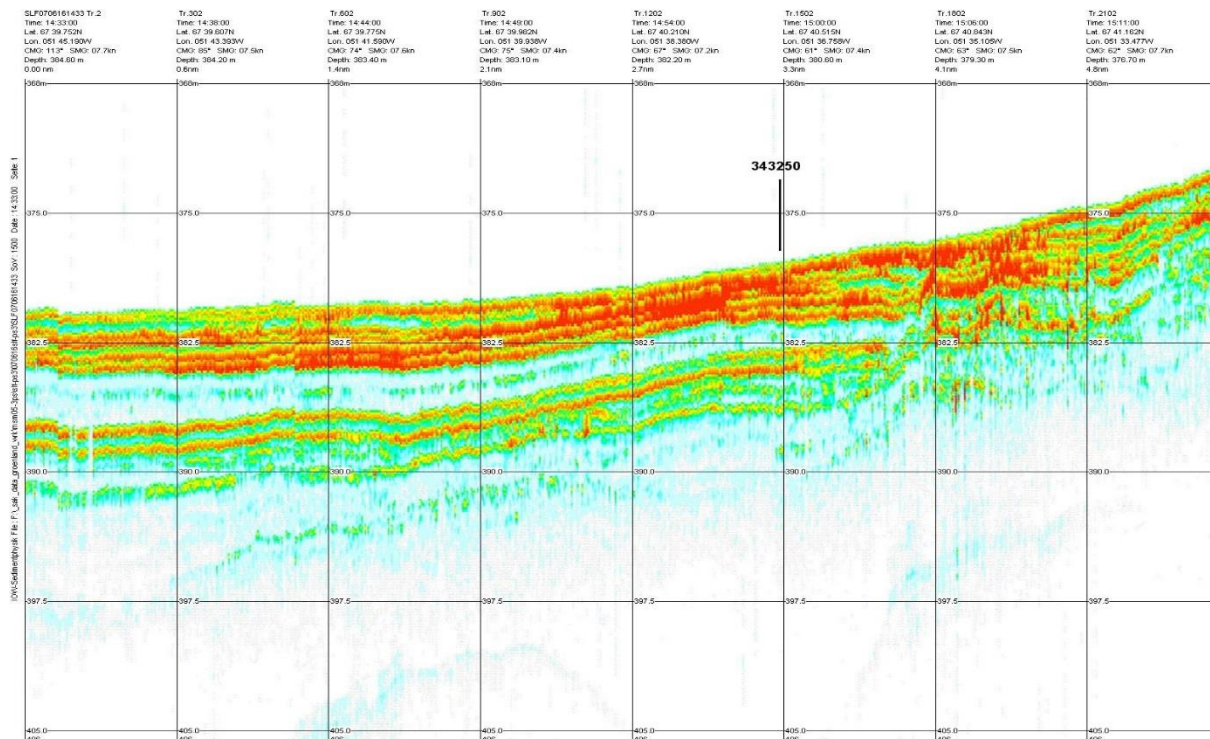


Fig. E6.1: Parasound record at station 343250.

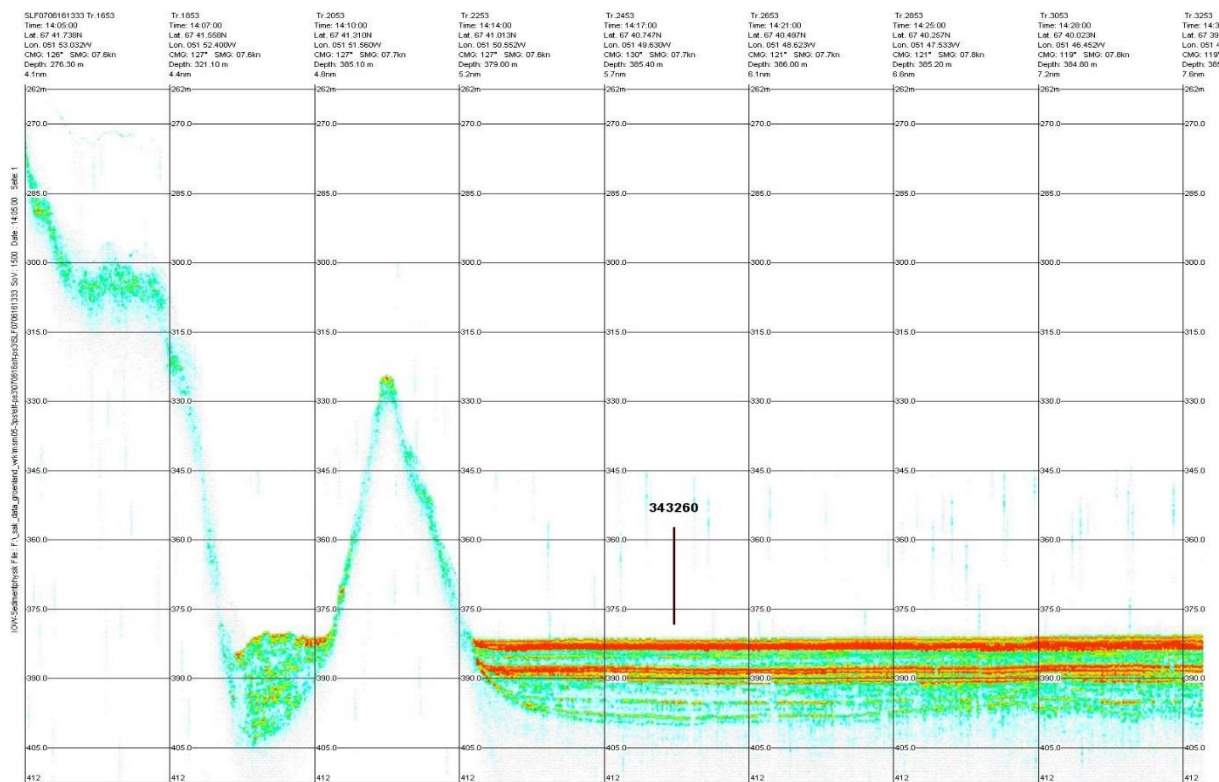


Fig. E6.2: Parasound record at station 343260.

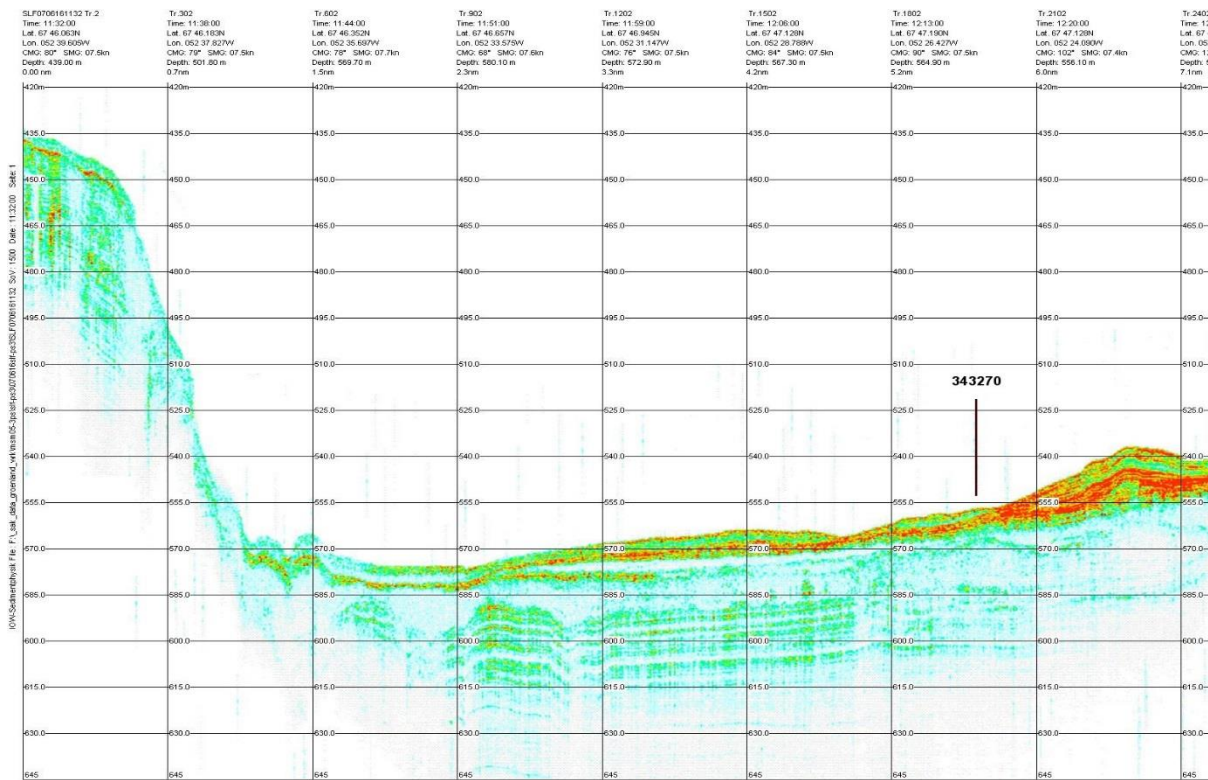


Fig. E6.3: Parasound record at station 343270.

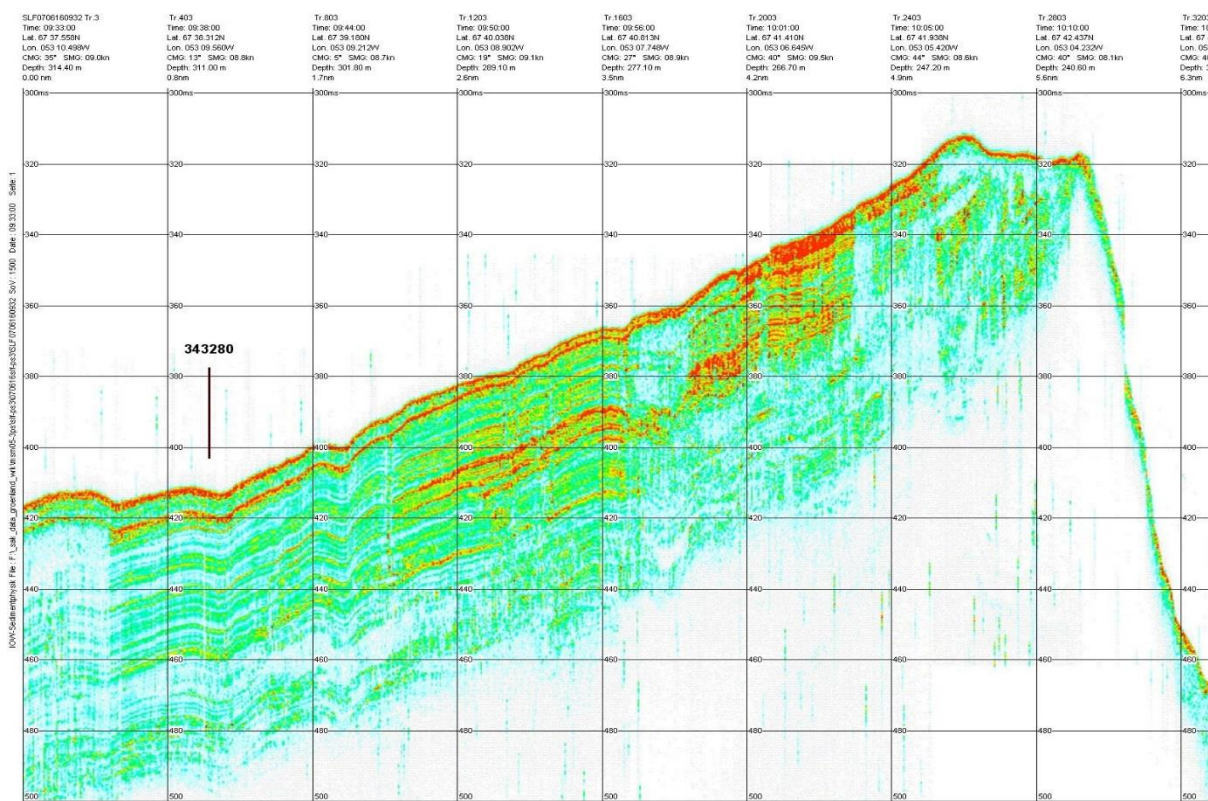


Fig. E6.4: Parasound record at station 343280.

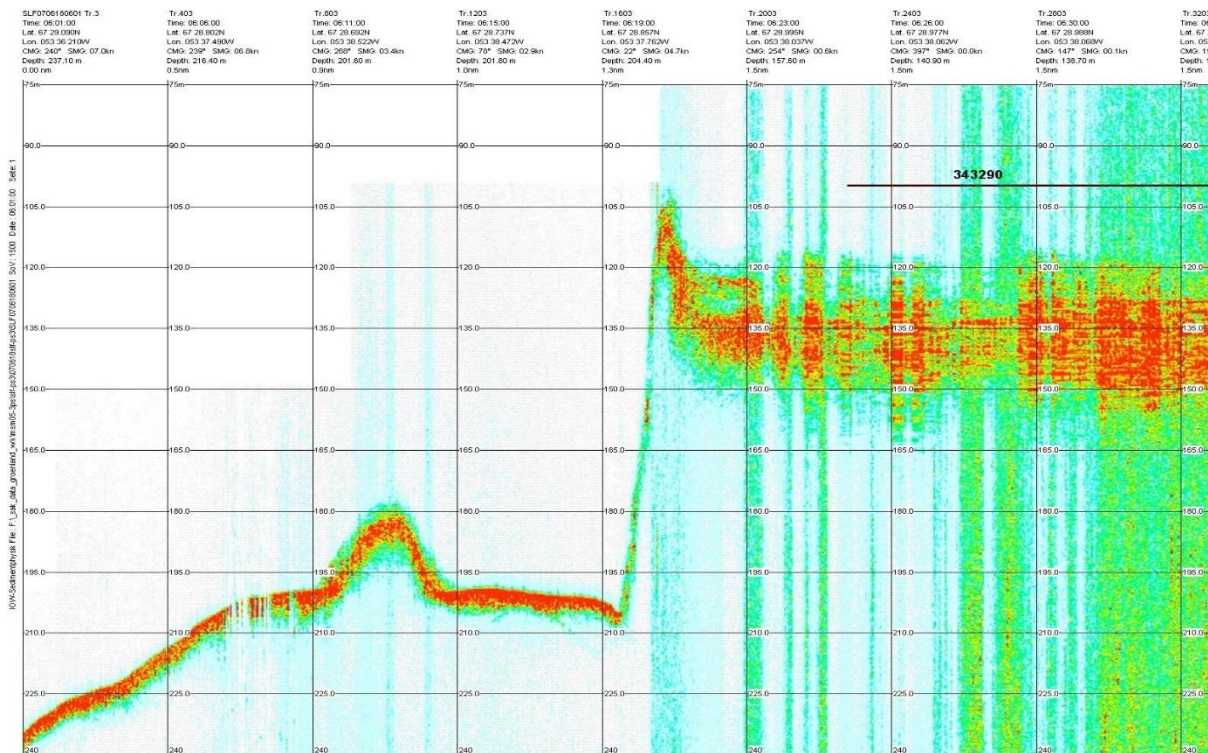


Fig. E6.5: Parasound record at station 343290.



Fig. E6.6: Parasound record at station 343300.

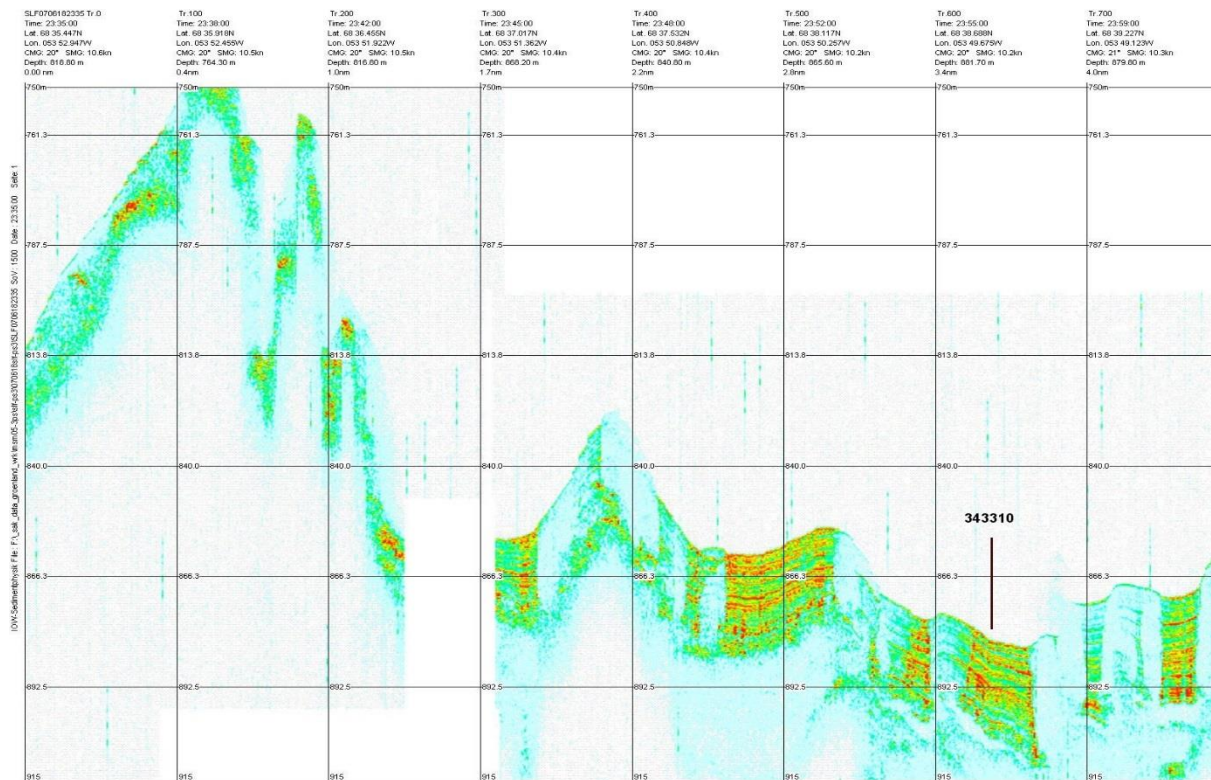


Fig. E6.7: Parasound record at station 343310.

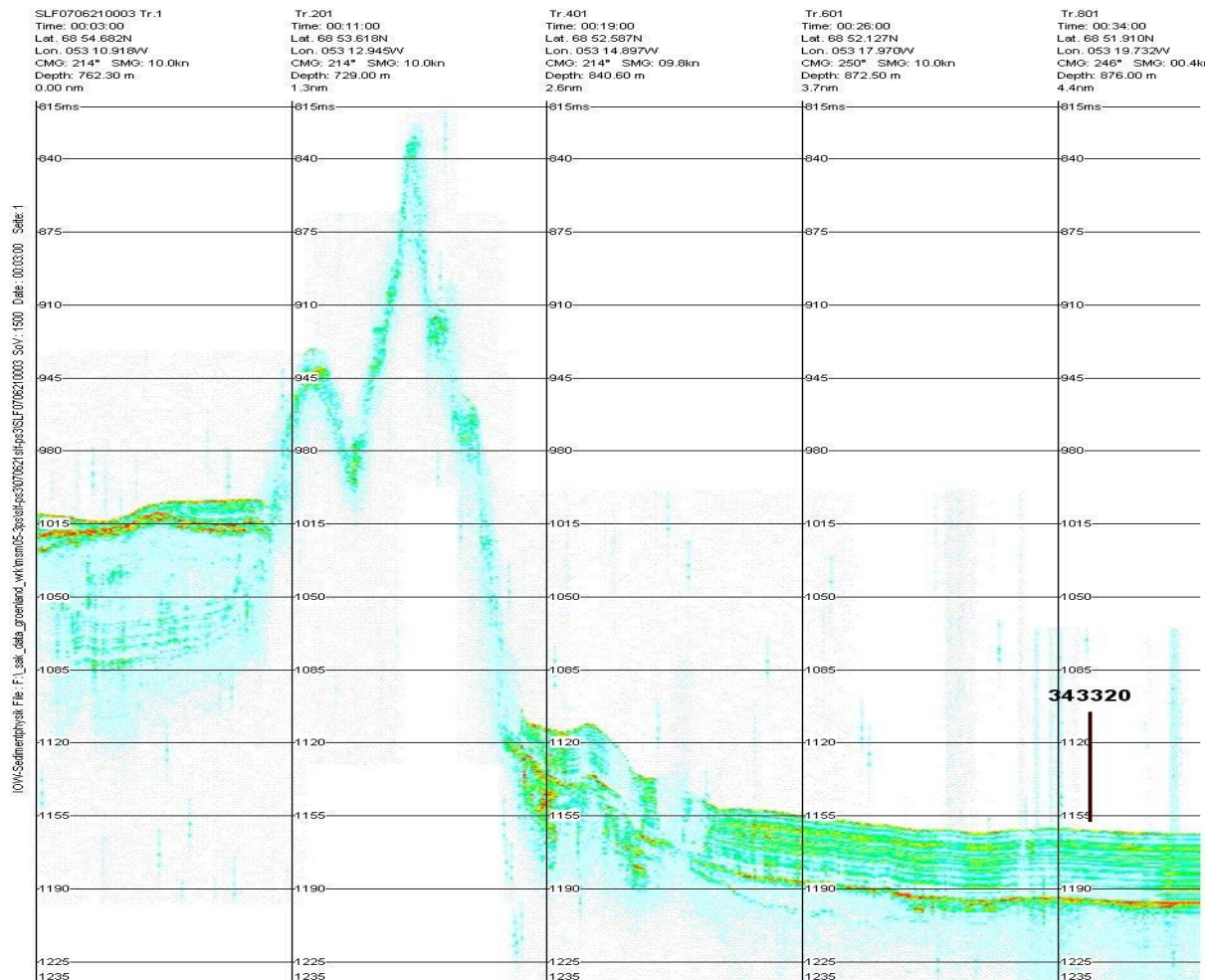


Fig. E6.8: Parasound record at station 343320.

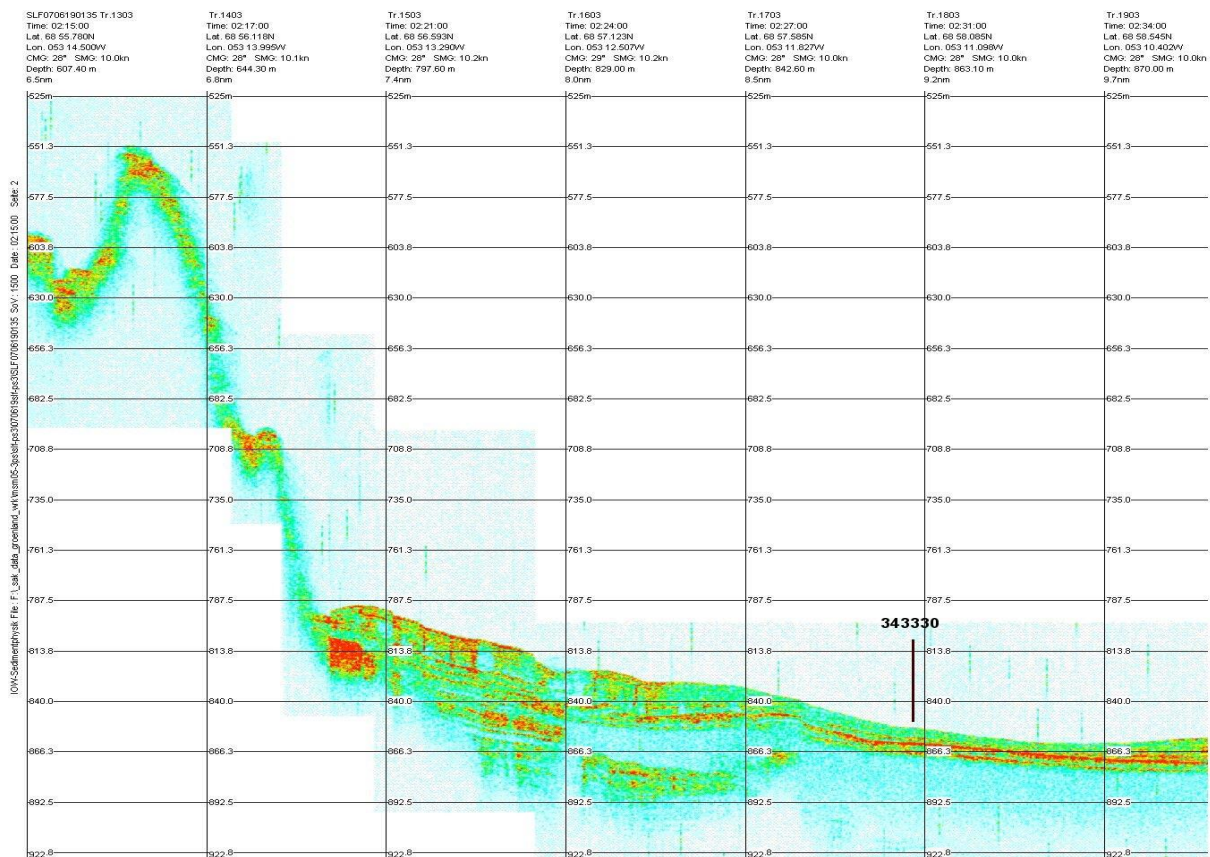


Fig. E6.9: Parasound record at station 343330.

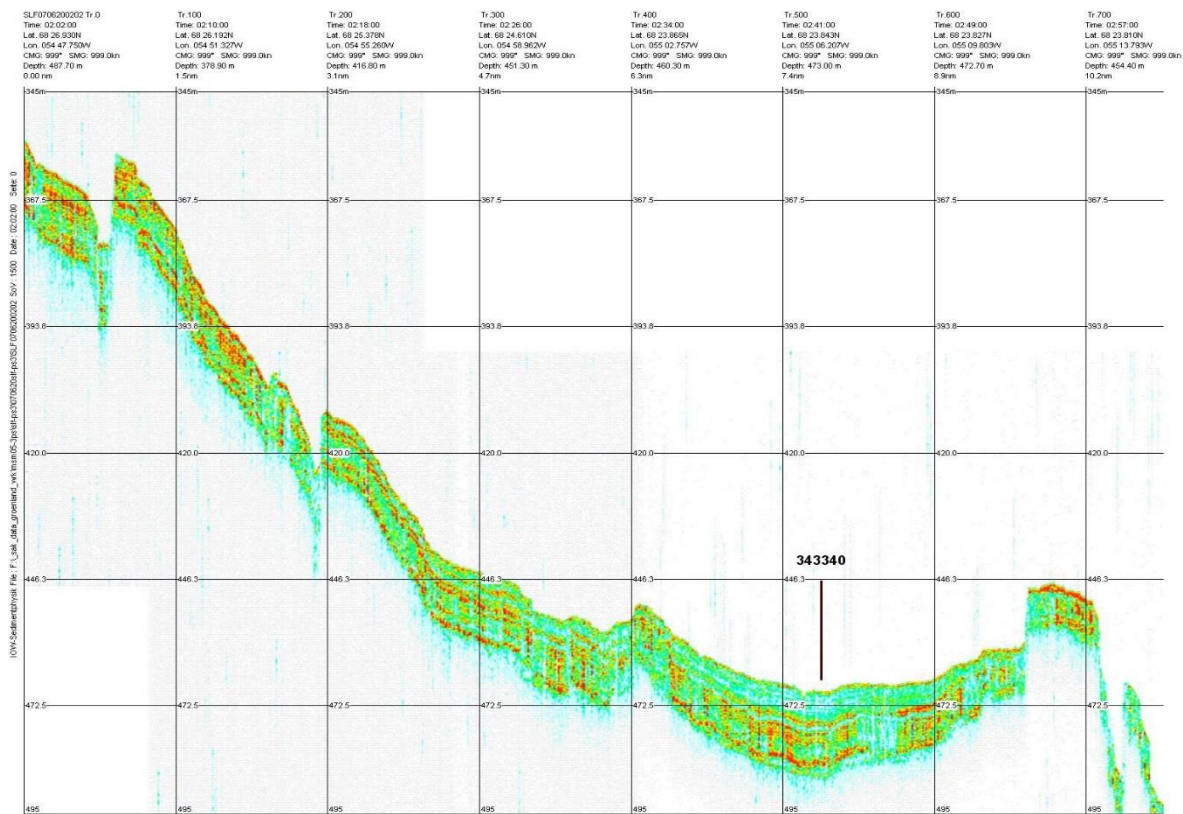


Fig. E6.10: Parasound record at station 343340.

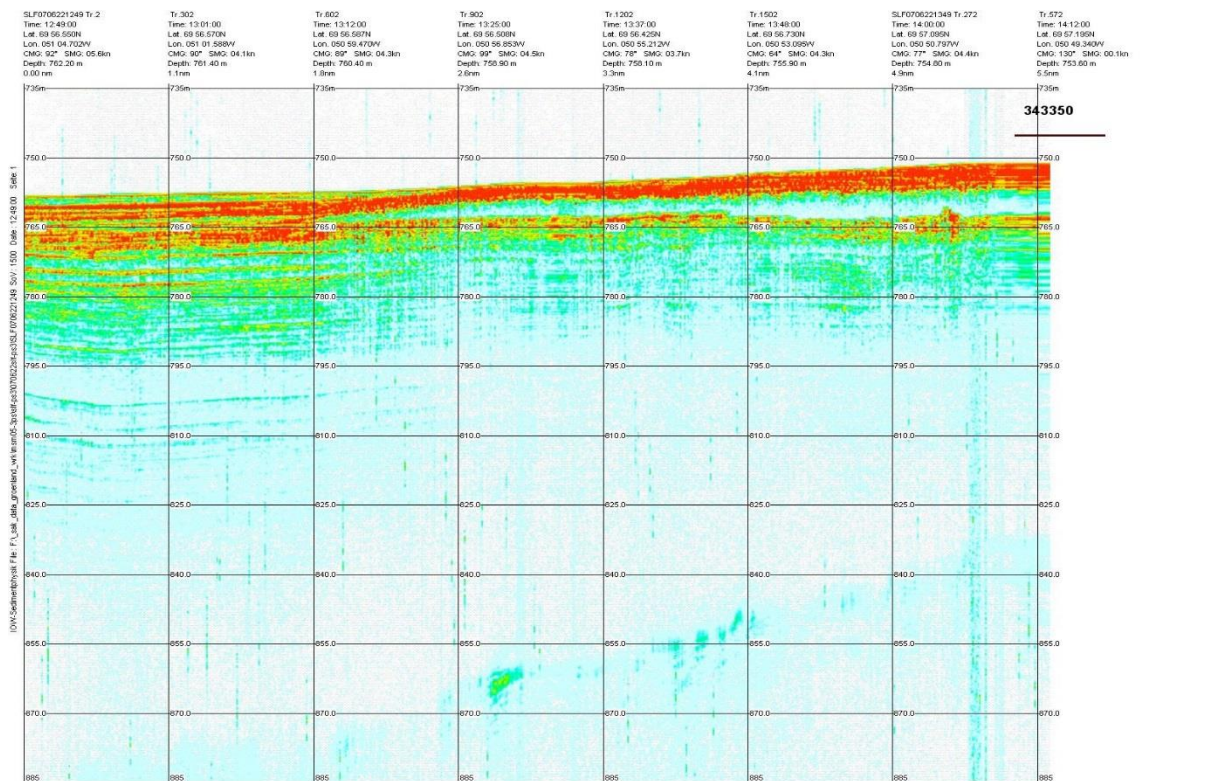


Fig. E6.11: Parasound record at station 343350.

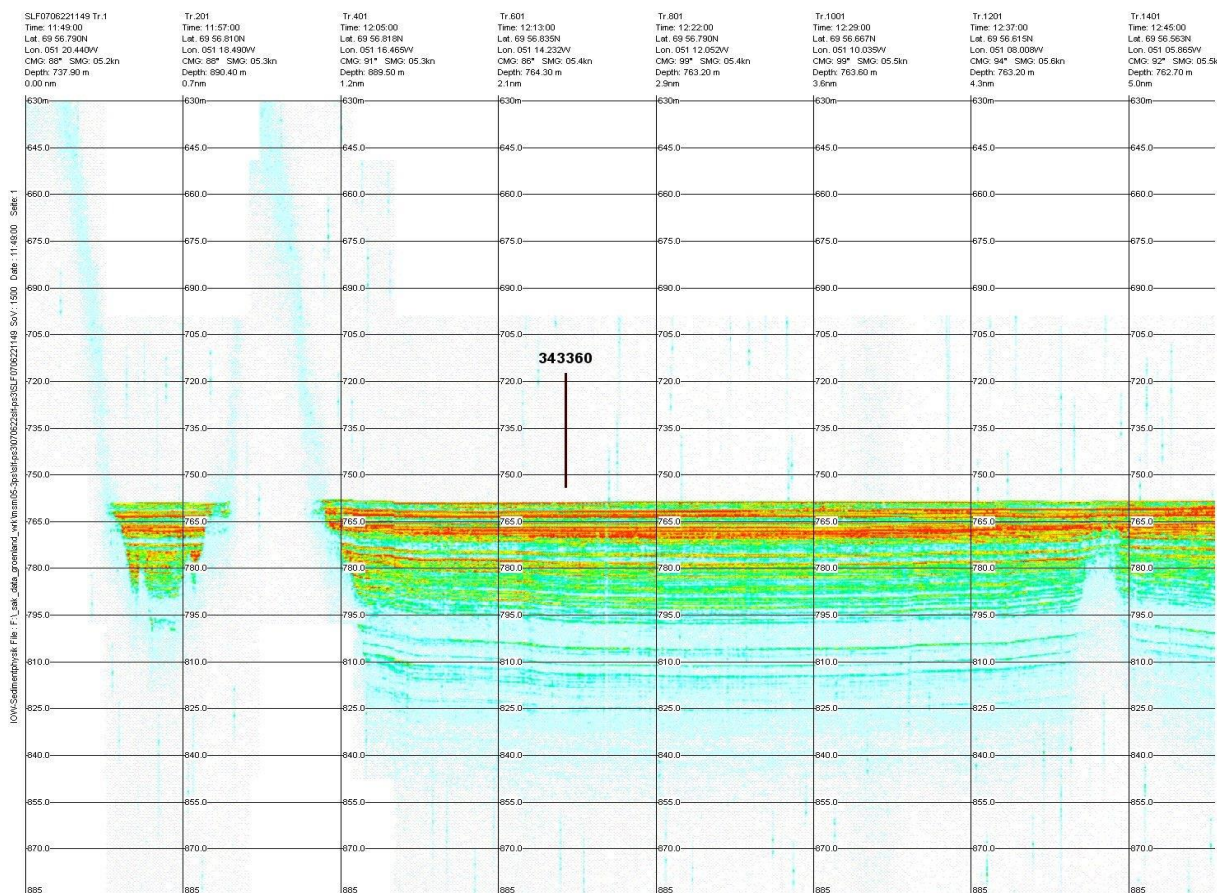


Fig. E6.12: Parasound record at station 343360.

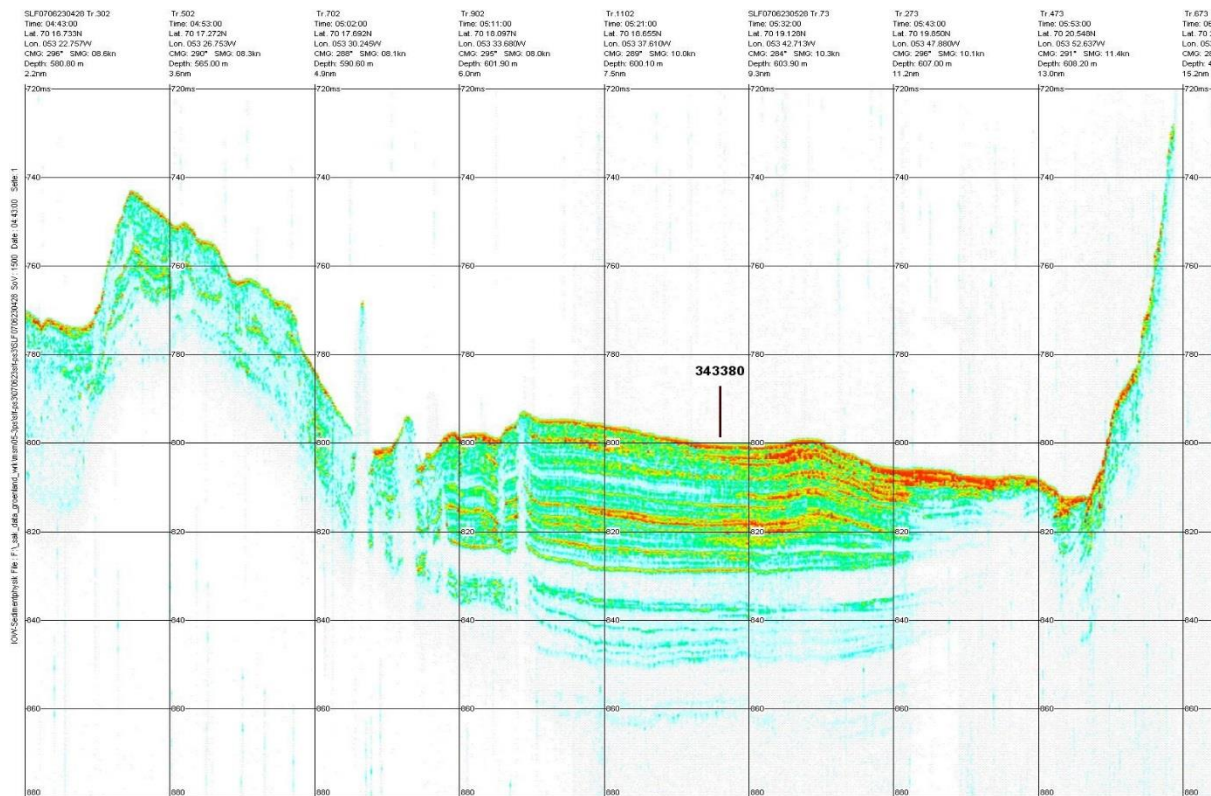


Fig. E6.13: Parasound record at station 343380.

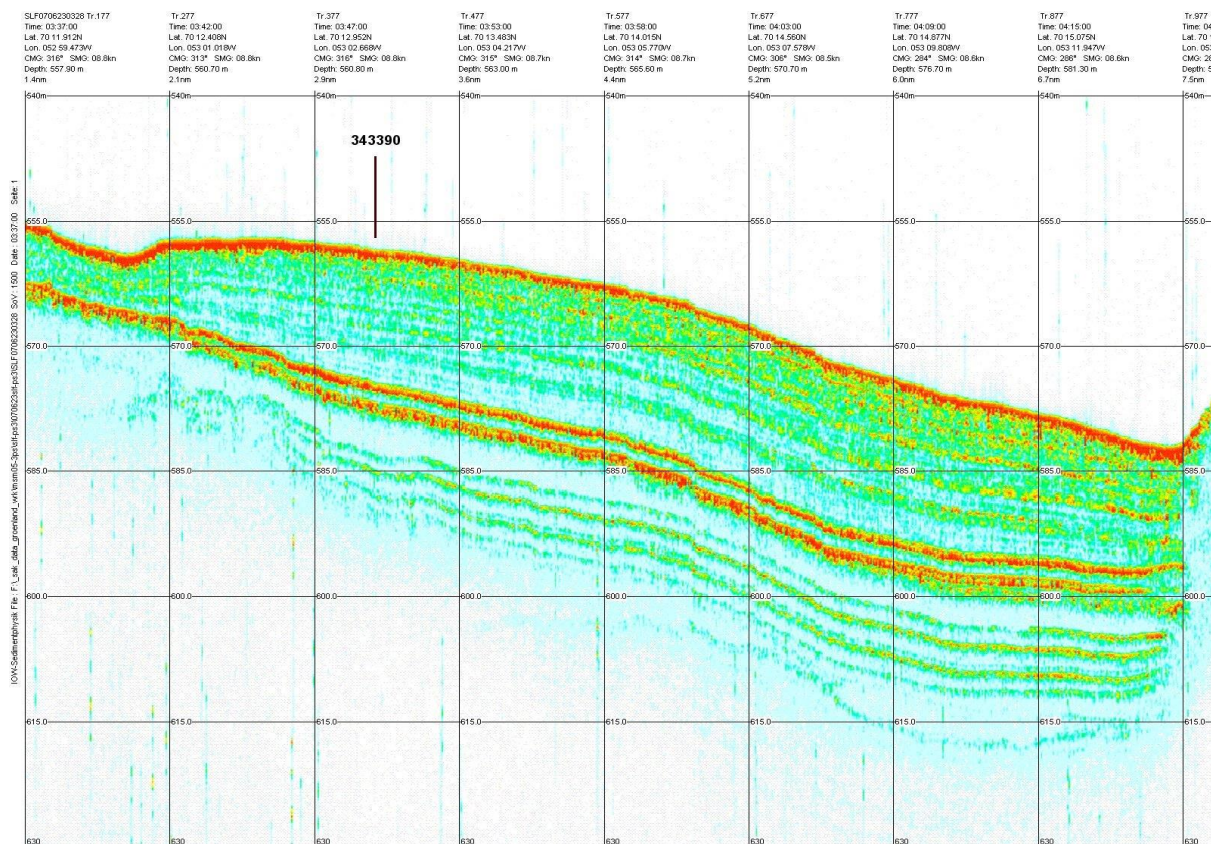


Fig. E6.14: Parasound record at station 343390.

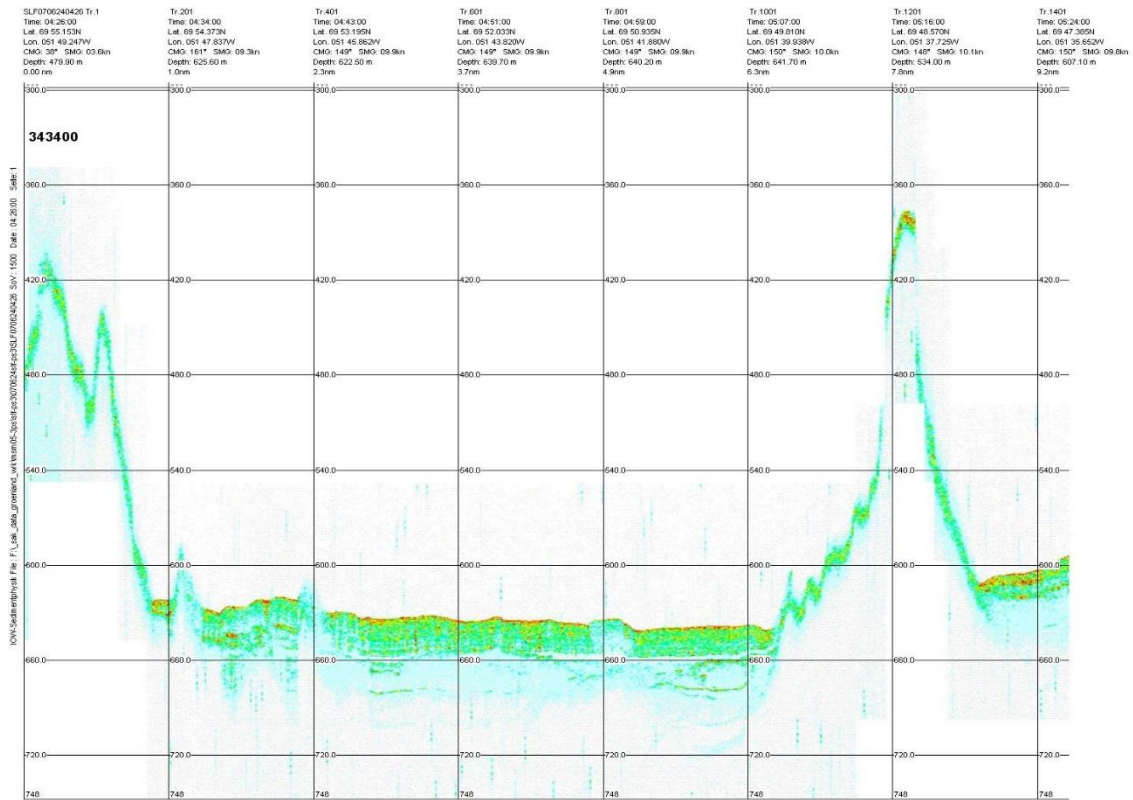


Fig. E6.15: Parasound record at station 343400.

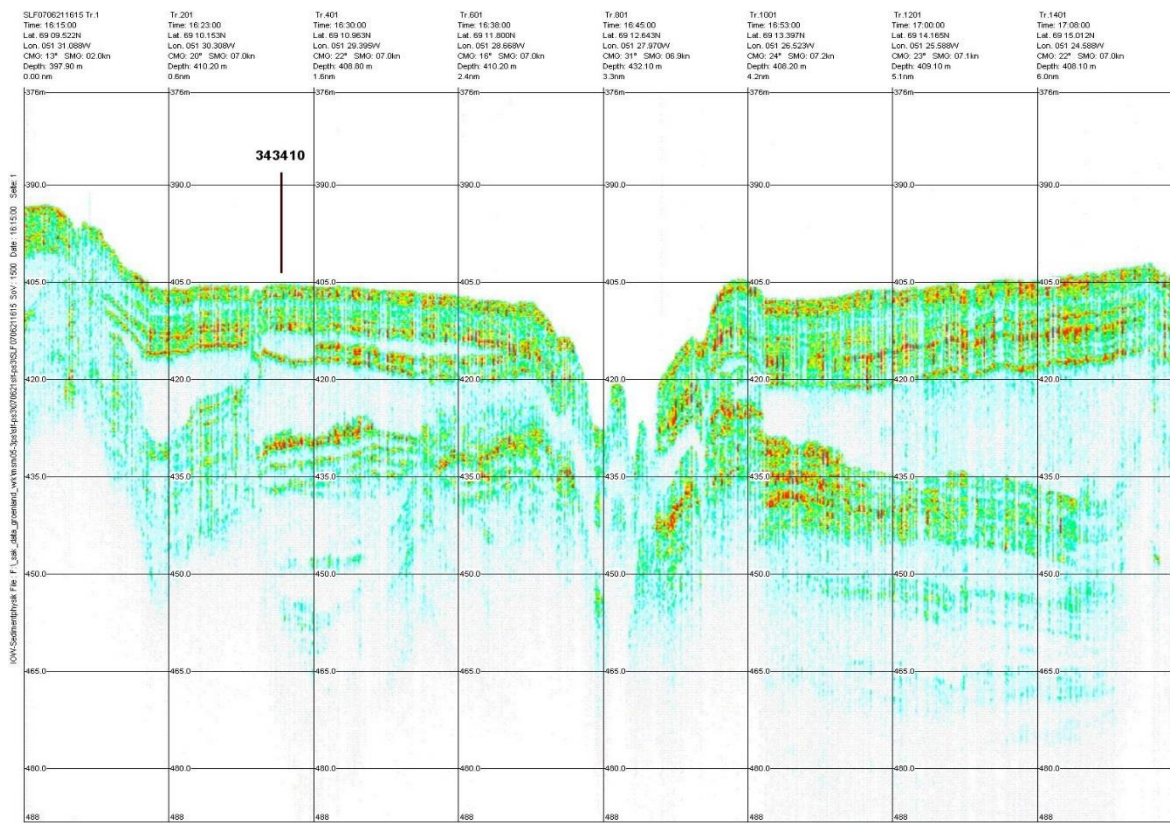


Fig. E6.16: Parasound record at station 343410.

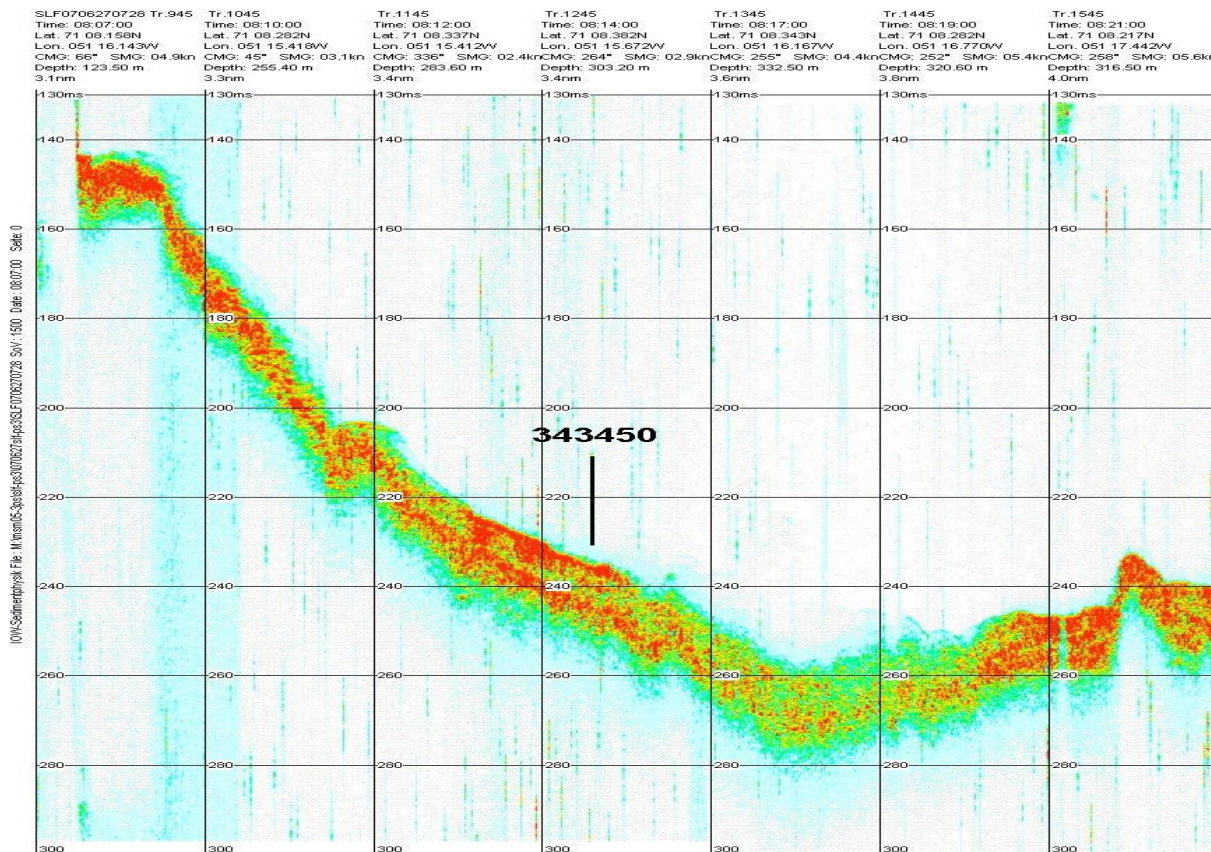


Fig. E6.17: Parasound record at station 343450.

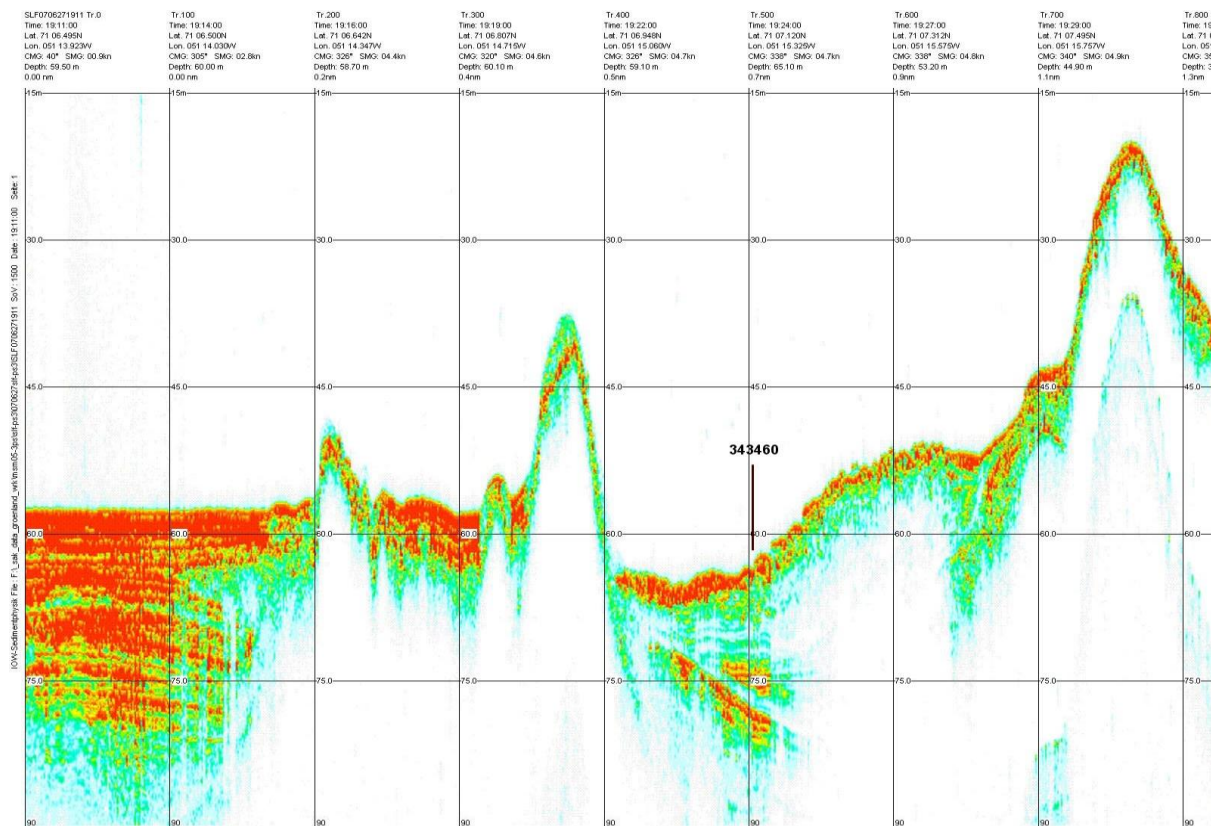


Fig. E6.18: Parasound record at station 343460.

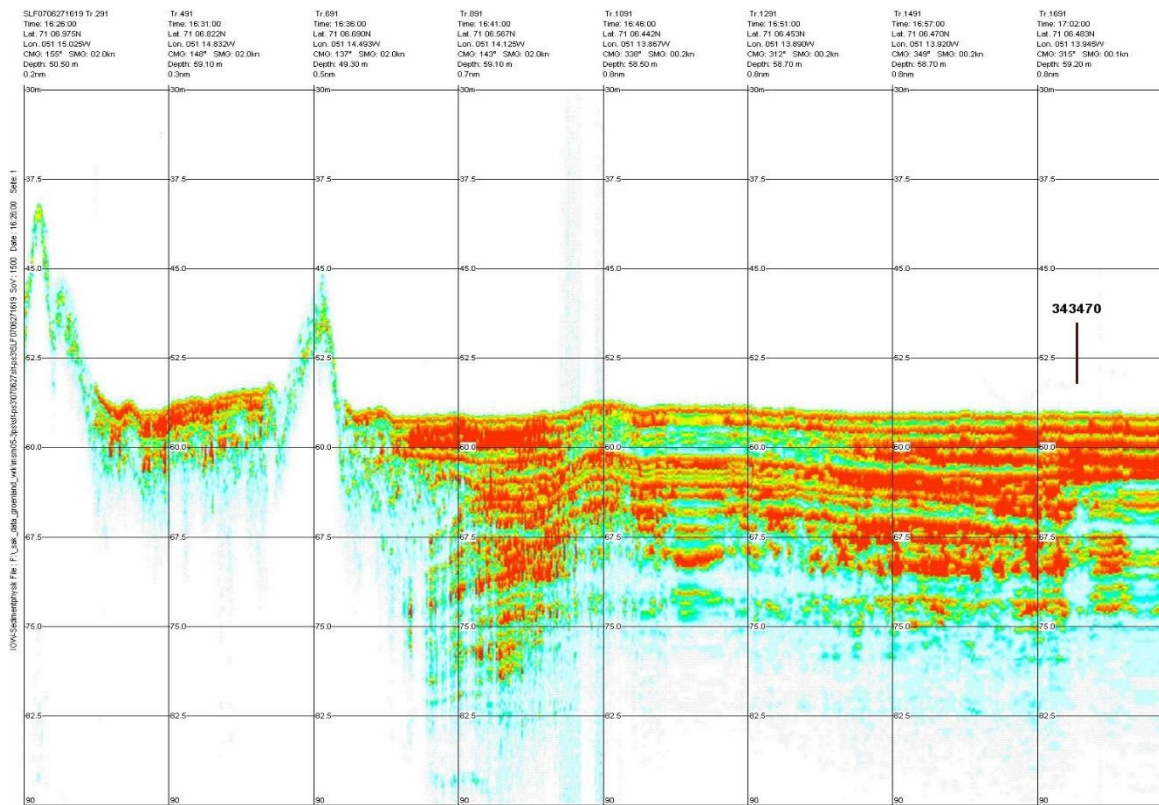


Fig. E6.19: Parasound record at station 343470.

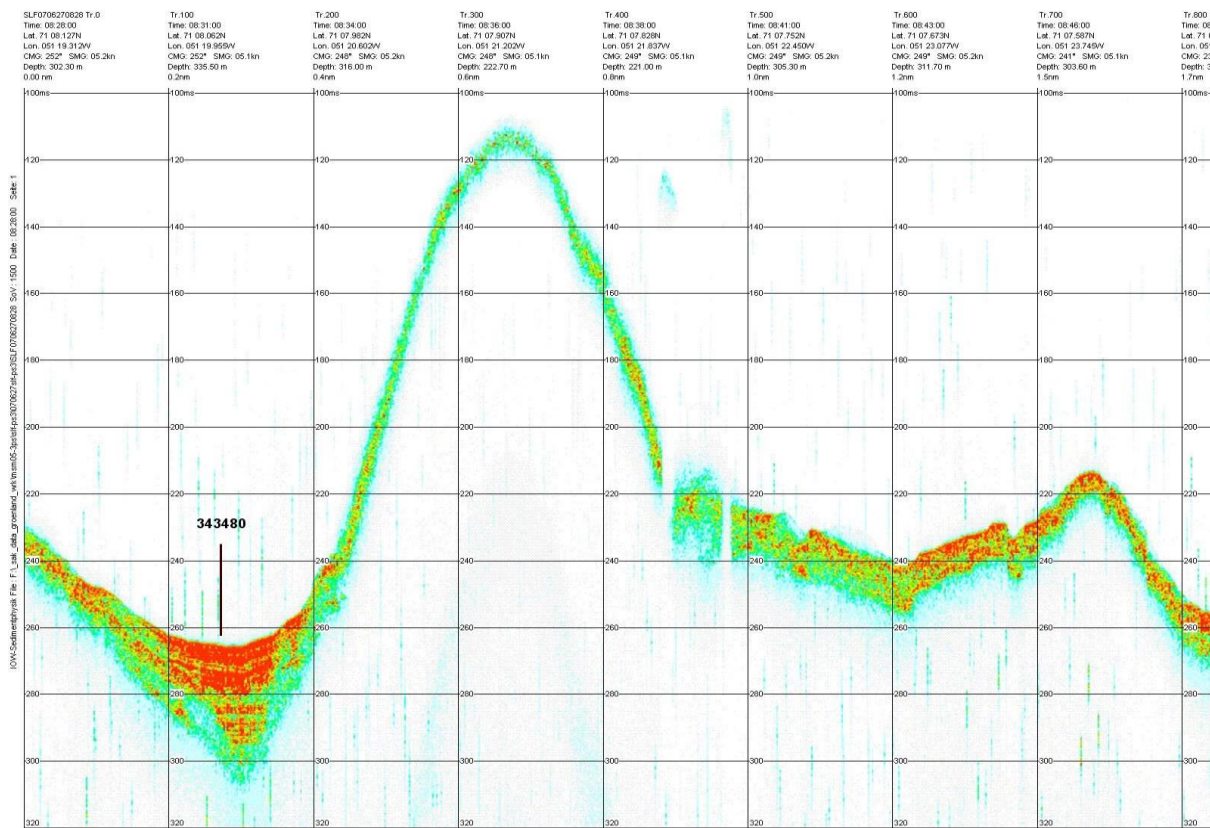


Fig. E6.20: Parasound record at station 343480.

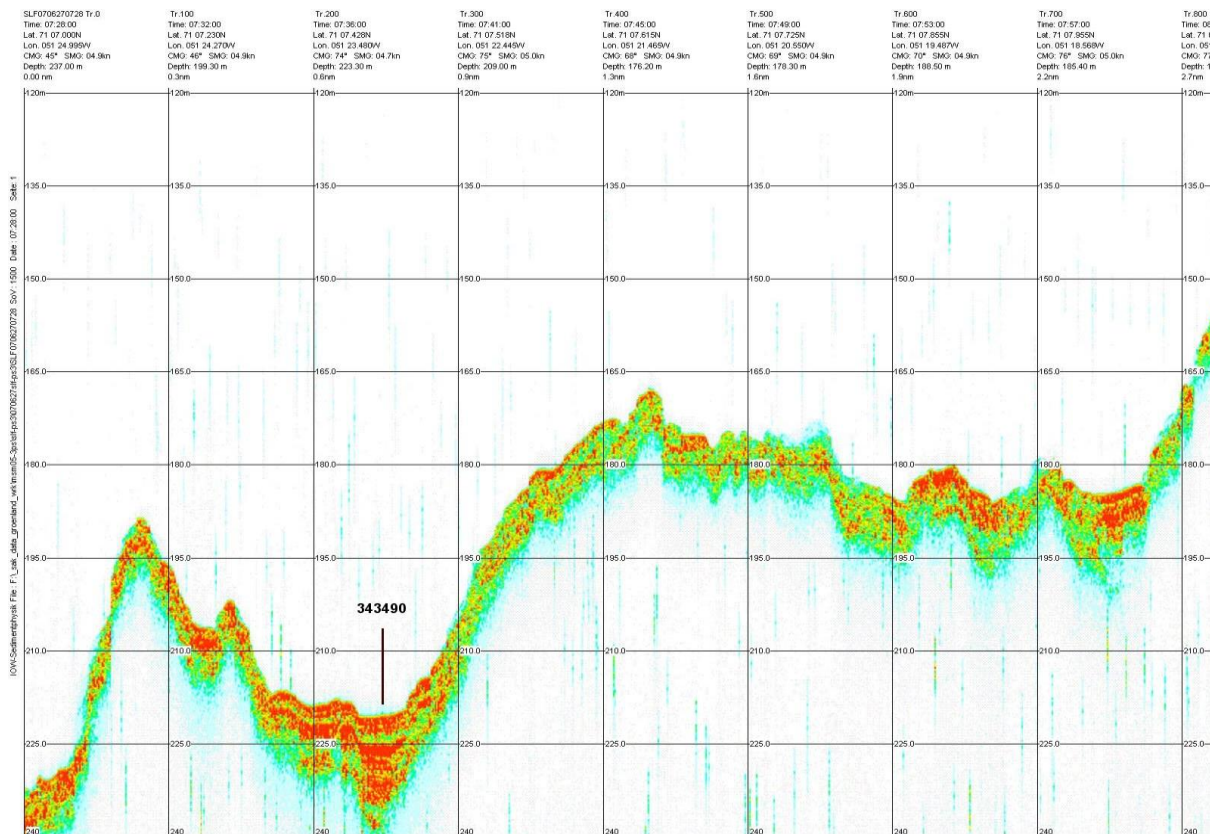


Fig. E6.21: Parasound record at station 343490.

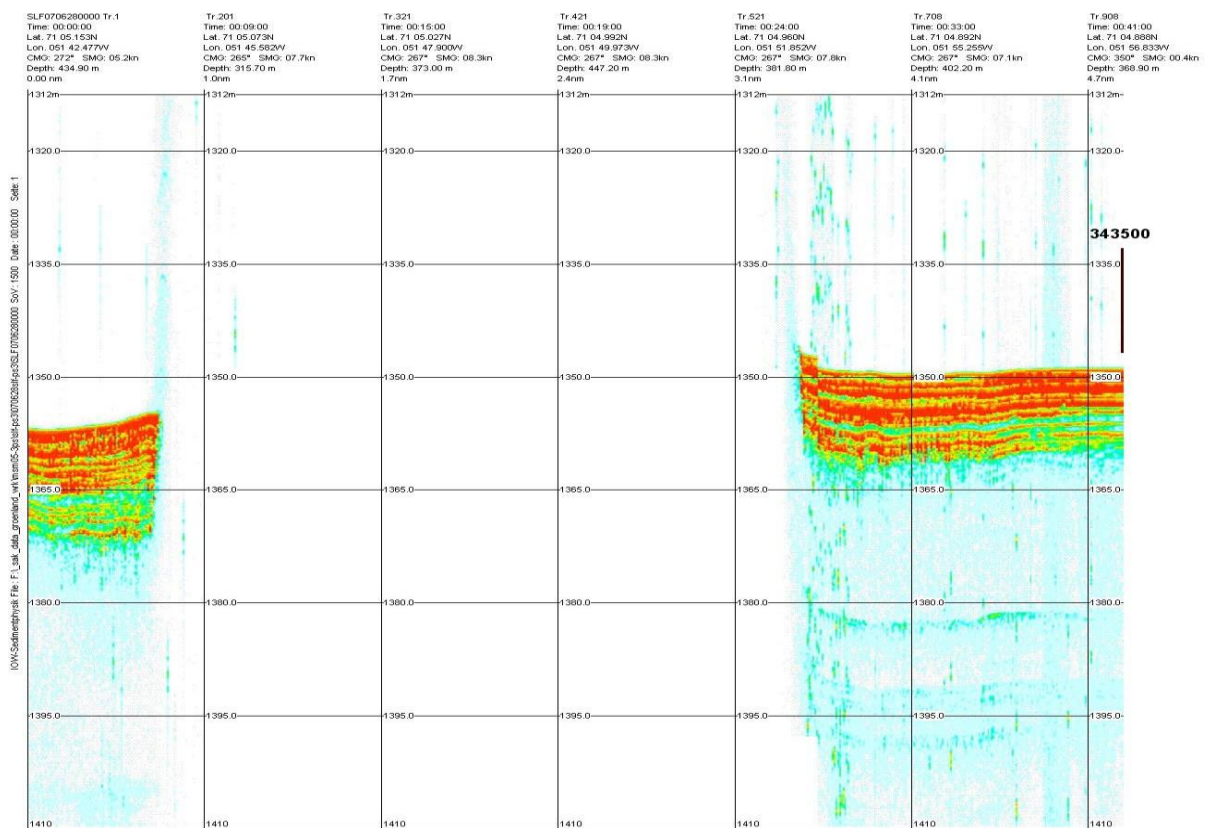


Fig. E6.22: Parasound record at station 343500.

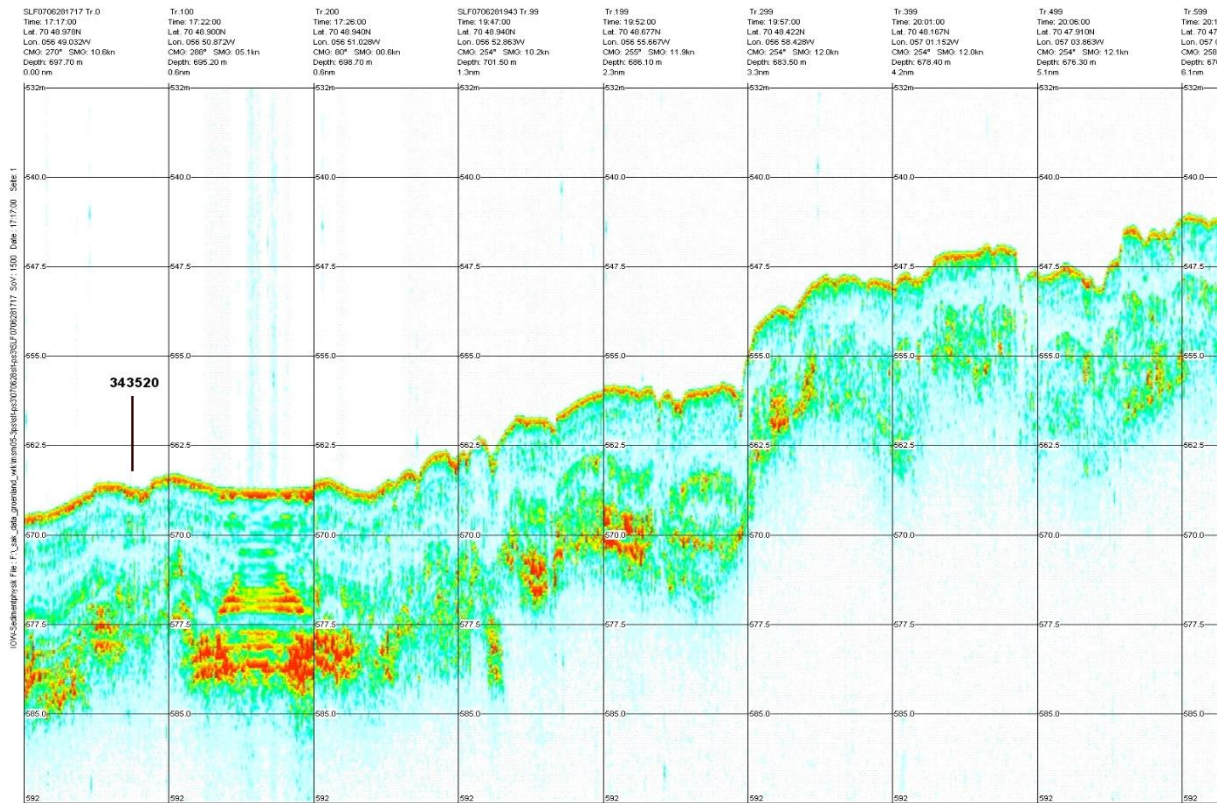


Fig. E6.23: Parasound record at station 343520.

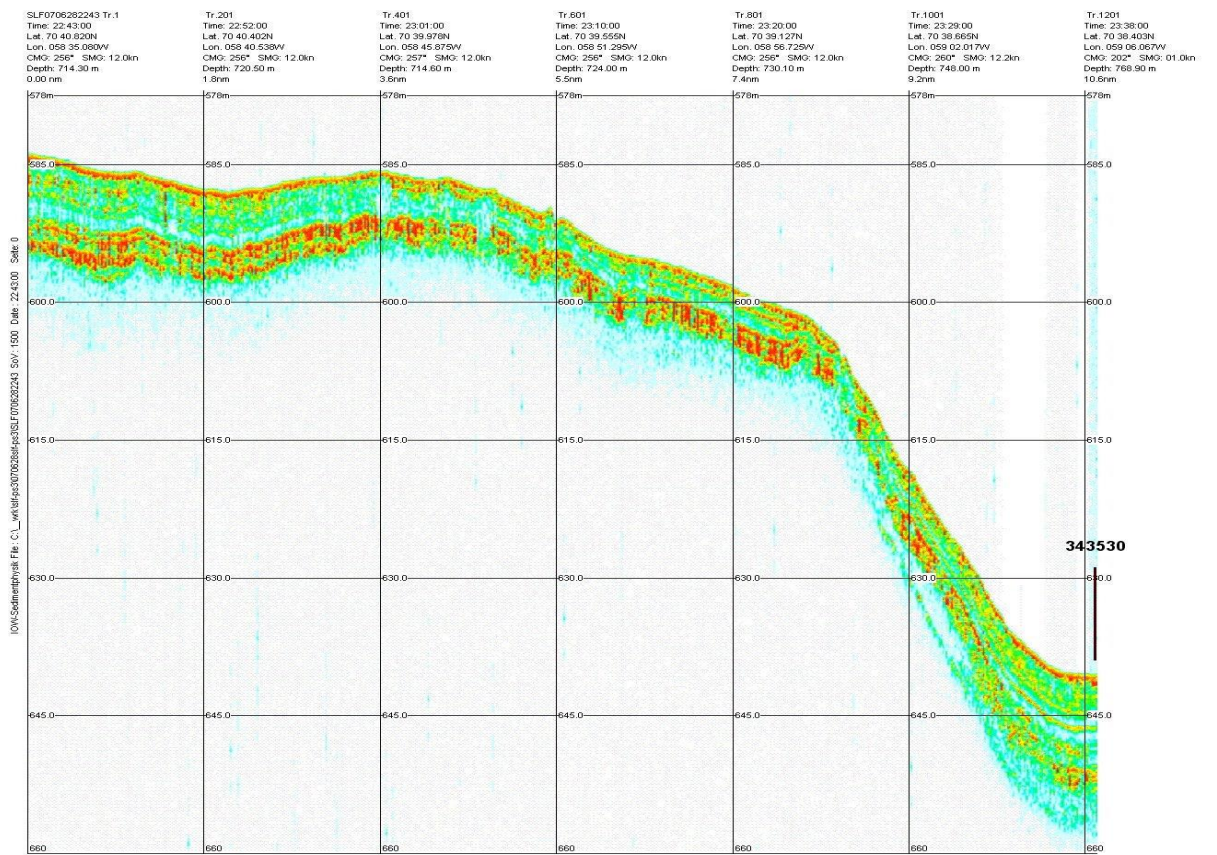


Fig. E6.24: Parasound record at station 343530.

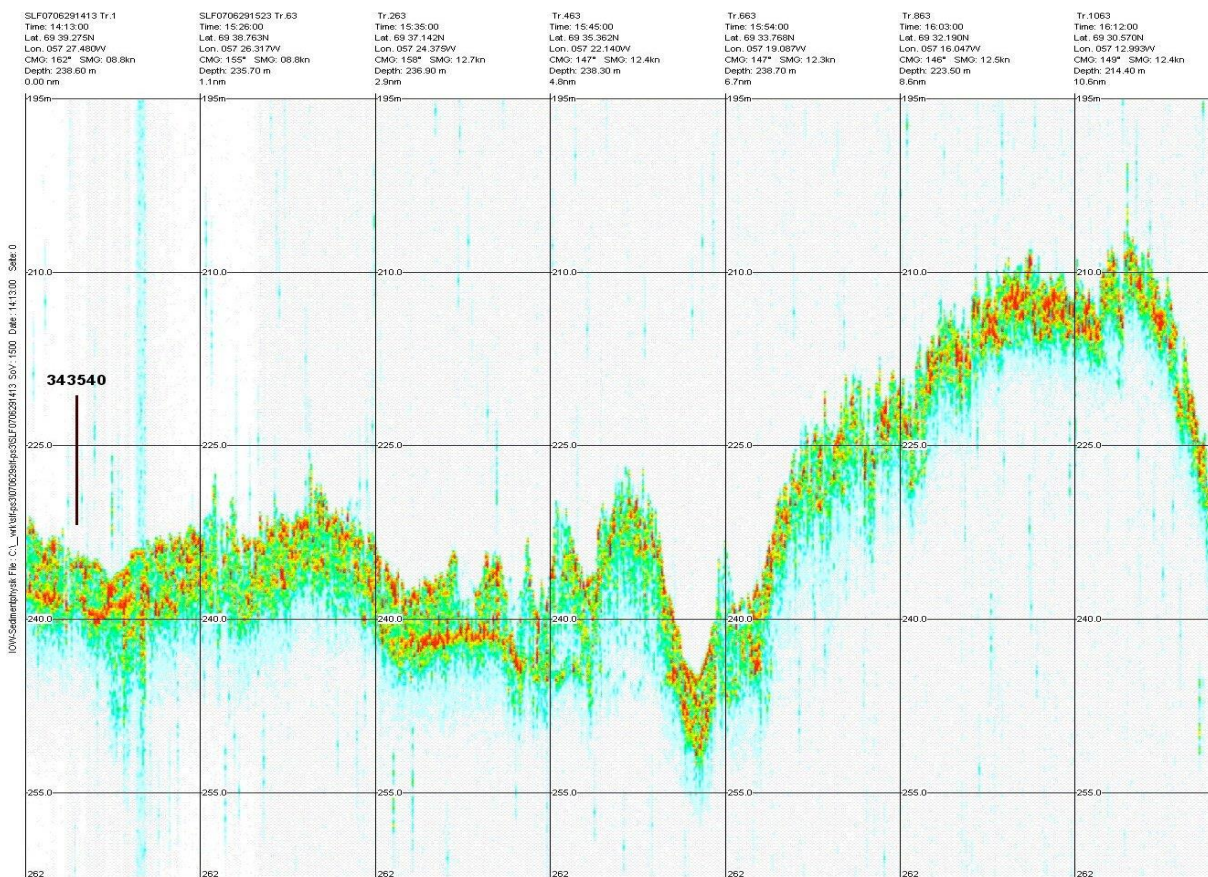


Fig. E6.25: Parasound record at station 343540.

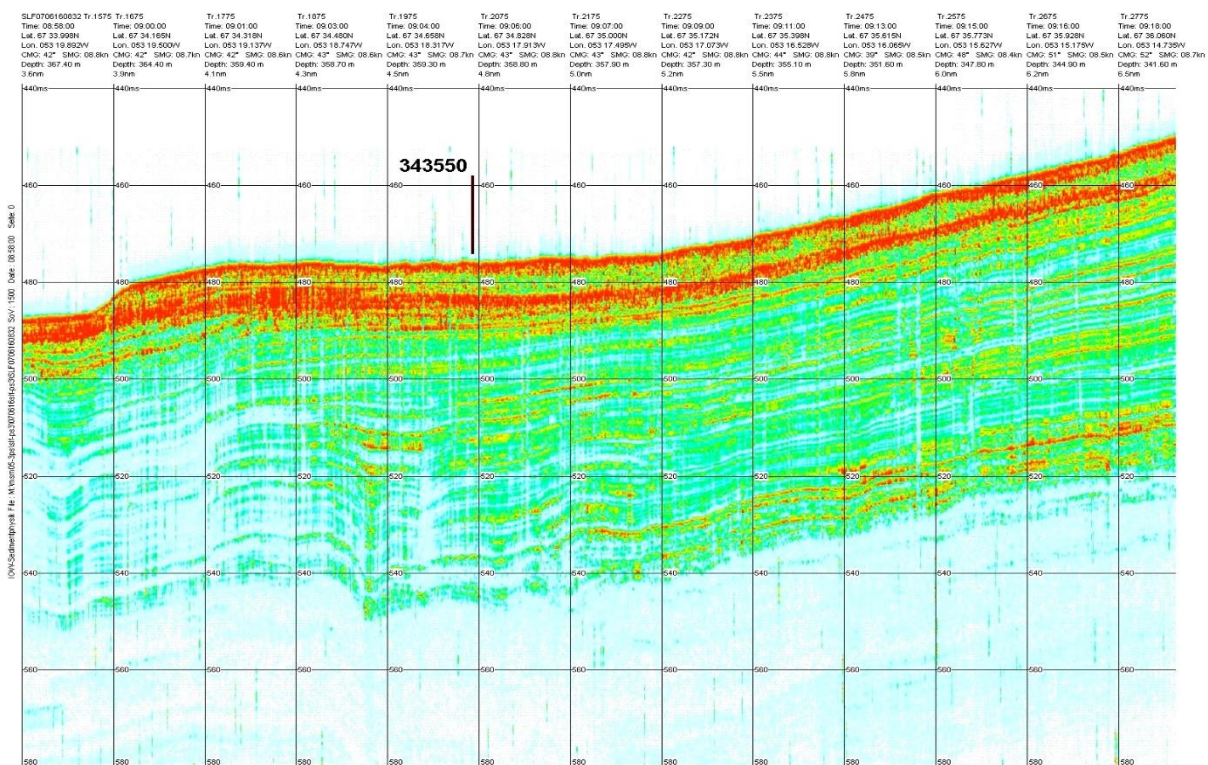


Fig. E6.26: Parasound record at station 343550.

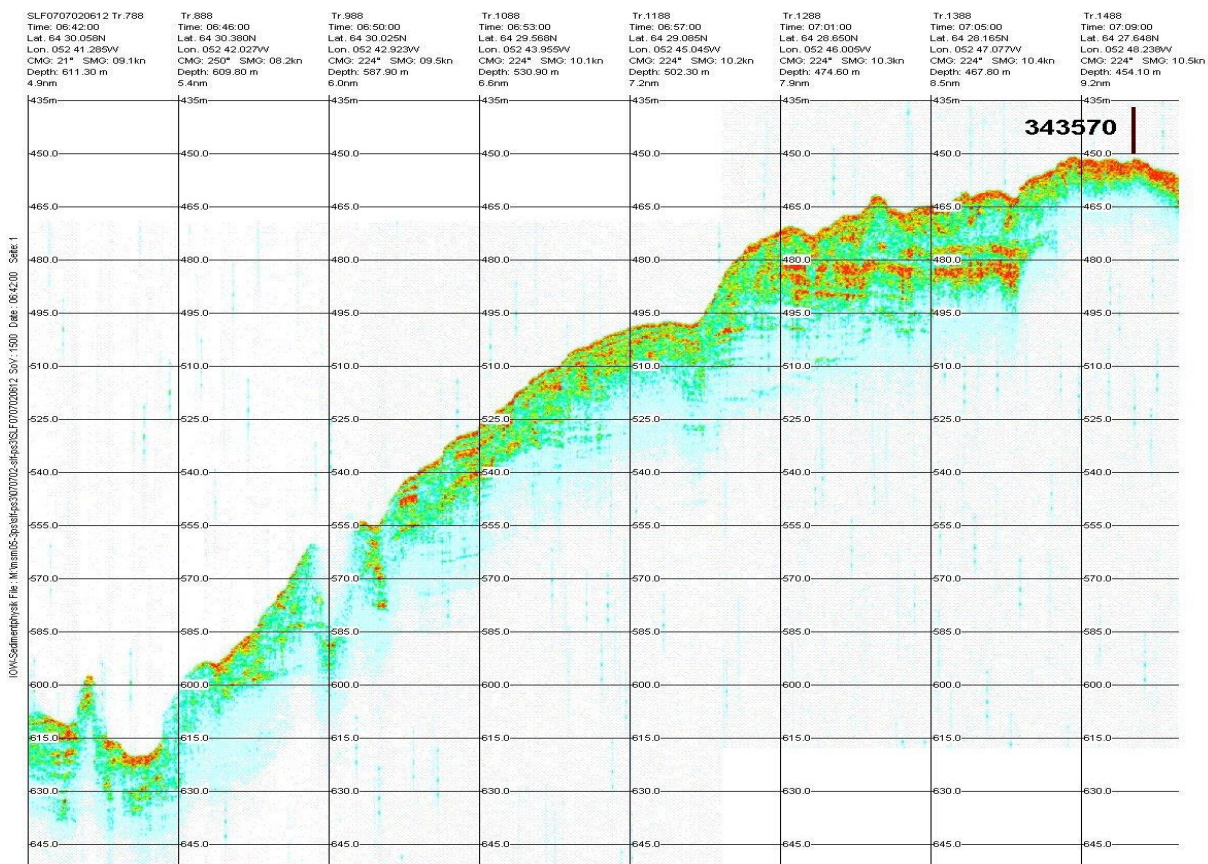


Fig. E6.27: Parasound record at station 343570.

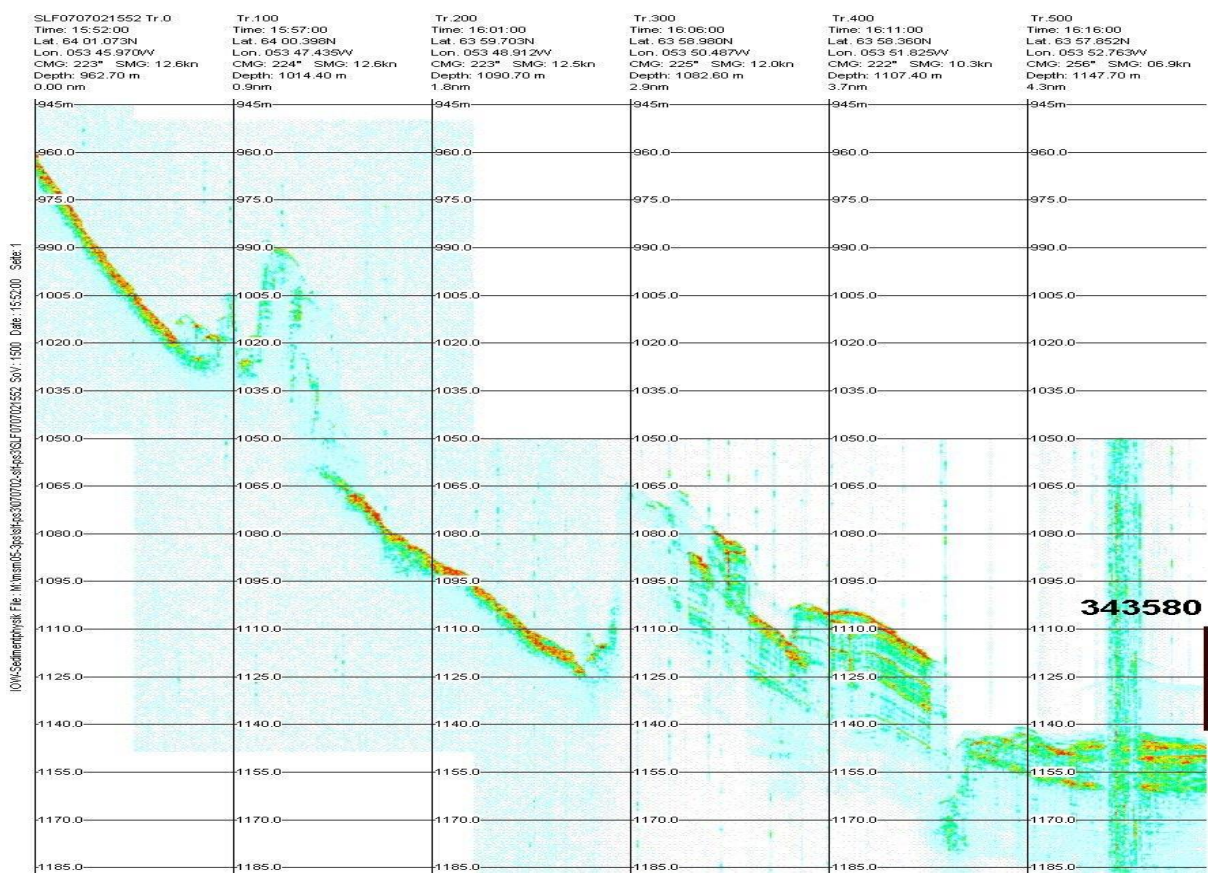


Fig. E6.28: Parasound record at station 343580.

## 7. Core lists

## Core List

Projekt:

Cruise: MSM 05/3

RV- Stat. Code	RV MSM	Area Nordre Stroemfjord	Year 2007	Month June	Day 16	Start (UTC) 17:26:08	IOW- Station ID 343250	
Lat. 67°44.00' Long. 51°20.00'	Water depth start 377,2	Station description No. Of Cores: 11 MUC Positioning System: GPS Geoid: WGS84 Stationsname:						
Core	Time (UTC)	Real Position Lat. Long.	Depth (m)	Gear	Corerlength (m)	Penetration / Gain (m)	Scientist/ Institute	Comment
-1	17:27:02	67°40,478 51°36,930	377,4	CTD			Waniek (IOW)	
-2	18:37:24	67°40,478 51°36,929	377,1	MUC	0,6	0,45	Endler, Krauss (IOW) Rysgaard (GINR) Mikkelsen (GEUS) Witkowski (US)	#1 Endler #2 Krauss #3 subsampled by Rysgaard, Mikkelsen, Witkowski
-3	19:33:42	67°40,479 51°36,930	377,9	BC	0,6	0,5	Rysgaard (GINR)	Thrown away
-4	21:27:55	67°40,478' 51°36,928'	379,3	MUC	0,6	0,34	Rysgaard (GINR)	#1-8 subsampled
-5	22:26:58	67°40,478' 51°36,927'	380,6	GC	6 (foil)		IOW	no gain

## Core List

Projekt:

Cruise: MSM 05/3

RV- Stat. Code	RV MSM	Area Nordre Sroemfjord	Year 2007	Month June	Day 17	Start (UTC) 11:18:26	IOW- Station ID 343260	
Lat. 67°40,600' Long. 51°49,06'	Water depth start 383,1	Station description No. Of Cores: 4 MUC, 2 GC Positioning System: GPS Geoid: WGS84 Stationsname:						
Core	Time (UTC)	Real Position Lat. Long.	Depth (m)	Gear	Corerlength (m)	Penetration / Gain (m)	Scientist/ Institute	Comment
-1	11:20:09	67°40,599' 53°06,600'	383,0	CTD			Waniek (IOW)	Dropt into sediment
-2	12:22:15	67°40,598' 51°49,058'	383,9	MUC	0,6	0,46	Endler, Krauss (IOW) Witkowski (US) Mikkelsen (GEUS)	#1 Endler #2 Krauss #3,4 subsampled by Witkowski, Mikkelsen
-3	13:39:58	67°40,599' 51°49,056'	384,1	GC	6 (foil)	4,3	Mikkelsen (GEUS)	thrown away, subsampled by Mikkelsen
-4	15:31:55	67°40,597' 51°49,052'	383,4	GC	12 (liner)	6,3	Endler (IOW)	Core for Endler
-5	15:06:00 – 17:00:00	67°40,597' 51°49,053'	383,1	GPS-Buoy			Dietrich (TUD)	
-6	16:48:51	67°40,594' 51°49,051'	383,4	GC	12 (liner)	8,07	Krauss (IOW) Snowball (GBSC) Richter (NIOZ)	Core for Krauss, MagSus and XRF done onboard

## Core List

Projekt:

Cruise: MSM 05/3

RV- Stat. Code	RV MSM	Area Nordre Stroemfjord	Year 2007	Month June	Day 17	Start (UTC) 19:39:56	IOW- Station ID 343270	
Lat. 67°40,60' Long. 52°25,20'	Water depth start 554,9	Station description No. Of Cores: 4 MUC Positioning System: GPS Geoid: WGS84 Stationsname:						
Core	Time (UTC)	Real Position Lat. Long.	Depth (m)	Gear	Corerlength (m)	Penetration / Gain (m)	Scientist/ Institute	Comment
-1	19:50:55	67°47,158' 52°25,195'	554,9	CTD			Waniek (IOW)	
-2	20:51:05	67°47, 158' 52°25,199'	554,9	MUC	0,60	0,20	Endler (IOW) Witkowski (US) Mikkelsen (GEUS) Rysgaard (GINR)	#1 Endler #3,4 subsampeld by Witkowski, Mikkelsen, Rysgaard
-3	19:50:00- 20:50:00	67°47,158' 52°25,195'	554,9	GPS-Buoy			TUD	

## Core List

Projekt:

Cruise: MSM 05/3

RV- Stat. Code	RV MSM	Area Nordre Stroemfjord	Year 2007	Month June	Day 18	Start (UTC) 00:19:36	IOW- Station ID 343280	
Lat. 67°38,46' Long. 53°09,46'	Water depth start 311,08	Station description No. Of Cores: 5 MUC; 1 GC Positioning System: GPS Geoid: WGS84 Stationsname:						
Core	Time (UTC)	Real Position Lat. Long.	Depth (m)	Gear	Corerlength (m)	Penetration / Gain (m)	Scientist/ Institute	Comment
-1	00:25:05	67°38,459' 53°09,458'	311,08	CTD			Waniek (IOW)	
-2	01:10:09	67°38,459' 53°09,456'	311,08	MUC	0,6	0,28	Endler (IOW) Lloyd (DU) Mikkelsen (GEUS) Witkowski (US) Rysgaard (GINR)	#1 Endler #2,3,4,5 Lloyd, Mikkelsen, Witkowski, Rysgaard,
-3	01:43:32	67°38,457' 53°09,458'	311,08	GC	6	7,10		Core in foil
-4	02:42:25	67°38,456' 53°09,460'	311,16	GC	12	3,72	Moros (IOW) Snowball (GBSC) Richter (NIOZ)	Core for Moros, MagSus and XRF done onboard
-5	03:31:32	67°38,455' 53°09,460'	310,78 at 304,0 groundcontact	GC	6			Thrown away

## Core List

Projekt:

Cruise: MSM 05/3

RV- Stat. Code	RV MSM	Area Nordre Stoemfjord	Year 2007	Month June	Day 18	Start (UTC) 10:44:22	IOW- Station ID 343290	
Lat. 67°29' Lon. 53°38'	Water depth start 126,50 m	Station description    No. Of Cores: Positioning System: GPS                      Geoid: WGS84                      Stationsname:						
Core	Time (UTC)	Real Position Lat. Long.	Depth (m)	Gear	Corerlength (m)	Penetration / Gain (m)	Scientist/ Institute	Comment
-1	11:29:27	67°28,997' 53°37,998'	124,99	CTD			Waniek (IOW)	Abbruch 11:34:40
-2	11:46:46	67°28,999' 53°37,998'	128,94	BC	0,6		Rysgaard (GINR)	No gain

## Core List

Projekt:

Cruise: MSM 05/3

RV- Stat. Code	RV MSM	Area Disko Bay	Year 2007	Month June	Day 19	Start (UTC) 11:18:14	IOW- Station ID 343300	
Lat. 68°28.312' Long. 54°0,122'	Water depth start 518,7	<b>Station description</b> No. Of Cores: 3 MUC; 1 GC Positioning System: GPS Geoid: WGS84 Stationsname:						
Core	Time (UTC)	Real Position Lat. Long.	Depth (m)	Gear	Corerlength (m)	Penetration / Gain (m)	Scientist/ Institute	Comment
-1	11:24:44	68°28,312' 54°00,118'	519,0	CTD			Waniek (IOW)	
-2	12:22:32	68°28,311' 54°00,118'	519,5	MUC	0,6	0,32	Moros, Endler (IOW) Lloyd (UD) Mikkelsen (GEUS) Rysgaard (GINR) Witkowski (US)	#1 Moros (sliced) MagSus done onboard #2 Endler #3 Subsampled by Lloyd, Mikkelsen, Rysgaard, Witkowski
-3	13:03:13	68°28,311' 54°00,118'	518,1	GC	6 (foil)	7		Thrown away
-4	14:06:00	68°28,311' 54°00,119'	519,4	GC	12 (liner)	11,40	Moros (IOW) Snowball (GBSC) Richter (NIOZ)	Core for Moros, MagSus and XRF done onboard
-5		68°28,312' 54°00,118'		GPS-buoy			TUD	

## Core List

Projekt:

Cruise: MSM 05/3

RV- Stat. Code	RV MSM	Area Disco Bay	Year 2007	Month June	Day 19	Start (UTC) 16:01:23	IOW- Station ID 343310	
Lat. 68°38,872' Long. 53°49,493'	Water depth start 853,8	Station description No. Of Cores: 7 MUC; 2 GC Positioning System: GPS Geoid: WGS84 Stationsname:						
Core	Time (UTC)	Real Position Lat. Long.	Depth (m)	Gear	Corerlength (m)	Penetration / Gain (m)	Scientist/ Institute	Comment
-1	16:32:15	68°38,872' 53°49,485'	849,7	CTD			Waniek (IOW)	
-2	17:24:56	68°38,869' 53°49,486'	852,3	MUC	0,6	0,35	Moros, Endler (IOW) Mikkelsen (GEUS) Rysgaard (GINR) Witkowski (US)	#1 Moros (sliced) MagSus done onboard #2 Endler #3-7 subsampled by Witkowski, Rysgaard, Mikkelsen
-3	18:18:50	68°38,869' 53°49,487'	856,4	GC	6 (foil)	7		Thrown away
-4	19:57:36	68°38,864' 53°49,490'	854,7	GC	18 (liner)			Broken liner
-5	21:35:59	68°38,861' 53°49,493'	855,8	GC	12 (liner)	9,39	Moros (IOW) Snowball (GBSC) Richter (NIOZ)	MagSus, XRF done onboard
-6	23:08:03	68°38,859' 53°49,496'	856,3	GC	12 (liner)	9,11	IOW/GBSC	After MSCL to Lund

## Core List

Projekt:

Cruise: MSM 05/3

RV- Stat. Code	RV MSM	Area Disco Bay	Year 2007	Month June	Day 21	Start (UTC) 00:40:11	IOW- Station ID 343320	
Lat. 68°51,880' Long. 53°19,72'	Water depth start 864,7	Station description No. Of Cores: 8 MUC Positioning System: GPS Geoid: WGS84 Stationsname:						
Core	Time (UTC)	Real Position Lat. Long.	Depth (m)	Gear	Corerlength (m)	Penetration / Gain (m)	Scientist/ Institute	Comment
-1	00:45:24	68°51,879' 53°19,719'	864,8	CTD			Waniek (IOW)	
-2	01:56:15	68°51,879' 53°19,719'	861,8	MUC	0,6	0,53	Moros, Endler (IOW) Witkowski (US) Rysgaard (GINR) Mikkelsen (GEUS)	#1 Moros (sliced) MagSus done onboard #2 Endler #3-8 subsampled by Witkowski, Rysgaard, Mikkelsen

## Core List

Projekt:

Cruise: MSM 05/3

RV- Stat. Code	RV MSM	Area Disco Bay	Year 2007	Month June	Day 20	Start (UTC) 20:35:35	IOW- Station ID 343330	
Lat. 68°58,077' Long. 53°11,109'	Water depth start 828,6	<b>Station description</b> No. Of Cores: 8 MUC; 1GC Positioning System: GPS Geoid: WGS84 Stationsname:						
Core	Time (UTC)	Real Position Lat. Long.	Depth (m)	Gear	Corerlength (m)	Penetration / Gain (m)	Scientist/ Institute	Comment
-1	20:40:38	68°58,076' 53°11,104'	828,6	CTD			Waniek (IOW)	
-2	22:00:02	68°58,076' 53°11,105'	830,4	MUC	0,6	0,31	Moros, Endler (IOW) Lloyd (DU) Mikkelsen (GEUS) Witkowski (US) Rysgaard (GINR)	#1 Moros (sliced) MagSus done onboard #2 Endler #3-8 subsamped by Lloyd, Witkowski, Mikkelsen, Rysgaard
-3	22:56:47	68°58,077' 53°11,104'	829,3	GC	12 (liner)	7,31	Moros (IOW) Snowball (GBSC) Richter (NIOZ)	MagSus, XRF done onboard
-4				GPS-buoy			Dietrich (TUD)	

## Core List

Projekt:

Cruise: MSM 05/3

RV- Stat. Code	RV MSM	Area Disco Bay	Year 2007	Month June	Day 20	Start (UTC) 10:30:15	IOW- Station ID 343340	
Lat. 68°23,838' Long. 55°07,790'	Water depth start 460,35	Station description No. Of Cores: 16 MUC; 3 GC Positioning System: GPS Geoid: WGS84 Stationsname:						
Core	Time (UTC)	Real Position Lat. Long.	Depth (m)	Gear	Corerlength (m)	Penetration / Gain (m)	Scientist/ Institute	Comment
-1	10:37:32	68°23,837' 55°07,787'	460,65	CTD			Waniek (IOW)	
-2	11:32:40	68°23,836' 55°07,786'	467,60	MUC	0,6	0,34	Moros, Endler (IOW) Mikkelsen (GEUS) Rysgaard (GINR) Lloyd (UD)	#1 Moros (sliced) MagSus done onboard #2 Endler #3-8 subsampled by Lloyd, Mikkelsen, Rysgaard
-3	12:27:33	68°23,837' 55°07,786'	462,75	MUC	0,6	0,34	Witkowski (US) Mikkelsen (GEUS) Rysgaard (GINR)	#1-8 subsampled by Witkowski, Mikkelsen, Rysgaard
-4	13:14:02	68°23,837' 55°07,786'	463,1	GC	6 (foil)	Ca. 6 m	Rysgaard (GINR) Mikkelsen (GEUS)	subsampled by Rysgaard, Mikkelsen
-5	14:18:35	68°23,835' 55°07,779'	461,2	GC	12 (liner)	10,74	Moros (IOW) Snowball (GBSC) Richter (NIOZ)	MagSus and XRF done onboard
-6	15:34:46	68°23,834' 55°07,773	461,3	GC	12 (liner)	11	Endler (IOW) Sandgren (GBSC)	After MSCL to Lund
-7				GPS-buoy			Dietrich (TUD)	

## Core List

Projekt:

Cruise: MSM 05/3

RV- Stat. Code	RV MSM	Area Torssukatak Fjord	Year 2007	Month June	Day 22	Start (UTC) 14:12:32	IOW- Station ID 343350	
Lat. 69°57,200' Long. 59°49,34'	Water depth start 723,9	Station description No. Of Cores: Positioning System: GPS Geoid: WGS84 Stationsname:						
Core	Time (UTC)	Real Position Lat. Long.	Depth (m)	Gear	Corerlength (m)	Penetration / Gain (m)	Scientist/ Institute	Comment
-1	14:15:01	69°57,196' 50°49,337'	723,8	CTD			Waniek (IOW)	
-2				GPS-buoy			Dietrich (TUD)	

## Core List

Projekt:

Cruise: MSM 05/3

RV- Stat. Code	RV MSM	Area Torssukatak Fjord	Year 2007	Month June	Day 22	Start (UTC) 17:32:16	IOW- Station ID 343360	
Lat. Long.	Water depth start 734,5	Station description No. Of Cores: 8 MUC; 1 GC Positioning System: GPS Geoid: WGS84 Stationsname:						
Core	Time (UTC)	Real Position Lat. Long.	Depth (m)	Gear	Corerlength (m)	Penetration / Gain (m)	Scientist/ Institute	Comment
-1	17:44:12	69°56,835' 51°13,611'	739,1	CTD			Waniek (IOW)	
-2	18:52:45	69°56,831' 51°13,659'	737,0	MUC	0,6			No gain
-3	19:47:54	69°56,832' 51°13,657'	731,36	MUC	0,6			No gain
-4	20:34:05	69°56,832' 51°13,658'	733,9	GC	12		Endler (IOW)	Upper 4m liquified/turbated while cutting sections.
-5	21:36:10	69°56,838' 51°13,660'	738,8	MUC	0,6	0,46	Moros, Endler (IOW) Lloyd (UD) Witkowski (US) Mikkelsen (GEUS) Rysgaard (GINR)	#1 Moros (sliced) MagSus done onboard #2 Endler #3-8 subsampled by Lloyd, Witkowski, Mikkelsen, Rysgaard
-6	17:44- 18:15	69°56,835' 51°13,611'	739,1	GPS-Buoy			Dietrich (TUD)	

## Core List

Projekt:

Cruise: MSM 05/3

RV- Stat. Code	RV MSM	Area Vaigat	Year 2007	Month June	Day 23	Start (UTC) 11:51:34	IOW- Station ID 343370	
Lat. Long.	Water depth start 312,2	Station description    No. Of Cores: Positioning System: GPS                      Geoid: WGS84                      Stationsname:						
Core	Time (UTC)	Real Position Lat.   Long.	Depth (m)	Gear	Corerlength (m)	Penetration / Gain (m)	Scientist/ Institute	Comment
-1	11:56:02	70°36,278' 54°31,637'	313,4	CTD			Waniek (IOW)	

## Core List

Projekt:

Cruise: MSM 05/3

RV- Stat. Code	RV MSM	Area Vaigat	Year 2007	Month June	Day 23	Start (UTC) 17:42:01	IOW- Station ID 343380	
Lat. Long.	Water depth start 579,7	Station description No. Of Cores: 8 MUC; 1 GC Positioning System: GPS Geoid: WGS84 Stationsname:						
Core	Time (UTC)	Real Position Lat. Long.	Depth (m)	Gear	Corerlength (m)	Penetration / Gain (m)	Scientist/ Institute	Comment
-1	17:45:01	70°19,042' 53°41,690'	580,0	CTD			Waniek (IOW)	
-2	18:46:10	70°19,041' 53°41,692'	578,2	MUC	0,6	0,33	Moros, Endler (IOW) Sandgren (GBSC) Lloyd (DU) Mikkelsen (GEUS) Witkowski (US)	#1 Moros (sliced) MagSus done onboard #2 Endler #3 Sandgren #4-8 subsampled by Lloyd, Mikkelsen, Witkowski,
-3	19:28:05	70°19,041' 53°41,692'	578,4	GC	12 (liner)		Moros (IOW) Snowball (GBSC) Richter (NIOZ) Lloyd (UD)	Core for Moros, MagSus and XRF done onboard, Corecatcher subsampled by Lloyd

## Core List

Projekt:

Cruise: MSM 05/3

RV- Stat. Code	RV MSM	Area Vaigat	Year 2007	Month June	Day 23	Start (UTC) 21:56:53	IOW- Station ID 343390	
Lat. 70°13,178' Long. 53°03,320'	Water depth start 537,9	Station description No. Of Cores: 8 MUC; 1 GC Positioning System: GPS Geoid: WGS84 Stationsname:						
Core	Time (UTC)	Real Position Lat. Long.	Depth (m)	Gear	Corerlength (m)	Penetration / Gain (m)	Scientist/ Institute	Comment
-1	22:01:02	70°13,176' 53°03,194'	537,7	CTD			Waniek (IOW)	
-2	22:53:31	70°13,177' 53°03,195'	537,3	MUC	0,6	0,25	Moros, Endler (IOW) Lloyd (UD) Mikkelsen (GEUS) Rysgaard (GINR)	#1 Moros (sliced) MagSus done onboard #2 Endler #3-8 subsampled by Lloyd, Mikkelsen, Rysgaard
-3	23:29:49	70°13,176' 53°03,194'	537,6	GC	12 (liner)	5,06	Moros (IOW) Snowball, (GBSC) Richter (NIOZ) Lloyd (UD)	MagSus and XRF done onboard Corecatcher subsampled by Lloyd

## Core List

Projekt:

Cruise: MSM 05/3

RV- Stat. Code	RV MSM	Area Vaigat	Year 2007	Month June	Day 24	Start (UTC) 03:42:00	IOW- Station ID 343400	
Lat. 69°55,09' Long. 51°49,31'	Water depth start 501,0	Station description No. Of Cores: Positioning System: GPS Geoid: WGS84 Stationsname:						
Core	Time (UTC)	Real Position Lat. Long.	Depth (m)	Gear	Corerlength (m)	Penetration / Gain (m)	Scientist/ Institute	Comment
-1	03:42:00	69°55,09' 51°49,31'	501,0	CTD			Waniek (IOW)	

## Core List

Projekt:

Cruise: MSM 05/3

RV- Stat. Code	RV MSM	Area Disco Bay	Year 2007	Month June	Day 24	Start (UTC) 11:59:34	IOW- Station ID 343410	
Lat. Long.	Water depth start 398,6	Station description No. Of Cores: 1 MUC Positioning System: GPS Geoid: WGS84 Stationsname:						
Core	Time (UTC)	Real Position Lat. Long.	Depth (m)	Gear	Corerlength (m)	Penetration / Gain (m)	Scientist/ Institute	Comment
-1	12:02:22	69°10,998' 51°29,499'	398,5	CTD			Waniek (IOW)	
-2	12:42:58	69°10,998' 51°29,499'	398,7	MUC	0,6	0,39	Endler (IOW)	#1 Endler

## Core List

Projekt:

Cruise: MSM 05/3

RV- Stat. Code	RV MSM	Area Uummanaq Fjord	Year 2007	Month June	Day 26	Start (UTC) 04:20:00	IOW- Station ID 343420	
Lat. 70°22,620' Long. 50°48,720'	Water depth start 833,0	Station description No. Of Cores: Positioning System: GPS Geoid: WGS84 Stationsname:						
Core	Time (UTC)	Real Position Lat. Long.	Depth (m)	Gear	Corerlength (m)	Penetration / Gain (m)	Scientist/ Institute	Comment
-1	04:28:00	70°22,62' 50°48,72'	830,4	CTD			Waniek (IOW) Shevchenko (SIO)	

## Core List

Projekt:

Cruise: MSM 05/3

RV- Stat. Code	RV MSM	Area Uummanaq Fjord	Year 2007	Month June	Day 26	Start (UTC) 10:10:26	IOW- Station ID 343430	
Lat. 70°29,570' Long. 51°37,117'	Water depth start 936,2	Station description No. Of Cores: 8 MUC; 1 GC Positioning System: GPS Geoid: WGS84 Stationsname:						
Core	Time (UTC)	Real Position Lat. Long.	Depth (m)	Gear	Corerlength (m)	Penetration / Gain (m)	Scientist/ Institute	Comment
-1	10:15:36	70°29,409' 51°35,860'	935,7	CTD			Waniek (IOW) Shevchenko (SIO)	
-2	11:41:53	70°29,409' 51°35,859'	935,7	MUC	0,6			No gain
-3	12:36:01	70°29,409' 51°35,859'	942,0	MUC	0,6			No gain
-4	13:31:49	70°29,388' 51°35,892'	934,6	MUC	0,6	0,52	Endler, Krauss, Perner (IOW) Mikkelsen (GEUS) Rysgaard (GINR)	#2 Endler #3 Perner #4 Krauss #1,5-8 subsampled by Mikkelsen, Rysgaard
-5	14:24:57	70°29,395' 51°35,881'	934,2	GC	12 (liner)	10,92	Krauss (IOW) Richter (NIOZ)	Core for Krauss, MagSus and XRF done onboard

## Core List

Projekt:

Cruise: MSM 05/3

RV- Stat. Code	RV MSM	Area Uummanaq Fjord	Year 2007	Month June	Day 26	Start (UTC) 18:27:45	IOW- Station ID 343440	
Lat. 70°39,786' Long. 52°06,479'	Water depth start 183,5	Station description No. Of Cores: Positioning System: GPS Geoid: WGS84 Stationsname:						
Core	Time (UTC)	Real Position Lat. Long.	Depth (m)	Gear	Corerlength (m)	Penetration / Gain (m)	Scientist/ Institute	Comment
-1	18:35:01	70°39,750' 52°06,855'	183,4	CTD			Waniek (IOW) Shevchenko (SIO)	
-2	19:42 – 23:46	70°39,750' 52°06,855'	183,4	Waterpump			Waniek (IOW)	

## Core List

Projekt:

Cruise: MSM 05/3

RV- Stat. Code	RV MSM	Area Quamarujuk Fjord	Year 2007	Month June	Day 27	Start (UTC) 10:34:03	IOW- Station ID 343450	
Lat. 71°08,368' Long. 51°15,409'	Water depth start 171,2	Station description No. Of Cores: 4 MUC; 1 GC Positioning System: GPS Geoid: WGS84 Stationsname:						
Core	Time (UTC)	Real Position Lat. Long.	Depth (m)	Gear	Corerlength (m)	Penetration / Gain (m)	Scientist/ Institute	Comment
-1	11:32:17	71°08,391' 51°15,844'	172,4	CTD			Waniek (IOW)	
-2	12:12:22	71°08,390' 51°15,845'	170,6	BC	0,6	0,55/0,45	Endler, Perner (IOW) Mikkelsen (GEUS) Rysgaard (GINR)	1 MUC-liner for Endler #1 2 MUC-liner sliced for Perner #2,3 1 MUC-liner sliced #4 for Mikkelsen further subsamplingby Rysgaard
-3	13:10:01	71°08,388' 51°15,840'	171,2	GC	6 (liner)	4,47	Perner, Krauss (IOW) Mikkelsen (GEUS) Richter (NIOZ)	Core for Perner MagSus and XRF done onboard corecatcher subsamped by Mikkelsen

## Core List

Projekt:

Cruise: MSM 05/3

RV- Stat. Code	RV MSM	Area Quamarujuk Fjord	Year 2007	Month June	Day 27	Start (UTC) 14:56:06	IOW- Station ID 343460	
Lat. 71°07,152' Long. 51°15,321'	Water depth start 64,1	<b>Station description</b> No. Of Cores: 2 MUC; 1 GC Positioning System: GPS Geoid: WGS84 Stationsname:						
Core	Time (UTC)	Real Position Lat. Long.	Depth (m)	Gear	Corerlength (m)	Penetration / Gain (m)	Scientist/ Institute	Comment
-1	15:15:12	71°07,154' 51°15,325'	63,3	BC	0,6	0,55/0,39	Endler, Perner (IOW)	1 core for Endler #2 1 core for Perner #1 scliced
-2	16:02:25	71°07,152' 51°15,320'	65,7	GC	6 (liner)	4,77	Perner, Krauss (IOW) Richter (NIOZ)	Core for Perner, MagSus, XRF done onboard
-3				GPS-buoy			Dietrich (TUD)	

## Core List

Projekt:

Cruise: MSM 05/3

RV- Stat. Code	RV MSM	Area Quamarujuk Fjord	Year 2007	Month June	Day 27	Start (UTC) 17:13:13	IOW- Station ID 343470	
Lat. 71°06,490' Long. 51°13,952'	Water depth start 59,23	Station description No. Of Cores: 5 MUC; 1 GC Positioning System: GPS Geoid: WGS84 Stationsname:						
Core	Time (UTC)	Real Position Lat. Long.	Depth (m)	Gear	Corerlength (m)	Penetration / Gain (m)	Scientist/ Institute	Comment
-1	17:52:15	71°06,491' 51°13,958'	59,29	BC	0,6	Loaded overtop	Perner (IOW)	Thrown away
-2	18:16:56	71°06,489' 51°13,951'	59,41	GC	6 (liner)	4,81	Perner, Krauss (IOW) Richter (NIOZ)	Core for Perner, MagSus and XRF done onboard
-3	18:55:01	71°06,489' 51°13,953'	59,49	BC	0,6	0,6	Endler, Perner (IOW) Mikkelsen (GEUS) Rysgaard (GINR)	1 core for Perner #1 scliced, 1 core for Endler #2 2 cores for Mikkelsen #3,4 1 core for Rysgaard #5

## Core List

Projekt:

Cruise: MSM 05/3

RV- Stat. Code	RV MSM	Area Quamarujuk Fjord	Year 2007	Month June	Day 27	Start (UTC) 20:12:17	IOW- Station ID 343480	
Lat. 71°08,03' Long. 51°20,23'	Water depth start 201,43	Station description No. Of Cores: 2 MUC Positioning System: GPS Geoid: WGS84 Stationsname:						
Core	Time (UTC)	Real Position Lat. Long.	Depth (m)	Gear	Corerlength (m)	Penetration / Gain (m)	Scientist/ Institute	Comment
-1	20:19:14	71°08,030' 51°29,226'	201,67	CTD			Waniek (IOW) Shevchenko (SIO)	
-2	21:02:28	71°08,030' 51°20,244'	201,71	MUC	0,6	0,17	Perner (IOW)	No gain
-3	21:17:09	71°08,028' 51°20,230'	201,97	MUC	0,6	0,34	Endler, Perner (IOW)	#1 sliced for Perner # 2 Endler
-4				GPS-buoy			Dietrich (TUD)	

## Core List

Projekt: Cruise: MSM 05/3

RV- Stat. Code	RV MSM	Area Quamarujuk Fjord	Year 2007	Month June	Day 27	Start (UTC) 22:01:15	IOW- Station ID 343490
Lat. 71°07.474' Long. 51°22.966'	Water depth start 223,84	Station description No. Of Cores: 2 MUC Positioning System: GPS Geoid: WGS84 Stationsname:					
Core	Time (UTC)	Real Position Lat. Long.	Depth (m)	Gear	Corerlength (m)	Penetration / Gain (m)	Scientist/ Institute Comment
-1	22:12:50	71°07,474' 51°22,958'	223,94	CTD			Waniek (IOW)
-2	22:43:04	71°07,474' 51°22,958'	224,04	MUC	0,6	0,28	Endler, Perner (IOW) #1 sliced for Perner #2 Endler
-3				GPS-buoy			Dietrich (TUD)

## Core List

Projekt: Cruise: MSM 05/3

RV- Stat. Code	RV MSM	Area Quamarujuk Fjord	Year 2007	Month June	Day 28	Start (UTC) 00:45:43	IOW- Station ID 343500
Lat. Long.	Water depth start 1345,2	Station description No. Of Cores: 3 MUC Positioning System: GPS Geoid: WGS84 Stationsname:					
Core	Time (UTC)	Real Position Lat. Long.	Depth (m)	Gear	Corerlength (m)	Penetration / Gain (m)	Scientist/ Institute Comment
-1	00:52:33	71°04,888' 51°56,846'	1345,2	CTD			Waniek (IOW) Shevchenko (SIO)
-2	02:17:26	71°04,888' 51°56,846'	1301,25	MUC	0,6	0,43	Endler, Perner (IOW) Mikkelsen (GEUS) #1 sliced for Perner, #2 Endler, #3 Mikkelsen

## Core List

Projekt:

Cruise: MSM 05/3

RV- Stat. Code	RV MSM	Area Uummanaq Fjord (Shelf)	Year 2007	Month June	Day 28	Start (UTC) 11:15:00	IOW- Station ID 343510	
Lat. 70°37,38' Long. 54°32,05'	Water depth start 285	Station description No. Of Cores: Positioning System: GPS Geoid: WGS84 Stationsname:						
Core	Time (UTC)	Real Position Lat. Long.	Depth (m)	Gear	Corerlength (m)	Penetration / Gain (m)	Scientist/ Institute	Comment
-1	11:15:00	70°37,34' 54°31,89'	285	CTD			Waniek (IOW)	

## Core List

Projekt:

Cruise: MSM 05/3

RV- Stat. Code	RV MSM	Area Uumannaq Fjord (Shelf)	Year 2007	Month June	Day 28	Start (UTC) 17:29:33	IOW- Station ID 343520	
Lat. 70°45,00' Long. 54°49,80'	Water depth start 557,5	Station description No. Of Cores: 8 MUC; 1 GC Positioning System: GPS Geoid: WGS84 Stationsname:						
Core	Time (UTC)	Real Position Lat. Long.	Depth (m)	Gear	Corerlength (m)	Penetration / Gain (m)	Scientist/ Institute	Comment
-1	17:36:43	70°48,949' 56°50,893'	557,3	CTD			Waniek (IOW)	
-2	18:30:11	70°48,950' 56°50,894'	545,3	MUC	0,6	0,4	Moros, Endler (IOW) Mikkelsen (GEUS) Rysgaard(GINR) Witkowski(US)	#1 sliced for Moros #2 Endler #3-8 subsampled by Mikkelsen, Rysgaard, Witkowski
-3	19:08:00	70°48,951' 56°50,898'	545,7	GC	12 (liner)		Moros, Krauss (IOW) Mikkelsen (GEUS) Richter (NIOZ)	Core for Moros, MagSus, XRF done onboard corecatcher subsampled by Mikkelsen
-4				GPS- Buoy				

## Core List

Projekt:

Cruise: MSM 05/3

RV- Stat. Code	RV MSM	Area Uumannaq Fjord (shelf)	Year 2007	Month June	Day 28	Start (UTC) 21:45:12	IOW- Station ID 343530	
Lat. 70°38,40' Long. 59°06,00'	Water depth start 618	Station description No. Of Cores: 8 MUC Positioning System: GPS Geoid: WGS84 Stationsname:						
Core	Time (UTC)	Real Position Lat. Long.	Depth (m)	Gear	Corerlength (m)	Penetration / Gain (m)	Scientist/ Institute	Comment
-1	23:49:15	70°38,399' 59°05,992'	626,2	CTD			Waniek (IOW)	
-2	00:52:44	70°38,399' 59°05,993'	641,27	MUC	0,6	0,27	Moros, Endler (IOW) Mikkelsen (GEUS) Rysgaard (GINR)	#1 sliced for Moros #2 Endler #3-8 subsamped
-3	02:03:00- 08:28:00	Water-Pump					Waniek (IOW)	
-4		GPS-Buoy					Dietrich (TUD)	

## Core List

Projekt:

Cruise: MSM 05/3

RV- Stat. Code	RV MSM	Area	Year 2007	Month June	Day 29	Start (UTC) 14:25:56	IOW- Station ID 343540	
Lat. Long.	Water depth start 228,6	Station description No. Of Cores: 8 MUC Positioning System: GPS Geoid: WGS84 Stationsname:						
Core	Time (UTC)	Real Position Lat. Long.	Depth (m)	Gear	Corerlength (m)	Penetration / Gain (m)	Scientist/ Institute	Comment
-1	14:32:10	69°38,959' 57°26,931'	230	CTD			Waniek (IOW) Shevchenko (SIO)	
-2	15:08:36	69°38,959' 57°26,933	229,2	MUC	0,6	0,24	Moros, Ender (IOW) Mikkelsen (GEUS) Ryssgaard (GINR)	#1 sliced for Moros #2 Ender #3-8 subsampled by Mikkelsen, Rysgaard
-3				GPS-Buoy			Dietrich (TUD)	

## Core List

Projekt:

Cruise: MSM 05/3

RV- Stat. Code	RV MSM	Area Nordre Stroemfjord	Year 2007	Month July	Day 1	Start (UTC) 00:50:54	IOW- Station ID 343550	
Lat.67°34.89' Long.53°18.00'	Water depth start 345,2	Station description No. Of Cores: Positioning System: GPS Geoid: WGS84 Stationsname:						
Core	Time (UTC)	Real Position Lat. Long.	Depth (m)	Gear	Corerlength (m)	Penetration / Gain (m)	Scientist/ Institute	Comment
-1	00:54:06	67°34,891' 53°17,998'	345,2	CTD			Waniek (IOW) Shevchenko (SIO)	
-2	01:38:21	67°34,890' 53°17,998'	345,1	MUC	0,6			No gain
-3	02:06:04	67°34,891' 53°17,998'	345,0	MUC	0,6			No gain
-4	02:33:37	67°34,889' 53°18,003'	344,5	GC	12 (liner)	5,82	Moros (IOW)	MagSus done onboard
-5	00:59- 02:42	67°34,891' 53°17,998'	345,2	GPS-Buoy			Dietrich (TUD)	

## Core List

Projekt:

Cruise: MSM 05/3

RV- Stat. Code	RV MSM	Area Godthabs Fjord (shelf)	Year 2007	Month July	Day 2	Start (UTC) 10:59:28	IOW- Station ID 343570	
Lat. 64°28.082' Long. 52°48,159'	Water depth start 440,3	Station description No. Of Cores: Positioning System: GPS Geoid: WGS84 Stationsname:						
Core	Time (UTC)	Real Position Lat. Long.	Depth (m)	Gear	Corerlength (m)	Penetration / Gain (m)	Scientist/ Institute	Comment
-1	10:58:11	64°27,586' 52°48,380'	440,0	CTD			Waniek (IOW) Shevchenko (SIO)	
-2	11:51:25	64°27,585' 52°48,380'	438,5	MUC	0,6	0,21	Endler, Waniek (IOW) Kuijpers (GEUS) Rysgaard (GINR) Witkowski (US)	#1,4 Endler #2 Kuijpers #3 sliced for Kuijpers #5-8 subsampled by Rysgaard, Witkowski
-3	12:27:50	64°27,585' 52°48,380'	439,3	GC	12 (liner)	2,44	Kuijpers (GEUS)	to Copenhagen
-4	10:59- 12:44	64°27,586' 52°48,380'	440,0	GPS-Buoy			Dietrich (TUD)	

## Core List

Projekt:

Cruise: MSM 05/3

RV- Stat. Code	RV MSM	Area Godthabs Fjord (shelf)	Year 2007	Month July	Day 2	Start (UTC) 16:21:24	IOW- Station ID 343580	
Lat. 63°57,80' Long. 53°53,00'	Water depth start 1110,9	Station description No. Of Cores: Positioning System: GPS Geoid: WGS84 Stationsname:						
Core	Time (UTC)	Real Position Lat. Long.	Depth (m)	Gear	Corerlength (m)	Penetration / Gain (m)	Scientist/ Institute	Comment
-1	16:30:21	63°57,802' 53°53,012'	1110,4	CTD			Waniek (IOW) Shevchenko (SIO)	
-2	17:49:44	63°57,864' 53°54,089'	1111,00	MUC	0,6	Ca. 30 cm	Endler, Waniek (IOW)	#1 Endler #2 subsampled by Waniek
-3	19:12- 01:35	63°57,94' 53°55,41'	1168,9	Waterpump			Waniek (IOW)	
-4	16:22- 17:27	63°57,86' 53°54,09'	1110,9	GPS-Boje			Dietrich (TUD)	

## Core List

Projekt:

Cruise: MSM 05/3

RV- Stat. Code	RV MSM	Area Godthabs Fjord	Year 2007	Month July	Day 3	Start (UTC) 08:00	IOW- Station ID 343590	
Lat. 64°21,96' Long. 51°36,31'	Water depth start	Station description No. Of Cores: Positioning System: GPS Geoid: WGS84 Stationsname:						
Core	Time (UTC)	Real Position Lat. Long.	Depth (m)	Gear	Corerlength (m)	Penetration / Gain (m)	Scientist/ Institute	Comment
-1	08:11	64°21,96' 51°36,34'	602,1	CTD			Waniek (IOW) Shevchenko (SIO)	
-2	10:15- 14:20	64°21,97' 51°36,28'	596,6	Waterpump			Waniek (IOW)	
-3	15:06:10	64°18,836' 51°37,936'	288,6	MUC	0,6			No gain
-4	16:09:26	64°21,491' 51°37,261'	581,6	MUC	0,6			No gain
-5	11:14- 13:25	64°21,97' 51°36,28'	600,7	GPS-Buoy			Dietrich (TUD)	

## 8. Sample List

### Andrzej Witkowski

#### 1. Inland samples collected from 4 GPS stations

- Moss – 19 samples
- Sands/sediments – 19 samples
- Moss squeeze – 11 samples
- Scarpe/pool rocks – 12 samples
- Macroalgae – 4 samples

#### 2. Samples collected onboard for analyses of the diatom assemblage and of phytoplankton for the uppermost sediment layer

- Gravity Corer – 1 sample
- MUC – 19 samples of 0-1 cm interval sediments
- Boxcorer – 2 samples (0-1 cm interval)
- CTD – 21 filters

So far 42 samples were prepared for microscopic analysis. Some samples were already studied by means of Scanning Electron Microscope (SEM) and Light Microscope (LM).

3. Selected MUC and gravity cores have been sampled at high-resolution, e.g., for the Multi-Cores the interval from 0 to 10 cm has been sampled at 0.5 cm steps and the Gravity-Cores have been sampled at 1 cm interval, for diatom assemblage studies and for reconstruction of palaeotemperature.

### S. Rysgaard, N. Risgaard-Petersen

(measurements performed on Multi-Cores)

Station#	date	Position °N	Position °W	Am ino aci ds	C H 4	bact eria	Org. C & N	13 C	15 N	O 2	DI C	NO 3	NH 4	N 2	N2 o	Dens ity & poro sity	Fora minifera
3432	16- 50	67° 40,481	51° 36,924				X	X	X	X						X	X
3432	17- 60	67° 40,599	51° 49,058				X	X	X	X						X	X
3432	17- 70	67° 47,158	52° 25,199				X	X	X	X						X	
3432	17- 80	67° 38,459	53° 09,458				X	X	X	X						X	
3432	18- 90	67° 28,999	53° 37,399				X	X	X	X						X	X
3433	19- 00	68° 28,311	54° 00,118				X	X	X	X						X	X



<b>Measurements made in upper 6 m of the water column</b>
---

Station#	date	Position °N	Position °W	TA	DIC	NO <sub>3</sub>	NH <sub>4</sub>	PO <sub>4</sub>	Si	CHLA
343250	16-jun	67° 40,481	51° 36,924	X	X	X	X	X	X	X
343260	17-jun	67° 40,599	51° 49,058	X	X	X	X	X	X	X
343270	17-jun	67° 47,158	52° 25,199	X	X	X	X	X	X	X
343280	17-jun	67° 38,459	53° 09,458	X	X	X	X	X	X	X
343290	18-jun	67° 28,999	53° 37,399	X	X	X	X	X	X	X
343300	19-jun	68° 28,311	54° 00,118	X	X	X	X	X	X	X
343310	19-jun	68° 38,874	53° 49,483	X	X	X	X	X	X	X
343340	20-jun	68° 23,837	55° 07,787	X	X	X	X	X	X	X
343330	20-jun	68° 58,076	53° 11,105	X	X	X	X	X	X	X
343320	20-jun	68° 51,879	53° 19,719	X	X	X	X	X	X	X
343350	22-jun	69° 57,196	50° 49,338	X	X	X	X	X	X	X
343370	23-jun	70° 36,277	54° 31,637	X	X	X	X	X	X	X
343390	23-jun	70° 13,176	53° 03,196	X	X	X	X	X	X	X
343410	24-jun	69° 10,998	51° 29,500	X	X	X	X	X	X	X
343420	26-jun	70° 22,620	51° 48,720	X	X	X	X	X	X	X
343430	26-jun	70° 29,408	51° 35,861	X	X	X	X	X	X	X
343440	26-jun	70° 39,750	52° 06,856	X	X	X	X	X	X	X
343450	27-jun	71° 08,392	51° 15,833	X	X	X	X	X	X	X
343510	28-jun	70° 37,241	54° 33,193	X	X	X	X	X	X	X
343520	28-jun	70° 48,946	56° 50,938	X	X	X	X	X	X	X
343530	28-jun	70° 38,399	59° 05,993	X	X	X	X	X	X	X
343540	29-jun	69° 38,925	57° 26,900	X	X	X	X	X	X	X
343550	30-jun	67° 34,891	53° 17,998	X	X	X	X	X	X	X
343570	02-jul	64° 27,582	52° 48,303	X	X	X	X	X	X	X
343580	02-jul	63° 57,580	53° 53,000	X	X	X	X	X	X	X
343590	03-jul	4° 21,9650	51° 36,278	X	X	X	X	X	X	X

## 9. Lithological core description

## Nordre Strømfjord

GC 343260-3-1  
 Lat 67°40,599'  
 Lon 51°49,056'

FS Maria S. Merian 05/03  
 Water depth: 384,1 m

### Coring depth

cm

18

- olive green, soft  
 - clay with silt

38

- slightly darker olive green  
 - silt  
 - some organic fragments  
 - more compact

110

- sticky silt with some clay

125

- olive green and black mottled  
 - clay rich silt

200

- olive green sand (→ well sorted)  
 - coarse at base  
 - gradually fining to the top  
 - fine sand at the top of the section

376

- olive green  
 - clay with some silt  
 - at 216-220 cm silt band (clay), increase of black stain  
 - at 240-245 cm coarse silt to fine sand, increase of black stain  
 - at 278-286 cm fine sand (quartz), increase of black stain  
 - at 294-303 cm siltband with darker stain

388

- olive green  
 - increase silt → clayrich silt (more than above)

430

- olive green  
 - sticky clay and silt  
 - black organic trace in it → occasionally molluscs

GC 343260-6-1  
 Lat 67°40,594'  
 Lon 51°49,051'

FS Maria S. Merian 05/03  
 Water depth: 383,4 m

### Coring depth

cm

44

### Lithological description

- light olive grey soft clay with some silt  
 occasional black sulphide staining, trace of capinations

- 58 - moderate to light olive grey silty fine sand with increasing black staining
- 107 - light olive grey silty clay with abundant black staining in discontinuous layers
  - shell debris at 62 cm
  - fine sand and silt layers at 10-12 cm and 89-100cm
- 121 - light olive grey silty clay with few black stains
- 126 - moderate olive grey silt and fine sand with black stained laminations
- 172 - light olive grey silty clay with abundant black stain laminations near top
- 207 - light olive grey clay and fine silt
- 270 - light olive grey clay with some silt, occasional black staining
- 307 - light olive grey silty sand becoming more coarse towards base
- 333 - light olive grey silty clay with black staining in pebbly form surrounded by fine sand and silt (disturbed during coring?)
- 407 - moderate to light olive grey well sorted sand becoming sand towards base
- 433 - moderate to light olive grey well sorted coarse sand towards
- 507 - light olive grey clay and silt with discontinuous black laminations with dark grey to black silt band 456-457 cm and 488-490 cm
- 607 - light olive grey clay and silt with faint black lamination and moderate olive green to grey fine sand and silt layer from 536- 539 cm
  - dark grey to olive green band at 558-560 cm
  - large granit boulder (ø8cm) at 560 cm
  - dark grey to black band band at 579-580
  - trace of gas bubbles towards base
- 632 - light olive grey clay and silt with trace of gas bubbles
- 638 - moderate olive grey fine sand and silt with trace of dark grey laminations
- 649 - olive green clay and silt with mottled black staining
- 699 - pale olive green clay and silt with occasional black staining
- 707 - moderate to light olive green fine sand and silt
- 718 - moderate to light olive green well sorted fine sand with some black staining
- 738 - pale grey olive green clay with silt
  - shell at 730 cm

- 760 - moderate to light grey olive green silt and fine sand with occasional plant fragments
- 807 - moderate to light grey olive green medium sand  
- becoming coarse towards base with trace of gas bubbles

GC 343280-3-1 FS Maria S. Merian 05/03  
 Lat 67°38,457' Water depth: 311,08 m  
 Lon 53°09,458'

Coring depth cm	Lithological description
110	- dark grey to black organic rich silty clay with abundant makroalgeae
445	- olive green silty clay with abundant black makroalgeae with common molluscs ( <i>Hiatella artica</i> )
485	- olive green sand and silt with very abundant molluscs ( <i>Pecten</i> ø 8 cm / <i>Hiatella artica</i> / <i>Cardium</i> ) - some dropstones at base
615	- olive green silty sand with rare shell fragments - with rare dropstones
690	- olive green silty clay with rare dropstones
710	- olive green silty clay with abundant dropstones (ø 3cm dropstone)

GC 343280-4-1 FS Maria S. Merian 05/03  
 Lat 67°38,456' Water depth: 311,16 m  
 Lon 53°09,460'

Coring depth cm	Lithological description
230	- light olive grey fine sand and silt with dark grey to black - makroalgeae abundant - occasional mollusc shells ( <i>Pecten</i> and <i>Hiatella artica</i> )
372	- light olive grey silty clay with trace of fine sand - with dark grey to black macroalgeae abundant - occasional mollusc shells ( <i>Hiatella artica</i> )

## Disko Bay/ Vaigat

GC 343300-4-1      FS Maria S. Merian 05/03  
 Lat 68°28,311'      Water depth: 519,4 m  
 Lon 54°00,119'

Coring depth cm	Lithological description
400	- mottled olive grey and moderate olive brown organic rich clay with occasional shell fragments
540	- mottled light olive grey and olive grey clay with rare shell fragments
740	- greenish grey to olive grey mottled clay - with occasional dropstones and rare shell fragments
1140	- light olive grey clay with occasional olive grey patches and occasional dropstones - rare shell fragments - trace of silt - from 900 cm the olive grey patches fade out

GC 343310-5-1      FS Maria S. Merian 05/03  
 Lat 68°38,861'      Water depth: 856,3 m  
 Lon 53°49,49'

Coring depth cm	Lithological description
400	- moderate olive brown and olive grey mottled organic rich clay
840	- moderate olive brown to light olive grey organic rich clay - from 640 cm on occasional shell fragments
939	- moderate olive brown to light olive grey organic rich clay with occasional olive grey vertical staining (possible plant fragments)

GC 343330-3-1      FS Maria S. Merian 05/03  
 Lat 68°58,077'      Water depth: 829,3 m  
 Lon 53°11,104'

Coring depth cm	Lithological description
267	- light olive grey to moderate olive brown clay with trace of silt and sand - occasional shell fragments
423	- moderate olive brown clay with bands of light olive grey

	clay
	- occasional shell fragments
427	- mid grey to light olive grey clay
433	- light grey to light olive grey well sorted medium sand
436	- medium grey well sorted medium sand with some dark grey graus and discontinuos olive grey clay band with sand
440	- light grey clay
520	- light olive grey clay with some silt and dark grey sulfide staining
	- occasional shell fragments
791	- with medium to light grey clay
	- pebbles and common dropstones and shell fragments
	- trace of sand

GC 343340-5-1      FS Maria S. Merian 05/03  
 Lat 68°23,835'      Water depth: 461,2 m  
 Lon 55°07,786'

<b>Coring depth</b> cm	<b>Lithological description</b>
100	- moderate olive brown organic clay with darker olive brown mottling
170	- same lithology with occasional polychaete tubes and occasional shells
440	- moderate olive brown to light olive grey clay with darker olive brown mottling - occasional polychaete tubes and shells - mottling might be in burrows
700	- light olive grey clay with olive grey mottling and occasional shell fragments with a trace of sand (from 6 m)
804	- light olive grey clay with olive brown infilled burrows - with occasional shell and dropstones becoming more common
900	- medium grey to olive grey clay with slightly darker olive grey mottling - with occasional dropstones and shelle fragments
1074	- same lithology with band of olive grey clay (lamination) common and rare shell fragments

GC 343380-3-1 FS Maria S. Merian 05/03  
 Lat 70°19,041' Water depth: 578,4 m  
 Lon 53°41,692'

Coring depth cm	Lithological description
12	- olive green clay with silt
13	- dark grey silt with clay
16	- brownish grey silt with clay
151	- light olive grey with olive grey mottling - silt with clay with slightly darker bands and occasional dropstones from 110-151 cm
154	- olive grey fine to medium sand
270	- light olive grey with olive grey mottling clay with a trace of silt
450	- occasional shell fragments - olive grey clay with trace of silt with some light olive grey mottling
680	- light olive grey clay with some olive grey mottling - trace of silt - shell fragments and dropstones - with trace of gas - with some darker olive grey banding and large dropstones (ø 5 cm) 598-602 cm

GC 343390-9-1 FS Maria S. Merian 05/03  
 Lat 70°13,176' Water depth: 537,6 m  
 Lon 53°03,194'

Coring depth cm	Lithological description
5	- olive grey silty fine sand
560	- light olive grey clay minor colour mottling - occasional dropstones below 170 cm - at 492-493 cm large dropstone

GC 343550-4-1 FS Maria S. Merian 05/03  
 Lat 67°34,889' Water depth: 344,5 m  
 Lon 53°18,003'

Coring depth cm	Lithological description
3	- greyish olive finesand
372	- light olive silty clay to slightly silt (gradually finer downcore)

	- with abundant molluscs shells and shell debris
	- some layers and pockets of silt to finesand
382	- light olive fine silty sand with clay
395	- light olive slightly silty clay
430	- light olive fine silty sand with clay
442	- light olive silty clay
454	- light olive silty fine sand with cla

## Uummanaq Fjord

GC 343430-5-1      FS Maria S. Merian 05/03  
 Lat 70°29,395      Water depth: 934,2 m  
 Lon 51°35,881

Coring depth cm	Lithological description
61	- Light olive grey, silty clay - From 18-41 cm colour mottling → some faint colour layering
65	- olive grey silty clay - sharp upper and lower boundary
65	- Light olive grey silty clay with minor fine silt
77	- Light olive grey clay
194	- Light brownish grey fine silty sand
197	- light olive grey clay
225	- olive grey silty clay - mottled and bioturbated
293	- light olive grey clay with 2 cm light brownish grey fine silty sand at base
317	- light olive grey clay with some layer or slightly darker material
405	- light olive grey clay - sand lense between 391 and 404 cm
424	- light olive grey clay alternating lighter and darker layers slightly mottled
440	- light olive grey clay predominantly darker than above
457	- light olive grey clay homogenously lighter than above
479	- light olive grey clay with some silt - 1 cm thick fine sand layer at 462 cm
496	- light olive grey clay isolated piece of gravel at 492 cm
513	- light olive grey clay with silty base
517	- light olive grey clay slightly darker than above
525	- lighth olive grey clay, homogenous
529	- light olive grey clay light mottled and bioturbated

553	- alternating lighter and darker lamination and mottling getting more homogenous towards base
571	- mainly darker layered mottled and bioturbated silty clay, light olive grey
601	- light olive grey clay, homogenous
643	- light olive grey clay, darker and lighter layered layer of finesand at 640 cm
664	- light olive grey clay mainly darker coloured clay - mottled and bioturbated
674	- light olive grey homogenous clay
730	- light olive grey clay faint layered some mottling near top - lower part more homogenous 1cm thick silt layer at base
845	- light olive grey homogenous clay - 3cm thick fine sand at base - dropstones at 826 cm
851	- light olive grey mottled and bioturbated (darker)
864	- light olive grey homogenous clay
1092	- olive grey clay - occasional silt, isolated lamina and occasional dropstones

**GC 343450-3-1**      **FS Maria S. Merian 05/03**  
**Lat 71°08,388'**      **Water depth: 171,2 m**  
**Lon 51°15,840'**

<b>Coring depth</b>	<b>Lithological description</b>
<b>cm</b>	
446	- light olive grey, silty clay with some color mottling and occasional dark mineral grains - occasional plant fragments - at 56-66 cm increases finesand content - maximum grain size feinsand

**GC 343460-3-1**      **FS Maria S. Merian 05/03**  
**Lat 71°07,152'**      **Water depth: 65,7 m**  
**Lon 51°15,321'**

<b>Coring depth</b>	<b>Lithological description</b>
<b>cm</b>	
36	- olive grey, silty clay
46	- multi colored finesand (darkgrey to greenish grey) → contains ore minerals?
63	- dominantly olive grey clay with finesand

70	- dark grey to greenish grey finesand
80	- olive grey silty clay with finesand
95	- dark grey finesand and olive grey silty clay
100	- olive grey silty clay with finesand
130	- alternaing olive grey silty clay with light brewish grey and greenish grey in cm-scale
144	- olive grey silty clay with mm-scale finesand
195	- olive grey silty clay with some mm-scale finesand
226	- olive grey silty clay with light brewish grey and greenish grey finesand layers
259	- olive grey silty clay with cm.scale layers of finesand
290	- intercalated olive grey with silty clay and cm-scale layers of finesand
347	- olive grey clay with some silt, some mm-scale sand layers
382	- olive grey clay with silt and distinct cm layers of finesand at 347 to 348 cm; 355-360 cm; 370-373 cm; 379-382 cm
415	- olive grey silty clay with mm-scale layers of blewish grey finesand
578	- olive grey clay with minor silt, few mm-scale layers of finesand - light greenish grey finesand layer at 515 to 516 cm

GC 343470-2-1      FS Maria S. Merian 05/03  
 Lat 71°06,489'      Water depth: 59,41 m  
 Lon 51°13,951'

<b>Coring depth</b> cm	<b>Lithological description</b>
420	- light olive grey clay with some minor silt - gradually darker downcore - at 30 to 119 cm black specks and lamination - permanent black band at 119 cm - occasional dropstones - band of white finesand at 249 cm - white band at 414 cm
481	- yellowish grey - clay with silt with occasional black mottling - lighter corlor bands of siltysand at depths of 444 to 446 cm and 454 to 471 cm

## Westgreenland Shelf

GC 343520-3-1      FS Maria S. Merian 05/03  
 Lat 71°06,489'      Water depth: 59,41 m  
 Lon 51°13,951'

Coring depth cm	Lithological description
458	- olive grey clay with minor silt, mainly homogenous - darker bands at 47 cm - shell fragments at 41 cm and 150 cm - darker coloring between 252 cm and 268 cm
586	- olive grey clay with minor silt slightly mottled faint dark specks - shell fragments between 480 cm and 488 cm
860	- olive grey clay with common mottling and darker specks - larger dark discolouration between 620 cm and 630 cm (flow structures?)
884	- olive grey clay with minor silt, occasional dropstones - olive grey clay with minor silt, slightly darker
936	- light olive grey clay with minor silt homogenous - occasional dropstones
974	- olive grey clay with minor silt homogenous with isolated lamina - sand lense (ø 4 cm) at 960 cm
1000	- light olive grey clay with minor silt - dropstone at 978 cm

## 10. XRF-Scans / Metadata plus selected plots

### XRF scanning metadata:

**Step size:** 1cm

**Slit width** (analyzed length in downcore direction): 1cm [16mm in crosscore direction]

**Counting time:** 30 seconds

**Tube voltage:** 10 kV (additionally 20kV for Quamarajuk Fjord core 343470-2)

**Tube current:** 150 mA

**Elements detected:** Al, Si, S, Cl, K, Ca, Ti, Mn, Fe (all with K lines)

### Additional settings for selected Quamarajuk Fjord cores:

20kV (Pd thin filter in front of incoming X-ray beam), 250 mA

**Elements detected:** Cu, Zn, Br, Rb, Sr (K lines), Pb (L lines)

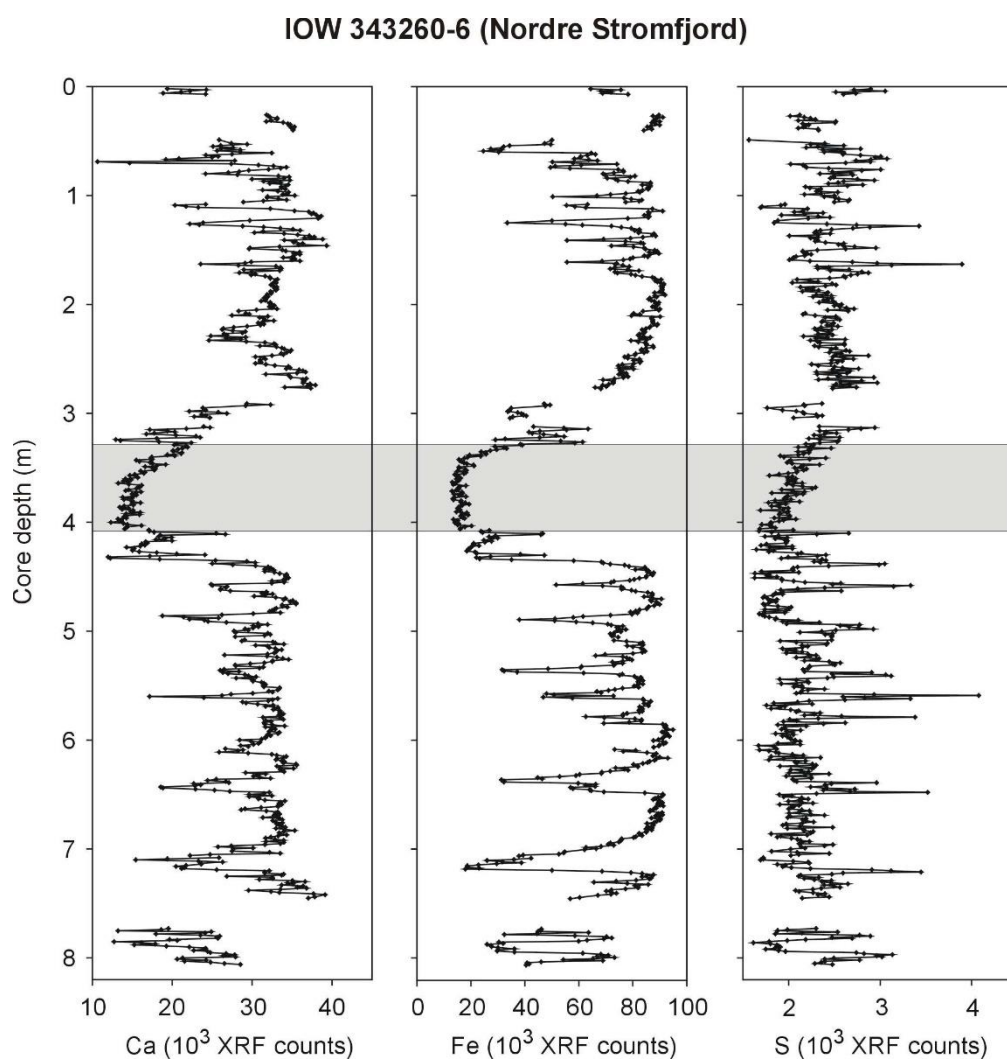


Fig.E10.1: Nordre Stromfjord core 343260-6. Sandy layers display lower counts for all major elements (shaded rectangle gives one example. Occasionally higher counts for sulfur (S) probably reflect presence of plant fragments.

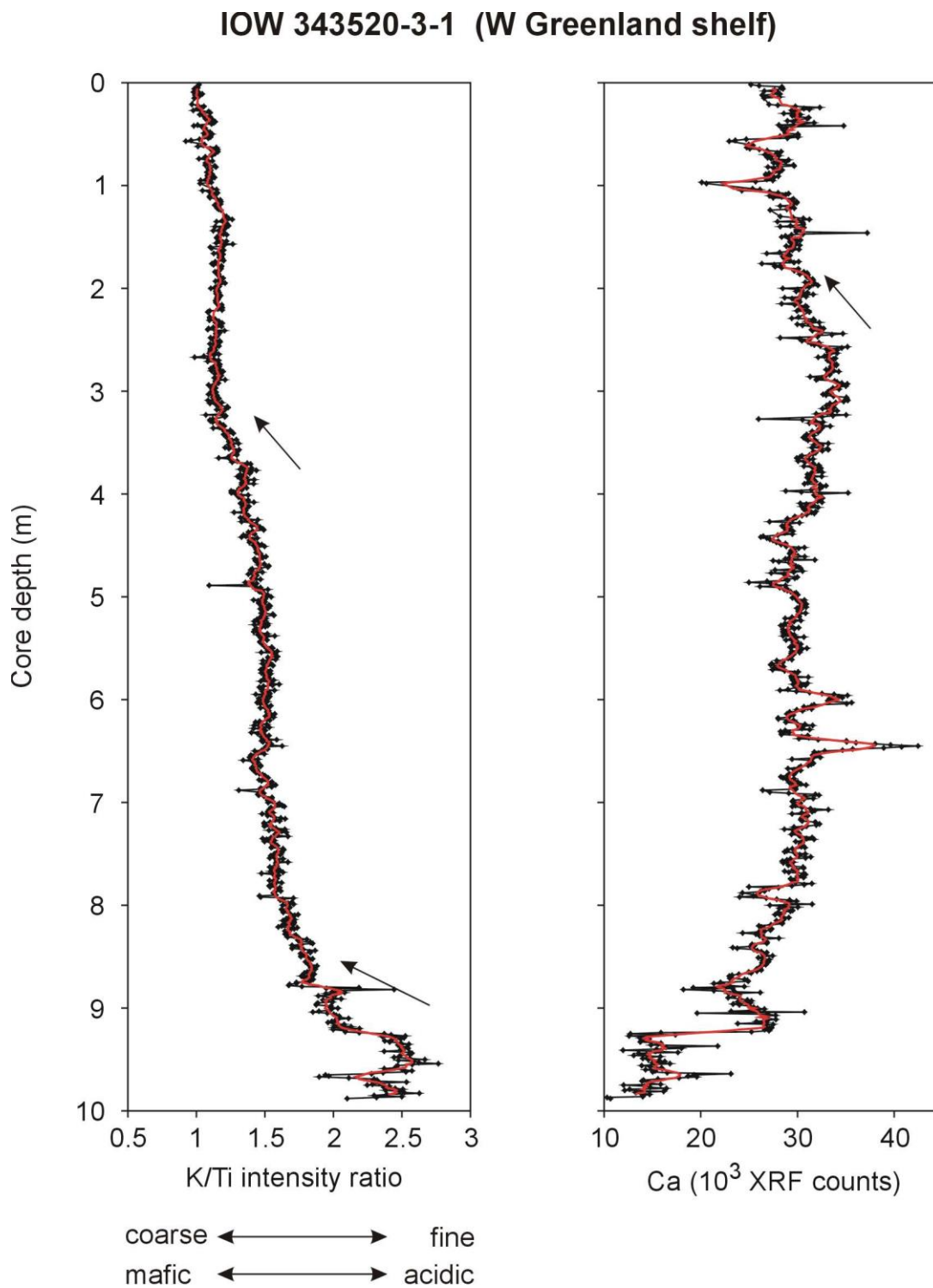


Fig.E10.2: West Greenland shelf core 343520-3-1. K/Ti intensity ratio reflects changes in grain size and/or provenance of the terrigenous fraction. Ca record corresponds to fluctuations of biogenic carbonate. Arrows highlight main shifts in both records.

### IOW 343470-2 (Qaumarujuk Fjord)

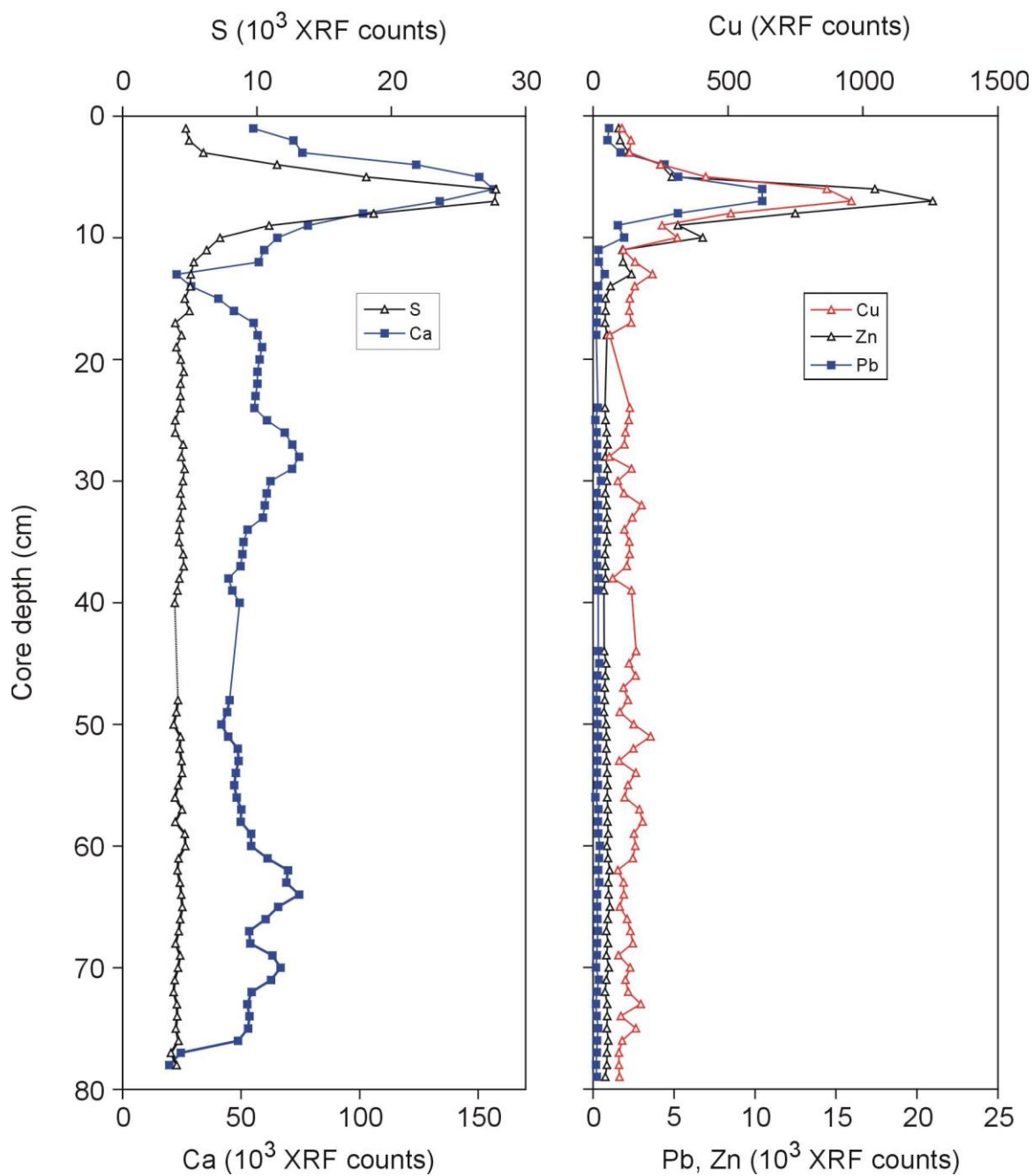


Fig.E10.3: Qaumarujuk Fjord core 343470-2 (first section). Concomitant enrichment of all elements displayed reflects anthropogenic mining activity (pyrite-bearing marble with high metal concentrations).

## 11. Magnetic susceptibility (MS) scanning of sediment cores collected during MSM05/03

MS units are in the SI system ( $10^{-5}$ )

### ***Nordre Strømfjord (sites 343250 and 343280)***

MS values range between  $700 \times 10^{-5}$  (site 343260-6-1) and  $20 \times 10^{-5}$  (site 343280-4-1). The highest values measured in gravity core 343260-6-1 are related to a series of sand layers. Upwards fining of the sediment above each sand layer is associated with gradually lower MS values. Gravity corer 343280-4-1 is characterised by MS values that increase from  $20 \times 10^{-5}$  in the lower parts to  $140 \times 10^{-5}$  in the upper 50 cm.

### ***Disko Bay and shelf to the west (sites 343300, 343310, 343330 and 343340)***

MS values in the multi-cores (sediments down to a depth of c. 40 cm) range between  $10 \times 10^{-5}$  in the unconsolidated surface sediments (high water content) to  $100 \times 10^{-5}$ . The lowest values are in the sediments in Disko Bay (343320-2-1) and the highest values are in sediments further to the west (343340-2-1).

### ***Vaigat Fjord (sites 343360 and 343380).***

MS values range between  $40 \times 10^{-5}$  SI (multicore 343370-1-1) and  $1300 \times 10^{-5}$  SI (gravity core 343380-3-1). MS values in gravity core 343380-3-1 are consistently higher than  $400 \times 10^{-5}$  SI.

*Uummannaq Fjord and shelf to the west (sites 343470, 343380, 343390, 343500, 343520, 343530 and 343540).*

Note that MS measurements of multi-cores 343500-2-1 and 343500-2-2 were contaminated by a metal ruler. These are not true measurements.

MS values range from below  $20 \times 10^{-5}$  SI in multi-core 343470-3-1 to  $400 \times 10^{-5}$  SI in multi-core 343540-2-1.

### **Geographic distribution of MS values**

Compared to sediments recovered in Disko Bay and the Uummannaq Fjord, MS values are significantly higher, by at least one order of magnitude, in the sediments recovered to the west of Disko Island and in the Vaigat Fjord. This contrast in the spatial distribution suggests that detrital sediment of basaltic origin from Disko Island dominates the magnetic properties of the sediments in the Vaigat Fjord and on the shelf to the west of Disko Island. On the other hand, detrital sediments originating from the mainland of Greenland, from areas with a sedimentary bedrock dominate the magnetic properties of sediments in Disko Bay and the Uummannaq Fjord. Variability of magnetic mineral concentration in the sediment sequences (multi-cores and gravity cores) is most likely related to changes in the relative contributions of these two magnetically contrasting sediment sources over time, but in combination with sediment sorting processes.

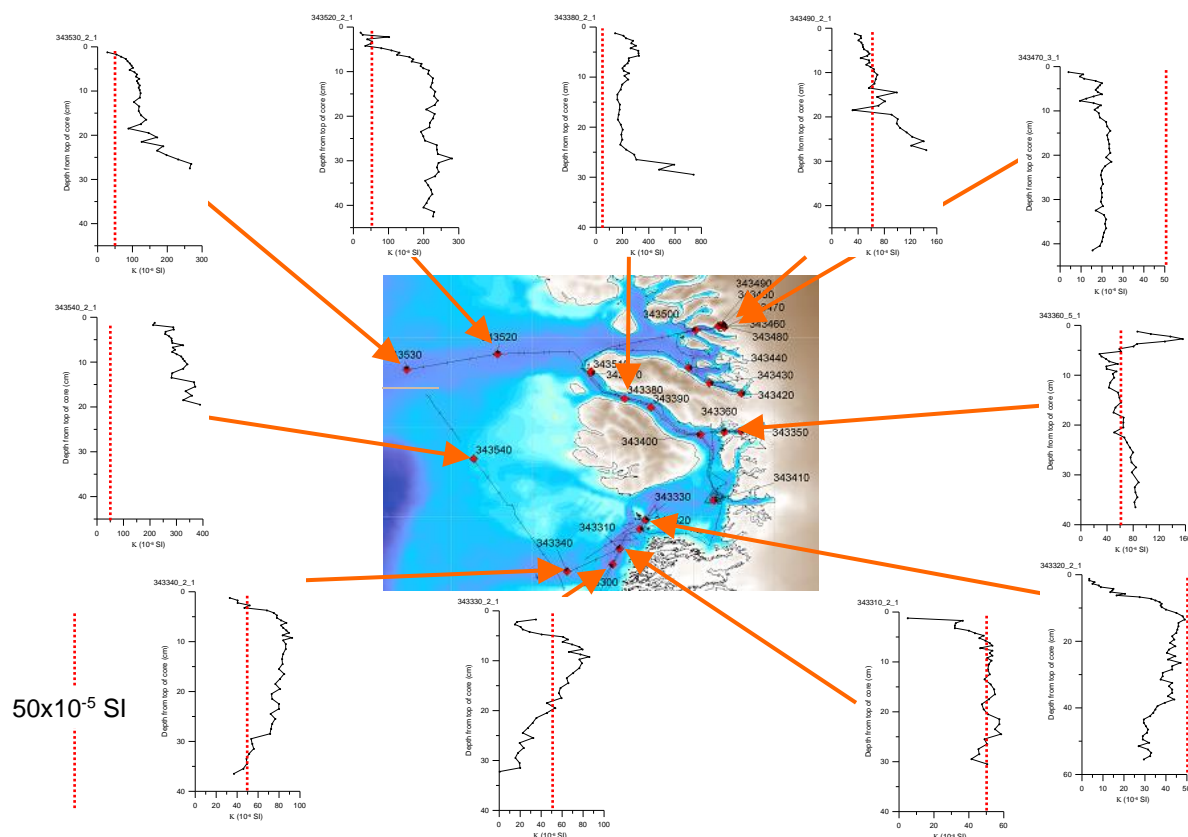


Fig.E11.1: Magnetic susceptibility measurements: Multi-cores from Disko Bay, Vaigat Fjord, Uummannaq Fjord and shelf to the west of Disko Island.

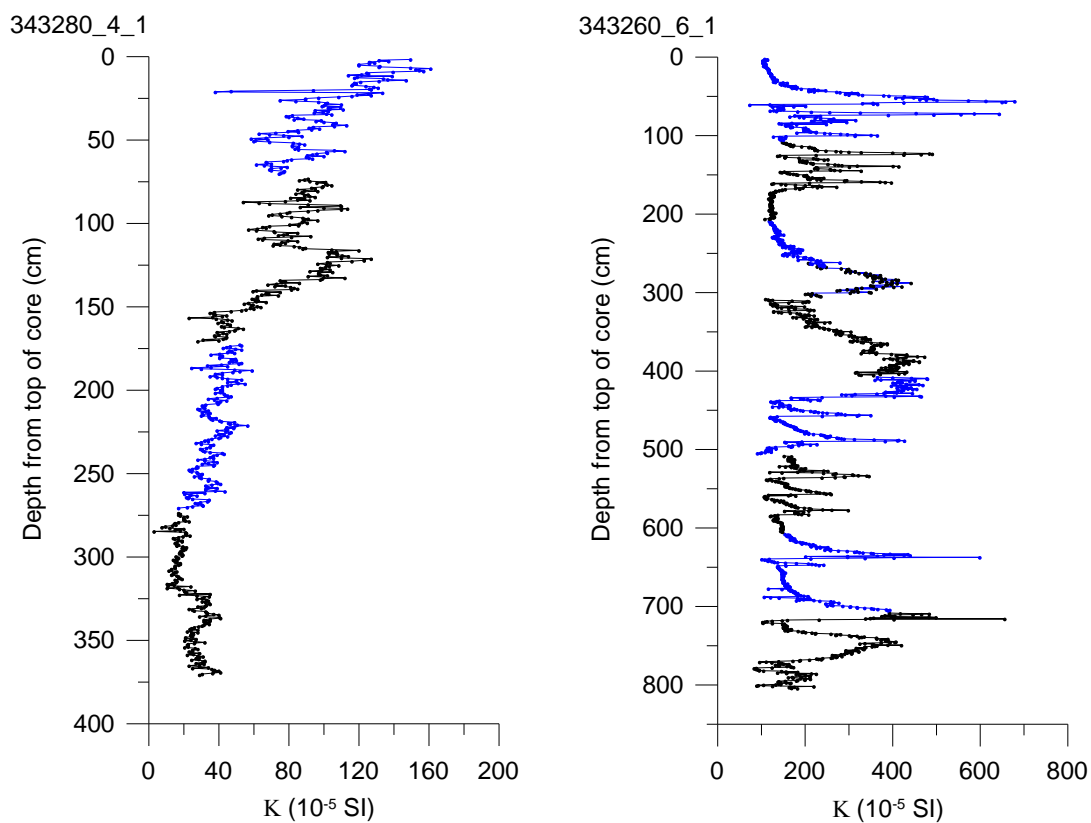


Fig.E11.2: Magnetic susceptibility data from Nørdre Strømfjord – gravity cores.

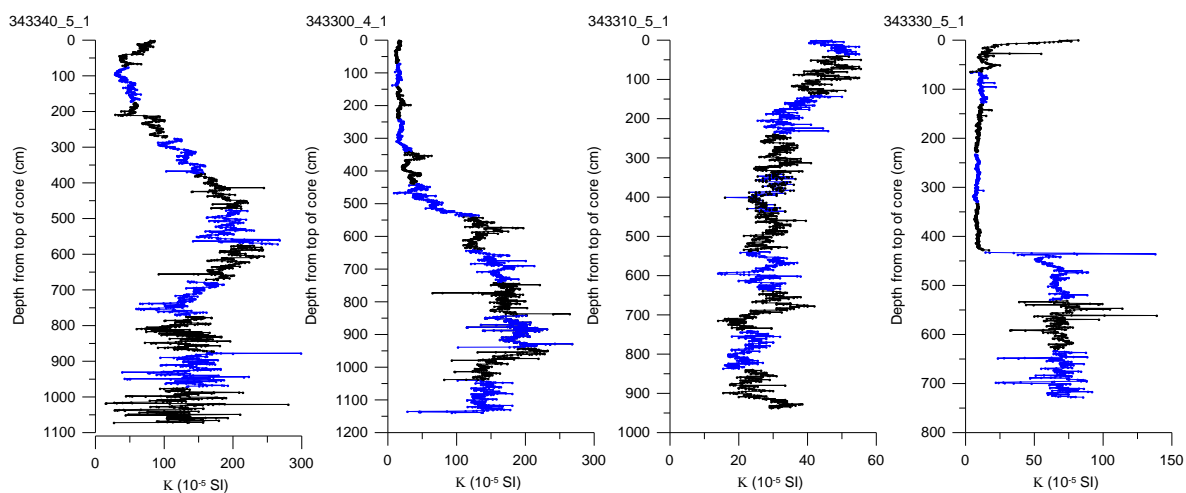


Fig.E11.3: Magnetic susceptibility data from Disko Bay and shelf to the west – gravity cores.

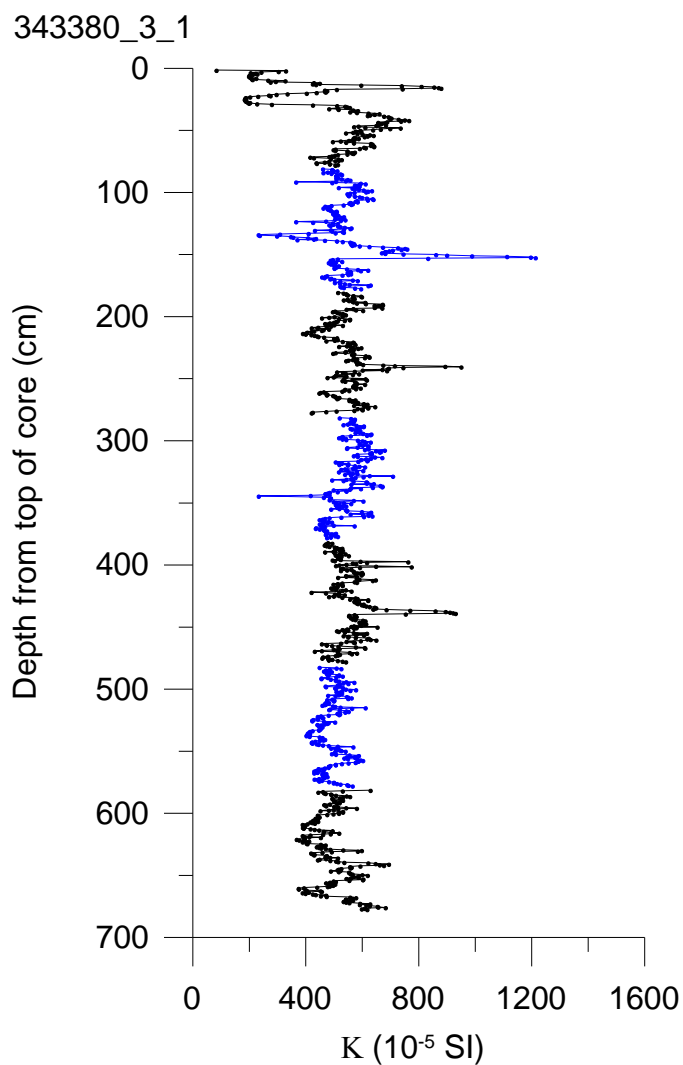


Fig.E11.4: Magnetic susceptibility data from Vaigat Fjord – gravity core.

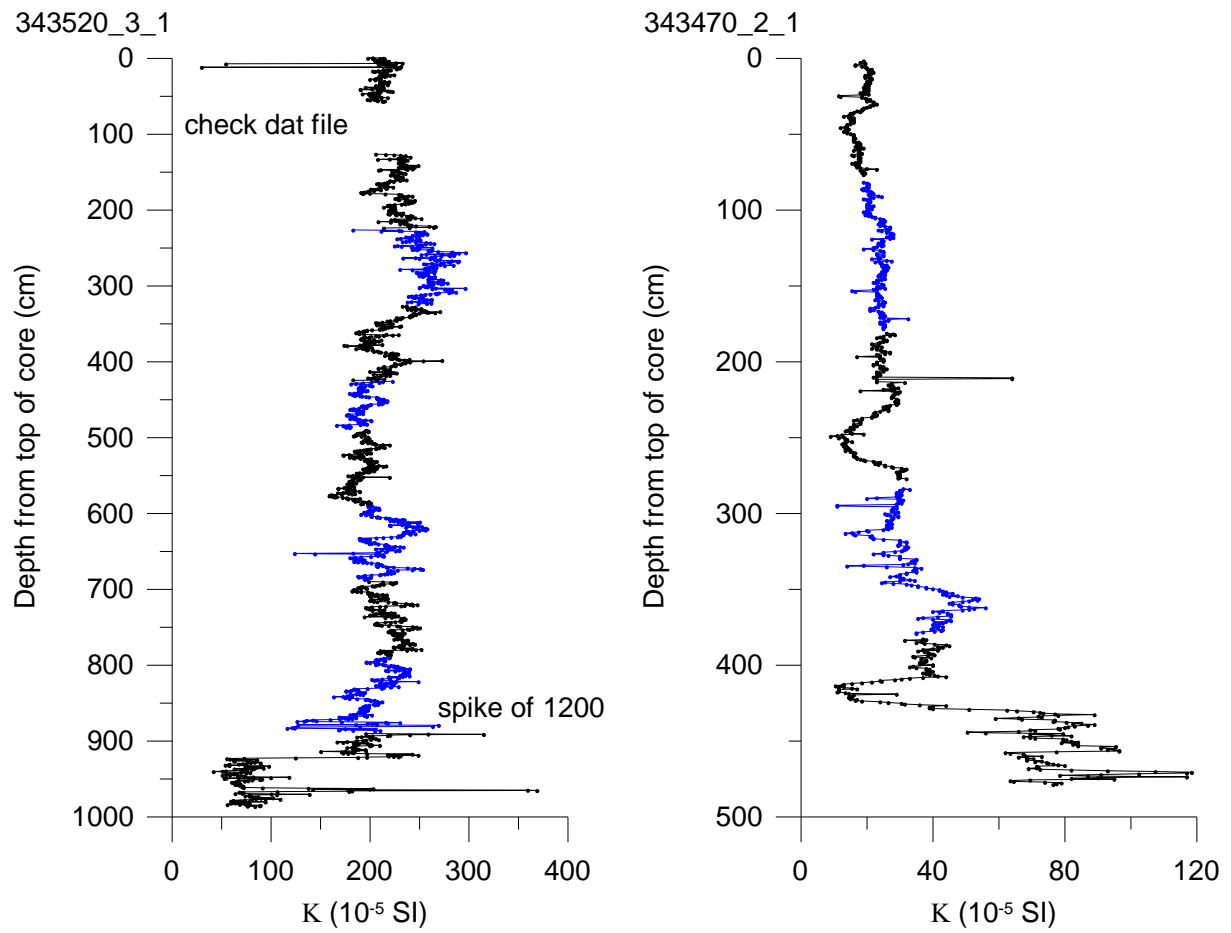


Fig.E11.5: Magnetic susceptibility data from Uummannaq Fjord and shelf to the west.

**12. Abstracts of seminars held during the expedition  
MSM 05/03**

15.6.2007

## Geodetic fieldwork: establishing GPS network of West Greenland

R. Dietrich, A. Richter

Technical University of Dresden, Mommsenstrasse 9, 01062 Dresden

The planned geodetic fieldwork has been conducted successfully. Our GPS network of West Greenland has been densified and extended to the north by the establishment and first observation of four new GPS markers. Based on the obtained observation data, exact marker coordinates have been determined in a global reference frame. The inference of recent crustal deformation rates, however, requires the repetition of the GPS observations on these markers. The pressure tide gauge records obtained at two locations in the Nordre Strømfjord allow the determination and analysis of the water-level changes in the fjord. The water-level variations are clearly dominated by the tidal signal with a range of 4 m. At this, the tidal amplitudes seem to increase towards the east. The tidal constituents resulting from a harmonic tidal analysis of the sea-level signal can be compared to the predictions of ocean tide models for a) a regional validation of the tide models, and; b) investigating the modification of the tidal signal within a long, narrow fjord. In addition, high-frequency sea-level changes such as surface seiches can be studied, and the simultaneously registered water temperature and conductivity records can be analysed regarding oceanographical questions.

18.6.2007

## Ice streams, climate and ocean circulation in Disko Bugt

J. Lloyd<sup>1</sup>, M. Moros<sup>2</sup>, A. Kuijpers<sup>3</sup>, A. Witkowski<sup>4</sup>, D. McCarthy<sup>1</sup>

<sup>1</sup>Department of Geography, University of Durham, UK, (j.m.lloyd@durham.ac.uk). <sup>2</sup>Leibniz Institute of Baltic Sea Research Institute Warnemünde, Germany. <sup>3</sup>Geological Survey of Denmark and Greenland, Copenhagen, Denmark. <sup>4</sup>University of Szczecin, Szczecin, Poland

There is increasing concern that key components of the cryosphere are responding to climate changes over recent decades, and may be susceptible to catastrophic collapse. Significant increases in velocity and ice production recently identified from several major ice streams draining the Greenland Ice Sheet suggest that rapid changes in ice stream and ice sheet dynamics may already be underway. Such dynamic response has important implications for sea-level rise and also freshwater flux induced changes in ocean heat transport and hence climate. The late Holocene provides an important time window from which to assess the significance of these recent events and, in particular, to establish whether they are exceptional or simply part of natural system variability. In this study we have investigated the relative activity of Jakobshavn Isbrae, the most important ice stream draining the West Greenland ice sheet, in particular the interaction between the ice stream and ocean temperature and air temperature forcing during the Holocene. Documentary evidence identifies a 25 km retreat of the Jakobshavn Isbrae terminus from the Neoglacial maximum position of AD 1850 and a recent abrupt velocity increase from 5 km a<sup>-1</sup> to 12.6 km a<sup>-1</sup> from AD 2000 associated with a further 12 km retreat of the ice front. The reason for this accelerated retreat is unclear. The ice stream may be responding to one or a

combination of changes in air temperature, ocean temperature, or internal ice sheet dynamics and constraining topography.

To assess the possible controls on Jakobshavn Isbrae we use a combination of documentary and instrumental records of ice margin position, air temperature and ocean temperature for the recent past and reconstructions based on marine cores and ice cores for the longer term record. Analysis of benthic foraminifera from marine cores beyond the influence of glacial meltwater provides evidence for variations in ocean water temperature over the past 3000 years. Marine cores close to the mouth of Jakobshavn Isfjord provide a record of the position and activity of the ice stream over the past 8000 years. Our data identifies the retreat of the ice stream from the pinning point at the mouth of Jakobshavn Isfjord into the deep fjord itself at *c.* 7 ka cal BP. We can also identify clear variations in ice stream behaviour (identified based on foraminiferal faunal changes and variations in sedimentation rate) correlating with climate events such as the 'MWP' and 'LIA'. We also show a strong link between air temperature forcing and changes in the relative strength of the West Greenland Current (ocean temperature) suggesting the ice stream is indeed sensitive to variations in air and ocean temperature forcing.

18.6.2007

### **Applications of X-ray fluorescence logging data**

T. Richter

Royal Netherlands Institute of Oceanography (NIOZ), P.O. Box 59, NL-1790 AB Den Burg (Texel),  
Netherlands

The principle of X-ray fluorescence (XRF) core scanning is briefly explained, and applications are presented based on case studies from the NE Atlantic Ocean. Distribution patterns of Ca and Fe can provide preliminary stratigraphic information on glacial-interglacial timescales, as interglacials are characterized by higher carbonate content and less terrigenous input. Element ratios and cross-elemental plots serve to enhance the signal-to-noise ratio of XRF logging results and help distinguishing between multiple sources for some elements. For example, combined use of Si and Al traces relative contributions of alumino-silicates vs. biogenic opal to total silicon. The coupled use of Fe, Ti and S can differentiate between a dominantly terrigenous supply of iron and distinct early diagenetic iron enrichments in oxidizing and reducing environments. Sr and Ca distribution patterns taken together define the relative importance of aragonite (high Sr) vs. calcite (low Sr). First results of onboard measurements on Nordre Stromfjord cores were also presented during the seminar.

21.6.2007

### **Arctic climate variations on millennial to multi-decadal scales**

Naja Mikkelsen

Geological Survey of Denmark and Greenland, Øster Voldgade 10,  
1350 Copenhagen, Denmark. Email: nm@geus.dk

The Arctic Ocean has since its formation passed through different physical and environmental stages. These stages witness a transition of the Polar Basin from a stagnant and oxygen deficient

ocean through a temperate upwelling basin into a cold and ventilated ocean, which today has profound impact on the global ocean circulation.

A major element in the evolution of Cenozoic environments has been the transformation of the global oceans from warm Eocene oceans with low latitudinal and bathymetric thermal gradients into the recent modes of circulation characterized by strong thermal gradients, oceanic fronts, cold deep oceans and cold high latitude surface waters. The climate on Earth has throughout the Cenozoic changed from one extreme (i.e. the Paleogene 'Greenhouse') to another (i.e. the Neogene 'Icehouse').

The sparse of knowledge about the role that the Arctic played in the maintenance and development of these climatic extremes is a major gap in our ability to understand and model global environmental change. Continuous data series from the Arctic Ocean is often a weak point in any global model. Data from paleoclimatic reconstructions are therefore important to improve our understanding of the behavior of the climate system over different time scales and are fundamental in providing data to validate models of climatic scenarios different from those covered by the short instrumental record.

21.6.2007

## **Palaeomagnetic secular variation and palaeointensity at high northern latitudes**

Ian Snowball, Per Sandgen and Raimund Muscheler  
GeoBiosphere Science Center (Quaternary Sciences), Lund University, Sweden

Palaeomagnetic data obtained from volcanic rocks, sediments and ceramics tell us how the direction and intensity of Earth's geomagnetic field varied in the past (systematic instrumental measurements began in the 18<sup>th</sup> century AD). The majority of palaeomagnetic data that cover the Holocene have been obtained from archaeological sites and lake sediments: very few data exist for the 70% of the Earth's surface that is covered by the ocean and the 10% covered by continental ice sheets. The aim of our participation in the MSM05/03 cruise was to recover high resolution marine sediments from Holocene sediment sequences in, or close to, Disko Bay for palaeomagnetic analyses. A Holocene palaeomagnetic master curve for Fennoscandia (Snowball et al. 2007) and similar data from two marine sediment cores on a sediment drift north of Iceland (Stoner et al. 2006) indicate that some features of secular variation were widespread in high northern latitudes. When converted to virtual geomagnetic poles (VGP's) they may indicate period of pole movement, but more data are needed to discriminate between the dipole field and higher term components. If we obtain good palaeomagnetic data from the sediments in Disko Bay we should be able to relatively date the sediment, which can be made more accurate if the sediments contain a valid relative palaeointensity signal. Onboard magnetic susceptibility measurements of split sediment core surfaces indicate that the last 7,000 years of sediment should contain a strong natural remanent magnetization (NRM).

21.6.2007

## Early diagenesis in Arctic marine sediments

Søren Rysgaard, Nils Risgaard-Petersen

Greenland Institute of Natural Resources, Nuuk – Greenland.

Present-day mineralization rates in coastal arctic sediments, covering oxygen respiration, denitrification, manganese, iron, and sulfate reduction as well as DIC and nutrient flux from the sediment were presented and discussed. In response to enhanced mineralization following sea ice break-up, sediment water fluxes of O<sub>2</sub>, DIC, NO<sub>3</sub><sup>-</sup> + NO<sub>2</sub><sup>-</sup>, NH<sub>4</sub><sup>+</sup>, urea, PO<sub>4</sub><sup>3-</sup>, and Si increase and rapidly recycle nutrients to the water column, indicating an efficient benthic-pelagic coupling in coastal arctic areas. Sediment porewater concentrations of O<sub>2</sub> are affected by the input of organic matter, leading to higher O<sub>2</sub> consumption rates near the sediment surface during summer. The depth distributions of e-acceptors (O<sub>2</sub>, NO<sub>3</sub><sup>-</sup>, Fe(III) and SO<sub>4</sub><sup>2-</sup>) and reduction rate measurements supports the classical orderly progression from O<sub>2</sub> respiration to NO<sub>3</sub><sup>-</sup> reduction followed by bacterial iron reduction and finally sulfate reduction. On an annual scale, O<sub>2</sub> respiration accounts for 38 % of total oxidation of organic carbon, denitrification; 4 %, iron reduction; 25 %, and sulfate reduction; 33 %. The benthic mineralization rates in arctic sediments are comparable with rates from much warmer locations, suggesting that benthic mineralization in these sediments is regulated by the availability of organic matter and not by temperature.

29.6.2007

## Deep-draft icebergs and late Quaternary oceanographic changes around Greenland

Antoon Kuijpers

Geological Survey of Denmark and Greenland, Oster Voldgade 10, DK-1350 Copenhagen K, Denmark.

Deep-tow side scan sonar and sub-bottom profiling both in the open North Atlantic (Iceland-Faeroe Ridge) and offshore Disko Bugt, West Greenland, have documented the presence of giant iceberg plow marks at water depths of almost 1000 m or more (1,2). The largest plow marks are about 750 m wide, while the height between bottom of the scours and rim crest is up to 40 m. A precise timing of these extreme iceberg scouring events is problematic, but sub-bottom profiling data from the North Atlantic plow mark site suggests that these episodes are likely to have occurred during glaciation(s) prior to the last (Eemian) Interglacial. It has been inferred that fast flowing ice streams from the glacial Greenland ice sheet may have been the source of these giant icebergs. During the last deglaciation, the Greenland Inland Ice rapidly withdraw from the Southeast Greenland (mid)shelf at a time coinciding with the Heinrich-1 event (14.2 ka <sup>14</sup> C). During the following c. 2000 years this area was characterised by the presence of a (semi)permanent sea ice cover. During this period both the East Greenland Current strength and the intensity of the Denmark Strait Overflow gradually increased, resulting in the appearance of well-ventilated bottom water masses in the Irminger Basin after 13.4 ka <sup>14</sup> C (3).

Late Holocene hydrographic changes in the Labrador Sea basin as documented from studies of West Greenland fjord cores appear to confirm a North Atlantic climate (temperature) seesaw, indicating, amongst others, the absence of Medieval warming in the West Greenland region.

During (European) colder climate conditions, as occurred during the 'Little Ice Age' and preceding 'Dark Ages', a positive sea surface temperature (SST) anomaly due to enhanced inflow of 'warm' Irminger Sea Water was a typical feature of the Labrador Sea (4). Interestingly, such a pattern did also appear at the end of the 1920's and prevailed until the end of the 1960's, with generally colder European winters having been common during that period since end of the 1930's. The same SST anomaly pattern was re-established once more in the late 1990's, which thus suggests the possibility of a colder type of European winter for the coming decade(s).

1 – KUIJPERS, A., WERNER, F. 2007. *Extremely deep-draft iceberg scouring in the glacial North Atlantic. Geo-Marine Letters* doi:10.1007/s00367-007-0059-1

2 – KUIJPERS, A., DALHOFF, F., BRANDT, M.P., HÜMBS, P., SCHOTT, T., ZOTOVA, A. 2007. *Giant iceberg plow marks at more than 1 km water depth offshore West Greenland. Marine Geology, in press*

3 – KUIJPERS, A., TROELSTRA, S.R., PRINS, M.A., LINTHOUT, K., AKHMETZHANOV, A., BOURYAK, M.F., LASSEN, S., RASMUSSEN, S., JENSEN, J.B., 2003. *Late Quaternary sedimentary processes and ocean circulation changes at the Southeast Greenland margin. Marine Geology* 195, 109-129

4 – SEIDENKRANTZ, M.S., AAGAARD-SØRENSEN, S., SULSBRÜCK, H., KUIJPERS, A., JENSEN, K.G., KUNZENDORF, H., 2007. *Hydrography and climate of the last 4400 years in a SW Greenland fjord: implications for Labrador Sea palaeoceanography. The Holocene* 17,3, 387-401

30.6.2007

## Aeolian and ice transport and fluxes of matter (including ecotoxicants) in the Arctic

V. Shevchenko

Shirshov Institute of Oceanology, Moscow, Russia (IORAS), Nakhimovsky Prospekt 36, 117997 Moscow

Numerous studies have shown that aerosols in the Arctic are of importance for atmospheric chemistry and climate. But up to now aerosols of the Arctic are studied insufficiently. We began aerosol research in the marine boundary layer over the seas of the Russian Arctic in 1991. For comprehensive study of the amount and composition of aerosols we used a system of complementary and sometimes even overlapping methods. In August-September the mass concentration of insoluble coarse fraction varied from 0.02 to 1.38  $\mu\text{g}/\text{m}^3$ . Organic matter (fibers of vegetation, pollens, diatoms) is the main component by mass. Content of organic carbon varies from 7.54 to 48.9%. Mineral particles also play an important role. Some "fly ash" particles (from 0.5 to 10  $\mu\text{m}$ ) have been found in most mesh samples. The quantity of these particles increases near Norilsk and the Kola Peninsula. A catastrophic increase of element content due to anthropogenic factor in the summer-autumn time has not been found.

The average, over the three methods, vertical flux of insoluble aerosols in the Arctic comprises about 300  $\text{mg m}^{-2} \text{ year}^{-1}$ , what is far higher than formerly accepted. This value calls for refinement. The contribution of aeolian material to formation of the geochemical properties of the suspended matter, cryosols and bottom sediments in the Arctic is roughly equal to contribution of the suspended matter of rivers and ice rafted material. The income of organic matter from the atmosphere is also of great significance. For many chemical elements (Pb, Sb, Se, V etc.) in the Arctic the atmospheric source is principal. Our experience shows that along with the detailed study of the aerosol material in the atmosphere, thy systematic studies of lithology and geochemistry of snow cover are necessary, since it is a natural collector of both dissolved and particulate aeolian material. The corresponding studies of lithology and geochemistry of the sea ice are necessary as well. Thus, the study of aeolian material acquires a systematic and multidisciplinary character, what sharply increases the possibilities of interpretation. Now we

are only at the first stage of these studies, and further thorough and long joint work is needed. In our expedition we will try to continue such studies. It will be our input in the studies in the frame of project No. 323 of the International Polar Year 2007/08 (Aeolian and ice transport and fluxes of matter (including ecotoxicants) in the Arctic).

1.7.2007

## **Variation of Late Quaternary climate of the North Atlantic – Baltic realm as reflected in the sediments of the central Baltic Sea –**

J. Harff, R. Endler, S. Kotov

Leibniz Institute for Baltic Sea Research Warnemuende, Seestrasse 15, 18119 Rostock, Germany

Sediments of the Baltic Sea basins serve as a textbook in climate and environmental history of the Baltic area and the North Atlantic realm. The sedimentary facies of basin sediments in the central Baltic Sea correlates significantly with the climate conditions and their variations after the Last Glacial Maximum. During the Late Pleistocene and Early Holocene, continuous warming and resulting water level changes interfered with glacio-isostatic adjustment and caused abrupt incursions of ocean water into the Baltic basin, but also abrupt outflow of fresh water to the North Atlantic that obviously influenced the oceanic circulation pattern. During the late Holocene when the Baltic basin was permanently connected with the Atlantic Ocean the dynamics of the atmospheric circulation of the North Atlantic, but also its modification due to the variation of Eurasian anticyclones is reflected in the facies of sediments in the Baltic Sea. The facies variation points to a cyclic change of a continental climatic style with lower atmospheric temperatures and warmer maritime climatic conditions. In short cores of the Eastern Gotland Basin, transitions in sedimentary facies can be clearly allocated to climate shifts from the Medieval Climate Optimum to the Little Ice Age and the Modern Warm Period. Time series analysis of dated sediment cores sampled with gravity corers covering a time span of the last 11000 years reveals periodicities of climate proxy-parameters from 400 through 500 to 900 years correlating significantly with the oxygen isotope signals measured in Greenland ice cores. Periodicity analysis allows the development of predictive scenarios of the future development of climate parameters based on mathematical models of proxy-data variability from sediments and ice cores.

3.7.2007

## **Azores Front, Saharan dust and the biogeochemical properties of the Madeira Abyssal Plain (subtropical NE Atlantic) - case study at 33°N, 22°W.**

Joanna J. Waniek<sup>1</sup>,

V. Chavagnac<sup>2</sup>, D. Atkins<sup>2</sup> (NOCS, UK), T. Leipe<sup>1</sup>, R. Bahlo<sup>1</sup>, and D. Schulz-Bull<sup>1</sup>

<sup>1</sup>Leibniz Institute of Baltic Sea Research Warnemünde, Germany, <sup>2</sup>National Oceanographic Centre, Southampton, UK

The seminar focuses on the question “What is the reason for the strong year to year variations in surface production and associated export production in the Azores Front region in the subtropical Northeast Atlantic?” by examination of the possible causes a) Changes in the

thermocline, b) Azores Front meanders and c) Natural iron fertilization via Saharan dust. Previous studies of the region in the subtropical Northeast Atlantic have shown that: 1) Local meteorological forcing and surface production do not explain the variations in particle flux and its components on a year to year basis (Waniek et al. 2005a); 2) High particle flux signal always occurred when negative temperature anomaly was observed between September-January (just prior to the bloom period); 3) High particle flux signal occurs in years, in which the thermocline has a temperature less than 18°C; surface colder by approximately 1°C because of the cold, nutrient rich water advected southward by cyclonic eddies or meanders of the Azores Front; 4) DW, CaCO<sub>3</sub>, POC and PON show all similar patterns on an annual time scale. In contrast opal and lithogenic fraction differ; 5) since 1998 drastic change in the properties of the thermocline was observed (shallow Mixed Layer Depth, positive Sea Surface High Anomaly) in connection with relatively moderate particle flux and also less year to year variations (Waniek & Schulz-Bull, 2006). Those findings lead to the question “What is causing the differences in annual cycle between mass flux and lithogenic fraction?”, which was elaborated in the second part of the presentation.

Dust emissions from major worldwide desert areas supply several billion tons per year of particles to the open ocean. Its spatial and temporal variability in atmospheric dust flux has a significant impact on major environmental regimes as phytoplankton growth is relying on the essential micronutrient element available in dissolved form in the open ocean. Although a large quantity of micronutrient is provided by fluvial inputs, most of it is used within coastal areas and little is effectively delivered to the open ocean. In contrast, aeolian particles are directly delivered to the open ocean impacting the marine primary productivity. Here, we show that lithogenic aeolian particles delivered to the Madeira Abyssal Plain in the subtropical Northeast Atlantic have high occurrence of palygorskite and smectite without kaolinite associated with Sr isotopic compositions similar to North Eastern Atlantic aerosol indicating the Anti-Atlas Moroccan chain of Paleozoic age as the source region. The nutrient supply of Fe, P and Mn associated with the lithogenic particles are 5 times more important during a dust event than the general eolian input. This suggests that a significant proportion of the lithogenic elemental flux diffuses to the water column and is made available to the ecosystems. As a consequence, any environmental modification in this input may alter immediately global biogeochemical cycles, ecosystem production rate, and carbon dioxide export via the biological pump.

Jan Harff, Kerstin Perner, Matthias Moros  
(eds.):

Deglaciation history, coastal development,  
and environmental change in West  
Greenland during the Holocene: Results of  
the R/V “Maria S. Merian” expedition  
MSM05/03, 15<sup>th</sup> June to 4<sup>th</sup> July 2007

## CONTENT

### Abstract

1. Introduction
  2. Methods and devices
    - 2.1 Subbottom profiling
    - 2.2 Multibeam echo-sounding
      - 2.2.1 Kongsberg (Simrad) EM-120 deep-water multibeam echosounder
      - 2.2.2 Kongsberg (Simrad) EM-120 shallow-water echosounder
      - 2.2.3 EM-120 multibeam data processing
    - 2.3 Hydrography
      - 2.3.1 Continous underway measurements
      - 2.3.2 Hydrochemistry
    - 2.4 Sediment Sampling
    - 2.5 Lithological core description
    - 2.6 Diatomological investigation
    - 2.7 Biogeochemistry Magnetic susceptibility measurements
    - 2.8 XRF-Scanning Geodetic measurements
    - 2.9 SPM and aerial dust sampling
  3. First results
    - 3.1 Mapping
      - 3.1.1 Mapping Ilulissat Icefjord
      - 3.1.2 Morphology of the Ilulissat Ice fjord area
      - 3.1.3 Mapping ice berg drift in the Davis strait
    - 3.2 Biogeochemistry - early diagenesis in fjord and bay sediments
    - 3.3 Disko Bay, fjord, and shelf sediments – paleoceanographic /paleoclimatological Interpretation
      - 3.3.1 Analyses during the expedition
      - 3.3.2 Data Analyses
    - 3.4 Anthropogenic impact on Qaumarujuk Fjord environment
    - 3.5 Geodetic measurements
    - 3.6 SPM an aerial dust
  4. Summary
- References  
Enclosures

